HPV-16 E6, hDlg and Connexin 43 in Cervical Carcinogenesis

By

Peng Sun M.D & M.Sc

A Thesis Submitted for the Doctorate of Philosophy

University of Glasgow

Division of Cancer Sciences and Molecular Pathology,

Section of Squamous Cell Biology & Dermatology

&

Division of Virology, IBLS

November 2005

Division of Cancer Sciences and
Molecular Pathology, Section of
Squamous Cell Biology &
Dermatology
University of Glasgow
Glasgow
Scotland, UK

Division of Virology, IBLS
University of Glasgow
Virology Institute
Glasgow
Glasgow G11 5JR
Scotland, UK

SUMMARY

Disruption of gap junctional intercellular communication and/or Connexins (the channel proteins of gap junctions) is frequently reported in malignant cell lines and tumours. Many tumor cells exhibit aberrant gap junctional intercellular communication (GJIC), which can be restored by transfection with Connexin genes. Of the Connexin family, Connexin 43 has attracted the most attention as it is widely expressed in many tissues and Connexin 43 gap junctions correlate with various physiological functions. Connexin 43 is a short-lived protein (half-life of 1–3 h in cultured cells), both lysosomes and proteasomes having been reported to be involved in its degradation.

Certain human papillomaviruses (HPV) associated with the development of cancers, especially of the cervix, have been reported to downregulate GJIC in vitro. There is also evidence for reduced gap junctions in cervical dysplasia. The association between HPV and GJIC, and the mechanism and consequence of deregulated GJIC in cervical tumour progression, remains unclear. In HPV-16 associated cervical cancer, the viral oncogene E6 inactivates the tumour suppressor p53, but also has p53-independent functions in tumour progression. One of these may involve interaction with hDlg (the human homologue of *Drosophila* Discs Large), a tumour suppressor present in epithelial cells at sites of cell-cell contact and which regulates cell polarity and attachment. hDlg contains three PDZ protein-protein interaction domains, the second PDZ domain of which binds E6. Connexin 43 also has a PDZ binding domain in its C-terminus.

Previously, it was demonstrated that Connexin 43 relocates from the membrane to the cytoplasm in a novel HPV-16 E6-containing cervical epithelial cell line (named W12GPXY) that is fully transformed and invasive and deficient in gap-junctional intercellular communication (Aasen T et al., 2003 Oncogene 22, 7969- 7980).

The overall aim of this project was to investigate the relationship of loss of gap junctions to malignant progression by comparing the properties of W12GPXY with those of the non-malignant parental cell line, W12G, from which W12GPXY was derived.

First, microarray was used to identify global differences in RNA expression between the two cell lines, large differences were seen in expression of angiogenesis-related genes and they were confirmed by Real-Time RT-PCR for three genes, IL-8, VEGF and FGF-2. No significant differences were noted for connexin genes but there were differences in MAGUK family members including hDlg.

However, protein expression studies by western blot and immunofluorescence staining showed a significant increase (2.9 fold) of HPV-16 E6 in W12GPXY cells, which co-localises with hDlg in the cytoplasm. Connexin 43 also binds hDlg. Treatment of W12GPXY cells with Leptomycin B to trap E6 in the nucleus or siRNA knockdown of E6 abrogate the relocation and co-location of hDlg and endogenous wild type Connexin 43 and restore Connexin 43 gap junction at points of cell-cell contact. Further, when C33a cells (HPV-negative cervical tumour cells which normally retain large Connexin 43 gap junctions) are transfected with HPV-18 wild type E6, changes in localisation of Connexin 43 and hDlg are consistent with those in W12GPXY cells. However, C33a cells transfected with a mutant E6 lacking the hDlg

binding site retain Connexin 43 gap junction plaques. Finally, Connexin 43 associates with hDlg through its PDZ-binding domain and this is required for its relocalisation to the cytoplasm in W12GPXY cells. The results suggest that increased cytoplasmic E6 associated with malignant progression of W12GPXY cells redistributes Connexin 43 from membrane junctions into the cytoplasm by a mechanism involving binding of hDlg to the Connexin 43 C-terminal tail. The findings have uncovered a new role for hDlg in trafficking of Connexin 43. It also provides a novel mechanism for the loss of gap junctional intercellular communication during malignant progression of squamous epithelial cells.

The specific roles played by lysosomes and proteasomes in the degradation of Connexin 43 in W12GPXY cells were also studied. The results suggest the involvement of both proteolytic pathways, although the lysosome seems to be the major compartment for Connexin 43 degradation. Association with HPV-16 E6 and hDlg together with proteasome activity seems to be required for Connexin 43 redirection from the cell membrane and transport into the lysosomal degradation pathway. Taken together, these results suggest that Connexin 43 gap junction intercellular communication was lost from the cell membrane requiring maintenance of E6 and hDlg complexes for proteasomal internalization and consequently transport into lysosomal compartment for degradation in W12GPXY cells.

LIST OF CONTENTS

LIST OF FIGURES

Page

TABLE LIST

Page

LIST OF ABBREVIATIONS

APS	Ammonium persulphate
BPV	bovine papillomavirus
CIN	Cervical intraepithelial neoplasia
DAPI	4',6'-diamino-2-phenylindole hydrochloride
DMEM	Dulbecco's modified Eagle's medium
DMSO	Dimethyl sulphoxide
EGF	epidermal growth factor
FCS	fetal calf serum
GJ	gap junction
GJIC	gap junction intercellular communication
H&E	haematoxylin and eosin
hDlg	human homologue of *Drosophila* Discs Large
HPV	human papillomavirus
IF	immunofluorescence
IgG	immunoglobulin G
IP3	inositol-1,4,5-triphosphate
kDa	kilodalton
KGM	keratinocyte growth medium
LY	lucifer yellow
MAGUK	membrane-associated guanylate kinase homologue

mRNA	messenger ribonucleic acid
NCR	none coding region
NGS	normal goat serum
NHS	normal horse serum
PBS	phosphate buffered saline
PCR	Polymerase chain reaction
PDZ	PSD95/Dlg/ZO-1 family
PI	propidium iodide
PKC	protein kinase C
LD -rich	leucine and aspartic acid – rich
RT	reverse transcriptase
SCC	squamous cell carcinoma
SDS	sodium dodecyl sulphate
SV 40	simian virus 40
UV	ultraviolet

ACKNOWLEDGEMENTS

Firstly I would like to express my thanks to my supervisors, Dr Malcolm B. Hodgins, Dr Mike Edward and Dr Shelia V.Graham, for the opportunity of exploring this project in the Dermatology Department and Virology Institute of Glasgow University. Thank you for the great support and guidance and invaluable expertise as well as the patience.

Many thanks for a variety of past and present members in both Dermatology and Virology for their support and help through the project. In particular I would like to thank Dr Sarah Cumming for her constant support and encouragement. I would like to thank Eve Kandyba, Steven Milligan, Graham Chadwick and Irene Campbell for their technological support and friendship. I would thank for my friends and colleagues who were there for me in both good times and challenging times, Thanaporn Veerapraditsin, Sarah Mole and Louise Yule.

I would thank Dr Giorgia Riboldi-Tunnicliffe and Dr Pawel Herzyk for their support and association with the microarray experiments and data analysis.

Finally, I am gratefully to my family, especially my mother and brother, for their endless encouragement and love during the course in Glasgow.

The author received funding from Glasgow University Studentship and ORS studentship during the course. Unless otherwise stated, all the work presented in the thesis is by the author's own efforts.

CHAPTER 1. INTRODUCTION

1.1 Papillomavirus

The viral etiology of warts was discovered around 100 years ago when McFadyan and Hobday in 1898 transmitted dog warts by ultrafiltered wart lysates. Nine years later, Ciuffo in Italy used the same method to produce warts successfully after self-inoculation of similar filtrates from human papillomas (zur Hausen, 1994, 1996). Papillomaviruses (PVs) were firstly described in cottontail rabbits in 1933 by Shope, these viruses were originally classified as members of the papovavirus family which was named using the first two letters of the major genera: papilloma, polyoma and simian vacuolating virus 40 (Howley, 1995). However, papillomaviruses (e.g. bovine, cottontail rabbit, and human papillomaviruses) and polyomaviruses (e.g. murine polyomavirus and simian virus 40) differ in diameter, genome size, protein composition and size, and capsomere morphology and size (Baker et al., 1983 and 1989); recently, papillomaviruses and polyomaviruses were divided into two DNA tumor virus subgroups. The more researchers studied them, the more PV subtypes have been widely defined throughout the animal kingdom such as in birds, mammals and human. PV infections have been proven to cause wart generation in squamous epithelia. Furthermore, human papillomavirus (HPVs) infection in the basal layers of mucosal and cutaneous epithelium causes benign hyperproliferative lesions (de Villers, et al., 1981; Kizyzek, et al., 1980). During the last two decades, HPVs were detected in genital warts leading to cervical cancer and PVs have been proved to be the most important oncogenic pathogenically associated virus group (Lowy, et al., 1994; zur Hausen, 1991). All the PV types possess a common structure: they are small nonenveloped viruses with 55nm-diameter icosahedral protein capsids containing double stranded DNA genomes of approximately 8,000 bp (Bunney et al., 1992). Most of the phylogenetic studies on HPVs are based on their genotype properties. More than 200 HPVs have been identified and at least 78 HPV genomes are

completely characterised Figure (1) (Chen et al., 1995). Different types of HPVs are associated with warts or cancers in the cervix and anogenital tract sites, oral cavity and skin (Melbye and Frisch, 1998; de Villiers et al., 1999; Harwood et al., 1999). It is clear that HPVs are prevalent and are transmitted through sexual activities and infections rates are high in both male and female population (Bosch et al., 2002). A number of epidemiology studies demonstrated the close linkage between HPV infection and development of cervical cancer. The association of HPVs with different diseases is presented in Table (1).

Site	HPV-associated disease	HPV types
Skin	Wart	1, 2, 3, 4, 7, 10, 26, 27, 28, 29, 41, 48, 60, 63, 65, 75, 76, 77,.....
	EV wart	5, 8, 9, 12, 14, 15, 17, 19, 20, 21, 22, 23, 24, 25, 36, 37, 38, 46, 47, 50,.....
Oral Cavity	FEH	13, 32, 57, 72, 73
Larynx	Papilloma	6, 11
Anogenital tract	Genital warts	6, 11
	Intraepithelial neoplasia	34, 40, 42, 43, 44, 53, 54, 55, 59, 61, 62, 64, 67, 68, 71, 74
	Intraepithelial neoplasia and cancer	**16**, **18**, **31**, 33, 35, 38, 45, 51, 52, 56, 58, 69,.....

Table 1: HPVs and their associated diseases. HPV 16, 18 and 31 were classified as high risk HPVs.

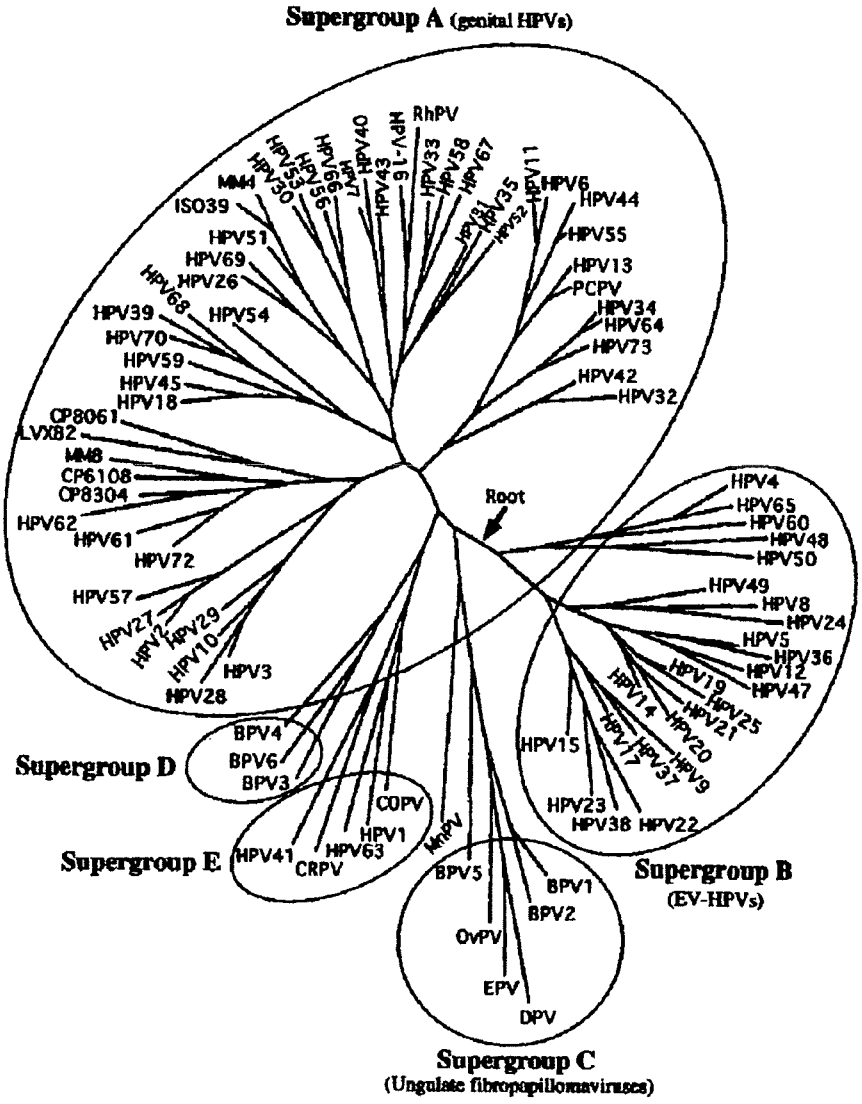

Figure 1: Phylogenetic tree of PV types. There are 5 supergroups in PV phylogenetic tree, subgroup A contains the most members including high risk HPVs (taken from Chan et al., 1995).

1.2 HPVs and cancer

Following Shope's discovery, Rous confirmed papillomavirus infection could link to cancer initiation and promotion and suggested PVs could be the first identified DNA tumor virus (Rous and Kidd, 1936; Kidd and Rous, 1940). Although HPV infections had been identified as the most common sexually transmitted disease producing common epidermal warts in the anorectum, hands, feet, and knees; it was only in 1980s that a clear connection was elucidated between HPV infection and 99.7% cervical cancer cases, and leading to the discovery of the first identified viral oncogenes that constituted a risk factor for widespread human cancer (Gissmann et al, 1983; 1984; Munoz, 2000). HPV DNA sequences found in cervical carcinoma cell lines were the first clue to the role that high-risk types 16 and 18 play in altered cell growth (Schwarz et al., 1985; Schneider-Gadicke and Schwarz, 1986). Further studies in cervical cancer cell lines have demonstrated many of the harmful effects of HPV in terms of cellular mutations (Havre et al., 1995; Liu et al., 1997) and genomic integrity (Hashida and Yasumoto, 1991). Additionally, since then HPV infections have also been found associated with some cases of oral cancer, other anogenital cancer, oesophageal cancer, non-melanoma skin cancer and lung cancer (Munger et al., 2004). The association between HPV and various cancers is presented in Table (2). Cervical cancer is the second most common cancer among women worldwide, each year more than 450,000 women are diagnosed with cervical cancer and over 200,000 women die of this disease (Daley, 1998). The mean incidence of cervical cancer in developing countries (19.2 cases per 100,000 women) was approximately twice more than in developed countries (10.6 cases per 100,000 women), which also happened for cervical cancer mortality (Drain et al., 2002).

The progress and outcome of an HPV infection depends on HPV type, anatomical features of the infection, location and the timing of cellular differentiation (Bosch et al., 2002). Starting in 1976, thereafter rapidly fostered by technological advances, the puzzling complexity of the HPV group became evident. These viruses can be divided in to two clinical groups, the mucosal

infecting and cutaneous infecting HPVs; within each subfamily, individual virus can be defined as high risk or low risk according to the propensity for malignant progression of the lesion that they cause (Jenson et al., 1991). HPV genotypes 6, 11, 40, 42-44, 53-55, 57, 59, 61, 67, 69, 71, 74 and 82 only cause gential warts (condyloma, acuminata); HPV types 31, 33, 35, 39, 51, 52 and 58 carry an intermediate risk; and HPV type 16, 18, 45 and 56 are a high risk subfamily which are associated with squamous intraepthelial lesions leading to high-grade dysplasias and malignant cervical cancer (Roman and Fife, 1989; Park et al., 1995). HPV 16 is the most prevalent virus to infect the cervix and is associated with the entire range of intraepithelial lesions to invasive squamous cell carcinoma, followed in prevalence by HPV-18, HPV-31 and the others (zur Hausen, 2002).

Infection by HPVs is believed to occur through microwounds of the epithelium by attachment to a cell surface receptor such as α6β4-integrin or heparin and entry into the basal layer cell nucleus. Cells in the basal layers consist of stem cells and transit-amplifying cells that are continuously dividing and provide a reservoir of cells for the suprabasal region (Hummel et al., 1992). During HPV maintenance and progression, the productive life cycle of the virus is directly linked to the differentiation program of the infected epithelial host cells (Howley and Lowy, 2001; Stubenrauch & Laimins, 1999), Figure (2). Following HPV entry, there is a viral gene expression cascade activated to establish around 50 copies of viral DNA episomes per cell that are stably maintained in the undifferentiated basal layer cells through the infection course and that replicate in synchrony with host cell division (LaPorta & Taichman, 1982; Howley and Lowy, 2001). In the HPV-infected differentiating cell, the viruses maintain the correct environment to stimulate the host cells in G1 into S-phase and to reactivate the host replicative machinery to allow virus vegetative replication for the virus to thrive (McMurray et al., 2001).

Cancer type	**Percent HPV- positive**
Cancer of the cervix	95%
Anal and perianal cancer	70%
Vulval cancer	50%
Vaginal cancer	50%
Penile cancer	50%
Cancer of the oropharyngeal region	20%
Cancer of the esophagus	10%-20%
Squamous cell carcinoma of the skin	70%-80%
Basal cell carcinoma of the skin	50%

Table 2. Approximate percentage of HPV-positive human cancers (Adapted from zur Hausen, 1999)

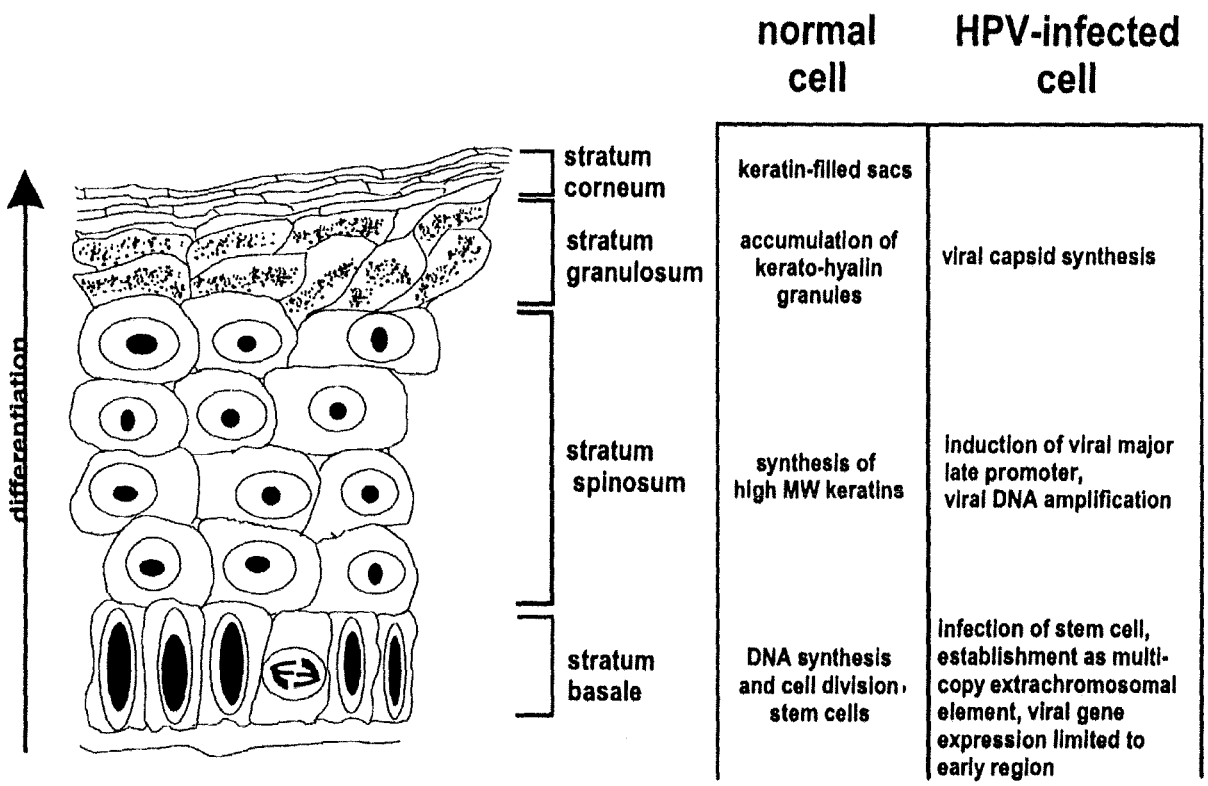

Figure 2: The differentiation-dependent changes in normal and HPV-infected epithelial cells (taken from Stubenrauch and Laimins, 1999).

1.3 The HPV Genome and Its Contribution to Malignancy

The HPV genome typically consists of eight open-reading frame sequences, located on only one of the strands of DNA, and is divided into a ~ 4 kb region encoding six early-phase genes (E) (E1-E7), a ~3 kb region encoding two late-phase genes (L1 and L2) and a ~ 1 kb viral noncoding long control region (LCR) which regulates E and L gene expression. The HPV16 viral genome also has the P_{97} early promoter, immediately upstream of E6 ORF; and the P_{670} late differentiation induced promoter, locating in the E7 ORF (Grassmann et al., 1996; Desaintes & Demeret, 1996). The open reading frames of the HPV 16 genome are shown in Figure (3).

1.3.1 HPV E1 and E2

The early genes serve to regulate the transcription of DNA, while the late genes encode the capsid proteins involved in viral spread (Stoler et al., 1989). The E1 and E2 proteins play important roles in regulating the transcription and replication of the viral genome, E2 is especially involved in regulating the transcription from the viral long control region. E1 protein is essential for viral replication; it is a DNA-dependent, ATP-dependent helicase which is responsible for recruiting the cellular DNA replication initiation machinery via E2 which binds to specific sequences at the origin of replication (Richman et al., 1997). The E1 binding site is an AT rich region which lies between the E2 binding sites. E1 binds weakly to DNA but the affinity is increased in the presence of E2 (Desaintes & Demeret, 1996). E2 is a DNA binding transcription factor interacting with an $ACCN_6GGT/ACCN_6GTT$ motif in the viral LCR (Hirt et al., 1996; Marshall et al., 1989). E2 binds to the motifs as a dimer through a domain in its C-terminal part, where E2 demonstrates the function of both a replication initiator and an E6/E7 transcriptional modulator. In morphologically normal, but HPV-infected basal cells, HPV gene expression is inhibited by E2 at normal levels (Cripe et al., 1987). HPV DNA is frequently

integrated into the host genome in cancer cells where the break point in the viral genome occurs consistently within the E1/E2 region, and once the E2-controlled regulation of E6/E7 expression is lost, E6 and E7 will be inappropriately expressed (Hubert & Laimins, 2002).

1.3.2 HPV E1^E4 and E5

The HPV E4 and E5 ORFs are expressed during the early phases of the viral life cycle but only as the third and fourth ORFs on polycistronic transcripts and little E4 and E5 proteins are sythesized (Remm et al., 1999). In contrast, on epithelial cell differentiation, E4 and E5 are expressed as the first and second ORFs of late transcripts. Actually, E4 is the virus protein most abundantly transcribed and highly expressed in a wart (Howley, 1996). The E4 ORF lacks an initiator AUG codon and translates with the first 5 amino acids of E1 to generate E1^E4 fusion proteins using the E1 sequence for translation initiation (Holey, 1996). High risk E1^E4 proteins bind and disrupt the cytoplasmic keratin networks in differentiated cells and interact with an RNA helicase, E4-DBD, which is a member of a helicase family involved in mRNA splicing, transport as well as initiation of translation (Doorbar et al., 1991; Yoshioka et al., 2000). Another character of HPV-18 and HPV-16 E1^E4 is they can induce a G_2 arrest in a variety of cell types, but how this happens is still not clear (Davy et al., 2002; Nakahara et al., 2002).

The HPV-16 E5 protein is a small 84 amino acid hydrophobic protein localized to the endoplasmic reticulum and Golgi apparatus but also found on cellular membranes (Conrad et al., 1993). It acts as a ligand for membrane proteins, including growth factor receptors, interacts with and also modulates ERK1/2 and p38 MAP kinase activation by an EGFR-independent pathway (Crusius et al., 2000). E5 can also stabilize and inhibit the degradation of the complex between epidermal growth factor (EFG) and its receptor (EGFR), resulting in enhanced MAP kinase activity (Gu & Matlashewski, 1995). The binding between E5 protein and ductin, a

16kDa subunit of the vacuolar ATPase, results in down- regulation of gap junction intercellular communication and disturbance of the H^+ transport function of vacuolar ATPase to inhibit endosomal acidification, prolonging the active signal from the EGFR and interfering the endosomal compartments pH (Conrad et al., 1993; Straight et al., 1995; Briggs et al., 2001). The effects of E5 on cell growth have been difficult to study due to its low (usually non-detectable) level of expression in stable cell lines. The E5 gene is frequently deleted during the viral integration, although it is thought to play an important role in malignant transformation. Recent studies showed HPV E5 had an important activity in late gene amplification and expression in differentiated suprabasal epithelial cells suggesting that E5 had a role in the late phase of the viral life cycle (Longworth & Laimins, 2004).

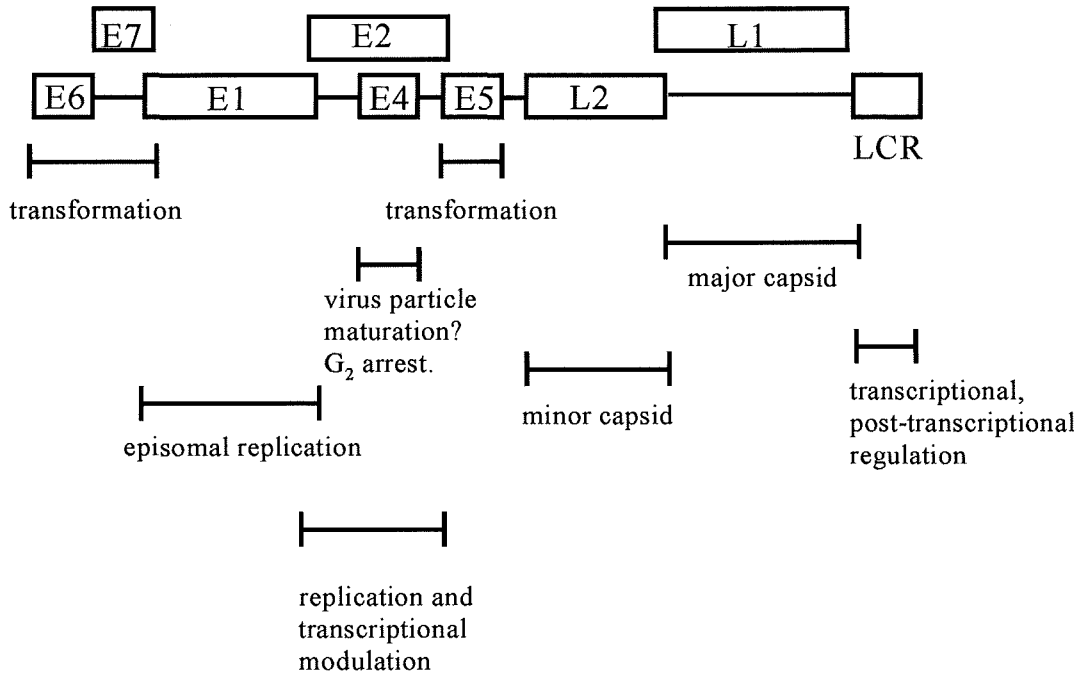

Figure 3: Genomic organisation and gene functions of HPV -16.

1.3.3 HPV E6 and E7

High risk HPV E6 and E7 emerge as most important for growth stimulation and cell transformation. Both represent related proteins that even individually can immortalize a variety of human cell types. Their cooperation synergistically exerts overlapping effects on cell cycle control, and in combination, they efficiently immortalise human keratinocytes (Gissmann, 1992). During the progression from the premalignant to malignant phase of high-risk HPV-associated disease, the viral DNA genome is integrated into the host chromosome, resulting in over expression of the viral oncoproteins E6 and E7 (Jeon and Lambert, 1995).

HPV E6 protein is a 151 amino acid (18 kDa) polypeptide in which there are four Cys-x-x-Cys motifs forming two zinc-finger domains, one highly conserved C-terminal PDZ (PSD-95/Dlg/ZO-1)-binding domain, and one LD-rich site (Kiyono et al., 1997; Tong et al., 1997). A schematic representation of high risk HPV E6 and its binding proteins is shown in Figure (4). E6 is one of the earliest expressed genes during the HPV infection. Although E6 is small, it is a multifunctional oncoprotein that induces several important effects upon the viral life cycle and host cell maturation processes, involving gene transcription, cell proliferation, apoptosis and immortalization (McMurray et al., 2001). The first insights into the action of E6 have come by studying its interactions with p53. p53 is a well-characterized tumor suppressor that regulates the expression of proteins involved in cell cycle control, including the cyclin dependent kinase inhibitor, p21. In the nucleus, E6 binds to the tumor suppressor p53 via an interaction with E6-associated protein (E6-AP), a cellular E3-ubiquitin protein ligase, and targets p53 for ubiquitination and degradation (Huibergtse et al., 1991). The cellular p53 protein is a transcription factor for cell cycle arrest and apoptosis related gene expression by which cells respond to environmental stress. In response to DNA damage, p53 is activated and detains the

cell in G1, presumably to allow time for DNA repair; p53 mediates this G1 arrest by inducing high levels of the cdk inhibitor $p21^{cipl}$ (cdk interacting protein-1) and $p14^{ARF}$ resulting in either G1 or G2 arrest (DeWeese et al., 1997; Samuel et al., 2002), as well as apoptosis (Hawley et al., 1989). E6 also inhibits p53 function by retaining p53 in the cytoplasm to block its entrance into the nucleus, independently of the degradation pathway (Thomas et al., 1999). It was identified that in human cervical carcinoma-derived malignant cell lines (CaSki and SiHa) the whole HPV 16 genome was harboured and HPV 16 E6 with E7 can induce morphologic transformation in mouse 3T3 cells as well as the immortalization of human mammary epithelial cells (Androphy et al., 1987; Kyono et al., 1998). Unlike E7, E6 alone was not efficient at immortalizing human keratinocytes, the process requires the expression of both E6 and E7 (Howley et al., 1989). Only high-risk HPV E6 directs ubiquitin degradation of p53, low risk HPV E6 protein has relatively low binding affinity for p53, which may partly account for the less aggressive functional properties (Kehmeier et al., 2002).

Recent studies have identified p53-independent activities of E6 that are important for immortalization of human cells. E6 mutants of HPV-16 have been identified that are unable to degrade p53 but retain the ability to immortalize mammary epithelial cells; consistently, other E6 mutants retain the ability to degrade p53 but have lost the ability to immortalize (Liu et al, 1999). One of the important onco-functions that appears to improve E6 transforming ability is its association with the PDZ family of proteins. PDZ proteins contain a conserved domain associated with the PSD-95, Dlg, and ZO-1 proteins (hence the name PDZ, the detail of this protein family will be described in Charpter 1.4.). The PDZ domain is often found in proteins localized at areas of cell-cell contact, such as tight junctions in epithelial cells. The PDZ proteins probably act as molecular scaffolds to aid in signal transduction (Graven and Bredt, 1998; Gompert, 1996). High risk HPV E6 containing a carboxyl terminal PDZ protein binding motive

X-(S/T)-X-(V/I/L)-COOH also has been reported to interact physically with several cytoplasmic proteins including the PDZ domain-containing proteins MAGI-1, ZO-1, MUPP-1, hScrib and hDlg. Such interactions might alter cell signalling cascades or cause changes in cell structure (Chen et al., 1995; Tong & Howley, 1997; Nakagawa and Huibregtse, 2000; Gao et al., 2001; Thomas et al., 2002; Watson et al., 2003). Binding of these PDZ proteins and high risk HPV E6 results in E6AP mediated ubiqitination and proteolysis (Gardiol et al., 1999; Nakagawa and Huibregtse, 2000). The PDZ binding sites in low risk HPV E6 proteins have much lower binding affinity than high risk HPVs and since most of these PDZ containing proteins are involved in negatively regulating cellular proliferation, it is conceivable that these PDZ interactions may contribute to hisk HPV E6 transformation activity. The importance of this interaction has been confirmed in experiments with transgenic mice expressing E6 proteins that lack the PDZ binding domain. These mice retain the ability to inactivate p53 but do not develop the epidermal hyperplasias that are frequently seen in wild-type E6 transgenics (Nguyen et al., 2003). It is not clear which signalling pathways are impacted by E6 binding to PDZ proteins or which PDZ family members are most important for these phenotypes. The elucidation of these pathways is of great importance for our understanding of HPV pathogenesis.

Another major function of the high-risk E6 proteins that is important for immortalization is their ability to activate the expression of the catalytic subunit of telomerase, hTERT which results in cell immortalization in early-passage human keratinocytes and mammary epithelial cells (Klingelhutz et al, 1996; Nakamura et al., 1997; Munger et al., 2002). Telomerase is a four-subunit ribonucleoprotein enzyme that synthesizes telomere hexamer repeat sequences by reverse transcript an RNA template and maintains the telomeric DNA at the ends of linear chromosomes (Lustig, 2004). Telomerase activity is usually restricted to embryonic cells and is

absent in somatic cells. The lack of telomerase activity results in a shortening of telomeres, with successive cell divisions eventually leading to senescence. In contrast, in most cancers, reactivation of hTERT expression occurs and leads to reconstitution of telomerase activity (Liu, 1999). E6 appears to activate hTERT transcription through the combined action of Myc and Sp-1 (Greenberg et al., 1999; Key et al., 2000). Recent studies have shown that E6 can bind to both Myc and its cofactor Max, leading to transcriptional activation of the hTERT promoter (Veldman et al., 2003). Analysis of E6 mutants that discriminate between the ability to degrade p53 and to activate hTERT demonstrated that the latter activity is most important for immortalization.

As described, E6 is a multifunctional protein. The high-risk E6 proteins interact with a number of other cellular proteins, such as p300/CBP, and the interferon regulatory factor IRF-3, which are important for normal cell differentiation and cell cycle progression to alter cellular gene expression (Werness et al., 1990; Patel et al., 1999; Zimmermann et al., 1999; Ronco et al., 1998). They can enhance the expression of the oncogene product c-myc (Hurlin et al., 1995). A number of additional cellular protein targets of high risk HPV E6 have been identified, including paxillin, a focal adhesion protein, which appears to be involved in bovine papillomavirus E6 transformation by disturbing the actin cytoskeleton; E6BP protein (also known as ERC-55), a calcium-binding protein, suggesting the interaction might affect calcium-induced differentiation of E6 expressing cells; and Bak, a member of Bcl-2 family.

Among E6 oncofunctions, it appears that p53 degradation is most important for full transformation and that binding of PDZ proteins and activation of hTERT expression are necessary for immortalization.

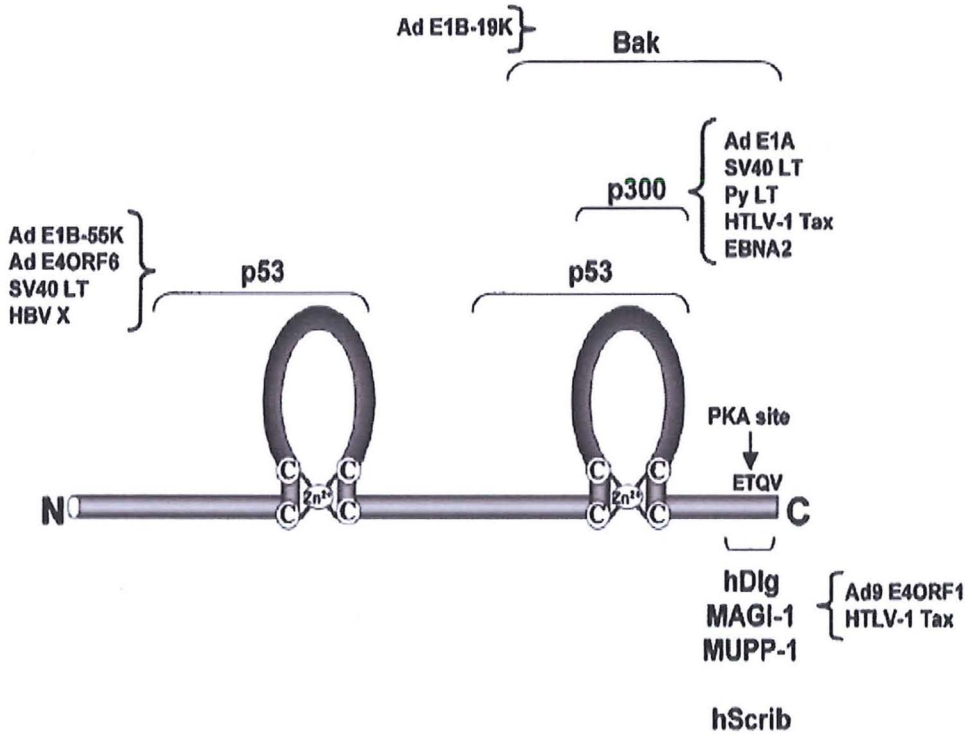

Figure 4: The high-risk HPV E6 protein. Schematic diagram of E6 showing the two zinc fingers, together with the regions involved in interactions with cellular proteins that are also targeted by the oncoproteins of other viruses. Also shown is the C-terminal PDZ binding motif, ETQV, and the overlapping site of PKA phosphorylation is arrowed (adapted from Mantovani and Banks, 2001).

The high risk HPV E7 like other oncoproteins encoded by DNA viruses, also associates with and modifies the functions of cellular protein complexes. There are two Cys-X-X-Cys motifs separated by a 29 amino acid spacer in the C-terminus via which E7 dimerizes as a zinc binding protein (McIntyre et al., 1993). E7 protein is a 98 amino acid nuclear protein with casein kinase II phosphorylation sites at serine residues 31 and 32 (Barbosa et al., 1990; Storey et al., 1990). Many of the interactions between E7 and cellular proteins involve the factors that regulate cell growth, especially the transition from the G1 of the mitotic cycle into S phase (Munger & Howley, 2002). The HPV-16 E7 binds to the tumor suppressor retinoblastoma protein (pRb) and other members of the pRb family proteins e.g. p105 and p130; and regulates their phosphorylation state to affect the cell cycle via a region analogous to the conserved region 2 of adenovirus E1A. This is critical for E7-induced cell transformation (Phelps et al., 1992). E7 preferentially interacts with hypophosphorylated pRb, resulting in the cell entering S phase. Hypophosporylated pRb normally represses E2F transcription factors, in G0/G1 phase. The sequestering of pRb by E7 results in stimulation of expression of genes involved in cell cycle progression and DNA synthesis such as DNA polymerase-α and thymidine kinase (Chittende et al., 1991; Martin et al., 1998). The binding between pRb and high risk HPV E7 also induces the destabilisation of pRb via promoting pRb proteolytic degradation, which contributes to HPV E7 induced cellular transformation and cell apoptosis (Jone et al., 1997; Boyer et al., 1996). Low risk HPV E7 binds to pRb with a lower affinity and has less phosphorylation by casein kinase II than high risk HPV E7. Consistent with these differences, low risk HPV E7 is not thought sufficient to transform cells (Gage et al., 1990; Barbosa et al., 1990).

In addition to pRb binding and degradation, like other viral oncoproteins, high risk HPV E7 also targets inhibitors of cyclin-dependent kinase that are critical regulators of cell cycle arrest during keratinocyte differentiation. As previously discussed, HPV must force the host cell to provide

DNA replication components and activities to amplify the viral genome in the absence of normal growth signals. For that, E7 targets cyclinE-cdk2 (which regulates initiation of S phase) and cyclinA-cdk2 (which regulates the progression of S phase) to extend the duration of replicative competence in the host cells. The binding and abrogation of inhibitors such as $p21^{CIP1}$ and $p27^{KIP1}$ by E7 may contribute to maintenance of a replication-competent cellular environment in differentiated epithelial cells (Cheng et al., 1995; Missero et al., 1996; Zerfass-Thome et al., 1996; Jones et al., 1997). $p21^{CIP1/WAF1/SDI1}$ binding with E7 can block the inhibition of both cyclin/cdk activity and PCNA-dependent DNA replication (Funk et al., 1997 Jones et al., 1997); $p27^{KIP1}$ is a regulator of TGF-β induced cell growth inhibition in keratinocytes, its binding with E7 may result releasing from TGF-β-associated growth arrest (Pietenpol et al., 1990).

The E7 protein also recruits histone deacetylases to repress the transcription of E2F factors involved in regulating transcriptional cell cycle progression and/or cellular differentiation (Brehm et al., 1998). Additionally, E7 interacts with members of the AP-1 family of transcription factors, including c-Jun, JunB, JunD and c-Fos, which are found to regulate early mitogenic effects on cell differentiation (Antinore et al., 1996). Finally, E7 targets the interferon-inducible signal cascade by inhibiting the IRF-1 and NFkappaB function and this could lead to the impairment of the IFN response in HPV-infected cells (Perea et al., 2000).

1.4 MAGUK proteins

All the members of membrane-associated guanylate kinase homologue (MAGUK) family are scaffold proteins that recruit different molecular components into localized macromolecular complexes with their protein partners, which are thought to be involved in cell signalling cascades and cell morphology organisation. These proteins are associated with the plasma

membrane typically at cell-cell contact sites in multicellular animals from *Drosophila* to mammals (Dimitratos et al., 1997; 1999). Our current knowledge of MAGUK activity, includes two overlapping functions: 1) to localize, recruit, and organise other proteins at the plasma membrane in order to allow extracellular signals to initiate a response from intracellular signalling transduction pathways; 2) to act as a molecular scaffold or anchoring proteins crucial in controlling cytoarchitecture and maintaining cell junction structure. In some cases, the PDZ domains are even involved in clustering of Shaker-type K^+ ion channels in cell membrane specialization (Kim et al., 1995).

MAGUKs appear to be critical in allowing the efficient transduction of extracellular signals via localised biochemical interaction (Spiro et al., 1999). MAGUK proteins have a multidomain organisation (from N- to C-terminus) including one or three PDZ domains, an SH3 domain and a region homologous to guanylate kinase (GUK). All these domains are involved in protein-protein interactions; in some MAGUKs there is also a HOOK domain and a Lin-7 binding/Veli-binding domain as well as the CaM kinase and calmodulin-binding domains in Lin-2-like MAGUKs. All these motifs can be associated with specific targets (Fanning & Anderson, 1996; Dimitratos et al., 1997). PDZ domains are 80-100 amino acid domains named for their presence in the MAGUK proteins: post-synaptic density protein-95 kDa (PSD-95), the *Drosophila* tumor suppressor Disc-large (Dlg) and ZO-1 (Doyle et al., 1996; Dimitratos et al., 1997) and they are the best characterized protein binding domains in MAGUK proteins. Data from X-ray crystallography and from binding specificity assays using the oriented peptide library technique show that PDZ domains can bind to three different types of targets: 1) to a specific (S/T)-X-(V/I) C-terminus motif, 2) to another PDZ domain, and 3) to an internal target motif (Morais etal., 1996; Songyang et al., 1997; Tsunoda et al., 1997; Shieh & Zhu 1996). GUK domains in MAGUKs, excluding Dlg-like and ZO-1 like proteins, contain a GMP binding site and an ATP

binding site similar in structure and GUK activity to the guanylate kinase that converts GMP to GDP using ATP as the phosphate donor (Dimitratos et al., 1997; Anderson, 1996; Stehle & Schulz, 1990); SH3 domains (src homology 3) have been described in numerous cytoskeletal and signalling proteins, where they mediate direct protein-protein association and direct subcellular localisation and formation of multiprotein complexes. Unfortunately, interactions between the GUK domains of the MAGUKs and other proteins are not well characterised (Mayer, 2001).

1.5 Dlg and hDlg

Several MAGUK proteins are important components of junctional complexes. The Dlg protein is localised in various *Drosophila* epithelia at both smooth and septate junctions. They are specialised apicolateral cell junctions necessary for normal epithelial cell polarity and are considered to be the equivalent of mammalian tight junctions (Hough et al., 1997; Woods et al., 1997). In epithelia, cell proliferation is partly controlled by local cell-cell interactions and lost of hDlg in epithelial cells indicated increased cell proliferation and caused neoplastic growth (Dimitratos et al., 1997). A detailed study of mice transgenic for Dlg protein lacking individual domains (as detailed below) has shown the essential functions of the domains by rescuing of the wild type from the mutant background (Woods et al., 1996; Hough et al., 1997; Lue et al., 1996):

1) Both PDZ_1 and PDZ_2 domains are sufficient for Dlg association with a 30-kDa NH2-terminal domain of the cytoskeleton actin-binding family protein 4.1 that is conserved in ezrin/radixin/moesin (ERM) proteins, although the link between Dlg and the cytoskeleton is not very clear.
2) The PDZ_2 domain is necessary for restricting Dlg membrane localisation to the septate junctions. In its absence the protein is localised over the entire plasma membrane.

3) Both PDZ_2 and PDZ_3 are required for cell proliferation control but not for epithelial structure. In the absence of either domain the protein rescued normal epithelial structure, but the rescued imaginal discs failed to support normal cell proliferation. This confirms that Dlg may have a direct role in proliferation control signalling pathways.
4) The SH3 domain is required for both growth control and maintenance of the epithelial structure.
5) The HOOK domain is essential for Dlg attaching to the plasma membrane and maintaining epithelial structure. In the absence of this domain, the protein is mainly found in the nucleus.
6) The GUK domain is not directly involved in cell proliferation regulation but rather serves for Dlg stabilisation.

Mammalian Dlg family members display similar structural characteristics to *Drosophila* Dlg. Absence of Dlg in *Drosophila* or of mammalian Dlg in neuromuscular junctions indicates that this protein is involved in loss of synaptic bouton integrity (Lahey et al., 1994). Other studies have shown the loss of Dlg can disrupt both microfilaments and the microtubule networks (Woods et al., 1996). Therefore, Dlg plays a vital role in cell junction component organisation and cell-cell interactions. Another MAGUK protein member, ZO-1, which also has a C-terminal proline rich extension is a major component of tight junctions and may be involved in organising these junctions by recruiting a complex with occludin and binding with both actin microfilaments and α-catenin (Haskins et al., 1998; Itoh et al., 1997; Furuse et al., 1994). This suggests that the MAGUK family is closely linked to the recruitment and function of cell junctions. Although most mammalian Dlg homologues were first identified in neuronal tissues, all of these proteins are expressed in a variety of non-neuronal cell types including epithelial cells. In epithelial cells, recruitment of Dlg to cell-cell contact sites is regulated by E-cadherin, furthermore, Dlg binds to E-cadherin and localises together at adherens junctions (Reuver &

Garner, 1998; Ide et al., 1999). hDlg is located at intercellular contact sites in epithelial cells where it can bind to other cellular proteins including adenomatous polyposis coli (APC), a tumour suppressor, involved in the Wnt signalling pathway (Matsumine et al., 1996; Goode and Perrimon, 1997). hDlg like other MAGUKs proteins also contains the protein interaction domains SH3, HOOK, guanylate kinase homologue and three PDZ domains (Matsumine et al., 1996; Marfatia et al., 1996; Craven and Bredt, 1998). The PDZ domains in hDlg have 80-90 amino acids, which bind with high affinity to C- terminal 4-amino acid motifs in partner proteins ending with carboxyl-terminal valine, isoleucine or leucine (V, I or L) (Harris and Lim, 2001). Previous studies have identified several viral oncoproteins including high-risk HPV E6 and Adenovirus 9 E4-ORF1 and the Tax oncoprotein of HTLV-1 (Lee et al., 1997; Suzuki et al., 1999) as proteins that can target hDlg, and in some cases E6 has been shown to target these proteins for proteasome-mediated degradation (Gardiol et al., 1999; Kuhne et al., 2000; Massimi et al., 2004). Therefore, hDlg is proposed to be involved in the oncogenic transformation processes of diverse viruses (Kiyono et al., 1997; Lee et al., 1997). Importantly, only high risk HPV E6 can lead to hDlg degradation, and PDZ binding motifs are only present in high risk HPV E6 (Gardiol et al., 1999). In addition, hDlg degradation is independent of high risk HPV E6 induced p53 degradation, highlighting hDlg as a viral oncoprotein target tumor suppressor for HPV cervical carcinoma pathogenesis (Gardiol et al., 1999). High risk HPV E6 first interacts with the second PDZ domain of hDlg through a consensus PDZ-binding motif (X-S/T-X-V/I) located at the E6 C-terminus, subsequently recruiting endogenous ubiquitin ligase for ubiquitination and degradation of hDlg (Pim et al., 2000). A diagram of this process is shown in Figure (5).

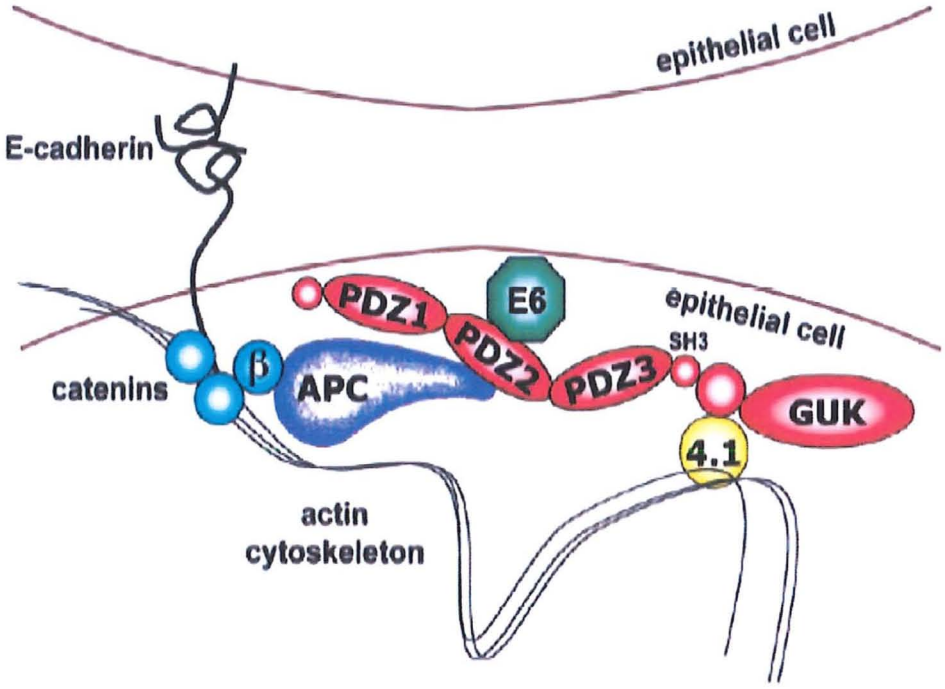

Figure 5: Schematic diagram showing the location of hDlg at the membrane-cytoskeleton interface of epithelial cells at regions of cell-cell contact. Here hDlg co-localizes with E-cadherin and binds the APC tumour suppressor, which in turn regulates β-catenin. The interaction between hDlg and APC is via PDZ domain 2 and this is the same domain targeted by the high risk HPV E6 proteins. Also shown is the interaction with protein 4.1, which connects hDlg to the actin cytoskeleton (adapted from Mantovani and Banks, 2001).

1.5.1 hDlg cellular trafficking and degradation

Previous studies found MAGUKs are associated with the cytoskeleton network. Microtubules were also found binding to PSD-93 *in vivo*, a member of MAGUKs, via its guanylate kinase (GK) domain binding to microtubule-associated protein 1A; GK domain truncations were found to disrupt the GK/MAP-1A interaction in another member of MAGUKs, *Drosophila discs-large* (Dlg) (Brenman et al., 1998; Kloker et al., 2002). Moreover, with its GK domain, hDlg was found binding to GAKIN, a microtubule-interacting protein, in the cytoplasm of human T lymphocytes. The interaction suggested GAKIN acted as a cargo vesicle which facilitated hDlg coupling to the microtubule-based cytoskeleton and was vital for intercellular trafficking of hDlg and its associated protein complexes (Hanada et al., 2000; Asada et al., 2003). The detail of the association between hDlg and the cytoskeleton and trafficking of hDlg to specialized cellular sites are still under investigation.

Besides the association with the microtubule network, hDlg has also shown to be connected with the actin cytoskeleton through binding with hCASK and the 4.1/ERM cytoskeletal proteins to organsize cell membrane junctions and extracellular matrix (Lue et al., 1996; Nix et al., 2000).

Although the details of hDlg degradation are not completely clear at this stage, the discovery of its binding to high risk HPV E6 elucidated an important route for its degradation. Previously, hScribble, a MAGUKs protein family member expressed at epithelial tight junctions, was shown to be a substrate for E6/EAP ubiquitin degradation (Nakagawa and Huibregtse, 2000). hDlg was also recently found to be degraded via the proteasomal pathway, by binding to high risk HPV E6 but independent of E6-AP (Mantovani et al., 2001; Grm and Banks, 2004). It was proposed that the degradation mechanism of hDlg was complicated differed according to various cellular condition. This still has to be further clarified.

1.6 Gap junctions, connexon and connexins

Cells in tissues and organs co-ordinate their activity by communicating directly with each other. Among the various cell contact mediated processes, gap junctions allow direct communication between adjacent cells (Fleming et al., 2000). Gap junctions were firstly defined morphologically as special cell-cell contacts with narrow 2-3nm gaps that allowed direct intercellular exchange of critical regulatory ions and small molecules (e.g Ca^{++}, C-AMP, glutathione), as well as macro-molecular materials of less than 1 kDa (amino acids; sugars, nucleotides, but not nucleic acids), between the opposing cells, providing direct coordination of electrical and metabolic functions, proliferation and differentiation (Cocle and Carfield, 1986; Churchchill and Louis, 1998; Evans and Martin, 2002). For example, the skin has numerous gap junctions involved in the co-ordination of keratinocyte growth and differentiation, whereas the abundance of gap junctions is thought to regulate the recycling of potassium ions during auditory transduction in the sensory inner ear epithelia (Choudhry et al., 1997; Kikuchi et al., 1995). GJIC is found in all multicellular animals (Bargiello et al., 1987; Warner, 1988) and GJIC function is regulated by the number of intercellular channels present in the plasma membrane and the functionally permeable states of the channels.

Gap junction numbers on cell membranes are regulated by several means: 1) connexin gene transcription regulation; 2) gap junction protein amount synthesised in the endoplasmic reticulum; 3) gap junction protein delivery to either the cell membrane or the lysosomes for degradation directly from the trans-Golgi network (Qin et al., 2003); 4) connexins can be endocytosed via clathrin-coated pits; 5) from the endosome, connexins can be either recycled to the cell membrane or diverted to the plasma membrane or to lysosome for targeted degradation. Gap junction channels are typically open at rest and only close under specific circumstances;

however, the gating mechanism of gap junctions is the most complex of any ion channel. The elementary gating of the gap junction channel is controlled by multiple factors including calcium concentration, pH, voltage difference between the cells, phosphorylation of connexin C-terminus and a number of physiological stimuli, typically associated with increased cell division, such as growth factors and oncogenes (Harris, 2001; Lampe and Lau, 2000). The component proteins of gap junctions also have significant impacts on the selective permeability properties of the junctions (Steinberg et al., 1994; Brissette et al., 1994).

Gap junction channels are intercellular structures formed of two "hemi-channels" or connexons. The connexons reside on the plasma membrane of cells and have three conserved cysteines in each extracellular loop to form the intramolecular disulfide bridges, so that connexons can dock end-to-end to another one on the neighbouring cell, forming a continuous aqueous pore through the lipid bilayer. A number of connexons cluster into supramolecular domains forming the familiar gap junction plaques between the adhesive cells (Zampighi et al., 1980; Sikerwar et al., 1981; Kumar and Gilula, 1994). The hexameric connexon is formed by six identical connexins (homologous connexons) or some combination of expressed connexins (hybrid or heterologous connexons) (Rook et al., 1992; Trosko and Ruch, 1998). An image of gap junction intracellular communication structure is shown in Figure (6).

The gap junction proteins, connexins, have a common topology: four hydrophobic transmembrane α helices anchored into the lipid bilayer of the cell membrane; two extracellular loops allowing channels to couple with the opposing connexon; one cytoplasmic loop; and a N- and C-terminal region located on the cytoplasmic membrane face. The connexin sequences are most conserved in the transmembrane and extracellular domains and the key functional differences between connexins are determined by amino acid differences in these domains; while the most sequence variation happens in the cytoplasmic loop and C-terminus (Bruzzone et al.,

1994; White et al., 1995). A schematic diagram of a general connexin is shown in Figure (7). Various functional properties have been assigned to specific linear domains in connexins. Site-directed mutation analyses have shown the second extracellular domain and the middle of cytoplasmic portion are responsible for heterotypic compatibility and facilitating docking between opposing connexins, whereas the first extracellular loop might be part of a voltage sensing mechanism (White et al., 1994; 1995; Bruzzone et al., 1994). The third transmembrane domain is suspected to contribute to the channel wall formation (Unwin, 1989; Rubin et al., 1992). It has been reported that the sequence and the length of the connexin cytoplasmic loop and C-terminus serves as a gating control particle like a "ball and chain" model, where the carboxyl tail swings around to interact with the intracellular loop. This may be critical in regulating connexin chemical gating and pH sensitivity (Anumonwo et al., 2001, Moreno et al., 2002). The deletion of some connexin C-termini seems to have little effect on assembly of gap junctions, yet several residues in most connexin (except connexin 26) C-terminal domains are phosphorylation targets for more than one protein kinase, suggesting connexins could have functions independent of the gap junction exchange channel (Morley et al., 1996; Homma et al., 1998; Kadle et al., 1991; Kanemitus et al., 1997; Martin et al., 2000). Functional studies on connexin carboxyl tails also suggested they can interact with other cell junctional proteins and a number of cytoplasmic partners (Furuse et al., 1993; Singh and Lampe 2003). Finally, the N-terminus behaves as a calmodulin-binding domain and plays an important part in connexin membrane targeting and insertion. Connexin N-terminus also plays an important role in controlling gap junction voltage gating mechanisms (Welsh et al., 1982; Suchyna et al., 1993; Martin et al., 2000). Since the first cloned connexin gene was reported in 1986, 20 mouse and 21 human connexin genes have been identified. Connexins can be divided into three subgroups (α,β and γ) with respect to their extent of sequence identity and length of cytoplasmic loop

(Table 3) (Eiberger et al., 2001; Sohl and Willecke, 2004). Connexin 43 is regarded as the most widely expressed connexin and intensive investigations have been carried out to search for linkages between its mutations/cellular changes and human diseases. Several studies have shown that Connexin 43 is involved in regulating cell proliferation and cell signalling cascades independently of GJIC functions. For example, Connexin 43 can be phosphorylated on tyrosine residues in the C-terminus by Src and this can activate anti-apoptotic progression through the Src/ERK signalling pathway (Plotkin et al., 2002). Connexin 43 also promotes degradation of S phase kinase-associated protein 2 (Skp2), the human F-box protein that regulates the ubiquitination and degradation of p27 (Zhang et al., 2003).

Gap junctions mediate cell coupling in almost all tissues, the size and number of gap junctions per cell depends on the cell cycle and physiological state of the organism/tissue and exposure to various environmental factors. Though evidence shows that expression of a single connexin in one cell is sufficient to establish gap junction intercellular communication, many cells contain more than one type of connexin. The observation of connexin expression in different organs or tissues suggests that the same connexin might be regulated distinctly in different cell types, some connexins are ubiquitously expressed but other connexin expression show restricted expression (Sohl and Willecke, 2004).

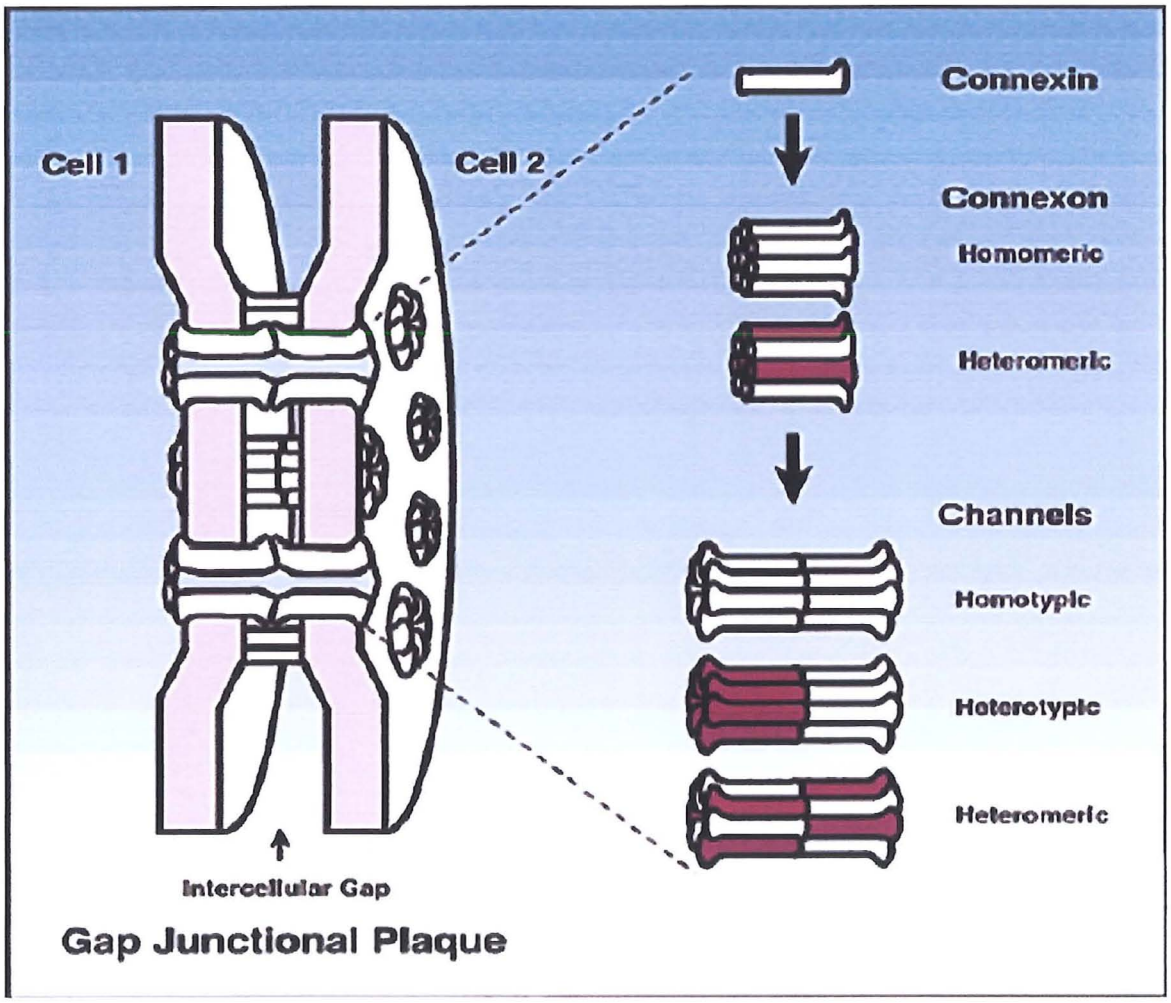

Figure 6: Model of gap junctions, connexons and connexins. Six homomeric/heteromeric types connexin subunits in each plasma membrane dock to generate the gap junction channel connecting two cytoplasmic compartments (adapted from Richard, 2000).

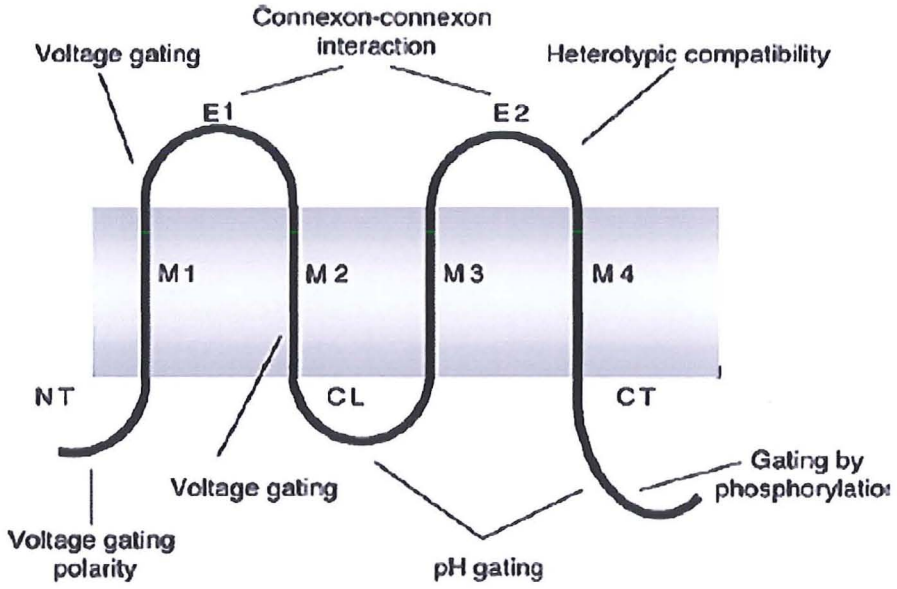

Figure 7: A schematic diagram of a general connexin including the structural motifs and their presumed functions. M1-M4, transmembrane domains 1-4; E1/E2, extracellular domain1 and 2; CL, cytoplasmic loop; NT; amino-terminus; CT, carboxy terminus compartments (adapted from Richard, 2000).

α-Group connexins		β-Group connexins	
mCx30.2	hCx31.9	mCx26	hCx25
mCx33	hCx37	mCx30	hCx26
mCx37	hCx40	mCx30.3	hCx30
mCx40	hCx43	mCx31	hCx30.3
mCx43	hCx46	mCx31.1	hCx31
mCx46	hCx50	mCx32	hCx31.1
mCx50	hCx62		hCx32
mCx57	hCx59		
γ-Group connexins		Non-grouped connexins	
mCx45	hCx45	mCx23	hCx23
mCx47	hCx47	mCx29	hCx30.2
		mCx36	hCx36
		mCx39	hCx40.1

Table 3: The connexin gene family and its subgroup distribution in mouse and human. This table reflects the current state of the sequence information available from the NCBI database (http://www.ncbi.nlm.nih.gov/genomes/static/euk _ g.html).

1.7 Connexin protein-protein interactions

Connexins have been traditionally regarded as simple gap junction channel proteins, but more and more evidence suggests connexins can interact with plasma membrane and cytoplasmic proteins either directly or forming multi-protein complexes to regulate cell structure and/or function (Zimmer et al., 1987; Fu et al., 2004). Such interactions tend to regulate connexin function at several levels, including connexin assembly, trafficking, gating and degradation. Furthermore, these interactions are associated with other cellular mechanisms responsive to stimulation or pathological conditions (Thomas et al., 2002; Moreno et al., 2002). Connexins have similar sequence from the N-terminus to the fourth transmembrane domain but can vary in their carboxyl terminal domains. There are protein-protein interacting motifs in these C-terminal domains which suggests these regions might play an important role in individual connexin gap junction independent functions (Toyofuku et al., 1998; Kausalya et al., 2001). Connexin 43 is the most studied gap junction protein, its C-terminus contains SH2, SH3 and PDZ binding domains that may facilitate the association of Connexin 43 and its binding proteins. A schematic diagram of possible protein interactions between the connexin 43 C-terminal domain and potential partners is shown in Figure (8). It has been shown that via the C-terminal domains, Connexin 43 and other several connexin types can interact with adherens junction-associated proteins, tight junction-associated proteins, cytoskeletal proteins and some protein kinases, including:

- ZO-1, a plasma membrane scaffolding protein belonging to the MAGUK family, which is an actin-binding, signal transduction molecule and cross linking protein that interacts with a large number of proteins involved in cell-cell contact. ZO-1 is specifically enriched at tight junctions of epithelial and endothelial cells (Stevenson et al., 1986). The C-terminal domains

of Connexins 43, 46 and 50 possess similar residues, which interact with the PDZ_2 motif in ZO-1 via its PDZ domain in several cell types and these interactions are regulated by phosphorylation via Src tyrosine kinases (Giepmans et al., 2001; Nielson et al., 2003; Toyofuku et al., 1998). The last four amino acids (DLEI) in the C-terminus of Connexin 43, especially the isoleucine site, were reported to be critical for binding with ZO-1 (Giepmans et al., 2001). The binding of ZO-1 and connexins suggests ZO-1 might serve as a scaffold in gap junction assembly and/or recruiting signal molecules for connexin mediated intracellular singalling.

- At cell contact sites, gap junctions are often seen by electron microscopy very close to adherens junctions (Peters et al., 1994). Functional inhibitors of Cadherin, (e.g.EDTA), can also disrupt gap junctions and inhibit cell coupling. Conversely, inhibition of Connexin 43 also can block adherens junction formation (Meyer et al., 1992; Hertig et al., 1996). In adherens junctions, the cadherin cytoplasmic domain binds to α/β-Catenin (Piepenhagen and Nelson, 1993). Both E-cadherin and α-catenin were found co-localised with connexin 26 and 32 during gap junction formation and β-catenin was co-localised with connexin 43 to form connexin 43/ZO-1/β-catenin complex for connenxin 43 plasma membrane targeting (Fujimoto et al., 1997; Wu et al., 2003).
- Previous work has shown connexin 43 gap junctions in a close association with cytoskeletal proteins. Several studies have shown connexin 43 binds to α- and β-tubulin via its C-terminal domain (Giepmans et al., 2001; Singh and Lampe, 2003). It seems the binding of connexin 43 to tubulin is involved in microtubule stabilisation and regulation of connexin 43 recruitment and distribution; furthermore, disruption of microtubules with nocodazole can inhibit connexin 43 recruitment on plasma membranes in NRK cells (Giepmans et al., 2001;

Guo et al., 2003; Thomas et al., 2001). Connexin 43 was found co-localised with F-actin in rat astrocytes in culture (Yamane et al., 1999); recently, Connexin 43 was found immunuprecipitated and co-localised with the actin-binding protein, drebrin (Butkevich et al., 2004). The authors suggested that the binding might direct connexins into degradative cellular pathways.

- All the known connexins, except Connexin 26 whose C-terminus is quite short, can be phosphorylated at their C-terminal domains (Herve and Sarrouilhe, 2002). Connexin 43 was found to be a substrate for more than 10 different protein kinases at different sites of its C-terminal domain (Herve and Sarrouilhe, 2002). Among them, Src was shown to regulate the interaction of connexin and ZO-1 (Toyofuku et al., 2001); Src phosphorylation on tyrosine residues in the Connexin 43 C-terminus can activate anti-apoptotic progression through the Src/ERK signalling pathway (Plotkin et al., 2002); and Connexin 43 phosphorylation by protein kinase C (PKC) was linked to the cell cycle phases and a reduction in gap junction channel conductance (Lampe et al., 2000; Solan et al., 2003). Phosphorylation of connexin 56 by PKC also caused decreased gap junction communication, whereas Connexin 32 phosphorylation by cAMP-dependent PKA caused improved intercellular communication (Saez et al., 1990; Berthoud et al., 2000).

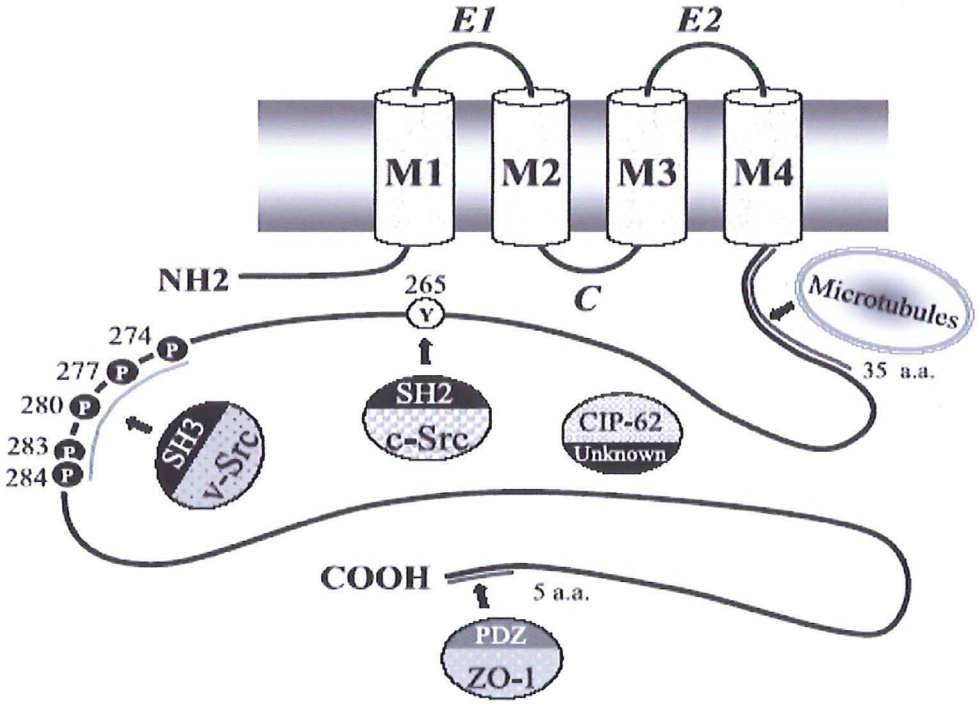

Figure 8: Connexin 43 C-terminal protein binding domains and their potential protein partners (Adapted from Herve et al., 2002).

1.8 Connexin cellular trafficking and degradation

The regulation of connexin assembly, trafficking and turnover may be important in the control of intercellular communication (Lampe et al., 1998; Alford and Rannels, 2001; Paulson et al., 2000). Connexins follow the general secretory pathway for most membrane proteins that are synthesized by membrane-bound ribosomes and delivered by vesicular trafficking from the endoplasmic reticulum via the Golgi apparatus to the cell membrane, although connexins are not glycosylated in the Golgi (Musil and Goodenough, 1993). Trafficking of Connexin 43 among these compartments requires interactions with cytoskeletal elements, the biological mechanism and process of this association is poorly understood.

Actin filaments and/or microtubules, could be involved in a number of aspects of gap junction assembly, such as restricting or facilitating the movements of connexins within the membrane, regulating or directing the transport of connexins from the cytoplasm to the plasma membrane, or affecting the recycling and turnover of connexins. There have been widely varying results in different system from previous studies addressing the relationship between gap junction assembly and actin filaments and/or microtubules (Martin et al., 2001; Johnson et al., 2002; Lauf et al., 2002).

Actin filaments have been observed closely associated with gap junctions although there is no evidence for their direct linkage (Woo-Kuen et al., 1994; Yamane, 1999). However, connexin association with actin-associated cell junction proteins, cadherins and ZO-1, raises the possibility that Connexin 43 can be indirectly linked to a cell surface network that includes actin filaments (Van Vee et al., 2002; Hernandez-Blazquez et al., 2001; Taliana et al., 2005). The role of cytoskeletal actin in gap junction assembly has been studied using cells treated with cytochalasin B to disrupt actin filaments. This has been reported to impair connexin 43 assembly and decrease GJIC (Wang and Rose, 1995; Theiss and Meller, 2002), or elongate gap junction

aggregates and a decrease the formation of plaque areas or not link gap junction assembly (Rassat et al., 1982; Kidder et al., 1987). Based on these varied studies, the precise role of the actin filaments in gap junction dynamics is not clear, particularly with regard to the assembly processes.

Binding studies have suggested there is a direct association between microtubules and Connexin 43 (Giepans et al., 2001; Singh and Lampe, 2003; Paulson et al., 2000; Lauf et al., 2002). Nocodazole, an inhibitor of tublin polymerization, has been employed to examine the mechanism of microtubules in transport of connexin 43. These experiments have shown that abnormal microtubule aggregation is accompanied by impeded translocation of connexin 43 from the cell interior to the plasma membrane, and a clear reduction of plasma-membrane-integrated Connexin 43 at cell contact points (Johnson et al., 2002; Guo et al., 2003; Giessmann et al., 2005). Furthermore, Nocodazole blocks the forskolin-enhanced increase in the expansion of gap junctions on the cell membrane and, in living MDCK cells, reduces the movement of transport intermediates containing green fluorescent protein-tagged connexion 43. Thus, microtubules appear to be necessary for enhanced GJ growth and likely for facilitating connexin trafficking under basal conditions (Jordan et al., 1999; Johnson et al., 2002).

Failure of integral membrane proteins to assemble/associate correctly in the ER/Golgi leads to degradation by either ubiquitin- proteasome or endosome-lysosome degradation system (Hurtley and Helenius, 1989; Arvan et al., 2002). The assembly of connexins into connexons has been reported to occur in the trans-Golgi network, but has been detected in the endoplasmic reticulum-Golgi intermediate subcellular compartments (Diez et al., 1999). Connexin transportation from the plasma membrane to the endosome is supposed to be mediated by the signals present from

connexin cytoplasmic domains like other membrane proteins (Thomas et al., 2003; Segretain et al., 2003).

Connexin 43 composes highly mobile plasma membrane domains with rapid turnover rates ranging in half-life from 1.5–5 h, depending on the cell type studied (Fallon and Goodenough, 1981; Laird et al., 1991; Laird, 1996; Gaietta et al., 2002). Previous work has shown both the lysosome and the ubiquitin-proteasome system to be involved in Connexin 43 degradation (Liang and Beyer, 1995; Laing et al., 1997). Connexin 43 lysosomal turnover seems to be primarily involved in the destruction of internalized gap junctions and degradation of overexpressed protein or even some native Connexin 43 delivered from early secretory compartments (Naus et al., 1993; Jordan et al., 1996; Qin et al., 2003; Leithe and Rivedal, 2004). Connexin 43 proteasomal turnover is mainly required for the degradation of mutant/misfolded Connexin 43 in the endoplasmic reticulum-associated degradation pathway; furthermore, proteasomal activity mostly affects the stability of newly synthesized plasma Connexin 43 (VanSLyke et al., 2000; VanSLyke and Musil, 2002; Leithe and Rivedal, 2004). However, the mechanisms that lead Connexin 43 to one or both degradation pathway is not clear.

1.9 Connexin and diseases

Gap junction deficiency and connexin mutations have been long speculated as being associated with a wide spectrum of human diseases, with clinical and genetic evidence. The relationships between connexins and human genetic diseases/connexin-deficient mouse models are shown in Table (4). Several transgenic and knockout model systems have provided evidence that gap junctions play a vital role in embryonic development. For example, GJIC is linked to chick limb bud patterning and connexin 43 distribution can affect mouse heart myocyte differentiation (Allen et al., 1990; Fromaget et al., 1992). Connexin 32 mutation is associated with a peripheral

neuropathy, X-linked Charcot-Marie-Tooth (CMTX) disease, which is a demyelinating syndrome with a progressive degeneration-induced defect in Schwann cells (Bergoffen et al., 1993; Nelis et al., 1999). In addition, connexin 32 knockout mice are more susceptible to chemically induced liver carcinogenesis (Nelles et al., 1996). As in skin, there are many connexins in the inner ear, and during auditory transduction through the inner ear, gap junctions supposedly precisely regulate ionic flow especially of potassium ions between the contacted sensory cells (Forge et al., 1999). It has been reported that at least five types of connexins, including connexin 26, 30, 31, 32 and 43, are involved in syndromic or nonsyndromic deafness (Kelsell et al., 2001). Connexin 26 is essential for cochlear cell function and survival in the inner ear and mutations in Connexin 26 are leading causes for genetic hearing impairment, while epidemiological trials have proved 50% of inherited asymptomatic sensoneural deafness is linked to connexin 26 mutations (Kelsell et al., 1997; Cohen-Salmon et al., 2002). Mutations of connexin 26 are increasingly found associated with skin development and processes such as skin wound healing and cell differentiation (Rouan et al., 2001; Brandner et al., 2003). Another type of skin disorder termed as erythrorokeratoderma variabilis (EKV) is linked to connexin 31 and 30.3 mutations (Richard et al., 1998; 2003); in the lens, mutations of connexin 46 and 50 are linked to cataract abnormalities (Pal et al., 2000). Connexin 43 mutations are involved with oculodentodigital dysplasia (ODDD), which is a human congenital disease characterised by abnormal face, eye, limb and dentition development (Paznekas et al., 2003). Gap junctions are vital in cardiac development and functions, they mediate electrical impulse spread and actuate synchronous contraction of the cardiac chambers. Connexin 43 is the major connexin expressed in adult mammalian myocardium and essentially responsible for electrical synchrony conduction (Severs, 2001). Furthermore, the connexin 43 deficiency could cause arrhythmic heart failure or dysfunction (Gutstein et al., 2001).

Mouse connexin	Cell and tissues with major expression levels	Phenotype(s) of Cx-deficient mice	Human hereditary disease(s)	Human connexin
	n.s.	n.s.	n.s.	hCx25
mCx26	breast, skin, cochlea, liver, placenta	lethal on ED11	sensorineural hearing loss, palmoplantar hyperkeratosis	hCx26
mCx29	myelinated cells	n.s.	n.s.	hCx30.2
mCx30	skin, brain, cochlea	hearing impairment	nonsyndromic hearing loss, hydrotic ectodermal dysplasia hair loss, nail defects and often mental deficiency	hCx30
mCx30.2	n.s.	n.s.	n.s.	hCx31.9
mCx30.3	skin	n.s.	erythrokeratoderma variabilis	hCx30.3
mCx31	skin, cochlea uterus, placenta	transient placental dysmorphogenesis	hearing impairment, erythrokeratoderma variabilis	hCx31
mCx31.1	skin	n.s.	n.s.	hCx31.1
mCx32	liver, Schwann cells, oligodendrocytes	decreased glycogen degradation, increased liver carcinogenesis	CMTX, (one of the hereditary peripheral neuropathies)	hCx32
mCx33	testis	n.s.		
mCx36	neurons retina	visual deficits	n.s.	hCx36
mCx37	endothelium, ovaries	female sterility, intensive bleeding	n.s.	hCx37
mCx39	n.s.	n.s.	n.s.	hCx40.1
mCx40	heart, endothelium	atrial arrhythmia	n.s.	hCx40
mCx43	many cell types and tissues	heart malformation and ventricular arrhythmia	visceroatrial heteroataxia?	hCx43
mCx45	heart, endothelia, neurons	lethal on ED 10.5	n.s.	hCx45
mCx46	lens	zonular nuclear cataract	congenital cataract	hCx46
mCx47	brain, spinal cord	n.s.	n.s.	hCx47
mCx50	lens	microphthalmia, zonular pulverulant and congenital cataract	zonular pulverulant cataract	hCx50
	n.s.	n.s.	n.s.	hCx59
mCx57	ovaries	n.s.	n.s.	hCx62

n.s. not studied. ED, embryonic days.

Table 4: Human inherited diseases associated with various connenxin mutations and the phenotypes in mouse models linked to connexin knock-outs (adapted from Evans and Martin, 2002).

1.10 Connexins and cancer

The hypothesis that gap junctional intercellular communication is involved in cancer progression arose from the observation that some types of cancer cells did not communicate through gap junctions (Loewenstein and Kanno, 1966; Kanno and Matsui, 1968). It seemed reduced gap junctional intercellular communication might be a general characteristic of cancer cells associated with uncontrolled cell growth (Loewenstein, 1979). It was postulated that lack of gap junctions (or lack of function) could prevent cell-to-cell diffusion of regulatory molecules or ions that was a prerequisite to cell growth control regulation (Loewenstein, 1979). A body of evidence has accumulated to show that GJIC may be lost during malignant progression, eg: HPV-positive cervical cancer (McNutt et al., 1971; Krutovskikh and Yamasaki, 1997; King et al., 2000; Aasen et al., 2003). Connexin 43, the most widespread connexin and a major component of gap junctions in stratified epithelia, has been seen to be down-regulated in epithelial carcinoma cells (Carystinos et al., 2001; Naus, 2002). Interestingly, several studies reported contradictory upregulation of gap junction in some cancer cells. For example: Connexin 26 is often upregulated in psoriatic epidermis and viral warts (Lucke et al., 1999). At least four different types of solid tumors were well coupled (Sheridan, 1970) and a rat bladder carcinoma cell line exhibited a better intercellular communication than their normal counterparts (Asamoto et al., 1994).

The PKC activators, phorbol esters, which are tumor promoters, are powerful gap junction intercellular communication inhibitors in various cultured cell lines, suggesting that inhibition of gap junctions is a prerequisite for cancer expansion (Kwak et al., 1995; Wagner et al., 2002). From then on, many accumulated data has shown most tumor promoters and oncogenes (such as ras, raf, src et al.) can inhibit gap junction intercellular communication in human or animal cell

lines at subtoxic doses (Beer et al., 1988; Budunova and Williams, 1994; Rivedal et al., 1996). Further evidence with specific connexin antibodies has shown in transformed cells, some tumor promoter agents not only decrease gap junction communication but also relocate connexins into cytoplasmic compartments (Bager et al., 1994; Krutovskikh et al., 1995), which suggests the cytoplasmic aberrant connexin was significantly associated with reduced gap junctions communication and increased cell hyperproliferation. Although there is no direct proof authenticating the lack of gap junctional intercellular communication as the cause of cell hyproliferation, it seems to favour cancer cell clonal expansion (Mesnil and Yamasaki, 1993). *In vitro* transformed fibroblast and epithelial cells either lack gap junction intercellular communication completely or are still able to communicate among themselves but are blocked from communication with surrounding normal counterparts (Enomoto and Yamasaki, 1984; Mehta et al., 1986). This supports the hypotheses that loss of gap junctions has a role in cancer progression. It is important to note in some transformed cases the molecular processes affecting cell coupling are different in human and in rat. For example, Connexin 32 is relocated in cytoplasmic compartments in human liver tumors, but it is completely deleted in rat liver tumors (Fitzgerald et al., 1989; Krutovskikh et al., 1994); while certain cancer cells still able to communicate through gap junctions despite their malignancy, show enhanced tumorigenicity after gap junctional intercellular communication abrogation which occurred in rat bladder squamous cell carcinoma cells (Asamoto et al., 1998). These accumulated data suggest that although aberrant cell coupling is an extensive phenotype in a wide range of transformed cells independent of original tissues, organs and species, the situation is much more complex than suspected and dependent on the individual characteristic of the original cells and tissue. Since many transformed/tumorigenic cells have been reported to exhibit reduction of gap junctional intercellular communication, it is interesting to investigate whether restoration of gap junction

capacity could normalize or delay the tumorigenicity in these cells. Some known antineoplastic agents such as retinoids, vitamin D and cAMP were found to upregulate gap junctional intercellular communication (Trosko and Chang, 2001). More importantly, *in vitro* and *in vivo* evidence has shown that transformed or tumorigenic cell lines transfected with wild type connexin cDNAs such as Connexin 43 and 26, which are normally expressed in cells from the originating tissue, have proportionally decreased cell proliferation, restored cell differentiation, induced cell apoptosis, and gap junction intercellular communication (Yamasaki et al., 1999; Mao et al., 2000; Tanaka and Grossman, 2001). However, it was reported that Connexin 43-transfected HeLa cells decrease invasive properties (Graeber and Hulser, 1998). These data suggest connexins might act as tumor suppressors affecting some cancer cells from certain types of tissue. So far, the role of gap junction intercellular communication and connexins in cell carcinogenesis is still unclear and under investigation.

1.11 Connexins and HPV associated Carcinogenesis

It was found that the number of gap junctions was decreased correlating with the severity of the morphological alteration in the dysplastic cervical epithelium and gap junction deficiency could occur during the development of HPV positive cervical malignant carcinomas (McNutt and Weinstein, 1969; McNutt et al., 1971). During malignant progression in HPV positive cervical carcinogenesis, cancer cells only arise from limited individual colonies of the HPV-infected immortal cells. Consequently, it was proposed that there are several important molecular and cellular changes other than inhibition of p53 and pRb participating in HPV-associated cancer progression. Gap junctional intercellular communication is abrogated in high-risk HPV-associated cancer cells such as HeLa. It was reported that gap junctional intercellular communication is reduced in HPV-16 transformed rat myoblasts although these cells are not

normal a target for HPV infection (Ennaji et al., 1995). BPV E5 was found to interact with 16kDa ductin/subunit c and was deemed responsible for the down-regulation of gap junction intercellular communication and the inhibition of acidification of endomembranes (Campo, 2002). HPV-16 E5 was suggested to reduce cell coupling in transfected HaCaT cells (Oelze et al., 1995). Connexin 43 which is the most common type in epithelia was found decreased in cervical dysplasia (King et al., 2000). Recently, our group demonstrated that Connexin 43 is relocated from the membrane to the cytoplasm in a novel HPV-16-containing cervical epithelial cell line that is fully transformed and invasive and deficient in gap junction intercellular communication, in contrast to the parental cell line in which connexin 43 localises to cell junctions, providing extensive gap junction intercellular communication (Aasen et al., 2003). HPV16 is the cause of over 60% of human cervical cancers. The high-risk HPV E6 proteins are found localized largely in the nucleus but also appear in the cytoplasm and HPV E6 is known to interact with several cytoplasmic proteins which could affect connexin assembly in the cytoplasm or gap junction targeting to the cell membrane which is believed to play a role during the initiation phase of invasion of cervical tumors. These results suggested that loss of gap junction intercellular communication may occur in a gradual fashion at a relatively late HPV-16 associated cervical carcinogenesis stage. The exact role of connexins and gap junction intercellular communication in HPV-associated carcinogenesis is yet to be investigated.

1.12 Project aim

The overall aims of this project were:

1) to identify gap junction related gene expression changes from immortal to invasive stage during the progression of HPV-16 positive cervical carcinogenesis;

2) to identify the relationship between the most common gap junction protein, Connexin 43, and hDlg, a tumor suppressor in MAGUK protein gamily;
3) investigation of the contribution of high risk HPV to loss of gap junction intercellular communication;
4) to investigate the mechanism of transporting and degradation of Connexin 43 in HPV positive cervical cancer.

Chapter 2: MATERIALS AND METHODS

2.1 Materials

2.1.1 Plasmids

p3XFLAG-CMV™-10 Expression Vector (E4401): For stable, cytoplasmic expression of N-terminal Met-3XFLAG fusion proteins. Stable expression is accomplished by neomycin selection (G 418 sulfate), ampicillin resistant.

p3XFLAG-CMV™-14 Expression Vector (E4901): For stable, cytoplasmic expression of C-terminal 3XFLAG fusion proteins. Stable expression was accomplished by neomycin selection (G 418 sulfate), ampicillin resistant.

Both of the plasmids were purchased from Sigma-Aldrich Company Ltd, UK. Map in Appendix 1&2.

2.1.2 Enzymes and kits

All the restriction enzymes and CIP were purchased from New England Biolabs, UK. Pfu polymerase, Taq polymerase, dNTPs, RNasin and RNase-free DNase 1 were purchased from Promega, UK. T4 DNA ligase, Oligo $dT_{(12\text{-}18)}$ primer and RNase H was purchased from Invitrogen, UK.

RNeasy mini kit and QIAquick gel extraction kit were purchased from Qiagen Ltd, UK. Superscript™ II Reverse Transcriptase Kit was purchased from Invitrogen, UK. Wizard Plus SV Minipreps DNA isolation system was purchased from Promega, UK.

2.1.3 Cell culture reagents

Dulbecco's modified Eagle's medium (DMEM), fetal calf serum (FCS), L-glutamine and trypsin were purchased from Gibco BRL, UK. Keratinocyte growth medium (KGM) was purchased from Cambrex Bio Science Walkesville Inc, UK.

LipofectamineTM was purchased from Invitrogen, UK. G418, ALLN, MG 132, Phalloidin-TRITC and Leptomycin B were purchased from Sigma-Aldrich Company Ltd, UK. All the cell culture plastics were purchased from Corning Inc., UK; or Nunc A/S, UK.

2.1.4 Common chemicals and buffers

All the chemicals were purchased from Sigma Chemical Co. or BDH Chemicals, UK except the following:

- 25nM $MgCl_2$, 10X PCR buffer, and1kb DNA ladder purchased from Promega, UK.
- Protein A-Sepharose beads, the Rainbow marker, ECL Western blotting reagents and Hybond-P nitrocellulose membrane purchased from Amersham Biosciences Ltd, UK.
- Agarose MP, protein inhibitor cocktail tablets, and ampicillin sodium BP purchased from Roche, UK.
- X-Omat film purchased from Kodak, UK.
- Formaldehyde, formamide from Fluka, UK.
- 30% Acrylamide, glacial acetic acid, Butan-2-ol, glycerol and isopropanol from Prolab, UK.

All the buffers were prepared following the comments in Table (5).

Table 5: Buffer comments.

Solution	Comment
5X agarose gel loading buffer	1xTAE, 1% SDS (w/v), 50% glycerol (v/v), 0.1 mg/ml bromophenol blue
citrate buffer	(prepared just prior to retrieving paraffin section antigen with the pressure cooker) mixed 18ml of solution A (9.6g citric acid in 500ml distilled water) with 82ml of solution B (14.7g Tris-Sodium-Citrate in 500ml distilled water) and made up to 1000ml.
Coomassie stain solution	0.02% (w/v) Coomassie Brilliant Blue^{TM}, 50% (v/v) methanol, 7% (v/v) acetic acid
Diethyl Pyrocarbonate (DEPC) treated dH_2O	200µl DEPC incubated with 500ml distilled water overnight at room temperature and autoclaved to inactivate DEPC
Destain	5% (v/v) methanol, 10% (v/v) acetic acid
Fix solution	20% sucrose (w/v), 5% formaldehyde (v/v) in PBS
IP buffer	1% Triton X-100, 0.5% CHAPS, 0.1% SDS with 15% fresh protein inhibitor cocktail (Roche, UK) in PBS
PBS	170mM NaCl, 3.4mM KCl, 10mM Na_2HPO_4, 1.8mM KH_2PO_4, pH7.2
PBS-Tween	PBS containing 0.05% (v/v) Tween 20
permeability solution	70% (v/v) acetone, 30% methanol (v/v)

7X protease inhibitor cocktail	one tablet dissolved in 1.5ml distilled water
2X protein loading buffer	125 mM Tris (pH 6.8), 4% SDS, 20% glycerol, 10% mercaptoethanol and 0.006% bromophenol blue, 15% (v/v) fresh protein inhibitor cocktail (Roche, UK)
10X SDS page running buffer	500mM Tris base, 500mM glycine, 1% SDS (w/v)
50X TAE	0.2M Tris base, 0.05 M EDTA (pH 8.0)
10X TBE	890mM TRIS, 890mM boric acid, 10mM EDTA
TE buffer	10mM Tris-HCl (pH 8.0), 1mM EDTA
Trypsin	0.25% (w/v) trypsin in Tris-saline containing phenol red, adjusted to pH 7.5 with $NaHCO_3$
Versene	0.6mM EDTA in PBS, 0.002% phenol red
Western blotting transfer buffer	25mM Tris base, 192mM glycine, 20% methanol (v/v)
Western blotting stripping buffer	0.288mM β-Mercaptoethanol, 2% v/v SDS, 62.5mM Tris pH 6.8

2.1.5 Antibodies

Table 6: List of antibodies, sources and dilutions.

Antibodies	*Antibody type*	*Catalogue or clone no.*	*Western blotting dilution*	*IFA dilution*	*Sources*
β-catenin	M AM	610156	1:100	1:100	Transduction Laboratories
E-cadherin	M AH	G-10	1:100	1:100	Santa Cruz Biot.
Cx26	M AM	138100	_	1:500	Zymed, UK
Cx26	R AR	71-0500	_	1:500	Zymed, UK
Cx30	R AM	71-2200	_	1:500	Zymed, UK
Cx43	R AH	from αα 363-382	1:1000	1:1000	gift from Dr E. Rivedal, Norway
Cx43	M AR	13-8300	_	1:500	Zymed, UK
Flag	R AR	F7425	1:320	1:160	Sigma, UK
GAPDH	M AH	H86540M	1:1000	_	Biodesign International
hDlg	M AH	sc9961	1:400	1:25	Santa Cruz Biot.
HPV-16 E6	R AG	sc1583	1:200	1:100	Santa Cruz Biot.
HPV-16 E7	M	ED17	1:100	_	Santa Cruz Biot.
involucrin	M	SY5	1:1000	1:1000	Sigma, UK
Ki-67	M AH	MIB-1	1:100	1:100	DAKO, UK
p53	M AH	_	1:1000	_	gift from Prof R White

pRb	R AR	_	1:1000	_	gift from Prof R White
tubulin	M AR	MCA77G	_	1:200	Serotec Ltd, UK
ZO-1	R AH	61-7300	1:250	1:100	Zymed, UK
Anti-mouse	FITC	FI2000	_	1:100	vector labs, UK
Ig	TexasRed	TI2000	_	1:100	vector labs, UK
	HRP		1:1000	_	Diagnostic Scot
Anti-goat Ig	FITC	F1763	_	1:100	Sigma, UK
Anti-rabbit Ig	FITC	FI1000	_	1:100	vector labs, UK
	TexasRed	TI1000	_	1:100	vector labs, UK
	HRP		1:1000	_	Diagnostic Scot
Anti-EEA1	M	Ab15846	_	1:500	Abcam Ltd.
Anti-EEA1	R AR	Ab2900	_	1: 250	Abcam Ltd.
Anti-MPR	M	Ab 2733		1:500	Abcam Ltd.
Anti-MPR	R AP	Ab16417		1:200	Abcam Ltd.
Anti-Golgi	R AR	GM130	_	1:400	Gift from Dr. Xiaohong Shi

- M, mouse monoclonal; R, rabbit polyclonal; AM, anti-mouse; AG, anti-goat; AH, anti-human; AR, anti-rat.

2.1.6 Cell lines

HaCaT – HPV negative spontaneously immortalized aneuploid human keratinocyte cell line (Boukamp et al., 1998)

W12 – HPV 16 positive but non-malignant cervical epithelial cell line developed from a low-grade lesion (Stanley et al., 1989)

W12E - Subclone from parental W12 cell line harbouring extrachromosomal copies of HPV 16, known as 20863 (Jeon et al., 1995).

W12G - Subclone from parental W12 cell line harbouring integrated copies of HPV 16, known as 20861 (Jeon et al., 1995).

W12GPX - Feeder-independent subclone established from W12G cell (Aasen et al., 2003)

W12GPXY - Feeder and mitogen-independent malignant subclone established from W12GPX cell, (Aasen et al., 2003)

W12GPXY$_{Wcx43}$ - W12GPXY cells stably transfected with the pC-terminus 3XFLAG-fused wild-type human Connexin 43 plasmid (original from p3X FLAG-CMVTM-14 plasmid) during this study.

W12GPXY$_{Tcx43}$ - W12GPXY cells stably transfected with the pC-terminus 3XFLAG-fused last 5 amino acids truncated human Connexin 43 plasmid (original from p3X FLAG-CMVTM-14 plasmid) during this study.

CaSki – HPV 16 positive cervical cancer cell line derived from cervical squamous cell carcinoma harbouring ~600 integrated viral copies (Pattillo et al., 1997).

C33a – HPV negative but p53 mutated cervical carcinoma cell line (Crook et al., 1991).

C33a$_{WHPV18E6}$ - C33a cells stably transfected with the pN-terminus 3XFLAG-fused HPV18 wild E6 plasmid (original from p3X FLAG-CMVTM-10 plasmid) during this study.

C33a$_{MHPV18E6}$ - C33a cells stably transfected with the pN-terminus 3XFLAG-fused Thr156Glu mutant HPV18 E6 plasmid (original from p3X FLAG-CMVTM-10 plasmid) during this study.

HBF - Human breast primary fibroblasts cells from reduction tissue.

2.2 Methods

2.2.1 Small scale preparation of plasmid DNA (mini-preps)

The small-scale extraction of plasmid DNA was prepared from the bacterial culture using Wizard Plus SV Minipreps DNA isolation system (A1330, Promega) following the manufacturer's protocol. Single colonies of transformed bacteria were dipped into 5 ml of L-broth containing 100μg/ml ampicillin and incubated with shaking overnight at 37 °C. Overnight-cultured bacteria were centrifuged to pellet at 14000 rpm for 4 minutes. The supernatant was removed and the pellet was resuspended in 250 μl of cell resuspension solution and gently mixed with 250 μl lysis buffer. 10μl alkaline protease solution was added and the mixture was incubated for 5 minutes at room temperature; sbsequently, 350 μl of neutralization solution was added to the lysate and centrifuged to remove the cell debris at 14000 rpm for minutes at room temperature. The supernatant containing the plasmid DNA was transferred into a spin column and centrifuged at 14000 rpm 1 minutes followed with two washes with the Wash Solution. The column was then

centrifuged at 14000 rpm for 2 minutes and the DNA eluted with 50 µl of TE buffer and centrifuged for 1 minute.

2.2.2 Large scale preparation of plasmid DNA (maxi-prep)

CsCl gradient was used to obtain a preparation of large scale of plasmid DNA. 500 ml of overnight bacteria culture containing 100µg/ml ampicillin was pelleted by centrifuging at 8000 rpm for 10 minutes at 4 °C and the pellet was thoroughly resuspended in 10 ml solution I (0.5 M TriHCl pH 8.0, 10 mM EDTA, 1 mg lysozyme). The cells were lysed by swirling with 20 ml fresh solution II (1% SDS, 0.2N NaOH) and incubated at room temperature for 10 minutes; 15 ml of ice cold solution III (3M potassium acetate, 11.5% acetic acid) was added and inverted and incubated on ice for 15 minutes to precipitate the protein complexes. The solution was centrifuged at 8000 rpm for 10 minutes at 4 °C and the supernatant was filtered into a fresh tube through gauze, then 26 ml of isopropanol was added to the filtrate and the mixture was incubated at room temperature for 10 minutes. The samples were centrifuged at 8000 rpm for 15 minutes at room temperature and the supernatant was decanted; the DNA pellet was air dried and resuspended in 5 ml of TE buffer, 5.4 g caesium chloride and 400 µl ethidium chloride (10mg/ml). The solution was centrifuged under vacuum at 48000 rpm for 16 hours at 4 °C. Following the centrifugation, the DNA/ethidium chloride band was extracted using a syringe with needle, the ethidium chloride was removed from DNA by repeated extraction with butan-2-ol. The plasmid DNA was finally collected with ethanol precipitation and resuspended in TE buffer.

2.2.3 Phenol:chloroform extraction

To purify the bulk nucleic acids solution, an equal volume of a 25:24:1 mixture of phenol:chloroform:isoamyl alcohol was added, mixed vigorously and centrifuged at 14000rpm for 5 minutes. The aqueous layer was transferred to a new tube and mixed with an equal volume of 24:1 chloroform:isoamyl alcohol and centrifuged as before. Finally, the aqueous layer was removed to another new tube and concentrated with ethanol precipitation.

2.2.4 Ethanol precipitation

Nucleic acids were precipitated by adding 2.5 volumes v/v ice-cold 100% ethanol and1/10 volume 3M sodium acetate, and incubated at -20 °C for 30~60 minutes, after which the the precipitated nucleic acids were collected by centrifugation at 1400rpm for 10 minutes. The pellet was washed with 70% ethanol and centrifuged at 14000rpm for a further 5 minutes, and the pellet was then air-dried and resuspended in 10-50 μl TE buffer.

2.2.5 DNA Agarose gel electrophoresis and recovery

Agarose gel electrophoresis was used for the separation, size determination and relative quantitation of DNA fragments. 1% (w/v) analytical grade agarose was heated up with 1× TBE/1xTAE buffer in a microwave until all the agarose was dissolved and poured onto the gel support tray at about 60°C. The gel with an inserted comb was left to solidify, the comb was removed and the gel placed in the electrophoresis tank with enough buffer covering the gel surface. A 10 μl aliquot of each DNA sample was pipetted with 2.5 μl 6x DNA loading buffer into the wells along with the appropriate DNA molecular weight marker. After the electrophoresis was carried out at 80~100 volts

for 1 hour, the gel was stained in ethidium bromide solution (1 μg/ml) and examined on a UV transilluminator, and photographs were taken with an Ultra Violet Products Gel Sytem, Image Store 7500. Agarose slices containing appropriate DNA fragments were excised with a scalpel from gels under long-wave UV transillumination and DNA was extracted and purified with a QIAquick gel extraction kit (28704, Qiagen) following the manufacturer's instruction. Briefly, the excised gel (no more than 400 mg) was mixed with 3 volumes (v/w) Buffer QG and incubated at 50°C for 10 minutes, then 1volume of isopropanol was added to the mixture. The solution was applied to the QIAquick column and centrifuged for 1 minute at 8000rpm, then DNA was washed with 0.75 ml Buffer PE and centrifuged for 1 minute at 14000rpm. The column underwent additional centrifugation for 1 minute and the DNA was eluted by adding 50 μl TE buffer and collected after 1 minute's incubation.

2.2.6 DNA restriction enzyme digestion and linearised plasmid DNA dephosphorylation

Restriction enzymes are sequence-specific endonucleases that cut DNA at specific sites. The digestion was assembled to 20/50 μl containing 400-600 ng DNA and 10 units of restriction digest enzyme per μg of DNA in 1x enzyme-special buffer. The reaction was incubated at 37°C (or the temperature specified by the supplier) for 2-3 hours or overnight and agarose gel loading buffer was added prior to electrophoresis; the second digestion was carried out following the first digestion, DNA purified by phenol choroform extraction and ethanol precipitation. To prevent self-ligation of the digested plasmid, the DNA was treated with calf intestinal phosphatase (CIP) to remove the phosphate group from the 5' terminus. The total 50 μl reaction contains digested DNA

and 1 unit of CIP per 5 µl of DNA in 1x CIP buffer, and the reaction was incubated at 37 °C for 30 minutes. The linearised, dephosphorylated DNA was then purified by phenol choroform extraction and ethanol precipitation.

2.2.7 PCR mediated site-directed mutagenesis and recombinant DNA

The human connexin 43 cDNA was cloned in to plasmid pcDNA3 and this plasmid (kindly provided by Dr D. Laird) was used as the template for PCR-mediated site-directed mutagenesis. The PCR primer sets:

Forward primers: 5'-CGACTCACTATAGGGAGACC-3'

Reverse primers: 5'-GGTCTGCTGCTGGCACGA-3'

were used to generate a mutant human connexin 43 cDNA fragment, in which the last five amino acids of the C-terminus are deleted. The PCR reactions were carried out with pfu DNA polymerase (M7741, Promega) to reduce reading error probability and followed the product protocol with annealing at 62°C. The PCR was set up in 50 µl volume containing: 1 µl pcDNA-Cx43 plasmid (~0.3 ng), 0.5µl pfu polymerase (M7741, Promega), 5 µl pfu PCR buffer, and 1µl 10 mM dNTPs. The PCR reaction was carried out under the following conditions: denatured the DNA at 95 °C for 3 minutes, and then thermal cycled at 94 °C for 30 seconds (strand separation), 62 °C for 45 seconds (primer annealing) and 72 °C for 30 seconds (strand elongation) for 30 cycles before another 72 °C for 10 minutes for a final extend step and then hold at 4 °C. The PCR mutant connexin 43 and the wild type connexin 43 fragment (isolated by digestion of pcDNA3-Cx43 with Hind III and Bam HI) were subcloned into the EcoR V/Hind III and Bam HI sites of p3X FLAG-CMVTM-14 expression vector plasmid (E4901, Sigma) to generate the pC-terminus 3XFLAG fused wild human Connexin 43 (pCFWCx43) and pC-

terminus 3X FLAG fused with truncated human Connexin 43 (pCFTCx43). The recombined plasmids were sequenced to confirm correct introduction of the desired mutation.

The HPV18 E6 wild type gene and E6 Thr156Glu mutation gene were cloned into pcDNA-3 plasmid by Dr Lawrence Bank's group and kindly provided by Dr Sally Roberts. The plasmids were sequentially digested with EcoRI and HindIII, then purified with phenol:chloroform extraction and ethanol precipitation. The vector p3x-FLAG-CMV^{TM}-10 expression plasmid (E4401, Sigma) was cut with EcoRI and HindIII and ligated to the wild and mutant HPV18 E6 DNA fragments. The constructs were transformed into DH5α and the positive colonies were selected and mini-preped to confirm the sequences.

2.2.8 DNA ligation

Digested and purified vector and insert DNA fragments were ligated in a 1:3 molar ratio. Reaction was carried out in 20 µl volume containing 1 unit of T4 ligase and total DNA 0.05-0.5 µg in 1x ligase reaction buffer, and the reaction incubated at 14 °C overnight before transformation of competent *E.coli*. All the recombinant DNA was sequenced (Glasgow University Molecular Biology Support Unit).

2.2.9 Competent *E.coli* preparation

To prepare the competent bacteria, a 1 ml overnight cultured *E.coli* strain DH5α was incubated into 100 ml L-Broth (10g NaCl, 16g Bactopeptone, 5g yeast extract in 1 liter water, pH7.5). The cells were grown for 3-4 hours at 37 °C in a shaking incubator until the OD_{550} was approximately 0.6. The culture was chilled on ice for 15-30 minutes and collected by centrifugation at 3000*g* for 15 minutes at 4°C. The cells were then

resuspended in 25 ml ice-cold 0.1 M $CaCl_2$ and incubated on ice for 45 minutes. The cells were then pelleted and resuspended with 10 ml ice-cold 0.1 M $CaCl_2$ and chilled on ice for 30 minutes followed by centrifugation. The pellet was resuspended in 3 ml of ice cold 0.1 M $CaCl_2$ and 15 % glycerol, then aliquoted and stored at -70°C until use.

2.2.10 Plasmid transformation and bacteria selection

For each transformation, 100 µl of competent DH5α cells was thawed on ice and approximately 15 ng of plasmid DNA was added and mixed gently and incubated together on ice for 30 minutes. The mixture was heat shocked by incubating at 42°C for 45 seconds and chilled on ice for 2 minute. 1 ml L-Broth was added to the cells which were incubated in a 37°C shaker for 1 hour. After the incubation, the cells were spun down and plated onto LB plate containing 100 µg/ml ampicillin which were then incubated at 37°C overnight. Colonies were picked with a sterile toothpick and placed in 5 ml L-Broth containing 100 µg/ml ampicillin and incubated in a 37 °C shaker overnight.

2.2.11 Quantification of oligonucleotides

The spectrophotometer (Eppendorf BioPhotometer) was used to determine the oligonucleotide concentrations by measuring the absorbance at 260 nm. Double-stranded DNA: 1 A_{260} equals 50 µg/ml.

Single-stranded DNA: 1 A_{260} equals 30 µg/ml.

RNA: 1 A_{260} equals 40 µg/ml.

The purity of oligonucleotides was determined by comparing readings at 260 nm and 280 nm (A_{260} and A_{280}), assuming a ratio of no less than 1.80 indicating the samples were protein free.

2.2.12 RNA isolation

Total RNA was extracted from $8x10^7$ cells using an RNeasy mini kit (74119, Qiagen), as specified by the manufacturer's instruction. The pelleted cells were lysed and homogenised in 4 ml of RLT Buffer by passing the lysate through an 18-20-gauge needle fitted to an RNase-free syringe several times. 4 ml of 70% ethanol was added to the sample and the mixture was transferred to an RNase mini spin column where total RNA binds selectively to the silica-based membrane. After 5 minutes centrifugation at 8000rpm, 4 ml of RW1 Buffer to the column and repeated the centrifugation, washed the column with 2.5 ml Buffer RPE twice and spun as previously described. The RNA was eluted in 50 µl RNase-free water and collected by centrifuging into a RNase-free tube and stored in -20 °C. The whole process was RNase protected and all the materials were DEPC-treated before used.

2.2.13 RT-PCR

For RT-PCR, the total RNA extract was treated with Rnase-free DNase to remove any potential contamination. 1 µg RNA was resuspended in 1X DNase I Reaction Buffer to a final volume of 20 µl and 1 units of DNase I (M0303S, New England Biolab) was added, mixed thoroughly and incubated at 37°C for 10 minutes. 0.2 µl of 0.5 M EDTA (to a final concentration of 5 mM) was added and heated inactivated at 75°C for 10 minutes. The reaction was diluted to 100 µl, stored at -70°C and used directly for RT-PCR.

RT-PCR was performed using Superscript™ II Reverse Transcriptase Kit (18064-022, Invitrogen) and followed the manufacturer's protocol. A 12 µl reaction containing 2.5 µg total RNA, 1 µl $Oligo(dT)_{12-18}$ (500 µg/ml) (18418-012, Invitrogen), 1 µl dNTP mix (10 mM each) and DEPC-treated water was heated at 65°C for 5 minutes and quick chilled

on ice. This solution was mixed with 4 µl 5x First-Strand Buffer, 2 µl 0.1 M DTT and 1µl RNasin® Plus RNase Inhibitor (N2661, Promega) and incubated at 42°C for 2 minutes. 1 µl Superscript™ II RT was added and the reaction was incubated at 42 °C for 50 minutes; then heating at 70°C for 15 minutes inactivated the reaction. To remove RNA complementary to the cDNA, 2 unit of RNase H (18021-014, Invitrogen) was added and incubated at 37°C for 20 minutes. cDNA was stored at 4°C. The PCR reaction was carried out with a final volume of 50 µl containing 2 units of Taq DNA polymerase (M1661, Promega), 2 µl dNTP mix (10 mM each), 3 µl of 25 mM $MgCl_2$, 1 µl of 10 µM of each primers, 5 µl of *Taq* DNA Polymerase Buffer and 1 µl cDNA as template. The PCR cycle was started with a hot start (3 minutes at 95°C in which the DNA Polymerase was added, followed by 2 minutes at 72°C), and then consisted of 30 cycles of denaturation at 94°C for 30 seconds, annealing at different temperature dependent on the different DNA primers for 45 seconds and elongation at 72°C for 30 seconds. The PCR was completed with a final extension at 72 °C for 10 minutes and held at 4°C. The product was checked after separation on a 1% agarose gel with ethidium bromide under the UV illumination.

2.2.14 Cell culture

W12GPXY, C33a, HaCaT, CaSki, HBF and J2 3T3 cells were cultured in Dulbecco's modified Eagle's medium (DMEM) supplemented with 10% FCS and L-glutamine (2mM); W12E, W12G and W12GPX cells were cultured in serum-free keratinocyte growth medium (KGM) (cc-3101, Cambrex). All cells were maintained under humidified 5% CO_2 95% air at 37°C and the medium changed every 3 days.

2.2.15 Preparation of cell stocks

After trypsinisation and counting, the confluent cells were resuspended in the appropriate growth medium at $1x10^6$ cells/ml with 15% DMSO in final concentration. 1 ml of cell suspension was aliquoted in vials and frozen at -70°C for 24 hours before transferred to in liquid nitrogen.

2.2.16 Total cell extract preparation

Confluent monolayer cells were washed with PBS twice and lysed in protein-loading buffer, 100µl /125 mm^2 on ice. The cell lysate was passed through a 18-20-gauge needle 8-10 times to shear the chromosomal DNA and collected in Eppendorf vials. The extract was boiled for 5 minutes and chilled on ice before centrifugation to pellet the cell debris. The cell lysate protein concentration was determined by the Bradford assay, and subsequently stored in -20°C.

2.2.17 SDS page

Proteins were separated on a vertical Polyacrylamide gel prepared with the Bio-Rad mini gel electrophoresis apparatus. The resolving gel and stacking gel (described as Table 7) were poured into the system and set one by one following the manufacturer's protocol. The gel assembly was submerged in 1x Tris-Glycrine buffer and 30 µl of each protein samples was loaded into the wells with 5 µl RainbowTM protein marker (RPN 756, Amersham Pharmacia biotech) in the first lane. The gel was run at 100 V until the dye front reached the end of the resolving gel.

2.2.18 Western blotting

Separated proteins were subsequently transferred to a nitrocellulose membrane (Hybond-P, Amersham Biotech) using a Bio-Rad transblot cell, following the manufacturer's

instructions. The process was carried out at 250 mA for 2 hours or 30 mA overnight at 4°C in Western blotting transfer buffer. The transferred membrane was preincubated for 1 hour at room temperature with 5% dried milk in PBS-0.1%Tween, before overnight incubation at 4°C with diluted primary antibody in PBS-Tween 1% dried milk on a rotating shaker. After 3x10 minute PBS-Tween washes, horseradish peroxidase (HRP)-conjugated secondary antibodies were diluted 1 : 1000 in PBS-Tween and incubated for 1 hour. The PBS-Tween washes were repeated 5 times and the membrane was developed with 1:1 mixture of the two supplied reagents of Amersham enhanced chemiluminescence (ECL) (RPN 2209, Amersham Biotech) kit for 1 minute and exposed to Kodak X-OMAT film. Bound antibodies were removed from the membranes by shaking the developed membrane in stripping buffer (0.288mM β-Mercaptoethanol, 2% v/v SDS, 62.5mM Tris pH 6.8) at 50°C for 30 minutes followed by 3x10 minutes PBS-Tween washes. The stripped membranes were stored at 4°C or reprobed with other antibodies.

Table 7: SDS-PAGE gel composition.

	12% Resolving gel	**15% Resolving gel**	**Stacking gel**
30% acrylamide	4.0 ml	5.0 ml	650µl
1.5M Tris pH8.8	2.5 ml	2.5 ml	-
1M Tris pH6.8	-	-	2.5 ml
10% SDS (w/v)	100 µl	100 µl	50 µl
10% APS* (w/v)	100 µl	100 µl	50 µl
TEMED	20 µl	20 µl	10 µl
dH_2O	3.3 ml	2.3 ml	3 ml

2.2.19 Co-immunoprecipitation

Confluent cells were washed twice with ice-cold PBS and scraped into 5 ml chilled IP buffer containing PBS, 1% Triton X-100, 0.5% CHAPS, 0.1% SDS with 15 % fresh protein inhibitor cocktail (Roche, UK). The cell lysates were incubated on ice for 15 minutes and the solutions sonicated for 1 minute on ice. Cell lysates were then cleared of cellular debris by centrifugation at 12000g for 10 minutes at 4 °C and the protein concentration determined by Bradford's assay. Primary antibodies were added to 100µg protein of each cell lysate and incubated for 2 hours at 4°C under agitation. Subsequently 40µg of reconstituted protein A-Sepharose was added (Amersham Biosciences, Inc) and the volume adjusted to 750µl. The samples were agitated at 4 °C for 4-5 hours. Immunocomplexes were then harvested by centrifugation and washed four times with 250µl ice-cold IP buffer and once with 25µl ice cold PBS. Proteins were solubilized by sonicating the complexes in PBS mixed with 5µl 6x protein loading buffer (1x buffer: 125 mM Tris (pH 6.8), 4% SDS, 20% glycerol, 10% mercaptoethanol and 0.006% bromophenol blue, 15% (v/v) fresh protein inhibitor cocktail (Roche, UK)) for 5 minutes on ice and separated by SDS-PAGE.

2.2.20 Transfection of cells

$1.5x10^5$ cells were seeded in 35mm petri dishes in 2 ml appropriate medium and incubated at 37°C until the cells were 80% confluent. The following solutions were prepared for each transfection: Solution A, 2 µg DNA diluted in 100 µl serum-free medium; Solution B, 3 µl LipofectamineTM (18324-012, Invitrogen) reagent diluted in 100 µl serum-free medium. Two solutions were combined and incubated at room temperature for 30 minutes to allow the DNA-liposome complexes to form. For each

transfection, cells were rinsed with 2 ml of serum-free medium and 800 µl of serum-free medium was added to the DNA-liposome mix which was applied to the pre-rinsed cells. Following 5 hours incubation at 37°C, 1ml of 20% FCS medium was added and the cells were incubated for 18 hours and then replaced with 2 ml fresh medium. After 72 hours transfection, stable transfected cells were selected in medium supplemented with 500 µg/ml G418 (A1720, Sigma) to obtain stably transfected cell lines.

2.2.21 Iontophoresis (cell microinjection)

90% confluent monolayer cells were washed twice with PBS and maintained in it before the iontophoresis. 4% Lucifer Yellow, a negatively charged fluorescent gap junction-permeable dye, was microinjected into the focalised cell with a freshly prepared fine glass capillary using 0.5 second pulses of 10nA at 10 Hz for 2 minutes. The injected cell was left for 1 minute, and the extent of cell coupling was measured by counting the number of cells that had clearly taken up Lucifer Yellow. Pictures were taken using a digital camera. The whole process was carried out under an Inverted UV fluorescence microscope in the dark.

2.2.22 Growth assay in vitro

$1x10^5$ cells were seeded in 35mm culture dishes and maintained in appropriate medium for 48 hours. Cells from three dishes were independently trypsinized and counted (Coulter counter) at selected intervals.

2.2.23 Organotypic raft culture

The *in vitro* living skin model system consisted of two components: a dermal equivalent made up of fibroblasts in a collagen matrix that is contracted and modified by the resident cells, and an epidermis that develops from keratinocytes "plated" on the dermal

equivalent. Type I collagen is extracted from rat tail tendons in 0.5 M acetic acid, precipitated by the addition of an equal volume of 10% w/v NaCl, redissolved in 0.25M acetic acid and extensively dialysed against 1/1000 acetic acid, with the final solution being adjusted to 2.5mg collagen/ml and stored at 4°C. The preparation of the dermal equivalent was carried out at 4°C and all the solutions were pre-chilled on ice. Collagen gel was prepared by mixing 8 volumes of collagen solution with 1 volume of 10x MEM, and 1 volume of 0.22 M NaOH, and the pH adjusted to 7.2 with NaOH. 1 volume of FCS containing$7.5x10^5$ human breast skin fibroblast/ml mixture was added and the gel was mixed thoroughly. The mixed gel was aliquoted as 3ml/dish into 35mm petri dish and allowed to set at 37°C for 15 minuets, after which 2 ml of DMEM containing 10% FCS was added and the gels detached from the dishes. The gels were incubated for approximately 10 days at 37°C in a humidified atmosphere of 5% CO_2 in air with medium changed every 2 days until the gels were contracted to fit 24 well multiwell dishes. The gels were transferred into the 24 well dishes and seeded $1x10^4$ cells seeded on the top of each gel and incubated for 24-48 hours until the cells on gel top were confluent. The gels were raised to the air-liquid interface on a stainless steel grid and incubated for 8-12 days with medium changes daily. The gels were harvested and fixed in 4% (v/PBS) formaldehyde overnight before being embedded into paraffin sets. 4μm sections were cut with Leitz 1501 rotary microtome and floated on a water bath at 45°C, lifted and fixed onto glass slides, and dried completely on a hot plate.

2.2.24 Haematoxylin and Eosin (H&E) stain

The slides with dried sections were incubated at 80°C for 1 hour and allowed to cool. The sections were deparaffinised and hydrated through a gradient of xylene for 5 minutes twice, absolute alcohol for 4 minutes twice and water 1 minute. The sections were stained with the following steps: immersed in haematoxylin for 4 minutes and washed in water, dipped in acid alcohol 5-10 second and rinsed with water, developed in Scott's Tap Water for 45 seconds and washed with water, stained in Putt's eosin for 5 minutes and washed in water to remove any remaining stain. The sections were dehydrated sequentially in alcohol for 4 minutes (2 change, 2 minutes each), and in xylene for 2 minutes (2 change, 1 minutes each). Finally the dried slides were fixed with Pertex mounting solution (CellPath, UK) using a coverslip. Pictures were taken with a Zeiss Axiovert S100 microscope.

2.2.25 Immunofluorescence staining of organotypic raft culture sections

The 4 μm paraffin-embedded sections were de-waxed and hydrated as described above. To retrieve antigen, the rehydrated sections were put into a pressure cooker, immersed in boiling citrate buffer, and microwaved at high power for 15 minutes, and left to cool for 20 minutes. The slides were rinsed with PBS for 5 minutes twice prior to incubation with PBS containing 20% FCS for 1 hour. The blocking solution was removed and then the sections were incubated with appropriate primary antibodies in PBS containing 1% FCS, 0.1% Tween, 1% BSA and 0.01% SDS (BSA and SDS only present for connexin stain) at 4°C in a humidified atmosphere overnight. The sections were washed with PBS 3x10 minutes and incubated with anti-mouse-fluorescein and anti-rabbit-texas-red-labelled secondary antibodies diluted 1:100 in PBS containing 1% FCS in a dark humidified box

for 1 hour. The slides were washed 4x10 minutes with PBS and mounted with Vectashield mounting medium with DAPI and finally a coverslip was fixed using nail varnish. Negative controls (no primary antibody) were included in all experiments. Images were taken using a Zeiss LSM510 Meta confocal microscope.

2.2.26 Immunofluorescence stain

Cell were grown on sterile 18 x 18 mm coverslips until 90% confluent, washed three times with PBS and fixed with Fix Solution (20% sucrose, 5% formaldehyde in PBS) for 10 minutes at room temperature. After three washes with PBS, the coverslips were permeabilised with 0.5 ml of a 70% acetone, 30% methanol solution for 5 minutes at -20 °C. The coverslips were washed three times with PBS and incubated in PBS containing 20% normal goat serum and/or 20% normal horse serum for 1 h at room temperature. Cells were incubated with primary antibodies diluted in 1% goat serum and horse serum in PBS for 1 hour at room temperature. Coverslips were washed in PBS six times before incubation for 1 hour with secondary antibodies labelled with fluorescein or Texas-Red diluted 1:100 in PBS (Vector laboratories). After washing in PBS six times, the coverslips were mounted with Vectashield mounting medium (with DAPI or propidium iodide as a nuclear stain). Negative controls (no primary antibody) were included in all experiments. Images were taken using a Zeiss LSM510 Meta confocal microscope.

2.2.27 Affymetrix arrays

A goal of this project was to generate a list of candidate genes, which were involved in the progression to late stage carcinogenesis in HPV 16 positive cervical cancer cell lines; and the gap junction-related proteins changes during this process.

In this study, Two-GeneChip®-array sets from Affymetrix (HG-U133) were used which created the selected sequence clusters from GenBank®, dbEST, and RefSeq and contained 22,283 (Chip A) and 22,645 (Chip B) probe sets derived from approximately 33,000 well-substantiated human genes. Affymetrix arrays are proprietary, based on direct photolithographic deposition of oligo probes on silicon wafers, which can give very reproducible results with high quality total RNA. In this array procedure, the biological noise was be accounted for with statistics using replicates of the conditions and the technical noise was modeled by the same research group in the same environment. Reproducibility of the chip set was examined by repeated tests on the same sample. The two duplicate chip sets (from two different manufacture lots) were tested on the same sample 6 months apart. All the array procedures were carried out following the manufacture's protocols.

The prepared total RNA samples stored at -70°C once extracted (described in 2.2.12) were submitted to the Sir Henry Wellcome Functional Genomics Facility, Glasgow University, who organized the whole experiment. The RNA quality and quantity at this stage are detected using the following machines: NanoDrop ND-1000 (NanoDrop Technologies) for quantity and the BioAnalyzer (Agilent) for quality control.

Briefly, following the recommendations from the manufacturers for each reaction, 10 μg total RNA was used to generate double-stranded cDNA by synthesising the first strands with T7-linked oligo$(dT)_{24}$ primers and Superscript II RT following the second strands synthesis. The double strand cDNA library was cleaned up according the protocol using the cDNA Cleanup spin column and cDNA Wash Buffer. The final labelling of the cRNA *in vitro* transcribed was performed with biotinyl-11-CTP and 16-UTP

ribonucleotides using Enzo HighYield RNA Transcript Labeling Kit (Enzo Diagnostics) at 37°C for 6 hours and purified using Qiagen Rneasy mini columns. Before hybridization with the U133 array chips, the labelled cRNAs were fragmented (10 to 11 μg/probe array) and maintained in a final hybridisation cocktail concentrated at 0.8 μg/μl. Hybridizations were preformed to the GeneChip set at 45°C for 16 hours in a rotisserie oven set at 60 r.p.m. The cRNA samples were first hybridized to Affymetrix Test 3 arrays for quality control and subsequently to Affymetrix Human Genome U133 A and B arrays. Finally, the fragmented cRNAs are hybridized to the GeneChip set by way of multiple 20 to 25 oligonucleotide probes specific for each gene, with each probe corresponding to a different region of the mRNA of interest. The probes specific for each mRNA are scattered across the surface of each GeneChip to control for technical issues that occur in each hybridization.

Following hybridization, the chips were washed and stained using Affymetrix fluidics stations. Staining was performed using streptavidin-phycoerythrin conjugate (Molecular Probes, Eugene, OR), followed by the addition of biotinylated antibody to streptavidin (Vector Laboratories) and finally with streptavidin-phycoerythrin conjugate. Probe arrays were scanned using the Affymetrix GeneArray Scanner at 488 nm and 3 μm per pixel. The scanned images were inspected and analyzed using established quality control measures.

2.2.28 Microarray data analysis

A fully automated analysis of Affymetrix GeneChips® is provided by the bioinformatics unit of MBSU in Glasgow University, which includes the raw data analysis, comparative data analysis and data automated annotation by iterative group analysis (iGA).

Raw data consists of files generated by the Affymetrix scanner and image-processing software: the image files (DAT) were converted to (CEL) files containing single intensity values for every probe (probe-level raw data). The files have then been taken for further analysis in three steps:

1. Low-level data normalization was done using the Robust Multichip Average (RMA) method implemented in the statistical analysis of Affymetrix oligonucleotide array probe level data included in the Bioconductor microarray analysis software (http://www.bioconductor.org). RMA performs the following operations (Irizarry et al., 2003):
    - Probe-specific background correction to compensate for nonspecific binding using perfect match distribution rather than perfect match-mismatch probe values
    - Probe-level multichip quantile normalization to unify perfect match distributions across all chips
    - Robust probe-set summary of the log-normalized probe-level data by median polishing
2. To identify differentially expressed genes in W12G and W12GPXY cells, RankProducts (RP) (Breitling et al., 2004), a method developed in the University of Glasgow, sorts all the genes according to their expression changes and provides statistical confidence levels. The value of Fold change and False Discover Rate (parameter like *p*-value in this programme) in the microarray result Table 8. was derived from RP analysis.

3. IterativeGroupAnalysis (iGA) is a method for automated functional interpretation to identify differentially expressed functional gene-classes (Breitling et al., 2004). All the genes shown in the microarray result Table 8 which have significantly changed between W12G and W12GPXY cells were nominated with the iGA programme and sorted in functional groups. iGA is based on using elementary statistics to identify those functional classes of genes that are significantly changed in an experiment and at the same time determines which of the class members are most likely to be differentially expressed. iGA assigns each gene to functional classes, e.g. based on its GeneOntology assignments. Whether the functional class was nominated was determined with the probability of change (PC-value). The PC-values, number of group members and of significantly changed genes are indicated. All genes are sorted according to metrics of differential expression (fold-change, *t*-statistics...), the choice of the optimal sorting method will depend on personal preferences and details of the experimental design, but has relatively little influence on the iGA results. The classes with the lowest PC-value are most significantly changed. As the PC-values are directly derived from *p*-values, they already give a good idea of the statistical significance of an observed change, after correcting for the effect of multiple testing, i.e. the fact that many hundreds of groups are tested for differential expression at the same time. At the same time, the PC-values are underestimating the true probability of changes, because they are based on determining the minimum *p*-value within each class. iGA yields a robust biological summary of transcriptional changes between W12G and W12GPXY

cells. The significance threshold for differentially expressed gene-groups in HG-U133A chips was set at with P-value changed more than 2.4e-0.4 and the threshold value in HG-U133B chips was 4.1e-0.4. In this thesis, all the individual genes nominated with iGA were sorted in functional groups although some of their false discovery rates were high.

2.2.29 Real-time reverse transcription polymerase chain reaction

Over recent years the employment of the method "real-time" reverse transcription polymerase chain reaction (RT-PCR) equipment has been widely used for the analyses of gene expression in a number of systems (Dhar et al., 2001; 2002; Hiratsuka et al., 2001). The objective of this study was to confirm the angiogenesis factors mRNA expression changes suggested from microarray analysis with SYBR Green RT-PCR using the GeneAmp 5700 Sequence Detection system. In contrast to other methods such as Northern hybridization, real-time RT-PCR is a technique with higher throughput and more quantitative capabilities. In quantitative RT-PCR, housekeeping genes are active references that are used to standardize between amounts of samples assayed. Glyceraldehyde-3-phosphate dehydrogenase (GAPDH) was used as housekeeping genes for studies involving mRNA measurements in this case.

Real-time PCR quantitative value was monitored with fluorescence after each of the repetitive cycles during the whole PCR process, which is especially sensitive during the early phase of the reaction. SYBR Green dye has a high affinity for double-stranded DNA (dsDNA) and exhibits enhancement of fluorescence upon binding to the dsDNA. The fluorescence spectrum resulted from the incorporation of SYBR Green I dye into the double-stranded DNA directly produced in PCR tubes during the PCR reaction, and

emission data were quantitated using the threshold cycle (C_T) value. In the GeneAmp® 5700 Sequence Detection System, the fluorescence of the SYBR Green dye is monitored at the end of the each cycle and C_T readings obtained represent measurements on the log scale. A melting point dissociation curve generated by the instrument was used to confirm that only a single product was present (Ririe et al., 1997). The major shortcoming of using SYBR Green in real time PCR is the dye can bind to all the double –stranded DNA which could leads to a false reading with undesired PCR products. To overcome this problem, it is vital to ensure that only one product is synthesised and no primer-dimer formed. To validate the specificity of a primer set, RNA (1 μg) and the RT negative were analyzed in triplicate to confirm that there was no fluorescence resulting from either genomic DNA contamination or from the RT step. Each PCR run also included triplicate wells of no template control (NTC) where RNase-free water was added to reaction wells (PE Biosystem GeneAmp® 5700 User Manual, 1998). The PCR products were collected and run on a 3% (w/v) agarose /TAE gel to confirm only one product size around 105 bp).

2.2.30 Primer design

The specific primers used for SYBR Green PCR are listed in Table (8). The primers were first designed using Primer Express Software version 1.0 (PE Applied Biosystems) on sequences attained from GenBank and primers were purchased from Sigma (Sigma Genosys, U.K). All primers were checked by running a virtual PCR, and the amplifications were analyzed for expected product.

Gene	Primer name	SYBR Green primer sequence (5'-3')	T_m[a] °C	Amplification size (bp)
VEGF	VEGF-For	AGAGCGGAGAAAGCATTTGTTT	58	106
	VEGF-Re	GCAACGCGAGTGTGTGTTTT	58	
FGF-2	FGF-2-For	CCAGGTAACGGTTAGCACACACT	59	108
	FGF-2-Re	CGACCCTCACATCAAGCTACAA	59	
IL8	IL8-For	TTCTTTAGCACTCCTTGGCAAAA	59	106
	IL8-Re	CTCTTGGCAGCCTTCCTGATT	59	
VPF	VPF-For	GGTGAGGTTTGATCCGCATAA	59	105
	VPF-Re	ACGAGGGCCTGGAGTGTGT	59	
GAPDH	GAPDH-For	CCCACAGCCTTGGCAG	59	102
	GAPDH-Re	ACCACAGTCCATGCCATCAC	59	

Table 8: Detail of the primers used for detection of angiogenesis factor genes by SYBR Green RT-PCR.

2.2.31 SYBR real- time quantitative PCR

SYBR Green PCR amplifications were performed in a GeneAmp 9600 thermocycler coupled with a GeneAmp 5700 sequence detection system (PE Applied Biosystems). The reactions were carried out in a 96-well plate in a 25-μl reaction volume containing 12.5 μl of 2×SYBR Green Master Mix (PE Applied Biosystems), 0.75 μl of 10 pmol/μl of both forward and reverse primers and 1 μl of different concentration total cellular cDNA. The thermal amplification and detection were performed using the GeneAmp 5700 system with the following profile: 1 cycle of 50°C for 2 minutes, 1 cycle of 95°C for 10 minutes, and 40 cycles each of 95°C for 15 s, 60°C for 1 minutes, and finally stored at 4°C. For determining the gene expression quantitative change between W12G and W12GPXY cells, the amounts of cDNA of W12GPXY cells used per SYBR Green PCR varied from 1.0 ng to 1.0 pg respectively. In each 96-well plate, a dilution series of the samples was run along with the control samples for the corresponding background and their GAPDH controls. Each sample was replicated two to three times.

2.2.32 Real time quantitative RT-PCR Pilot study

After SYBR Green PCR amplification, data acquisition and subsequent data analyses were performed using the GeneAmp 5700 sequence detection system (version 1.3). In the SYBR Green Master Mix, there is an internal passive dye, ROX, in addition to the SYBR Green dye. The increase in the fluorescence of SYBR Green against that of ROX is measured at the end of each cycle. A sample is considered positive when the change in the fluorescence of SYBR Green relative to that of ROX (ΔR_n) exceeds an arbitrary threshold value. The threshold value is set at the midpoint of the ΔR_n and the cycle number plot. For all the described amplifications, the threshold value of the ΔR_n was

considered to be between 0.1-0.3. The PCR cycle at which a statistically significant increase in the ΔR_n is first detected is called the threshold cycle (C_T). For data analyses, the C_T values were exported into a Microsoft Excel Worksheet for further statistical analyses. Regression analyses of the C_T values of cDNA dilution series were used to examine the amplification efficiencies of the genes.

Chapter 3. RESULTS 1

GLOBAL GENE EXPRESSION CHANGES DURING PROGRESSION OF HPV-16 CARCINOGENESIS

One goal of this project was to investigate gene expression changes during the progression of HPV-16 positive cervical carcinogenesis progression by comparing W12G and W12GPXY cell lines.

In the cervix, early squamous cell carcinoma lesions are characterised as cervical intraepithelial neoplasia (CIN), graded from CINI (mild dysplasia) to CINIII (carcinoma in situ). In 1989, Stanley et al. established the W12 cell line from an HPV 16 positive cervical CINI epithelial biopsy. In these cells, the viral DNA is stably maintained as around 100 extrachromosomal episomal copies (Stanley et al., 1989). In W12G cells, derived from W12 cells, HPV-16 DNA has integrated into the host cell chromosome in about 30 HPV-16 copies, but only E6 and E7 viral protein expression is detected. In W12G cells, the viral genomes are integrated as whole HPV 16 genome disrupted in the E2 open reading frame, which is quite similar to the integration in the HPV-16 positive cervical cancer cell line CaSki (Jeon et al., 1995). Although there are fewer HPV-16 copies in W12 G cells, the oncoproteins E6 and E7 are still expressed at higher levels than in any HPV-16 episomal containing cell population (Jeon and Lambert., 1995). However, W12G cells are still capable of undergoing terminal differentiation and are unable to form colonies in soft agar in spite of the increased viral oncoprotein expression and cellular growth advantage (Jeon et al., 1995).

As previously reported, W12GPXY cells were developed from W12 G cells without feeder-layer and growth factor support, and form malignant tumours in nude mice, although they did not form colonies in soft agar (Aasen et al., 2003). Giemsa staining

had shown in W12GPXY cells several chromosomal changes including ring-chromosome formation (Aasen, 2003).

3.1 Global mRNA expression changes between W12G and W12GPXY cells

3.1.1 Microarray analysis

From 1994, DNA microarrays have been utilized as a powerful tool in biomedical research as they can be used to determine the relative expression profiles of thousands of genes in given samples to predict genetic predisposition to disease, serve as a set of diagnostic markers, define better drug treatment options for existing diseases (pharmacogenomics), or mark the precise nature of disease progression.

To understand more about gene expression changes involved in late stages of HPV-16 positive cervical carcinogenesis progression, Affymetrix human array HG-U133 chips were used to compare mRNA transcription levels between W12G and W12GPXY cells; each sample group including three individual mRNA extracts, i.e. three mRNA preparations from three cell cultures; and the whole experiment was repeated.

After microarray analysis and hierarchical clustering, there were a total of 63 functional genes nominated by iterative Group Analysis (iGA) (see page 88-89), whose transcription expression values differed significantly between W12G and W12GPXY cells and these genes were sorted in different cell function groups with PC-value thresholds (see page 88). Among these genes, 26 were more highly expressed in W12G cells and 37 were more highly expressed in W12GPXY cells. Most of the genes are functionally related to cell growth regulation, cell and tissue metabolism regulation, and to vascular angiogenesis promotion. The results are presented in Table 9.

Table 9: microarray report comparing expressed functional genes in W12G and W12GPXY cells

- Genes more highly expressed in W12G cells are shown in red and genes more highly expressed in W12GPXY cells in green.
- False Discovery Rate shows the expected percentage of false positives when the differentially expressed gene-list was cut at the particular position associated threshold. Although some of genes in the table have high false discovery rate, it is still worth to present their transcription changes, especially those nominated in gene function groups.

Gene title	Gene symbol	Gene function	Fold change	False discovery rate
Cell cycle regulator				
cyclin-dependent kinase inhibitor 1C (p57, Kip2)	CDKN1C	G1 phase of mitotic cell cycle, cyclin-dependent protein kinase inhibitor activity, regulation of cyclin dependent protein kinase activity	29.71	0.00
insulin-like growth factor binding protein 3	IGFBP3	positive regulation of myoblast differentiation, negative regulation of signal transduction, positive regulation of apoptosis, insulin-like growth factor binding, protein tyrosine phosphatase activator activity	211.83	0.00
interleukin 8	IL8	regulation of retroviral genome replication, interleukin-8 receptor binding, chemokine activity, neutrophil activation, neutrophil chemotaxis, induction of positive chemotaxis, angiogenesis	127.87	0.00
Inhibin, beta A (activin A, activin AB alpha polypeptide)	INHBA	transforming growth factor beta receptor binding, activin inhibitor activity, negative regulation of follicle-stimulating hormone secretion	31.31	0.02
met proto-oncogene (hepatocyte growth factor receptor)	MET	hepatocyte growth factor receptor activity	6.90	0.81
interleukin 6 signal transducer (gp130, oncostatin M receptor)	IL6ST	oncostatin-M receptor activity	2.36	12.55
CDC42 effector protein (Rho GTPase binding) 3	CDC42 (EP3)	cytoskeletal regulatory protein binding	5.67	1.23
poliovirus receptor-related 2 (herpesvirus entry mediator B)	PVRL2	15026 - coreceptor activity	7.34	0.22
neuregulin 1	NRG1	receptor tyrosine kinase binding, transmembrane receptor protein tyrosine kinase activator activity	5.88	0.00
serine (or cysteine) proteinase inhibitor, plasminogen activator, urokinase	SERPIN B2	plasminogen activator activity	35.57	0.00

follistatin	FST	activin inhibitor activity, negative regulation of follicle-stimulating hormone secretion	53.03	0.00
transforming growth factor, alpha	TGFA	epidermal growth factor receptor activating ligand activity	6.88	0.77
jagged 1 (Alagille syndrome	JAG1	endothelial cell differentiation	6.19	0.95
parathyroid hormone-like hormone	PTHLH	cAMP metabolism	14.25	0.13
protein tyrosine phosphatase, dual specificity phosphatase 4	PTPRZ1	protein tyrosine/threonine phosphatase activity	21.74	0.04
cyclin-dependent kinase 6	CDK6	G1 phase of mitotic cell cycle, cytokinesis, regulation of cell cycle	18.39	0.00
plasminogen activator, urokinase receptor	PLAUR	U-plasminogen activator receptor activity	30.64	0.02
interleukin 1, beta	IL1B	interleukin-1 receptor binding	39.22	0.00
diphtheria toxin receptor (heparin-binding epidermal growth factor-like growth factor	DTR	epidermal growth factor receptor binding	30.06	0.02
chemokine (C-X-C motif) ligand 1	CXCL1	chemokine activity	21.81	0.04
Cell structure				
collagen, type VII, alpha 1 (epidermolysis bullosa, dystrophic, dominant and recessive)	COL7A1	collagen type VII	11.23	0.05
voltage-dependent anion channel	VDAC	voltage-dependent anion channel porin activity	2.57	8.45
TBC1 domain family, member 10	TBC1D10	microvillus	7.24	0.11
phytoceramidase, alkaline	PHCA	hydrolase activity, acting on carbon-nitrogen (but not peptide) bonds, in linear amides, ceramide metabolism, Golgi membrane, endoplasmic reticulum membrane	15.59	0.00
laminin	LAMC2	laminin-5	19.75	0.03
collagen, type XII, alpha 1	COL12A1	collagen fibril organization, collagen type XII, extracellular matrix structural constituent conferring tensile strength, skeletal development	30.46	0.00
microfibrillar associated protein 5	MFAP5	Microfibril	606.35	0.00
matrix metalloproteinase 10	MMP10	collagen catabolism	370.63	0.00
matrix metalloproteinase 1	MMP1	collagen catabolism	644.45	0.00
a disintegrin-like and metalloprotease (reprolysin type) with	ADAMTS1	extracellular matrix (sensu Metazoa), heparin binding	37.30	0.00

thrombospondin type 1 motif, 1				
histone 1	HIST1H1C	DNA topology	35.34	0.00
Cell metabolism				
emopamil binding protein (sterol isomerase)	EBP	cholestenol delta-isomerase activity, drug transporter activity, steroid delta-isomerase activity	62.42	0.00
nicotinamide N-methyltransferase	NNMT	nicotinamide N-methyltransferase activity	37.11	0.00
solute carrier family 2 (facilitated glucose/fructose transporter), member 5	SLC2A5	fructose transport	15.20	0.04
squalene epoxidase	SQLE	squalene monooxygenase activity, sterol biosynthesis	6.71	0.33
UDP glycosyltransferase 1 family, polypeptide A	UGT1	bilirubin conjugation, estrogen metabolism, UDP-glycosyltransferase activity	3.60	2.59
fatty acid desaturase 1, Sterol-C5-desaturase (ERG3 delta-5-desaturase homolog, fungal)-like	FADS1	C-5 sterol desaturase activity, sterol biosynthesis	3.30	3.47
ubiquinol-cytochrome c reductase core protein, binding protein	UQCRC	oxidative phosphorylation	5.38	0.64
protein-L-isoaspartate (D-aspartate) O-methyltransferase	PCMT1	protein repair	4.24	1.49
FK506 binding protein 5	FKBP5	FK506 binding, peptidyl-prolyl cis-trans isomerase activity, isomerase activity	107.38	0.00
hydroxyacyl-Coenzyme A dehydrogenase/3-ketoacyl-Coenzyme A thiolase/enoyl-Coenzyme A hydratase (trifunctional protein), alpha subunit	ACT-1	acetyl-CoA C-acetyltransferase activity	2.13	12.00
CGI-30 protein	CGI-30	peptidyl-diphthamide biosynthesis from peptidyl-histidine, diphthine synthase activity	4.99	0.64
biliverdin reductase A	BLVRA	biliverdin reductase activity	4.75	1.15
ARG99 protein	ARG99	adenosylmethionine decarboxylase activity, spermine biosynthesis	10.79	0.06
sulfatase 2	SULF2	heparan sulfate proteoglycan metabolism, carboxy-lyase activity	9.84	0.05
glutamate-ammonia ligase (glutamine synthase)	GLUL	glutamine biosynthesis, regulation of neurotransmitter levels, nitrogen fixation, glutamate-ammonia ligase activity	12.06	0.04

stearoyl-CoA desaturase (delta-9-desaturase)	SCD	stearoyl-CoA 9-desaturase activity	31.12	0.00
solute carrier family 7, (cationic amino acid transporter, y+ system) member 11	SLC7A11	cystine:glutamate antiporter activity, amino acid permease activity	15.56	0.08
NAD(P)H dehydrogenase, quinone 1	NQO1	NAD(P)H dehydrogenase (quinone) activity	2.21	17.60
gamma-glutamyltransferase 1	GGT1	gamma-glutamyltransferase activity	7.49	0.66
kynureninase (L-kynurenine hydrolase)	KYNU	kynureninase activity, tryptophan catabolism	629.18	0.00
hypothetical protein FLJ10808	FLJ10808	ubiquitin activating enzyme activity	12.12	0.32
dehydrogenase/reductase (SDR family) member 2	DHRS2	epithelial cell differentiation, alcohol dehydrogenase activity, progesterone metabolism, androgen metabolism, 9-cis-retinoic acid biosynthesis, - 3-alpha(17-beta)-hydroxysteroid dehydrogenase (NAD+) activity, racemase and epimerase activity	74.22	0.00
Cell development				
Pre-B-cell leukemia transcription factor 1, 3	PBX1	hindbrain development	9.11	0.11
3-hydroxy-3-methylglutaryl-Coenzyme A reductase	HMGCR	gonad development, hydroxymethylglutaryl-CoA reductase (NADPH) activity	6.11	0.43
apolipoprotein E, drebrin 1	DBN1	regulation of neuronal synaptic plasticity	3.63	2.73
ankylosis, progressive homolog (mouse)	ANKH	inorganic phosphate, diphosphate transporter activity, locomotory behaviour, regulation of bone mineralization	10.27	0.06
Cell angiogenesis				
vascular endothelial growth factor	VEGF	vascular endothelial growth factor receptor binding, positive regulation of vascular endothelial growth factor receptor signaling pathway, extracellular matrix binding	8.49	4.69
a disintegrin-like and metalloprotease (reprolysin type) with thrombospondin type 1 motif 1, fibroblast growth factor 2 (basic)	FGF2	heparin binding, angiogenesis	16.27	0.06
Cell immune response				
nuclear factor I/A	NFIA	viral genome replication	12.92	0.03
tropomyosin 1 (alpha)	TPM1	viral assembly, maturation, egress, and release	12.33	0.18

ribonuclease, RNase A family, 7	RNASE7	pancreatic ribonuclease activity, innate immune response, defense response to bacteria, ribonuclease activity	11.78	0.02

Interestingly, it was noted there were several gene transcriptions having unusually very large fold changes between W12G and W12GPXY cells in the microarray result analysis, e.g. IGFBP3 (211.83 fold), MMP10 (370.63 fold) and MMP1 (644.45 fold). To make sure there was no mistake in programme running, the raw data from the scanned image with the Affymetrix GeneArray Scanner was checked with the data analysis result. It was found in these genes the raw scanned data is consistent with the calculated fold changes (appendix 4).

We also selected out the connexins and PDZ containing protein gene expression data from the Rank Product analysis reports although some of their PC-value thresholds were higher than we defined in iGA analysis. In total 6 Connexins and 4 PDZ containing proteins were found expressed in the W12G and W12GPXY microarray lists. There were few apparent difference in connexin transcription levels between the two comparative cell lines except that Connexin 30, Connexin 26 and Connexin 45 were upregulated around three fold inW12GPXY cells. The PDZ containing proteins, ZO-1 and hDlg were around three fold more highly expressed in W12GPXY cells, while transcription of p55, a major human erythrocyte membrane protein also found in other tissues, was 7 fold higher in W12G cells than in W12GPXY cells. The results are presented in Tables 10a and 10b.

3.2 Real-Time Reverse Transcriptase-PCR Confirmed Differential Expression of Selected Genes in W12G and W12GPXY cells

To assess the validity of the microarray approach to identifying differentially expressed genes, quantitative real-time RT-PCR was performed on the mRNA prepared for microarray experiments. Angiogenesis is a key step in progression from

in-situ carcinoma to malignant tumour; furthermore, there are accepted functional assays for testing the significance of transcriptional changes in these factors to confirm the microarray results. Quantitative real-time PCR was carried out with three angiogenesis-related factor genes, VEGFC, FGF-2 and IL8, identified by this cDNA microarray analysis as having significantly higher expression in W12GPXY than in W12G cells. As controls for the angiogenesis factor family, VPF (expression not changed in W12GPXY cells compared to W12G cells) and GAPDH were also studied. For all the three expressed genes with differential expression on microarray, the quantitative real-time RT-PCR patterns corroborated the microarray data although the precise expression-fold changes by microarray analysis was higher than by RT-PCR. Moreover, the similarity in expression levels of mRNA for GAPDH and VPF between W12G and W12GPXY cells shown with quantitative real-time PCR were consistent with the microarray analyses. Quantitative real-time RT-PCR amplification was carried out with mRNA samples from W12G and W12GPXY cells (originally extracted at the same concentration): 1/10 diluted W12G mRNA comparing with a gradient of diluted W12GPXY mRNA from 1~1/10000 and no mRNA (XY-EM) as negative control; the results are shown in Figures 9 (a-d) and Table 11 (a-d).

Therefore, real-time quantitative PCR on selected representative genes demonstrated the functional integrity of our microarray in the appropriate identification of differentially expressed genes between W12G and W12GPXY cells, and highlighted the existence of variable (possibly coordinated) expression among similar functional individual genes.

Table 10 a: Microarray result of Connexin change in W12GPXY v W12G.

Gene bank accession	Connexins	Fold Change	False discovery rate
231771_at	connexin 30	3.33	2.14
223278_at	connexin 26	3.16	1.39
208460_at	connexin 45	3.00	3.80
206156_at	connexin 31.1	2.20	22.64
201667_at	connexin 43	1.22	6.66
215243_s_at	connexin 31	1.01	44.61

Table 10 b: Microarray result of PDZ proteins change in W12GPXY v W12G.

Gene bank accession	PDZ containing proteins	Fold change	False discovery rate
202743_at	phosphoinositide-3-kinase, regulatory subunit 3 (p55, gamma)	7.87	3.62
203230_at	dishevelled, dsh homolog 1 (Drosophila)	1.56	48.24
214168_s_at	tight junction protein 1 (zona occludens 1)	3.00	6.20
202516_s_at	discs, large homolog 1 (Drosophila)	3.62	4.08

- Gene more highly expressed in W12G cells are shown in red and genes more highly expressed in W12GPXY cells were in green.

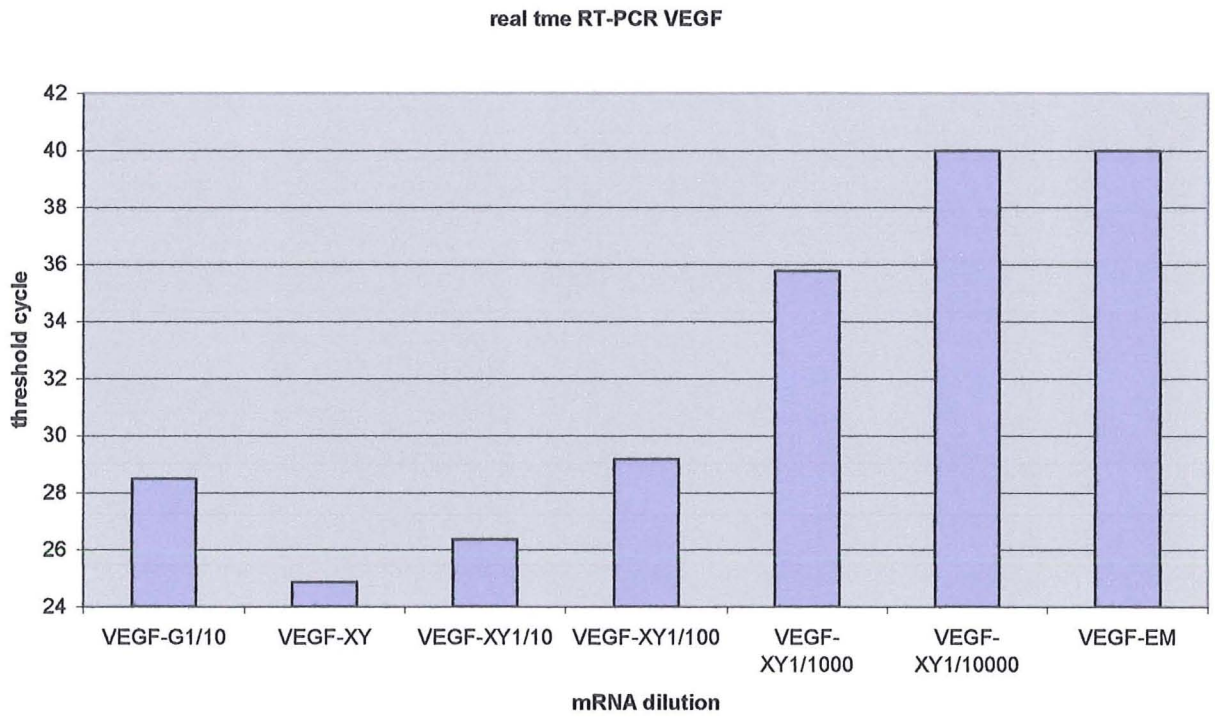

Figure 9 a: VEGF quantitative RT-PCR comparison of W12GPXY mRNA dilutions with W12G mRNA diluted in 1/10.

Name	Threshold cycle	Standard deviation threshold cycle
VEGF-G1/10	28.96	±0.61
VEGF-G1/10	28.1	±0.61
VEGF-XY	25.23	±0.38
VEGF-XY	24.7	±0.38
VEGF-XY1/10	26.28	±0.1
VEGF-XY1/10	26.41	±0.1
VEGF-XY1/100	29.17	±0.49
VEGF-XY1/100	28.48	±0.49
VEGF-XY1/1000	35.47	±3.2
VEGF-XY1/1000	34.80	±3.2
VEGF-XY1/10000	36.24	±0.83
VEGF-XY1/10000	35.07	±0.83
VEGF-EM	39.23	±14.69
VEGF-EM	40	±14.69

Table 11 a: Threshold cycle and Standard deviation Curve threshold cycle of VEGF in W12G and W12GPXY samples in quantitative real-time PCR.

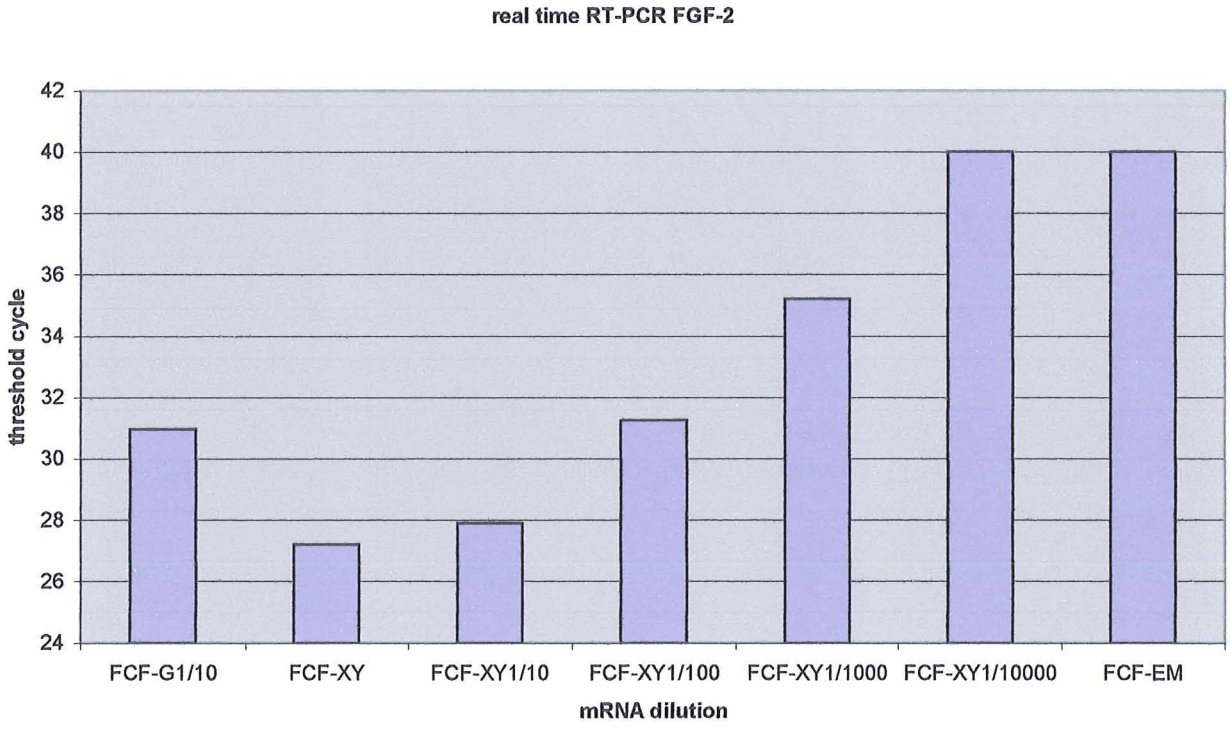

Figure 9 b: FGF-2 quantitative RT-PCR comparison of W12GPXY mRNA dilutions with W12G mRNA diluted in 1/10.

Name	Threshold cycle	Standard deviation threshold cycle
FGF-G1/10	31.05	±0.12
FGF-G1/10	30.87	±0.12
FGF-XY	27.19	±0.04
FGF-XY	27.24	±0.04
FGF-XY1/10	28.32	±0.38
FGF-XY1/10	28.67	±0.38
FGF-XY1/100	31.98	±1.03
FGF-XY1/100	31.53	±1.03
FGF-XY1/1000	35.39	±0.25
FGF-XY1/1000	35.04	±0.25
FGF-XY1/10000	40	0
FGF-XY1/10000	40	0
FGF-EM	40	0
FGF-EM	40	0

Table 11 b: Threshold cycle and Standard deviation Curve threshold cycle of of FGF-2 in W12G and W12GPXY samples in quantitative real-time PCR.

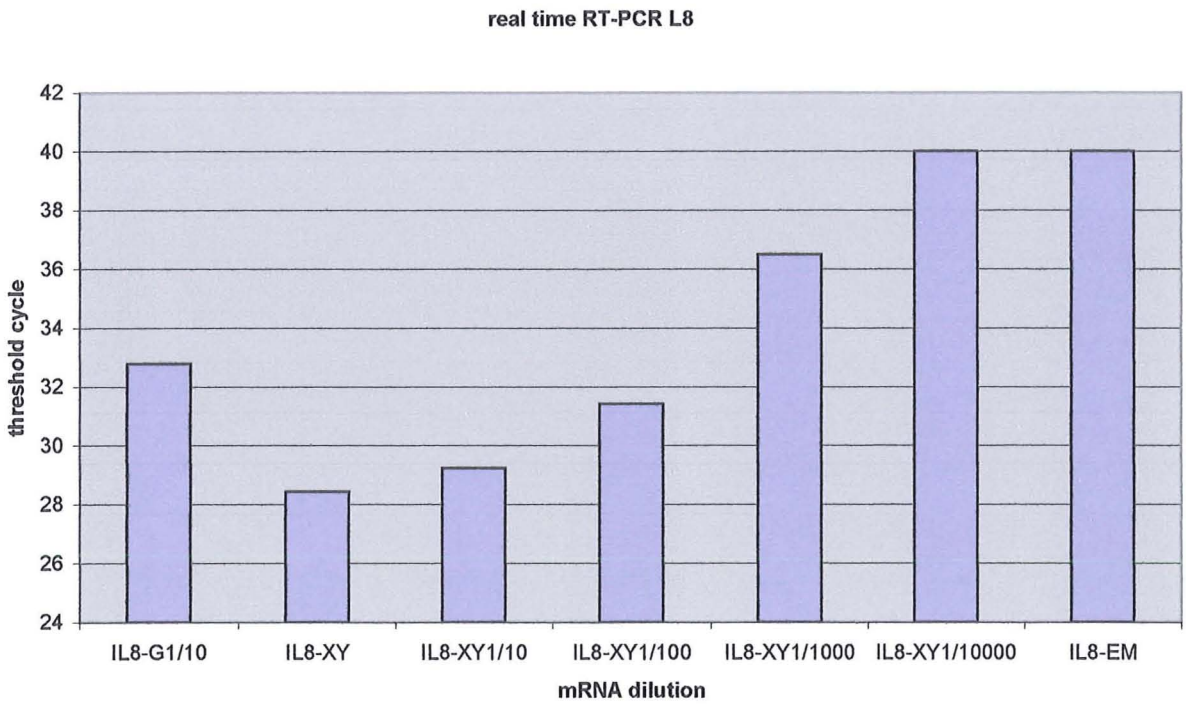

Figure 9 c: IL8 quantitative RT-PCR comparison of W12GPXY mRNA dilutions with W12G mRNA diluted in 1/10.

Name	Threshold cycle	Standard deviation threshold cycle
IL8-G1/10	32.57	±0.57
IL8-G1/10	32.98	±0.57
IL8-XY	28.65	±0.3
IL8-XY	28.23	±0.3
IL8-XY1/10	28.94	±0.41
IL8-XY1/10	28.52	±0.41
IL8-XY1/100	31.26	±0.91
IL8-XY1/100	31.55	±0.91
IL8-XY1/1000	35.68	0
IL8-XY1/1000	37.42	0
IL8-XY1/10000	40	0
IL8-XY1/10000	40	0
IL8-EM	40	0
IL8-EM	40	0

Table 11 c: Threshold cycle and Standard deviation Curve threshold cycle of of IL8 in W12G and W12GPXY samples in quantitative real-time PCR.

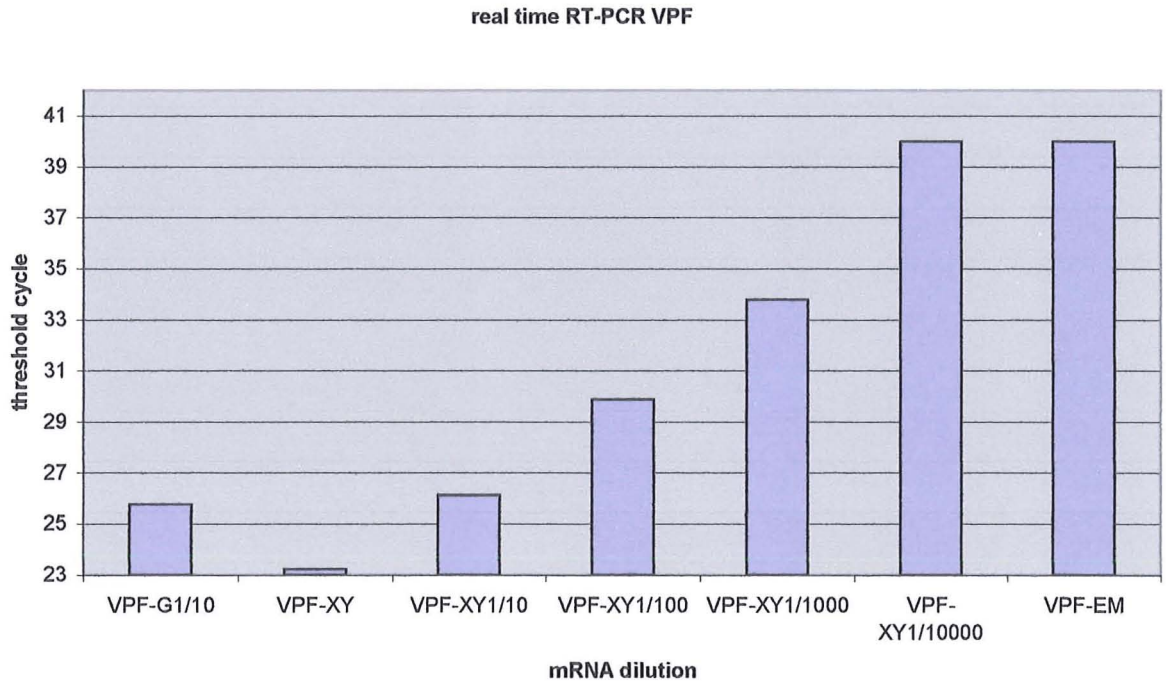

Figure 8 d: VPF quantitative RT-PCR comparison of W12GPXY mRNA dilutions with W12G mRNA diluted in 1/10.

Name	Threshold cycle	Standard deviation threshold cycle
VPF-G1/10	25.96	±0.37
VPF-G1/10	25.38	±0.37
VPF-XY	23.72	±0.14
VPF-XY	23.92	±0.14
VPF-XY1/10	26.21	±0.28
VPF-XY1/10	26.42	±0.28
VPF-XY1/100	29.39	±2.12
VPF-XY1/100	30.39	±2.12
VPF-XY1/1000	33.52	±0.4
VPF-XY1/1000	34.08	±0.4
VPF-XY1/10000	40	0
VPF-XY1/10000	40	0
VPF-EM	40	0
VPF-EM	40	0

Table 11 d: Threshold cycle and Standard deviation Curve threshold cycle of VPF in W12G and W12GPXY samples in quantitative real-time PCR.

Table 12: Nominated angiogenesis-related genes abnormally expressed in W12GPXY cells confirmed by quantitative RT-PCR.

Gene	Fold change shown from Affymetrix microarray	Fold change from quantity RT-PCR	Note
VEGFC	8.49	~10	vascular endothelial growth factor receptor binding, positive regulation of vascular endothelial growth factor receptor signaling pathway, extracellular matrix binding
FGF2	16.27	~10	angiogenesis , heparin binding
IL8	127.87	~20-30	Angiogenesis, regulation of retroviral genome replication, interleukin-8 receptor binding, chemokine activity, neutrophil activation, neutrophil chemotaxis, induction of positive chemotaxis
VPF	_	_	Vascular endothelial growth factor A precursor (VEGFA), Heparin binding, extracellular matrix binding, Growth factor activity
GAPDH	_	_	Glyceraldehyde-3-phosphate dehydrogenase (phosphorylating) activity, NAD binding

Abbreviations: VEGFC, vascular endothelial growth factor C; IL8, interleukin 8; FGF2, fibroblast growth factor 2; VPF, vascular permeability factor; GAPDH, glyceraldehyde-3-phosphate dehydrogenase.

3.3 HPV-16 oncoproteins and expression of the binding proteins

As W12GPXY cells were established from W12G cells, and W12GPXY cells showed more tumorigenic characteristics, the question arose of whether or not there is increased expression of viral oncogenes E6 and E7 in W12GPXY. To test this hypothesis, expression of HPV-16-E6, E7, p53 and pRb were analysed by Western blotting with whole cell lysates of HaCaT (HPV negative epithelia, immortalised, not transformed), C33a (HPV negative p53 mutant cervical cancer cell line), W12E (HPV-16 genome maintained as episomes, immortalised, not transformed cervical epithelial cells), W12G (integrated HPV-16 genome, immortalised, not transformed cervical epithelial cells (Jeon et al., 1995), W12GPX, W12GPXY (integrated genome, fully transformed cervical epithelial cells) cells (Aasen et al., 2003), and CaSki (HPV16 positive cervical cancer cell line).

E6 expression was readily detected in W12E, W12G, W12GPX and W12GPXY cells as expected (Fig (10). E6). Notably, there was approximately 2.9±0.36 (S.D.) times more E6 in W12GPXY than in W12G cells (quantified from densitometric scanning of films from 3 independent experiments); higher even than in CaSki cells. p53 level was checked to confirm that increased E6 could raise p53 degradation in the cell lines. In C33a cells, the mutant p53 expression was higher than p53 in HaCaT cells; while in the HPV16 positive cell lines, p53 was significantly decreased from W12G to CaSki cells and W12GPXY cells.

As HPV E7 binds to another important tumour suppressor, pRb, leading to the latter's degradation, the levels of E7 and pRb were also studied by western blot in the HPV16 harbouring cell lines. Consistent with a previous study (Jeon and Lambert, 1995), E7 was more abundant in W12G cells than in W12E cells; while in W12GPXY and CaSki cells there was increased E7 compared to level in W12G cells (Fig (11). E7).

In contrast, pRb in W12E and W12G cells was more abundant than in W12GPXY and CaSki cell lines, consistent with the known effect of E7 in down regulation of pRb.

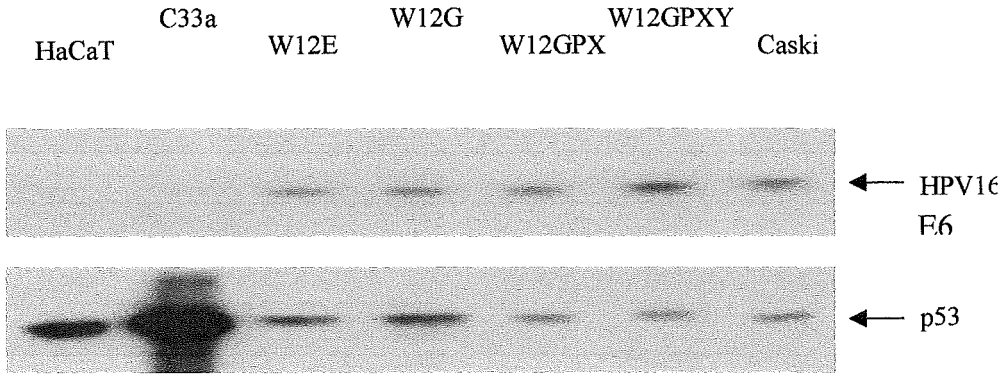

Figure 10: Western blot analysis of levels of HPV-16 E6, and p53 in epithelial cell lines.

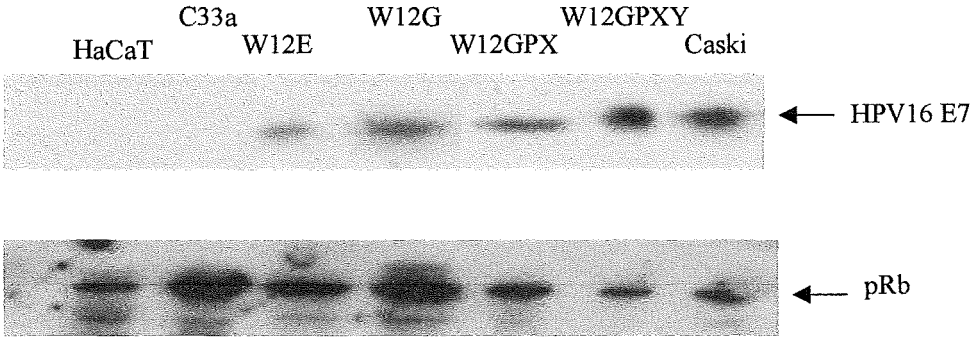

Figure 11: Western blot analysis of levels of HPV-16 E7, and pRb in epithelial cell lines.

3.4 Monolayer proliferation and differentiation

Ki67 is a marker for cell proliferation. It is a nuclear protein expresssed in proliferating cells and may be required for maintaining cell proliferation (as in HPV cervical neoplasia) (Isacson et al., 1996). Involucrin is a keratinocyte cornified envelope protein precursor, which is formed beneath the inner surface of the cell membrane during terminal differentiation. Involucrin first appears in the cell cytosol, but ultimately becomes cross-linked to membrane proteins by transglutaminase. In cervical dysplasia, involucrin expression was normally decreased. We took these two markers to analyse the further different carcinogenesis characteristics between W12G and W12GPXY cells.

Ki67 immuonofluorescence staining for the proliferative fraction was performed on W12G and W12GPXY after plating out for 60 hours. Positive stained cells were counted from three different fields under the microscope from each slide and for each sample two individual slides were checked. The percentage of Ki67 positive cells was assessed in each case and was found to be an average of 6 times more in W12GPXY (70%) cells than that in W12G (11%) cells Fig (12). Involucrin staining was analysed in monolayer cultured cells at 60 hours or 240 hours after plating out. The percentage positive cells were calculated as for Ki67. Involucrin immunostaining, was clearly increased after 240 hours in W12G cells; conversely, there was no significant change between 60 and 240 hours in cultured W12GPXY cells. Furthermore, in W12G raft culture sections, involucrin was mostly located in the upper and middle cell layers, but not in the basal cells. Involucrin was detected in all layers of W12GPXY cells on raft culture, although nearly all the cells invading into the collagen were negative Fig (13). Thus, W12GPXY cells appeared to have greater proliferative capacity but less differentiation potential than W12G cells.

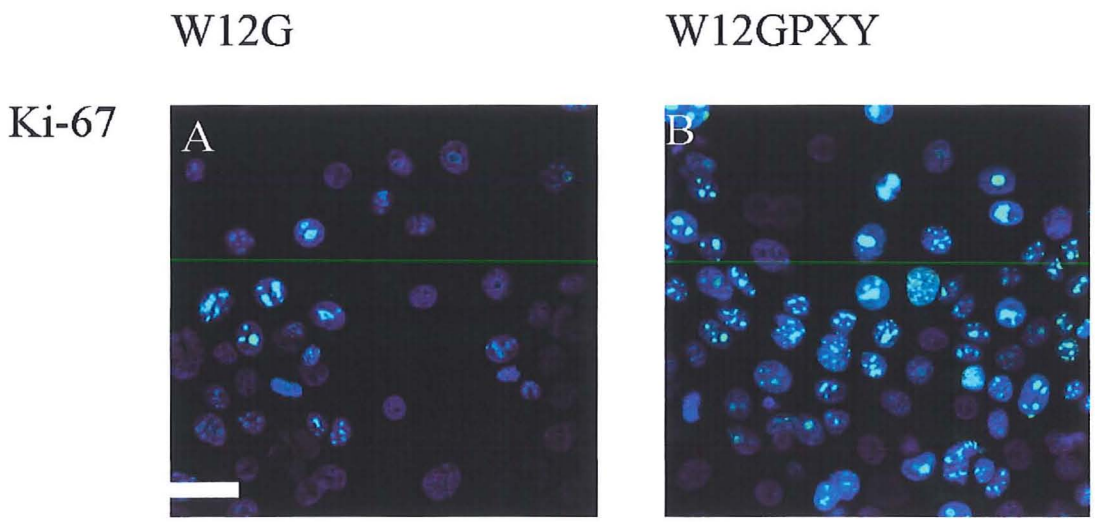

Figure 12: Ki67 immunofluorescence staining of W12G and W12GPXY cells in monolayer. The average percentage of Ki67 positive cells was ~12 % in W12G cells, and ~70 % in W12GPXY cells. Nuclei were stained with DAPI. Bar =20μm.

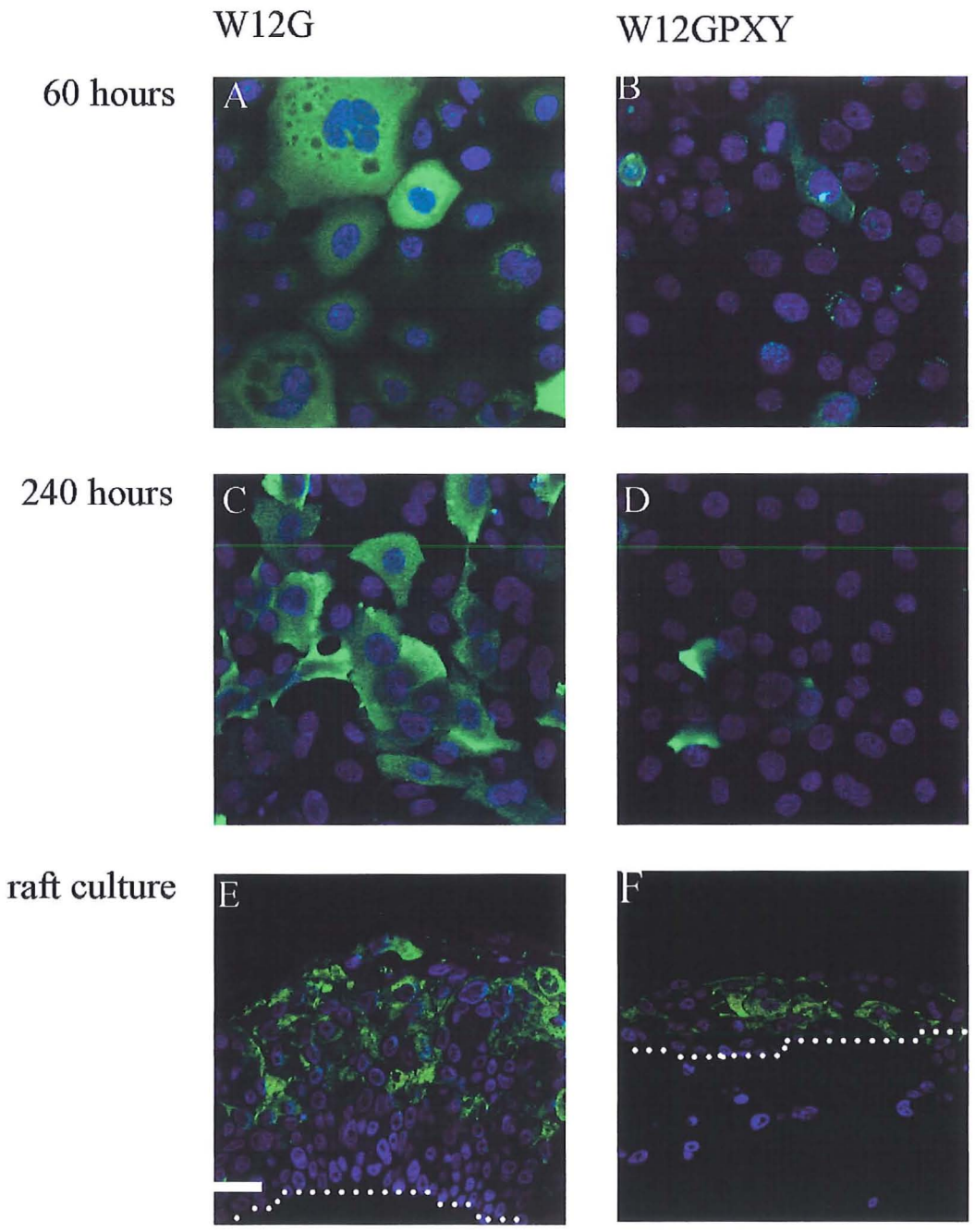

Figure 13: Involucrin immuonofluorescence staining of W12G and W12GPXY cells after monolayer cultured 60 hours (A, B), 240 hours(C, D) and raft culture sections (E, F). The average percentage of involucrin positive cells was ~10 % in W12G cells, and ~5 % in W12GPXY cells at 60 hour; while was ~80 % in W12G cells and ~7 % in W12GPXY cells at 240 hours. The white lines in (E, F) show the interface between cervical cells and collagen raft. Nuclei were stained with DAPI. Bar =10μm.

3.5 Connexin expression in W12G and W12GPXY cells

In previous experiments, it was demonstrated that, in contrast to the W12G parental cell line (Jeon et al., 1995), W12GPXY cells have lost intercellular gap junctional communication (as measured by transfer of Lucifer Yellow-CH) concomitant with redistribution of Connexin 43 from intercellular junctions in the plasma membrane into the cytoplasm (Aasen et al., 2003). To understand the mechanism regulating the redistribution of Connexin 43 and reduced cell coupling, firstly expression of Connexin 43 was analysed by Western blotting with whole cell lysates of W12E, W12G, W12GPX, and W12GPXY cells (Aasen et al., 2003). Consistent with the result of the microarray analysis, Western blotting demonstrated there is no obvious change in total amount of Connexin 43 between W12G and W12GPXY cell culture Fig (14, A); moreover, Connexin 43 phosphorylation patterns were similar in both cell lines Fig (14, B). However, when W12G and W12GPXY cells, on coverslips were immunofluorescence stained, Connexin 43 was identified mainly at cell-cell contacts on cell membrane, and the staining pattern was consistent with the presence of gap junction plaques in W12G cells Fig (15). However, only 35% of W12GPXY cells showed Connexin 43 positive stain and most of this was in the cytoplasm around the perinuclear region. Connexin 43 gap junction plaques were absent and little cell membrane staining was found in these cells. Interestingly, in W12GPXY cells that did stain the individual cytoplasmic Connexin 43 level seemed much higher than that seen on W12G cell membrane contacts. This could explain the reason for similar total Connexin 43 levels shown in Western blotting between W12G and W12GPXY cells Fig (15 C, F).

Although tried under different conditions with several other Connexin antibodies, it was difficult to detect the proteins in Western blotting of connexins other than

Connexin 43. However, immunofluorescence studies showed that in both cell lines, Connexin 26 was present in plasma membranes; with stronger staining at cell-cell contacts and larger membrane plaques in W12GPXY than in W12G cells (interesting in view of absence of LY-CH transfer between W12GPXY cells) Fig (15 A, D). Connexin 30 was also seen by immunofluorescence in both cell lines. Like the Connexin 26 pattern, it was present only on the plasma membrane and composed large plaques between the neighbouring cells Fig (15 B, E).

3.6 Other cell membrane proteins in W12G and W12GPXY cells

As HPV-16 E6 appears to target PDZ proteins and as ZO-1 (a PDZ protein) can associate with Connexin 43, hDlg and ZO-1 were analysed by Western blotting. ZO-1 was decreased from W12G to W12GPXY cells, and was hardly detected in CaSki cells. However, there was 2-3 fold more hDlg in W12GPXY cells than in W12G cells (consistent with mRNA upregulation from Microarray analysis), while the amount was less in CaSki cells (Fig (16)). More detailed study of hDlg will be described in the next chapter.

In previous studies, adherens junction proteins E-cadherin and β-catenin (also having been implicated in formation and stability of gap junctions) were reported to be reduced during cervical carcinogenesis (de Boer et al., 1999; Carico et al., 2001; Denk et al., 1997). However, Western blotting suggested there was no significant difference in amount of these proteins in HaCaT, W12G, W12GPXY and CaSki cells, although E-cadherin and β-catenin were dramatically decreased in C33a cells Fig (17). It was found that β-catenin located on plasma membranes especially at cell-cell contacts and there were no dramatic difference in staining between W12G, W12GPXY and CaSki cells, although there were more cytoplasm speckle staining

noted in W12GPXY cells Fig (18). Furthermore, it was previously shown that there was little difference in E-cadherin pattern between these cells (Aasen, 2003).

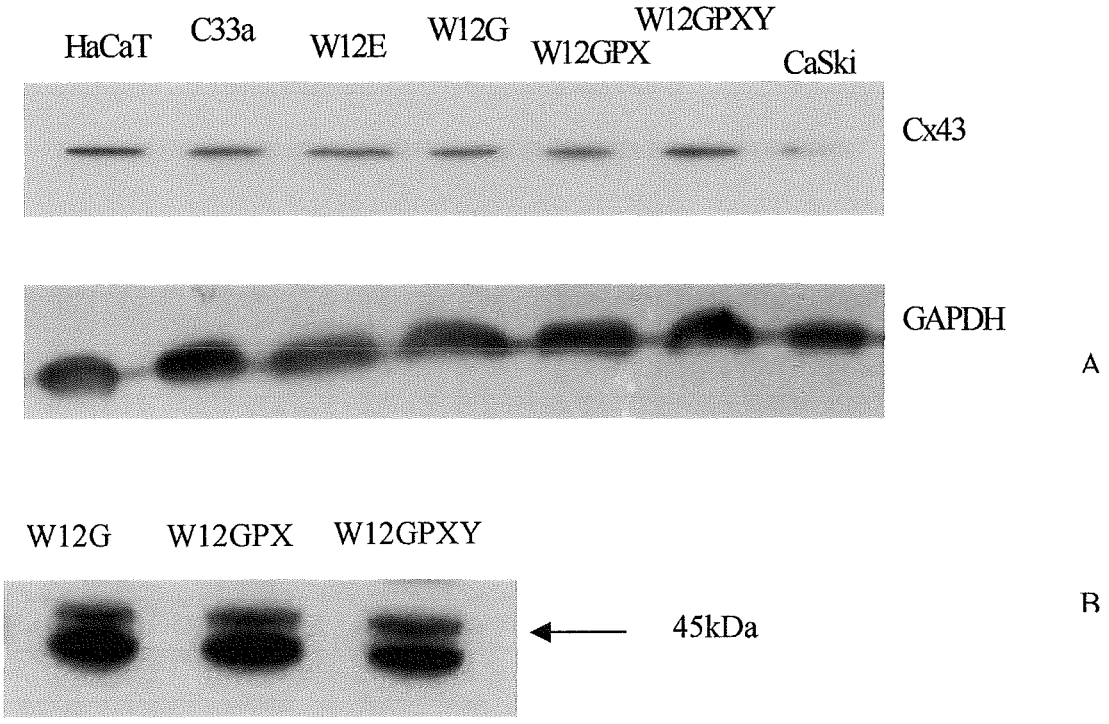

Figure 14: A, Western blot analysis of levels of Connexin 43 in epithelial cell lines; B, same Connexin 43 phosphorylation pattern in W12G, W12GPX and W12GPXY cells.

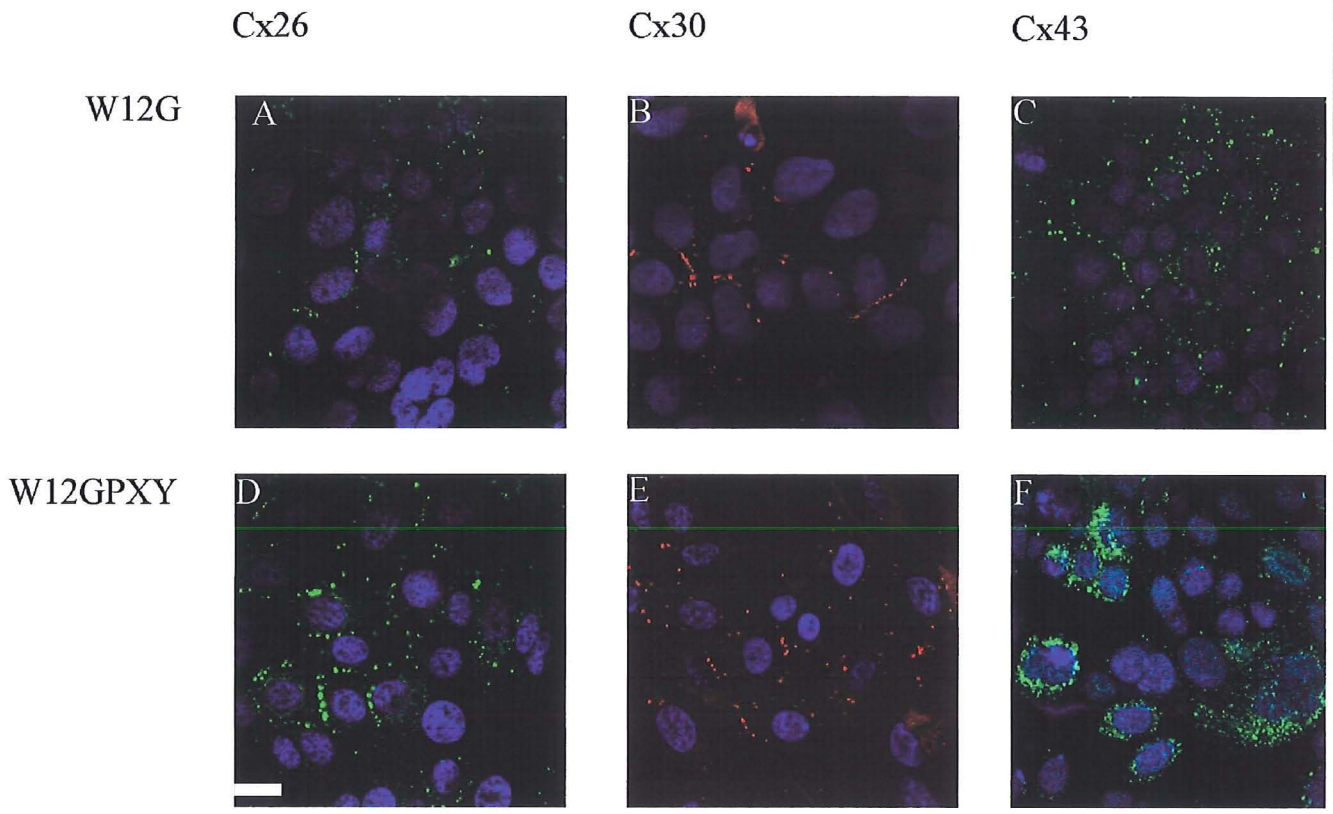

Figure 15: Connexin 26, Connexin 30 and Connexin 43 immuonofluorescence staining of W12G and W12GPXY cells in monolayer. Nuclei were stained with DAPI. Bar =20μm.

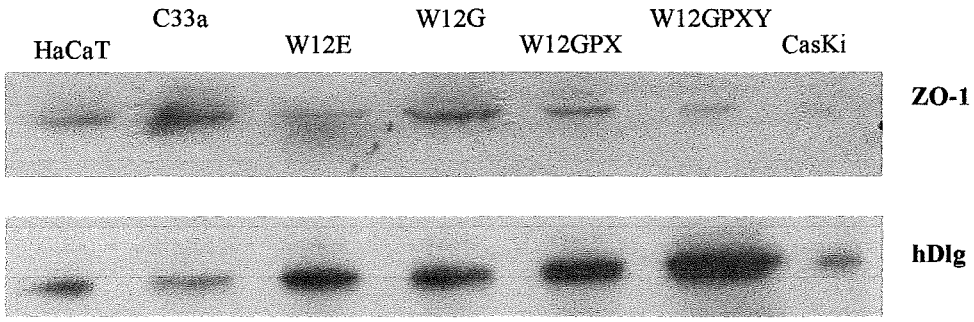

Figure 16: Western blot analysis of levels of ZO-1and hDlg in epithelial cell lines.

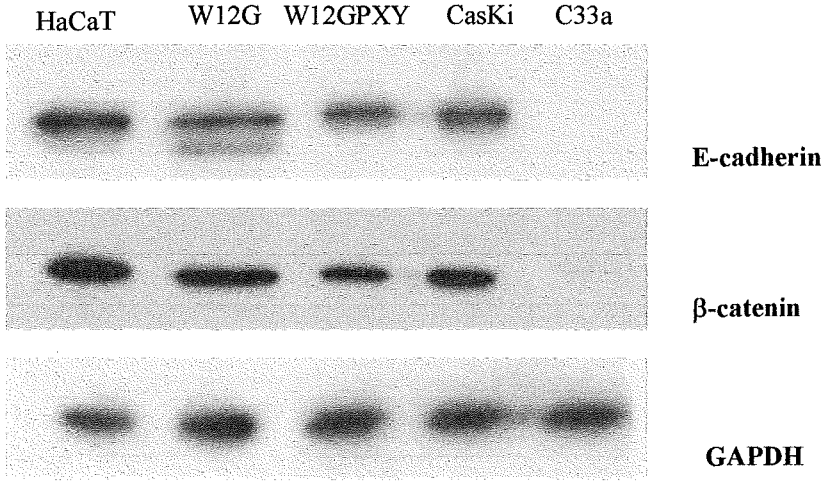

Figure 17: Western blot analysis of levels of E-cadherin and β-catenin in epithelial cell lines.

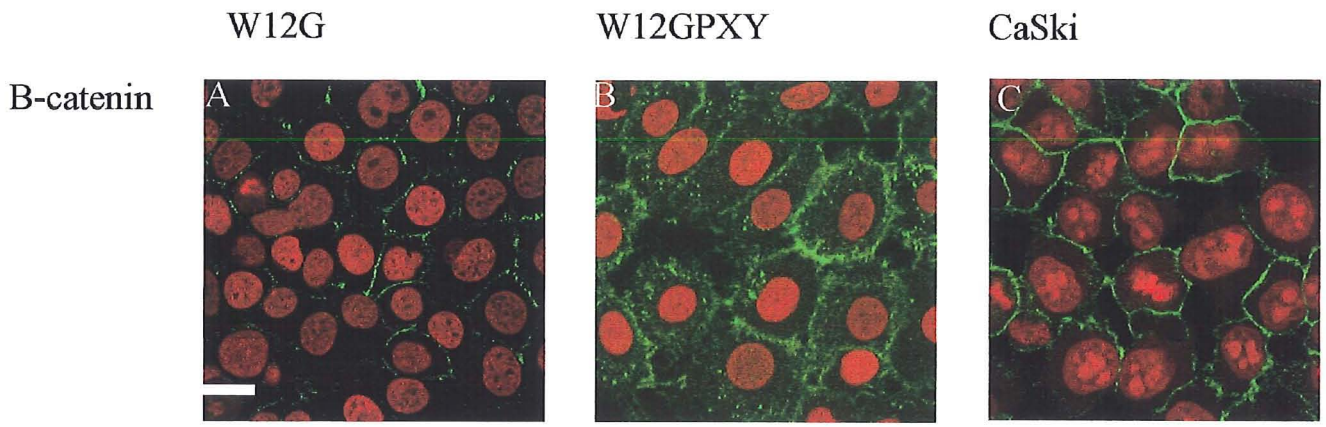

Figure18: β-catenin immuonofluorescence staining of W12G (A), W12GPXY (B) and CaSki(C) cells. Nuclei were stained with propidium iodide. Bar =20μm.

3.7 Cell morphology changes between W12G and W12GPXY cells

Previous studies have shown close links between cell junction complexes with the actin cytoskeleton: perturbation of cell junctions caused cellular actin cytoskeleton rearrangements (Watabe et al., 1994). Gap junction intercellular communication can affect actin stress fiber co-ordination in cultured astrocytes (Yamane et al., 2002). Phalloidin staining showed dramatic differences in actin filament distribution in addition to the cell junction changes between W12G and W12GPXY cells. In W12G cells, actin filaments were spread evenly in the cytoplasm. The cells were tightly associated with others, and were polygonal shape, quite similar to normal epithelial cells. In W12GPXY cells, actin filaments were concentrated on the cell edges and there were lots of projections around the cell membrane, where cells contacted less frequent and less organized. The cells were more elongated than W12G cells and the cell shape was more similiar to cancer cell morphology Fig (19, A).

When W12G and W12GPXY cells were grown as organotypic raft cultures, typical histological features indicated that W12G cells formed a stratified epithelium differentiated from basal layer to upper layers; the cells had close associated contacts and there was no obvious invasion into the collagen; W12GPXY cells showed little stratification and extensively invaded into the collagen raft Fig (19, B).

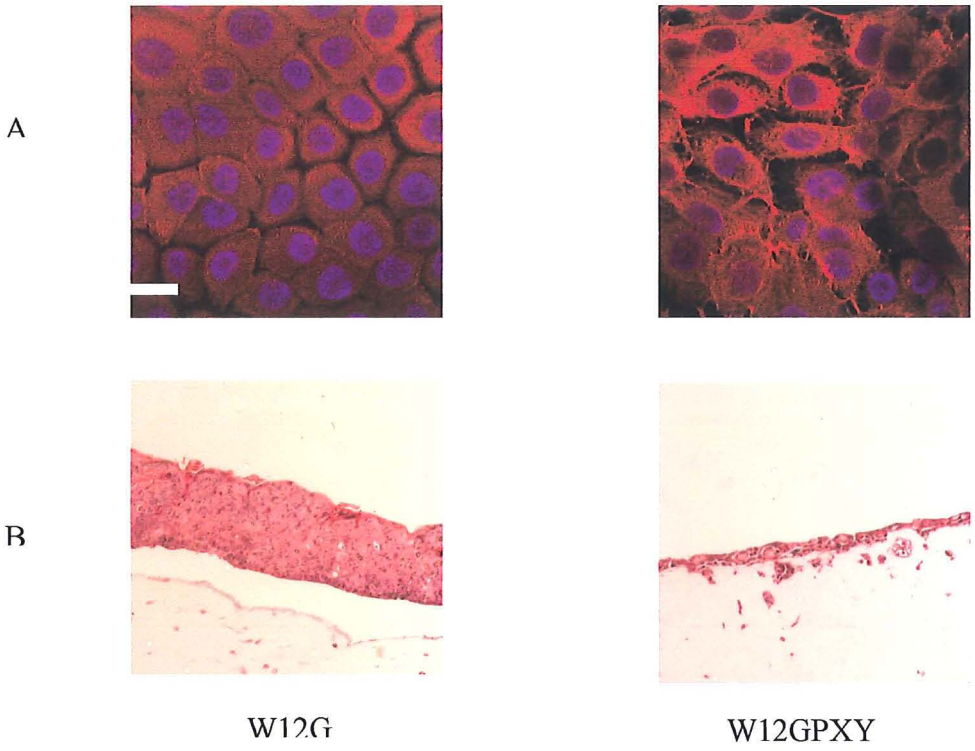

Figure 19: A, Phalloidin staining of W12G and W12GPXY cells; B, H&E stain of W12G and W12GPXY cells. Nuclei were stained with DAPI. Bar =20μm.

3.8 Discussion

Development of cervical cancer is closely associated with infection by high risk anogenital HPV and expression of its E6/E7 oncogenes. A key event in cervical tumour progression is the integration of the viral episomal copies into the host genome. Usually, this results in repression of expression of all virus proteins except for the viral oncoproteins E6 and E7 that become overexpressed, leading (among other changes) to uncontrolled cell cycle progression and inhibition of cell differentiation and apoptosis (zur Hausen, 2002). Cervical cancer progression is tightly linked to the interaction between the function of the HPV oncoprotein and the local cellular microenvironments, where cell-mediated responses are central in progression of squamous intra-epithelial lesions to cervical carcinoma. However, cervical carcinoma progression implies a complex and not entirely understood interaction between HPV oncoproteins and host factors. The microenvironment inside and around tumors is complex, involving interactions between extracellular matrix (ECM), growth factors, cytokines and cells. This microenvironment is modified by proteases produced by tumor or stromal cells (Wang and Hildsheim, 2005). These factors may influence the composition of the ECM around the plasma membrane and may also modulate gene expression of membrane components and future sequential cellular responses (Duffy, 1998). To investigate global gene expression changes during cervical cancer progression, microarray was employed to search for RNA-based biomarkers to define these pathological changes between the HPV 16 genome integrated cervical epithelial cell line W12G and a malignant cell line established from W12G cells, the feeder-layer and mitogen-independent line W12GPXY.

Microarray and quantitative real-time PCR results indicated there were significant increases in VEGFC, IL8 and FGF-2 mRNA expression in W12GPXY cells

compared with W12G cells. Such changes could be correlated with ability of W12GPXY cells to invade into collagen in organotypic raft culture compared with the non-invasive W12G cells. The disorganisation of epithelial junctions can lead to defective cell-cell adhesion, loss of cell polarity and unregulated cell proliferation, and therefore may represent a crucial step in tumourigenesis. This study found that ZO-1, a key tight junction protein at cell membranes, was significantly increased 3 fold at the mRNA level but decreased at the protein level in W12GPXY cells compared to W12G cells. On the other hand, the related PDZ protein, hDlg was increased in both mRNA and protein levels in W12GPXY cells. These data suggest that in our model of cervical cancer invasion, changes in Connexin 43 gap junctions could be associated with changes in malignant cancer cell microvascular invasion and metastatic spread. Previous studies reported the downregulation or loss of GJIC in HPV positive cervical tumours and malignant cell lines (Tomakidi et al., 2000; Faccini et al., 1996). However, our Western blot data revealed no significant changes of total connexin contents between W12G and W12GPXY cells, although they are completely deleted in HeLa and Caski cells (Aasen et al., 2003). However, immuonofluorescence staining of Connexin 43 demonstrated that Connexin 43 localization had transferred from plasma membrane gap junction plaques into the perinuclear cytoplasm concomitant with the loss of intercellular exchange of lucifer yellow. Interestingly, Connexin 26 and Connexin 30 still formed typical gap junction plaques at cell-cell contacts in W12GPXY cells; even though these cells could not transfer lucifer yellow. These results suggested that a specific change in permeability properties rather than a complete loss of gap junctions might be involved in the progression from W12G to invasive W12GPXY cells. Specific loss of Connexin 43 could be key to changing the signals exchanged between the cells in the later stages of cancer progression.

W12GPXY cells displayed many malignant tumour characteristics both in monolayer and organotypic raft culture such as hyperproliferation, hypodifferentation, lowered p53 and pRb levels. The multifunctional HPV-16 E6 oncoprotein seems to have roles in tumour progression that can facilitate malignant transformation of HPV-associated tumours (Song et al., 1999; 2000). E6 is a shuttling protein that can move between the nucleus and cytoplasm. Our results showed that the amounts and intracellular locations of HPV-16 E6 were distinctly different between W12G and the tumour-progressed W12GPXY cells (detailed study in next chapter). The increased amount of HPV-16 E6 in the latter cells was most pronounced in the cytoplasmic compartment suggesting the possibility of E6 actions in addition to the well-characterised E6-p53 pathway during the later stages of malignant progression. Thus, we hypothesized and focused on the proposal that the increased E6 in W12GPXY cells is directly/indirectly involved in targeting Connexin43 for its loss from cell membrane and accumulation in cytoplasm (or complete loss from the cell) resulting in loss of Connexin 43 gap junction functions. There is evidence from mouse papilloma cells that E-cadherin junction formation is required to transport Connexins from the cytoplasm to the sites of cell-cell contact at membranes (Hernandez-Blazquez et al., 2001). Altered E-cadherin expression has been reported in cervical dysplasia and cancer (Vessey et al., 1995). However, both W12G and W12GPXY display large amounts of E-cadherin in the membrane; in addition, the C33a cell line is E-cadherin negative (Vessey et al., 1995), yet it is very well coupled, and consistently displays large Connexin 43 membrane plaques. Furthermore, re-expression of Connexins by transfection of cancer cells was normally sufficient to restore GJIC (Jou et al., 1993; Trosko et al., 2001). In general, it seemed that loss of GJIC does not appear to be a necessary or a direct consequence of changes in cadherin based cell-cell adhesion.

Other candidate targets of E6 that might be involved in loss of gap junction are PDZ proteins. ZO-1 is a tight junction (TJ)-associated protein that belongs to the MAGUK family in which presence of the characteristic MAGUK modules (PDZ, SH3 and GK) are key. The modular organization of these proteins allows them to function as scaffolds, which associate with transmembrane tight juction proteins, the cytoskeleton and signal transduction molecules. Previous studies have suggested ZO-1 can bind to Connexin 43 and associate through its carboxyl cytoplasmic domain with the second PDZ domain of ZO-1 which may play an important role in Connexin 43-containing gap junctions (Giepmans and Moolenaar, 1998; Toyofuku et al., 1998). These conclusions were based largely on studies of cultured cells, and included coimmunoprecipitation, yeast 2-hybrid assays, transfection experiments, and co-immunofluorescence staining of Connexin 43 and ZO-1. There is consistent growing evidence that other MAGUK proteins (eg, ZO-1, dlg, PSD-95 and PSD-93) are involved in processes of cell junction assembling to membrane subdomains and ion channel aggregation (Migaud et al., 1998; Gonzalez-Mariscal et al, 2000; McGee et al., 2001). In this study, it was shown that the expression of both ZO-1 and the related protein hDlg were changed in W12GPXY cells compared to W12G cells..

The tumour suppressor Dlg and its human homologue hDlg, another membrane-associated guanylate kinase (MAGUK) family protein, have been found to be closely associated with regulation of cell architecture and control of cell proliferation and cell polarity (Woods et al., 1996; Goode & Perrimon, 1997; Bilder et al., 2000; Ishidate et al., 2000; Firestein & Rongo, 2001). In *Drosophila*, Dlg is located at septate junctions (Woods and Bryant, 1991) and genetic mutation causes tumour development in the imaginal disc. However, the role of Dlg as a tumour suppressor appears to be distinct

from its role in maintaining septate junctions and localising membrane proteins (Woods et al., 1996).

In view of the known interaction between ZO-1 and Connexin 43 and the tumor suppressor property of hDlg , it was decide to investigate further possible involvement of hDlg and E6 in the loss of Connexin 43 gap junctions in W12GPXY cells.

Chapter 4. RESULTS 2

HPV-16 E6 CAUSES REDISTRIBUTION OF CONNEXIN 43 IN CERVICAL CANCER CELLS VIA AN INTERACTION WITH hDLG AND LEADS TO LOSS OF GAP JUNCTIONAL INTERCELLULAR COMMUNICATION

In HPV-16 cervical carcinogenesis, the viral oncogene E6 inactivates the tumour suppressor p53, but also has p53-independent functions in tumour progression. E6 has been reported to interact with several cytoplasmic proteins including the PDZ domain-containing proteins MAGI-1, ZO-1, MUPP-1, hScrib and hDlg. Such interactions might alter cell signalling cascades or cause changes in cell structure (Chen et al., 1995; Tong et al. 1997; Nakagawa and Huibregtse, 2000; Gao et al., 2001; Thomas et al., 2002; Watson et al., 2003).

hDlg (the human homologue of *Drosophila* Discs Large), is a tumour suppressor present in epithelial cells at sites of cell-cell contact which regulates cell polarity and attachment. It contains several protein-protein interaction domains including three PDZ domains, the second PDZ domain of which binds E6. With those protein interaction domains, hDlg can form protein scaffolds and comprise macromolecular complexes with the protein partners that are thought to be involved in cell signalling cascades and cell morphology organisation. Previous studies have identified several viral oncoproteins including high-risk HPV E6 and Adenovirus 9 E4-ORF1 and Tax oncoprotein of HTLV-1 (Lee et al., 1997; Suzuki et al., 1999) as hDlg targeting proteins, and E6 has been shown to target hDlg for proteasome-mediated degradation (Gardiol et al., 1999; Kuhne et al., 2000; Massimi et al., 2004). Therefore, hDlg is proposed to be involved in oncogenic transformation processes of diverse viruses (Kiyono et al., 1997; Lee et al., 1997). In previous studies and this study, it was

shown hDlg relocalised from plasma membrane into cytoplasm in HPV positive cervical cancer (Watson et al., 2002).

Connexins, the proteins of vertebrate gap junctions, may also function as tumour suppressors, and Connexin 43, one of the most widely expressed connexins, also has a PDZ binding domain in its C-terminus, which can bind to several cell junctional MAGUK proteins such as ZO-1, ZO-2, and ZO-3). A body of evidence has accumulated to show that GJIC may be lost during malignant progression, eg: HPV-positive cervical cancer (McNutt et al., 1971; Krutovskikh and Yamasaki, 1997; King et al., 2000; Aasen et al., 2003). Connexin 43 relocates from the membrane to the cytoplasm in the novel HPV-16 E6-containing cervical epithelial cell line, W12GPXY, that is fully transformed and invasive and deficient in gap-junctional intercellular communication (Chapter 3 and Aasen et al., 2003). Several studies have shown that Connexin 43 is involved in regulating cell proliferation and cell signalling cascades independently of GJIC functions. For example, Connexin 43 can be phosphorylated on tyrosine residues in the C-terminus by Src that can activate anti-apoptotic progression through the Src/ERK signalling pathway (Plotkin et al., 2002), and Connexin 43 also promotes degradation of S phase kinase-associated protein 2 (Skp2), the human F-box protein that regulates the ubiquitination and degradation of p27 (Zhang et al., 2003). Therefore, the redistribution of Connexin 43 from cell membrane into cytoplasm may be a critical step in malignant progression in late stages of high risk HPV cervical carcinogenesis.

Results shown in Chapter 3. confirmed that E6 does not directly regulate expression of Connexin 43 protein in HPV-16-containing cervical tumour cells. Next, the possible mechanisms of Connexin 43 redistribution from cell-cell junctions into the

cytoplasm of W12GPXY cells were investigated. In this chapter, it is now shown that the W12GPXY cells express increased levels of cytoplasmic E6, which co-localises with hDlg and that, concomitant with its relocation into the cytoplasm, Connexin 43 also binds hDlg. Treatment of W12GPXY cells with Leptomycin B to trap E6 in the nucleus or siRNA knockdown of E6 abrogate the relocation and co-location of hDlg and endogenous wild type Connexin 43 and restore Connexin 43 gap junction at points of cell-cell contact. Further, when C33a cells (HPV-negative cervical tumour cells which normally retain large Connexin 43 gap junctions) are transfected with HPV-18 wild type E6, changes in localisation of connexin 43 and hDlg are consistent with those in W12GPXY cells. However, C33a cells transfected with a mutant E6 lacking the hDlg binding site retain Connexin 43 gap junction plaques. Finally, Connexin 43 associates with hDlg through its PDZ-binding domain and this is required for its relocalisation to the cytoplasm in W12GPXY cells. These results suggest that increased cytoplasmic E6 associated with malignant progression of W12GPXY cells redistributes connexin 43 from membrane junctions into the cytoplasm by a mechanism involving binding of hDlg to the connexin 43 C-terminal tail. The findings have uncovered a new role for hDlg in trafficking of Connexin 43. They also provide a novel mechanism for the loss of gap junctional intercellular communication during malignant progression of squamous epithelial cells.

4.1 hDlg can bind to both HPV-16 E6 and Connexin 43

Structural analysis has demonstrated that the second PDZ domain in hDlg can bind to the X-S/T-X-V/L protein motif in high risk HPV E6 proteins (Kiyono et al., 1997). In Connexin 43, the C-terminal sequence DLEI can bind to the second PDZ domain of the cell membrane protein ZO-1 that has many structural and functional similarities

with hDlg (both proteins are in the same MAGUK proteins subgroup) (Toyofuku et al., 1998; Giepmans and Moolenar, 1998). As expected, results showed that ZO-1 was expressed in the W12-derived cell lines (Fig.16, ZO-1) and immunoprecipitation confirmed that in W12G and in W12GPXY cells, ZO-1 was associated with Connexin 43 (Fig. 20A). Immunoprecipitation was taken to investigate possible interactions between HPV-16 E6, hDlg and Connexin 43 in the W12G and W12GPXY cell lines. Connexin 43 and hDlg were co-immunoprecipitated from both W12G and W12GPXY cell extracts (Fig. 20C) even though Connexin 43 is mainly located in connexons in the cell membrane in W12G cells but is located largely in the cytoplasm in W12GPXY cells (Figs. 21 H, N and K, Q). HPV-16 E6/ hDlg complexes were precipitated from both W12G and W12GPXY cells (Figure 20 B) but were much more abundant in the latter, probably as a result of the higher amounts of E6 in W12GPXY (Fig.11 E6 track 6). However, E6 precipitated Connexin 43 only in W12GPXY cells (Fig. 20 D). Thus it appeared that redistribution of Connexin 43 into the cytoplasm of W12GPXY cells correlated with binding to both hDlg and E6.

Next, I used immunofluorescence to investigate the subcellular location of these three proteins. HPV-16 E6 was abundant in the nucleus in W12G cells with some cytoplasmic staining (Fig. 21 B). In contrast, in W12GPXY cells the E6 stain was found not only in the nuclear but also in the cytoplasmic compartment (Figure 21 E). hDlg was mainly identified on the cell membrane and the cell margin in W12G cells (Fig. 21 A), but in W12GPXY cells most of hDlg was relocated to the cytoplasm and displayed a speckle pattern of staining (Fig. 21 D). There was strong co-staining of E6 and hDlg in the cytoplasm in W12GPXY cells but not in W12G cells (Fig. 21 compare C and F).

Connexin 43 was visualised mainly at positions of cell-cell contact, and the staining pattern was consistent with the presence of gap junction plaques on the plasma membrane in W12G cells (Fig. 21 H). However, in those W12GPXY cells, that retained Connexin 43, the protein was transferred into the cytoplasm and little cell membrane staining was found (Fig. 21 K) as observed previously (Aasen et al., 2003). In W12GPXY cells, cytoplasmic Connexin 43 clearly co-localised with hDlg in large aggregates (Fig. 21 L) while there was no clear evidence of co-location in W12G cells despite both proteins locating in or near the membrane (Fig. 21 I). Finally, when we examined the locations of E6 and Connexin 43 in W12G cells there was no co-localisation as each protein was detected in a different subcellular compartment (Fig. 21 O). However, in W12GPXY cells E6 and Connexin 43 co-localised in some areas in the cytoplasm (Fig. 21 R). These findings further support the hypothesis that increased cytoplasmic E6 protein in W12GPXY cells might lead to redistribution of Connexin 43 and hDlg.

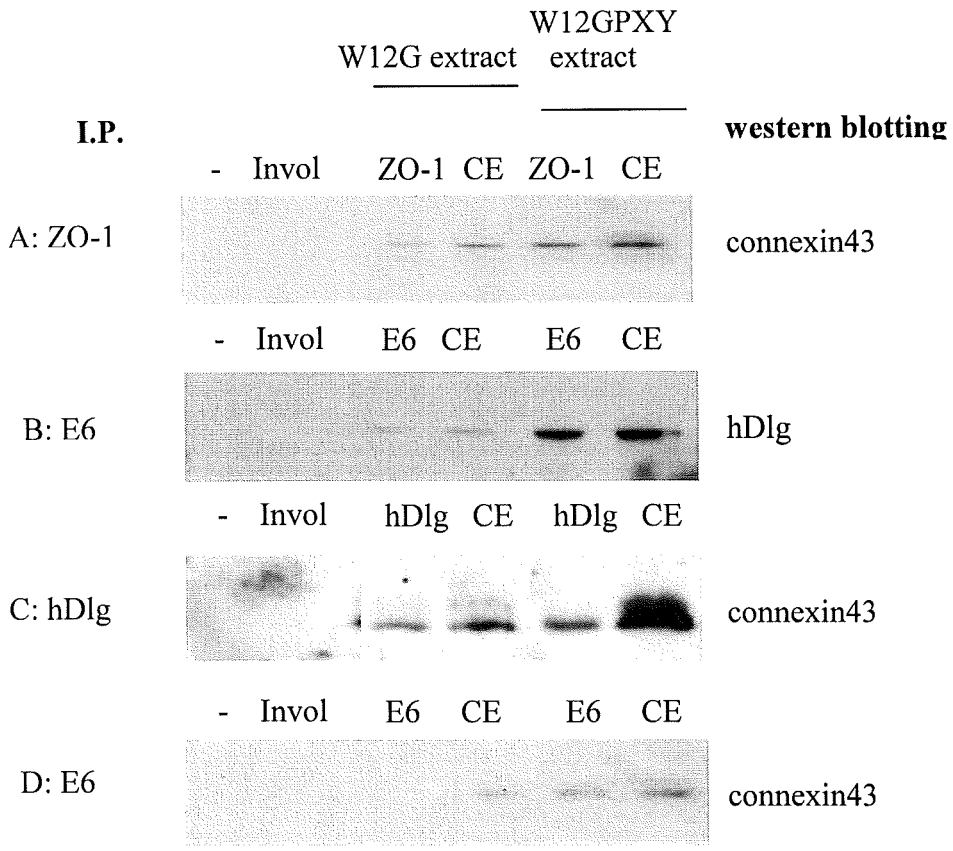

Figure 20: Co-immunoprecipitation of Connexin 43, hDlg and HPV-16 E6. A. Precipitation with ZO-1 antibody-linked beads and western blotting with an anti-Connexin 43 antibody. B. Precipitation with E6 antibody-linked beads and western blotting with an anti-hDlg antibody. C. Precipitation with hDlg antibody-linked beads and western blotting with an anti-Connexin 43 antibody. D. Precipitation with E6 antibody-linked beads and western blotting with an anti-Connexin 43 antibody. In each case the reverse experiment was also carried out, i.e. the antibody used for western blotting was linked to beads and the partner antibody used in western blotting, beads alone; Invol., involucrin antibody, CE, cell extract.

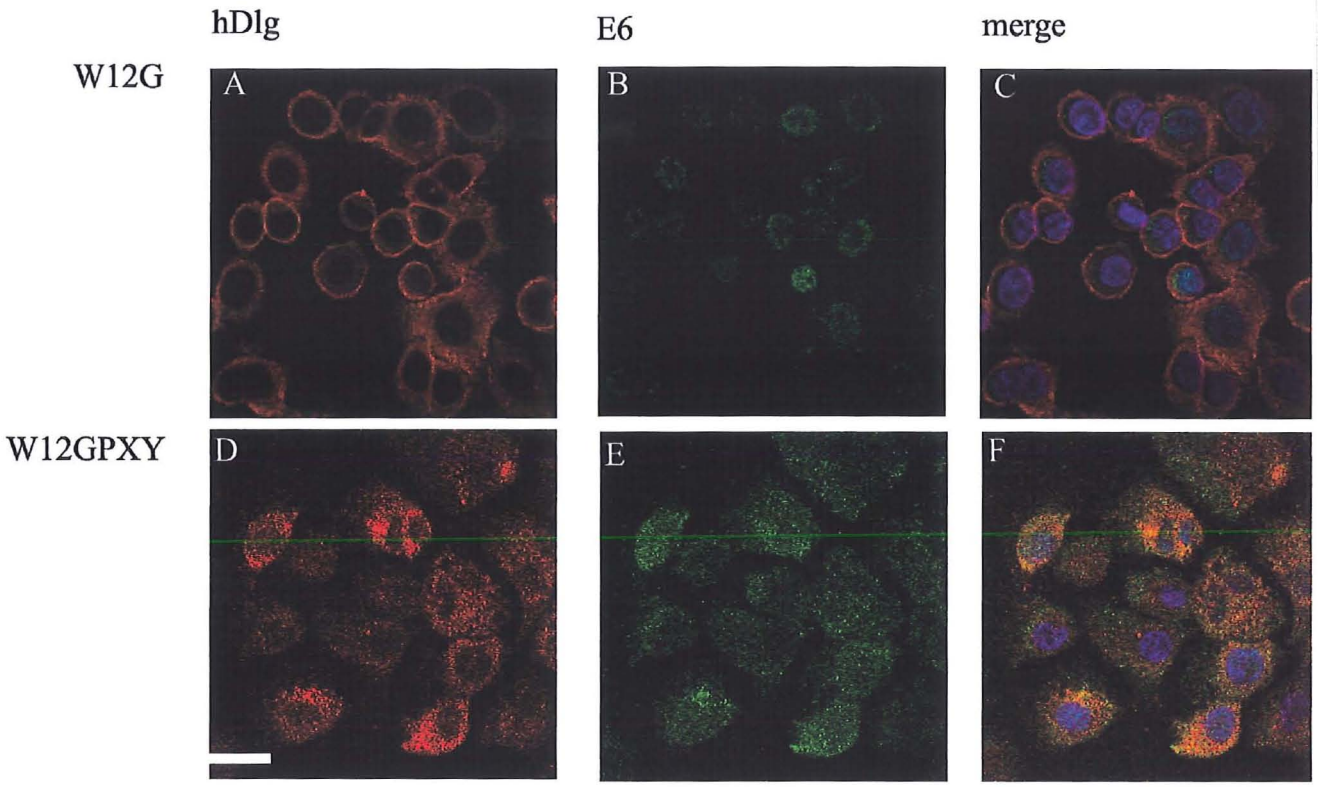

Figure 21: Co-immunofluorescence of W12G and W12GPXY cells. hDlg (A, D), E6(B, E), merge (C,F). Nuclei were stained with DAPI. Bars=10 μm.

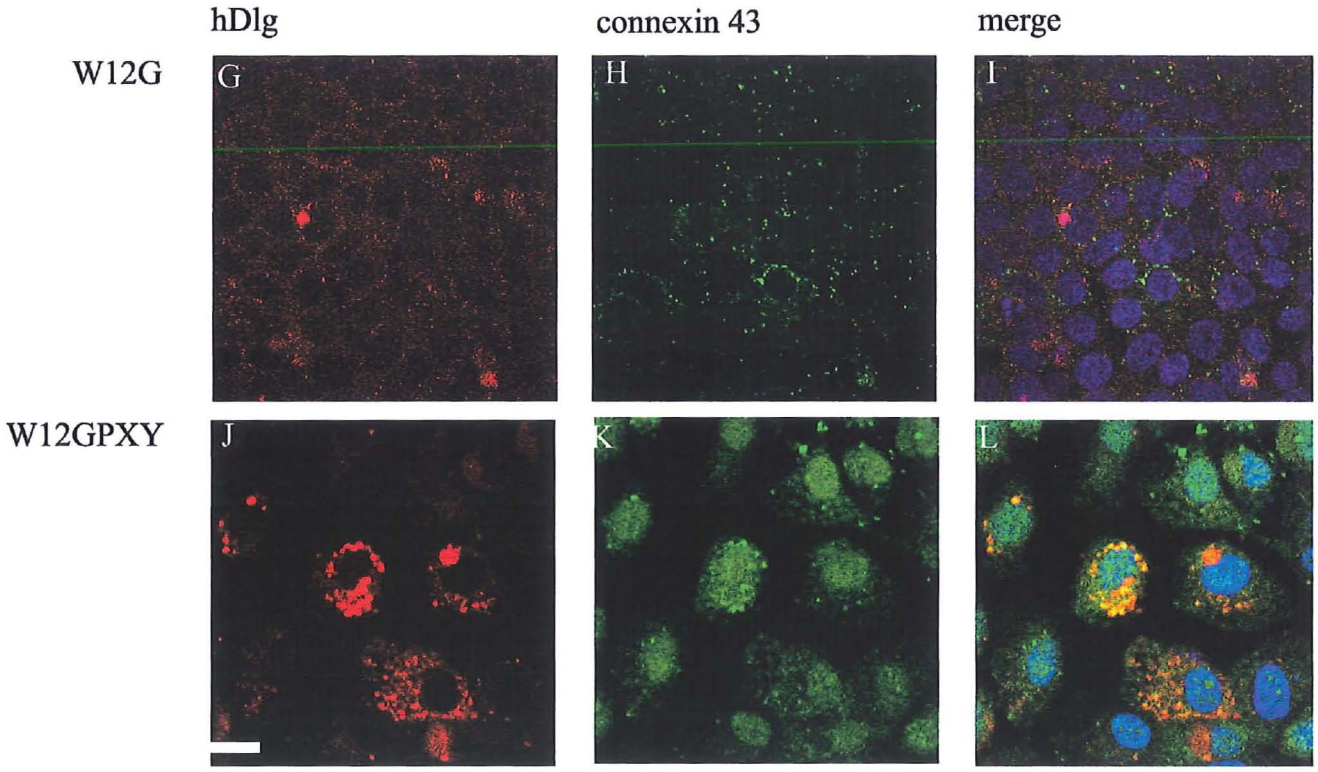

Figure 21: Co-immunofluorescence of W12G and W12GPXY cells. hDlg(G, J), Connexin 43(H, K), merge (I, L). Nuclei were stained with DAPI. Bars=10 μm.

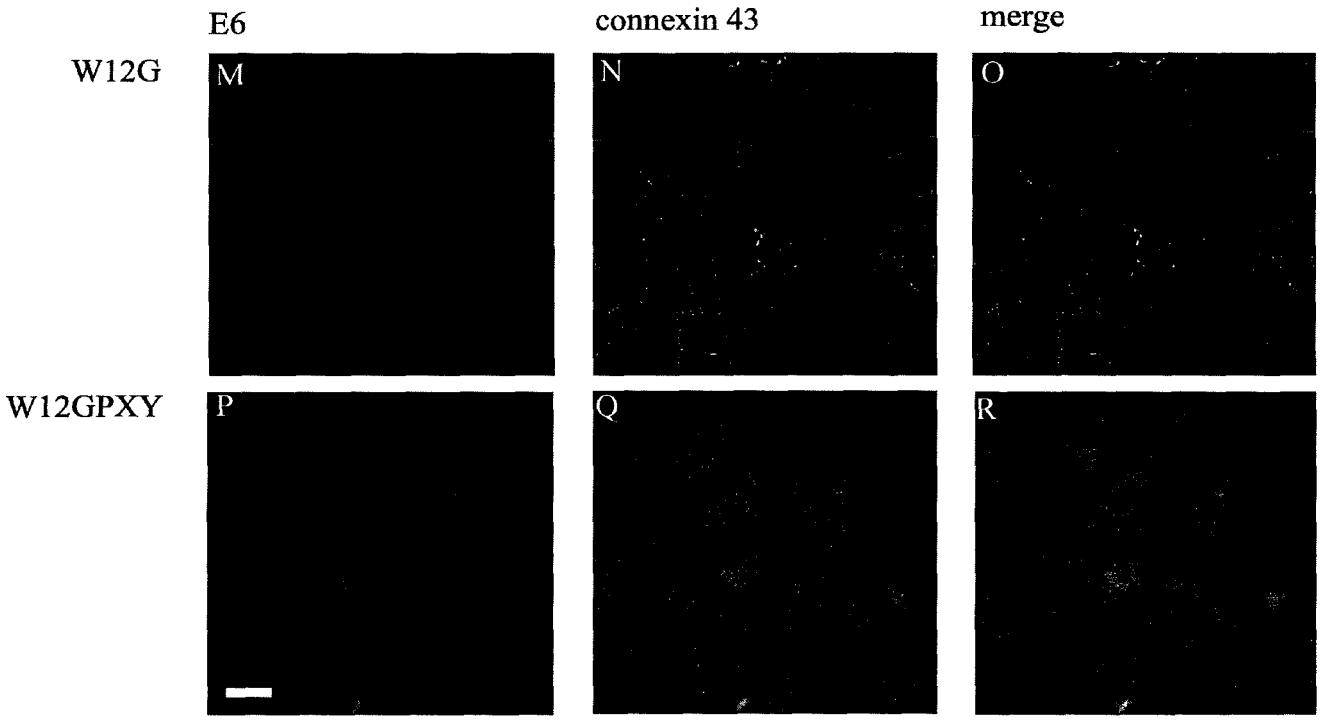

Figure 21: Co-immunofluorescence of W12G and W12GPXY cells. E6 (M, P), Connexin 43(N, Q), merge (O, R). Nuclei were stained with DAPI. Bars=0 μm.

4.2 Leptomycin B abrogates the relocation and co-localisation of hDlg and Connexin 43 into the cytoplasm of W12GPXY cells.

Given the evidence that in W12GPXY cells with increased cytoplasmic E6, hDlg and Connexin 43 were also relocated together into the cytoplasm, it was interesting to investigate whether the upregulated endogenous E6 was the vital reason for this interaction and relocation. If the HPV-16 cytoplasmic E6 protein was responsible for the co-localisation of hDlg and Connexin 43 in the cytoplasm of W12GPXY cells, then inhibition of nuclear export of E6 into the cytoplasm should disrupt formation of the E6/hDlg/Connexin 43 complexes, possibly leading to relocation of Connexin 43 to the plasma membrane. W12G cells treated with Leptomycin B (5 ng/ml Leptomycin B for 8 hours to inhibit nuclear protein export) had no change in localisation of either hDlg or Connexin 43 compared to untreated cells (Fig. 22 A-C). However, in W12GPXY cells, drug treatment resulted in loss of the cytoplasmic speckles containing hDlg and Connexin 43 and reappearance of Connexin 43 at the cell membrane (Fig. 22 E) that was not found in the mock-treated cells. Furthermore, most of Leptomycin B- treated W12GPXY cells microinjected with Lucifer yellow transferred the dye to the second or third layers of neighbouring cells, showing that functional Connexin 43 gap junction plaques were reformed at contacting plasma membranes after Leptomycin B treatment (Fig. 23 A). In these cells E6 was clearly localised mainly in the nucleus instead of in the cytoplasm, which suggested the cytoplasmic E6 was the trigger for redistribution of hDlg and Connexin 43 in W12GPXY cells (Fig. 22 K). Leptomycin B treatment also had a marked effect upon the shape of W12GPXY cells but not upon W12G cells: W12GPXY cell membranes lost projections and a layer of actin filament bundles was observed underlying the plasma membrane (Fig. 23 B).

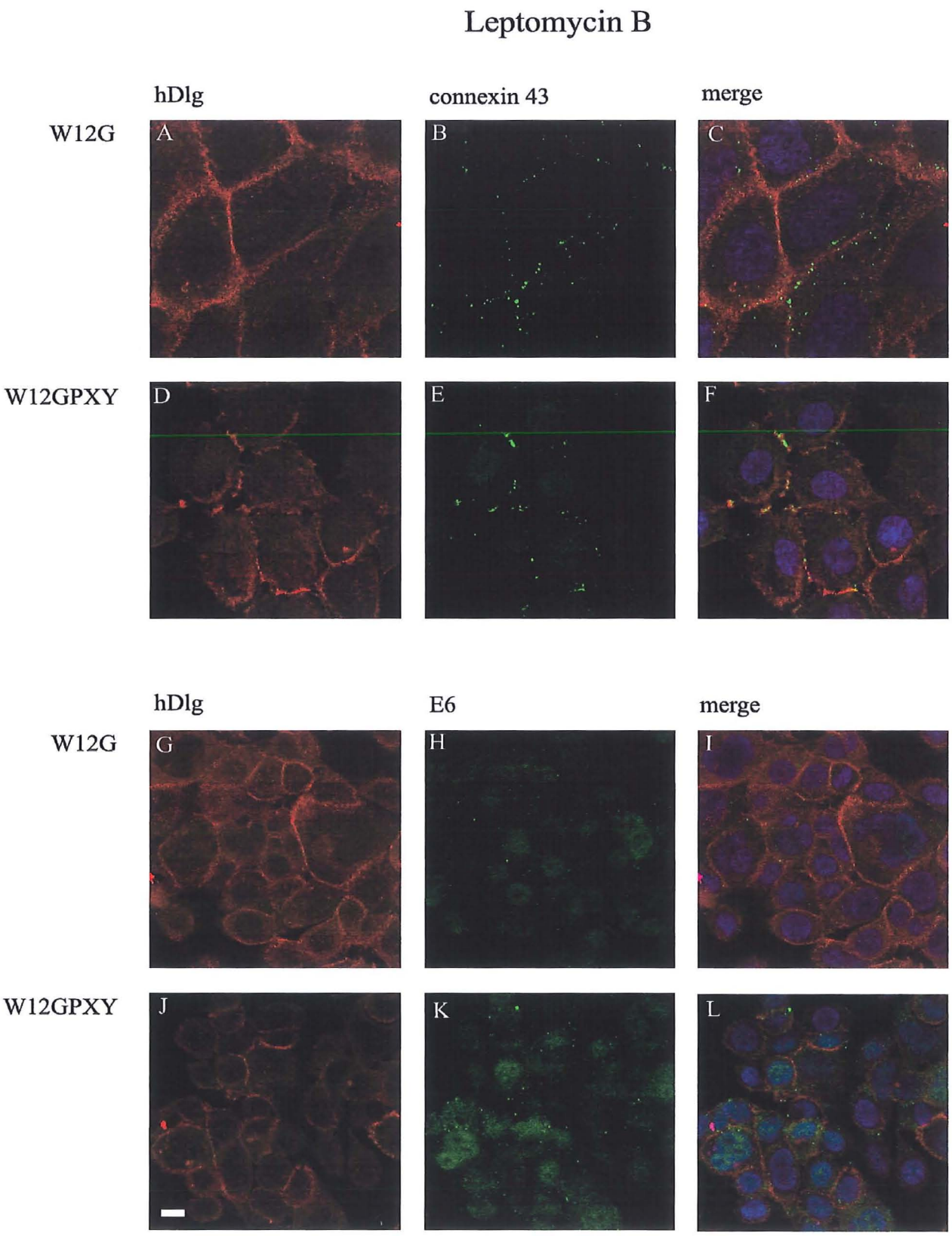

Figure 22: Co-immunofluorescence of Leptomycin B treated W12G and W12GPXY cells. hDlg (A, D), Connexin 43 (B, E), merge (C, F); hDlg (G, J), E6 (H, K), merge (I, L). Nuclei are stained with DAPI. Bars=20 μm.

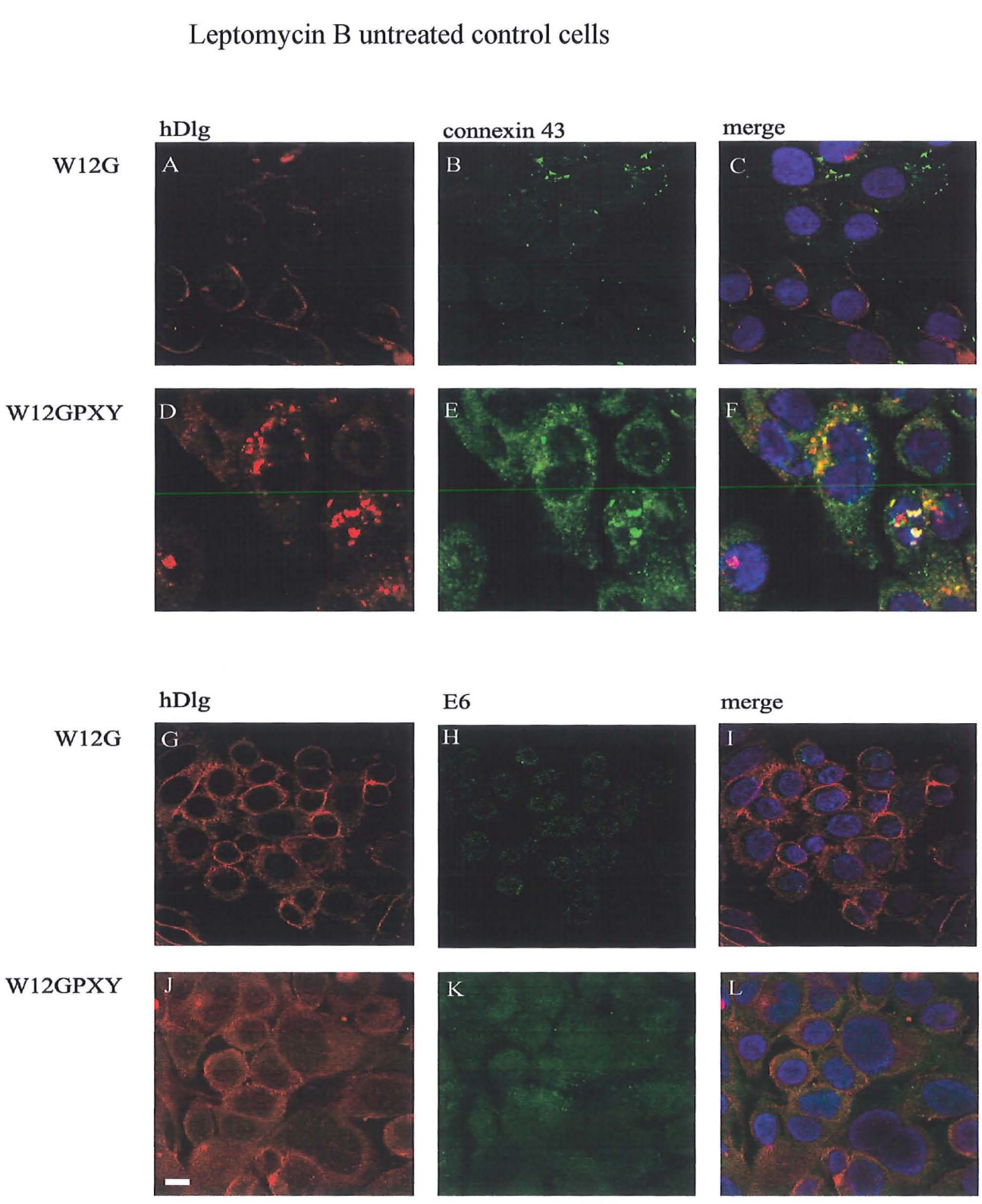

Figure 22-Control: Untreated W12G and W12GPXY cells for comparison with cells treated with Leptomycin B. Untreated control cells were given aqueous methanol diluent only. hDlg (A,D), Connexin 43 (B,E), merge (C,F); hDlg (G,J), E6 (H,K), merge (I,L). Nuclei are stained with DAPI. Bars=20 μm.

A

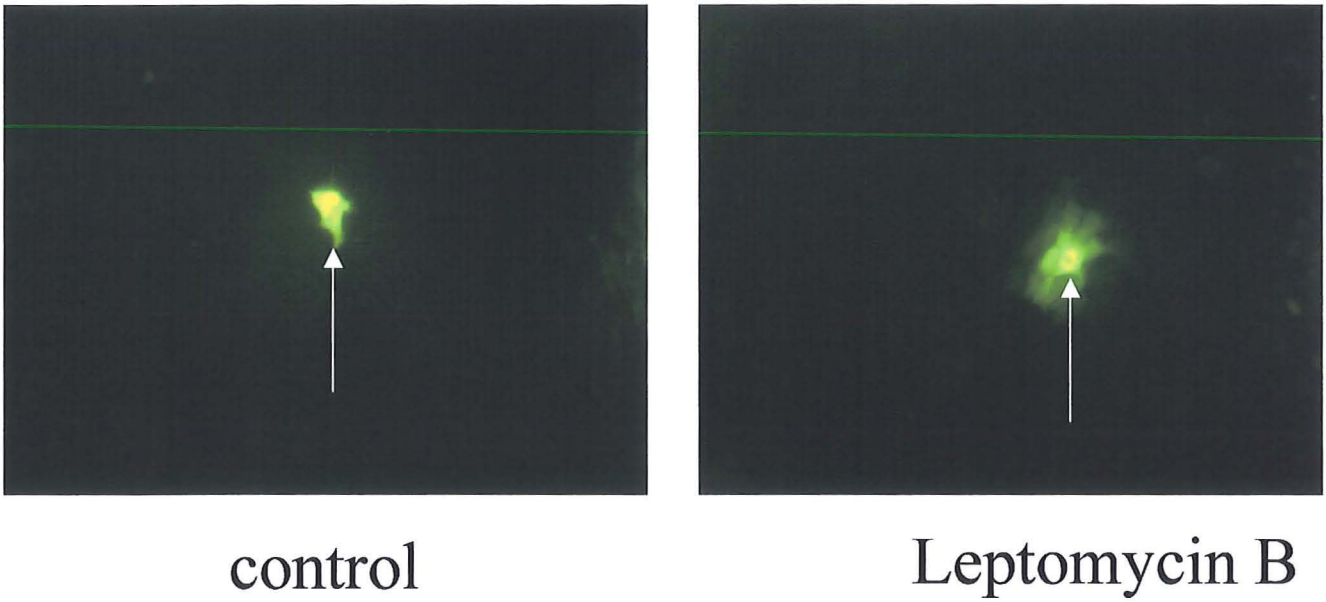

Figure 23 A: Leptomycin B treated and control W12GPXY cells were microinjected with Lucifer yellow. The white arrows point out the microinjected cells.

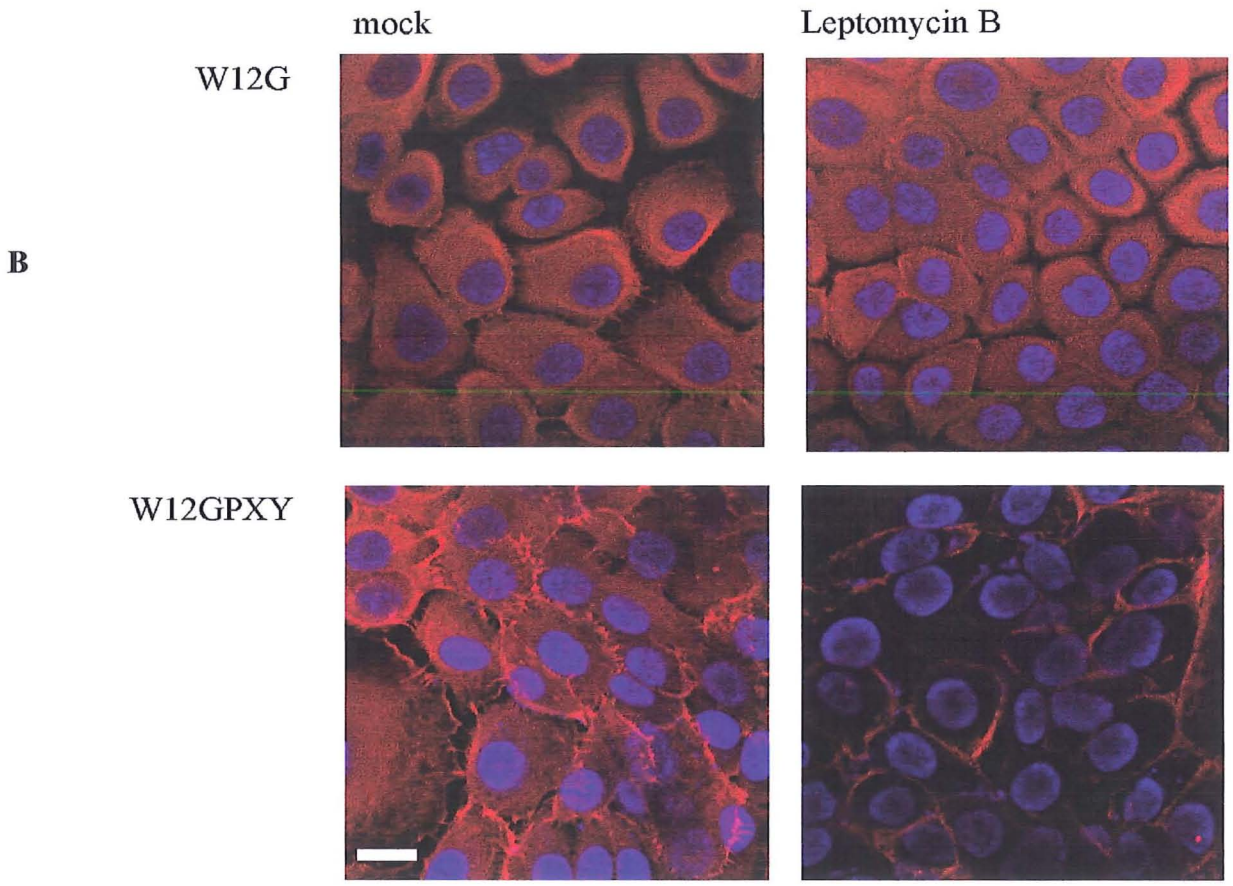

Figure 23 B: Phalloidin stain of Leptomycin B treated W12G and W12GPXY cells. Nuclei were stained with DAPI. Bars=20 μm.

4.3 siRNA knockdown of HPV16 E6 in W12GPXY cells redistributes Connexin 43 and hDlg from cytoplasm to plasma membrane and restores connexin 43 gap junction plaques at points of cell contact

To further confirm that elevated E6 protein caused relocation of Connexin 43 and hDlg from plasma membrane into cytoplasm, W12GPXY cells were transfected with siRNA directed against HPV16 E6. Western blots showed that siRNA against HPV16 E6 caused a marked decreased in total E6 protein in W12GPXY cells (Fig 24). This was accompanied by reversal of cytoplasmic co-localisation of Connexin 43 and hDlg, concomitantly with restoration of Connexin 43 gap junction plaques at points of cell-cell contact (compare Fig. 25 C, I). While mock transfection produced no change in cytoplasmic localisation of Connexin 43 and hDlg (Fig. 25 C), it was interesting to note that a control transfection with siRNA against BCR-ABL, while not restoring membrane localisation of Connexin 43 or hDlg, may have caused a subtle redistribution of the two proteins into smaller cytoplasmic aggregates (compare Figs. 25 C and F).

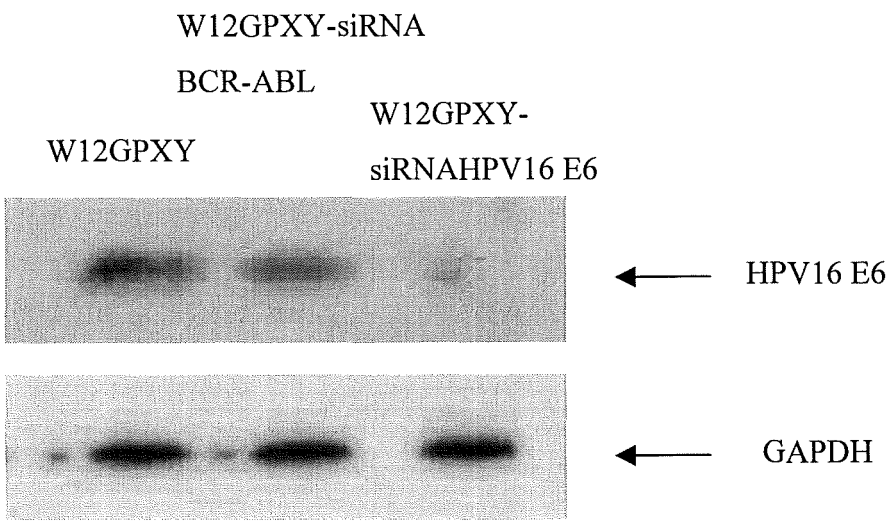

Figure 24. Western blot analysis of HPV 16-E6 in siRNA transfected W12GPXY cells. Track 1, W12GPXY cells treated with transfection reagents only; track 2, W12GPXY cells transfected with siRNA against BCR-ABL; track 3, W12GPXY cells transfected with siRNA against HPV-16 E6. Blots were reprobed with an anti-GAPDH antibody to demonstrate equal loading in each track.

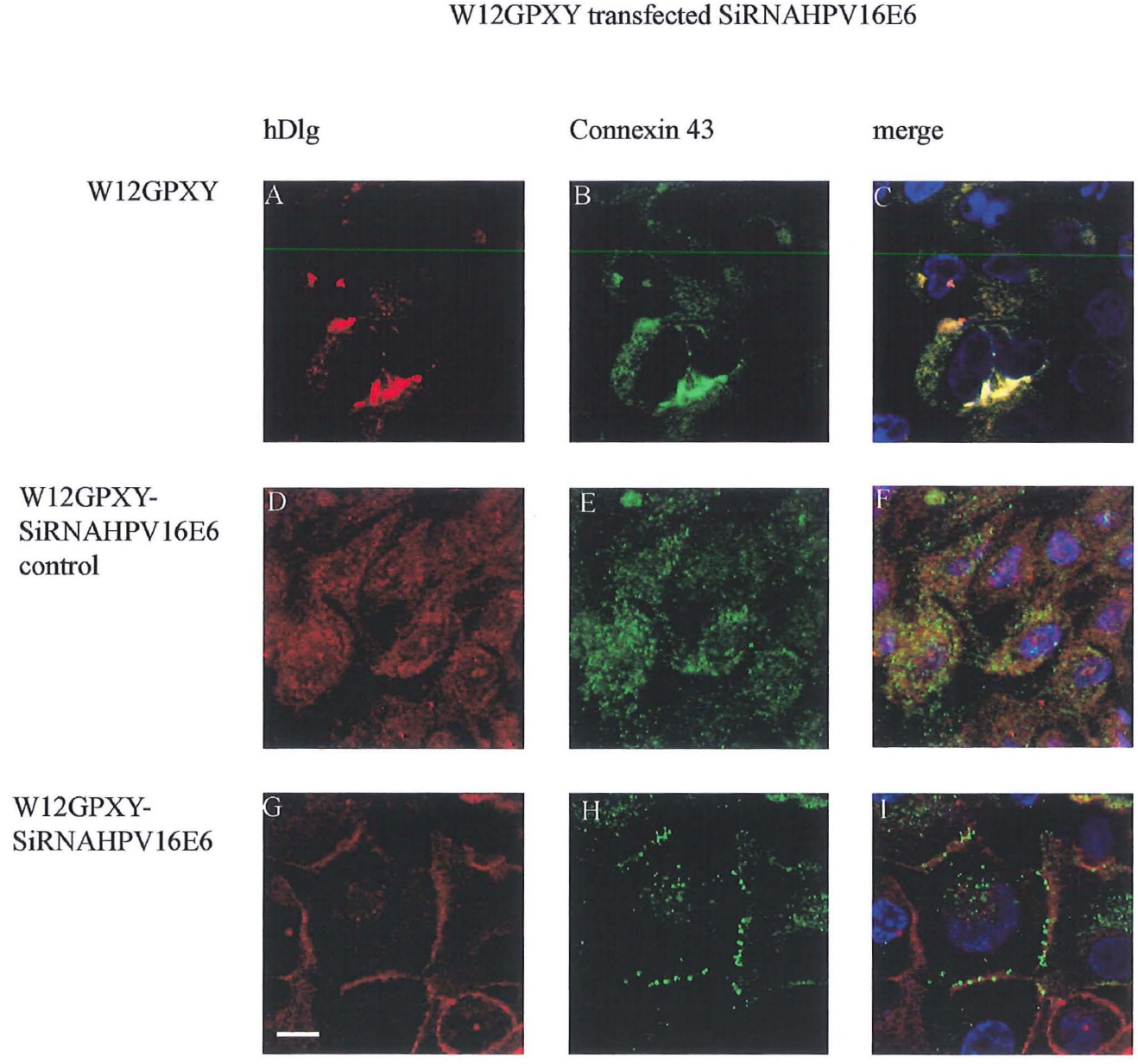

Figure 25: Co-immunofluorescence of W12GPXY cells transfected with siRNA. hDlg (A,D,G), Connexin 43(B,E,H), merge (C,F,I. Nuclei were stained with DAPI. Bars=20 μm.

4.4 Cervical keratinocytes transfected with wild type E6 display cytoplasmic relocalisation of Connexin 43 and hDlg.

To confirm the finding that E6 could mediate hDlg-connexin 43 re-location to the cytoplasm in HPV-16-transformed cells and E6 binding to the second PDZ domain was the vital trigger for hDlg-Connexin 43 association and relocation, C33a cells (a HPV-negative, but p53 mutant, cervical tumour line which displays large membrane Connexin 43 gap junction plaques) were transfected with empty vector (C33a-vec), a vector expressing HPV-18 wild type E6 (C33a-pNFWE6) and a vector expressing a mutant E6 lacking the hDlg binding site (C33a-pNFME6) (Gardiol et al., 1999). Firstly, in Western blot with the anti-flag antibody, it was shown there were amounts of HPV 18 wild/mutant E6 in the transfected cells (Fig. 26 A); then from IFA, it was suggested that the E6s were overexpressed both in nuclear and cytoplasm compartments (Fig. 26 B). In C33a and C33a-vec, transfected cells, most Connexin 43 and hDlg was detected on the cell membrane and Connexin 43 was present as gap junction plaques between the adjacent cells. (Fig. 27 ABC, DEF). In HPV-18 wild type E6 transfected cells (C33a-pNFWE6 cells) changes in localisation of Connexin 43 and hDlg were similar to those observed in W12GPXY cells. Most of Connexin 43 and hDlg was redistributed into the cytoplasm and the two proteins co-stained in large cytoplasmic speckles (Fig. 27 GHI). In contrast, in C33a cells transfected with the vector expressing a mutant E6 lacking the hDlg binding site, Connexin 43 was localised in gap junction plaques in the cell membrane and hDlg was also found in the membrane and periphery of the cell (Fig. 27 JKL).

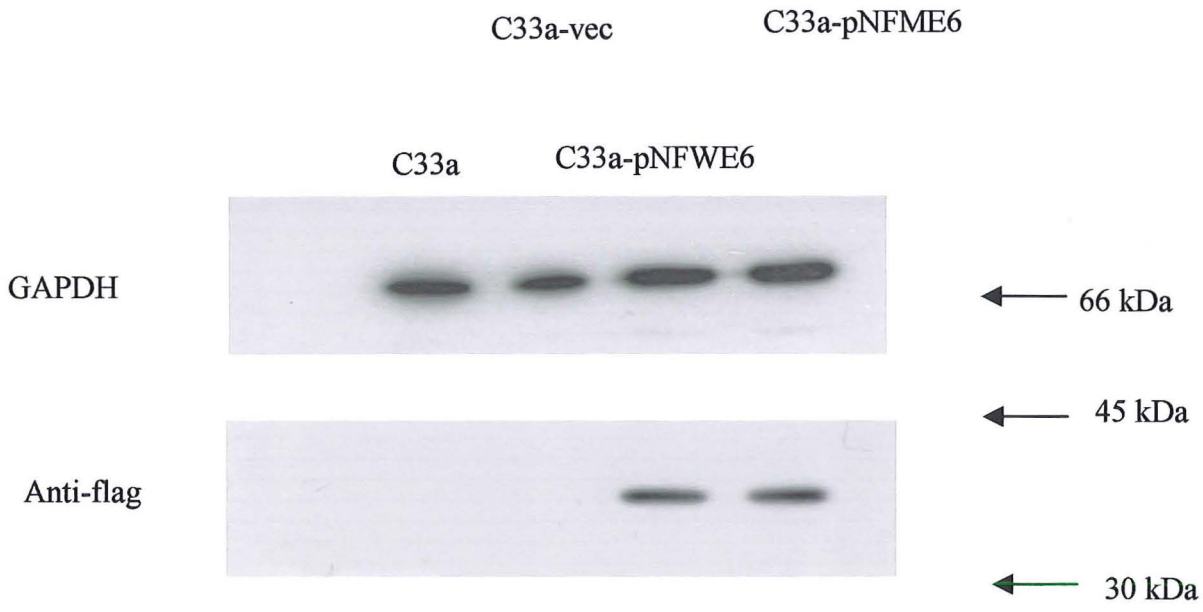

Figure 26 A: Western blot analysis of levels of flag fusion proteins in C33a, C33a-vec, C33a-pNFWE6 and C33a-pNFME6 cell lines. Blots were reprobed with an anti-GAPDH antibody to demonstrate equal loading in each track.

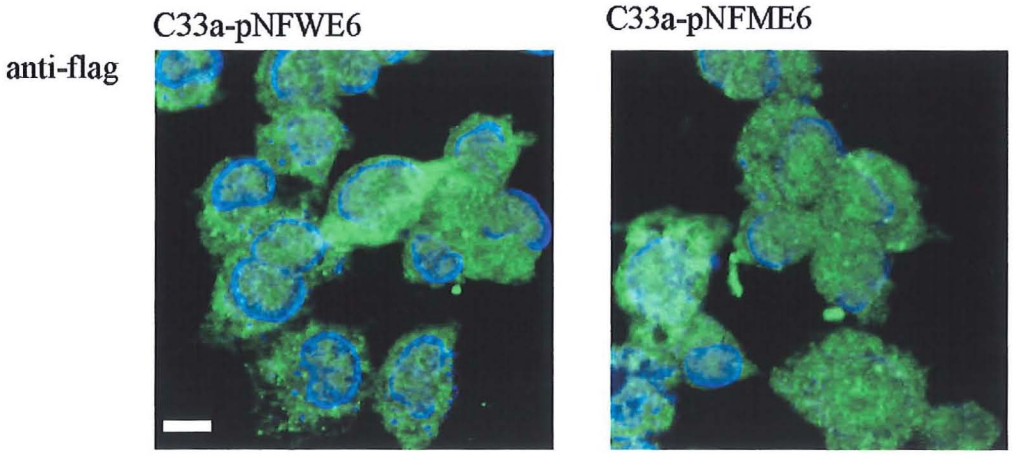

Figure 26 B: Immunofluorescence of C33a-pNFWE6 and C33a-pNFME6 stained with anti-flag to show cytoplasmic expression of E6 (green). Nuclei are stained with DAPI. Bars=10 μm.

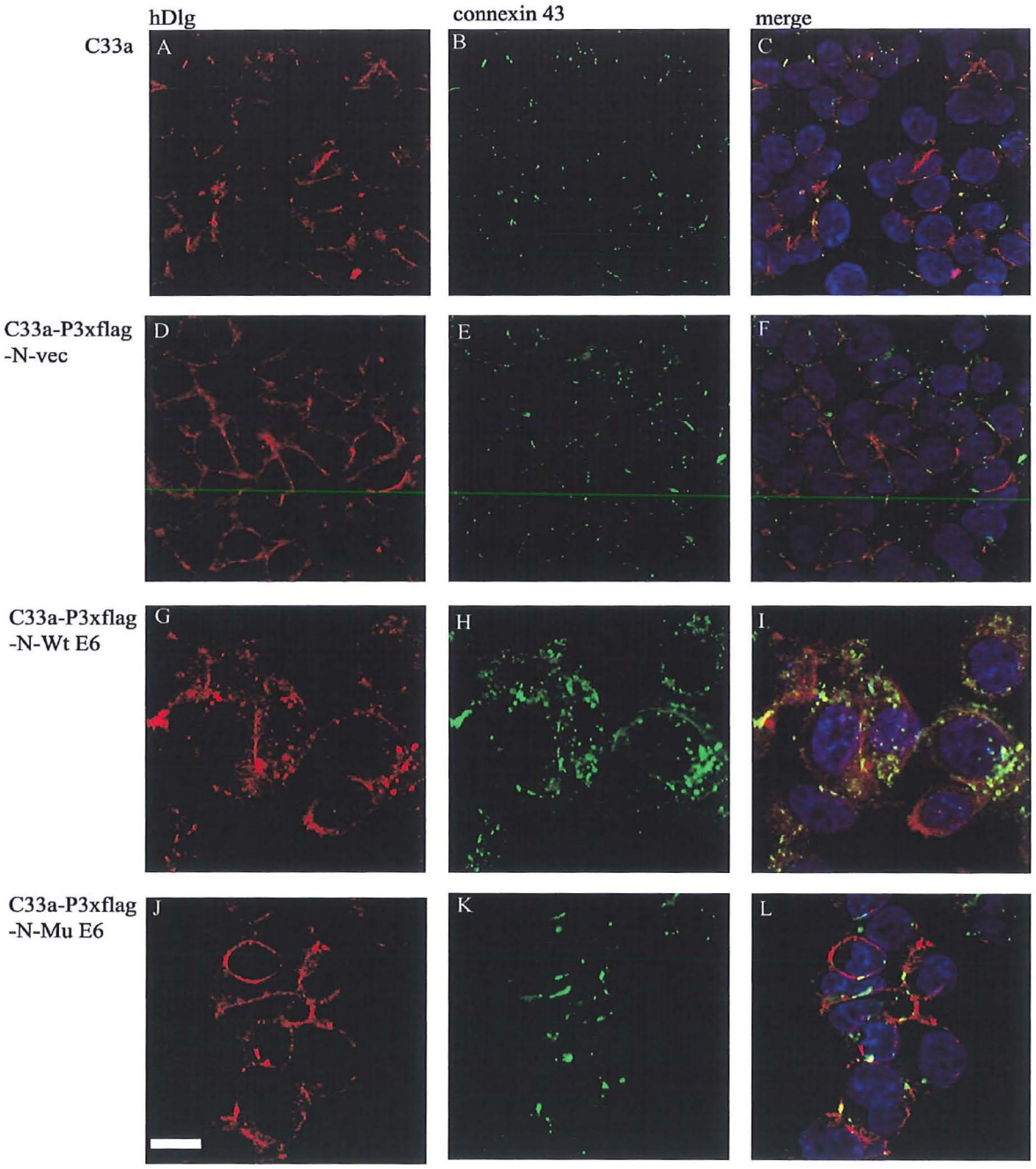

Figure 27: Immunofluorescence of C33a cells transfected with C33a-pNF (N-terminus flag empty plasmids), C33a-pNFWE6 (N-terminus flag-wild type HPV18 E6) and C33a-pNFME6 (N-terminus-mutated HPV 18 E6). hDlg (A,D,G,J), Cx43 (B,E,H,K), merge (C,F,I,L). Nuclei are stained with DAPI. Bars=10 μm.

4.5 Wild–type and C-terminal mutant Connexin 43 are differently localised in W12GPXY cells

To confirm that the last four amino acids DLEI in the C-terminus of Connexin 43 are key sites for binding to hDlg, mammalian expression plasmids for flag-tagged Connexin 43 and flag-tagged Connexin 43-Mu $tr_{378-382}$ were constructed. These were transfected into W12GPXY cells and stable cell lines selected. Anti-flag antibodies were used to detect Connexin 43 expressed from the transfected constructs. In W12GPXY cells transfected with wild- type Connexin 43-flag (vector pCFWCx43), both Connexin 43-flag and hDlg were detected in the cytoplasm and there was no staining found on the cell membranes (Fig. 28), and the two proteins were partially co-localised consistent with our previous results. In W12GPXY cells transfected with the Mu $tr_{378-382}$ Connexin 43-flag (vector pCFTCx43), the location of hDlg and Connexin 43 was quite different and there was no immunofluorescence co-stain of these two proteins. hDlg remained in the cytoplasm as in the cells transfected with a flag vector with no insert. Strikingly, most of Mu $tr_{378-382}$ Connexin 43-flag localised to cell membrane junction plaques at cell contacts. These data suggest that without the four C-terminal amino acids, DLEI, Connexin 43 can no longer associate with hDlg. Thus hDlg could be involved in the trafficking process of Connexin 43 between the plasma membrane and cytoplasm.

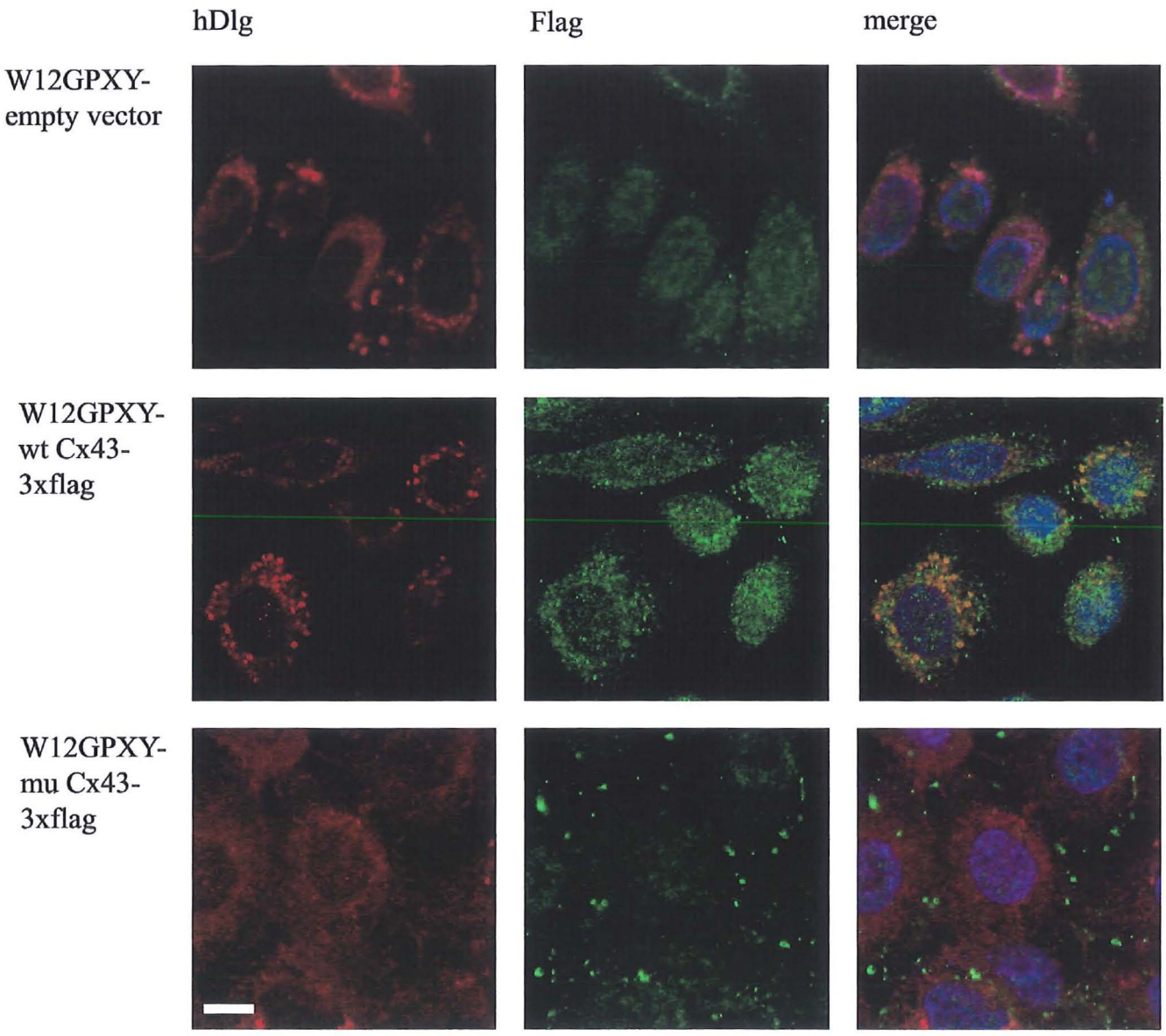

Figure 28: Co-immunofluorescence of W12GPXY cells transfected with C-terminal flag-tagged wild type and with C-terminal flag-tagged, C-terminal-mutated Connexin 43. hDlg (A,D,G), flag (B,E,H), merge (C,F,I). Nuclei are stained with DAPI. Bars=10 μm.

4.6 Discussion

The disorganisation of epithelial junctions can lead to defective cell-cell adhesion, loss of cell polarity and unregulated cell proliferation, and therefore may represent a crucial step in tumourigenesis. Connexin 43 is the most common unit of stratified epithelial cell gap junctions and, in keratinocytes in culture, its loss from the plasma membrane leads to loss of GJIC (Aasen et al., 2003; Shore et al., 2001).

The tumour suppressor Dlg and its human homologue hDlg, a membrane-associated guanylate kinase (MAGUK) family protein, have been found to be closely associated with regulation of cell architecture and control of cell proliferation and cell polarity and cell attachment (Woods et al., 1996; Goode & Perrimon, 1997; Bilder et al., 2000; Ishidate et al., 2000; Firestein & Rongo, 2001). The modular organization of these proteins allows them to function as scaffolds, which associate to transmembrane TJ proteins, the cytoskeleton and signal transduction molecules. In *Drosophila*, Dlg is located at septate juctions (Woods and Bryant, 1991) and genetic mutation causes tumour development in the imaginal disc. However, the role of Dlg as a tumour suppressor appears to be distinct from its role in maintaining septate junctions and localising membrane proteins (Woods et al., 1996).

High risk HPV E6 associates with hDlg and this association is important in cell transformation (Kiyono et al., 1997). The multifunctional HPV-16 E6 oncoprotein is known to have roles in tumour progression and can facilitate malignant transformation of HPV-associated tumours (Song et al., 1999; 2000). E6 is a shuttling protein that can move between the nucleus and cytoplasm. Our data show that the amounts and intracellular locations of HPV-16 E6 were distinctly different between W12G and the tumour-progressed W12GPXY cells. The increased amount of HPV-

16 E6 in the latter cells was most pronounced in the cytoplasmic compartment suggesting the possibility of E6 actions in addition to the well-characterised E6-p53 pathway during the later stages of malignant progression. This agrees with the observation that in HPV-associated cervical tumour samples, hDlg displayed an increased cytoplasmic localisation (Watson et al., 2002; Cavatorta et al., 2004). Finally, overexpression of HPV-18 E6 in SV40-transformed human keratinocytes resulted in marked reorganisation of the actin cytoskeleton and a decrease in intercellular adherens junctions, suggesting that the E6 PDZ-binding motif might regulate hDlg protein scaffolding complexes (Watson et al., 2003). The results in this chapter have shown that these E6 proteins bind to the second PDZ domain of the human homologue of hDlg through the high risk HPVs specific C-terminal XS/TXV/L (where X represents any amino acid, S/T serine or threonine, and V/L valine or leucine) motif that is similar to the interaction between the adenomatous polyposis coli gene product and hDlg; furthermore, it was found E6 mutants losing the ability to bind to hDlg was no longer able to target E6-dependent hDlg-Connexin 43 relocation from plasma membrane into cytoplasm. These results not only indicate the importance of E6 C-terminal region binding to the second PDZ site of hDlg in determining the binding specificity, but also imply that the E6 proteins of high-risk HPVs rather than low risk HPVs can bind hDlg through the common C-terminal motif. It suggested an intriguing possibility that interaction between the E6 protein and hDlg or other PDZ domain-containing proteins could be an underlying mechanism in the development of HPV-associated cancers.

Previous work demonstrated binding between the Connexin 43 C- terminus and ZO-1 (Geipmans and Moolenar, 1998). Now, our data has confirmed this association in the W12G and W12GPXY cell lines with I.P evidence, although the co-staining of

Connexin 43–ZO-1 was no as strong as Connexin 43-hDlg in W12GPXYcells. It is proposed there is competition between hDlg and ZO-1 for binding to Connexin 43 in W12GPXY cells, whether E6 could affect the competition and promote hDlg associated with Connexin 43 is interesting for further investigation. Recently hDlg was identified as a potential binding partner for the Connexin 43 C-terminal tail in a Tandem Mass Spectrometry (MS/MS) analysis screen (Singh & Lampe, 2003). Our studies now provide direct and indirect evidence that hDlg interacts with Connexin 43 via the latter's C-terminal PDZ-binding domain. This suggests that, similar to its homologue ZO-1, hDlg could be involved in assembly or disassembly of Connexin 43 gap junctions. The idea receives support from our finding that elevated amounts of cytoplasmic HPV-16 E6 in W12GPXY cells led to relocation of Connexin 43 from gap junction plaques into the cytoplasm in association with hDlg. Moreover, in W12GPXY cells, inhibiting E6 nuclear export by Leptomycin B or siRNA knockdown of E6 restored Connexin 43 to gap junction plaques on cell membranes. Furthermore, exogenous cytoplasmic expression of wild type HPV 18 E6, but not E6 lacking the hDlg binding site, in C33a cells resulted in redistribution of Connexin 43 from gap junctions into the cytoplasm in association with hDlg, demonstrating a causal relationship between E6 and redistribution of hDlg / Connexin and that the second PDZ ligand domain of high risk HPVs E6 is required for the induction of binding and relocation of hDlg-Connexin 43. Two other viruses, human T-cell leukemia virus (Rousset et al., 1998) and adenovirus 9 (Glaunsinger et al., 2000), encode oncogenes that bind PDZ domain-containing proteins. Interestingly, the PDZ ligand domain of adenovirus 9 oncoprotein, E4 ORF-1, has recently been found to be important for its oncogenic activities (Frese et al., 2000). The MAGUK family proteins (hDlg, ZO-1, ZO-2, PSD-95/SAP 90, p55 and others) display similar

modular structure composed of 2-3 PDZ domains, an SH3 domain and guanylate kinase homology (GuK) domain but hDlg also contains an NH_2-terminal domain, which is not found in other MAGUKs (Lue et al., 1994; 1996). The precise arrangement of ternary complexes between E6, hDlg and Connexin 43 remains to be determined (Appendix 5, p261). These results and ours indicate that interactions between viral proteins and PDZ domain-containing proteins constitute a general mechanism for virus-induced oncogenesis.

It is now clear that Connexin 43 can associate with both ZO-1 and hDlg within cells, but it remains to be seen whether or not it complexes with other MAGUK proteins having common second PDZ domains. Similarly, whether or not there is Connexin 43 binding competition between hDlg and ZO-1 needs to be investigated. Although it is still unclear what role hDlg plays in the transport cycle of Connexin 43, our immunoprecipitation data show that Connexin 43 and hDlg associate in both W12G and W12GPXY cells and in C33a cells. Thus binding between the last four amino acids in the Connexin 43 C-terminus and hDlg does not disrupt Connexin 43 trafficking from the ER to the cell membrane, and assembly into gap junctions when cytoplasmic levels of E6 are low. However, hDlg could play a key role in the relocation of Connexin 43 into the cytoplasm in W12GPXY cells when cytoplasmic E6 protein is abundant. In a scaffolding model, the different domains of hDlg serve as docking modules for the interactions with the different protein/polypeptides (Hung and Sheng, 2002). hDlg could function in the transport cycle of Connexin 43 by providing a docking platform for molecules involved in assembling or disassembling of gap junctions. Dlg and hDlg are important for adherens junction assembly and maintenance of actin filament and microtubule networks (Firestein and Rongo, 2001; Laprise et al., 2004; Watson et al., 2003). It is therefore noteworthy that the

restoration of Connexin 43 gap junction plaques in W12GPXY cells by Leptomycin B or siRNA knockdown of E6 was accompanied by changes in cell shape and rearrangement of the actin cytoskeleton. The present results suggest that binding with HPV-16 E6 may disrupt hDlg control of Connexin 43 trafficking, resulting in decreased formation of gap junctions on the cell membrane that may lead to tumour progression (Appendix 6, p262).

In conclusion, these findings highlight a role for hDlg in Connexin 43 trafficking between the plasma membrane and the cytoplasm. It is likely that this will be a significant mechanism leading to loss of GJIC during malignant progression of keratinocytes. It will be of interest to see whether or not hDlg is involved in loss of Connexin 43 gap junctional communication in non-HPV-induced tumours. There may be parallels to be drawn between the loss of gap junctional communication which results from the E6 – hDlg – Connexin 43 interaction described here and the disruption of Connexin 43 –ZO-1 interactions by Src (Toyofuku et al., 2001).

Chapter 5. RESULTS 3

THE TRAFFICKING AND DEGRADATION OF CONNEXIN 43 AND HDLG IN LATE STAGE OF HIGH RISK HPV POSITIVE CERVICAL CARCINOGENESIS

During protein synthesis and processing, the cell has an elaborate quality control system that monitors the whole procedure and functions rapidly to degrade aberrant proteins through the proteasomal and/or lysosomal degradation pathway (Ellgaard et al., 1999). Connexins, the integral membrane protein constituents of gap junctions, are degraded with a half-life 1.5-5 hours, much faster than most other cell surface proteins. Connexins, misfolded or abnormally assembled, are frequently retained in the endoplasmic reticulum and subject to endoplasmic reticulum-associated degradation by the ubiquitin-proteasome system (Viviana et al., 2004). In addition to this, it was shown that post-endoplasmic reticulum quality control mechanisms could lead to some mutant or non-native connexins being transported to the Golgi complex and post-Golgi compartments before intracellular disposal (Musil et al., 2000; Qin et al 2003). In some instances, it was proposed that connexins, like other membrane proteins, may undergo retrograde transport back to the endoplasmic reticulum with re-targeting to the endoplasmic reticulum-associated degradation pathway; or they are targeted directly into the endosomal system for vacuolar/lysosomal degradation and or may first be routed to the plasma membrane prior to their delivery to endosomal system for vacuolar/lysosomal degradation. It is also possible that a subset of newly synthesized connexins utilize early endosomes as a bio-synthetic intermediate during their first pass through the endomembrane system en route to the cell surface, and then undergo ubiquitination and proteasomal degradation in the plasma membrane (Laing and Beyer, 1995; Ellgaard et al., 1999; Benharouga et al., 2001; Tomas et al.,

2003). This membrane protein quality control targeting is likely not only to involve recognition of commonly expressed mutant connexins, but also possibly in wild-type connexins, especially ones at the cell surface with perturbation of local microenvironments essential for trafficking and stability of gap junction (Mazzoleni et al., 1996; Koval et al., 1997). One of the possibilities in connexin quality control system is postulated in Fig, 29. Although the degradation of connexin has been shown to be sensitive to inhibitors of either the lysosome or of the proteasome, the relative importance of proteasomal vs lysomal pathways in connexin degradation and how the processes are regulated to affect intercellular communication is not clear.

Previous reports and evidence presented in this thesis have indicated that viral oncoproteins might play a role in tumour promotion by their influence on the regulation of gap-junctional intercellular communication (Fletcher et al., 1987; Oelze et al., 1995). This chapter now looks at mechanisms underlying the virus-induced aberrant trafficking and delocalization of Connexin 43 in W12GPXY cells. From earlier results presented, it is postulated that hDlg acts in a manner analogous to an itinerant vesicular protein; initial HPV 16 E6 associated hDlg targeting to intracellular membrane compartments may participate in cellular trafficking and assembly of gap junction proteins.

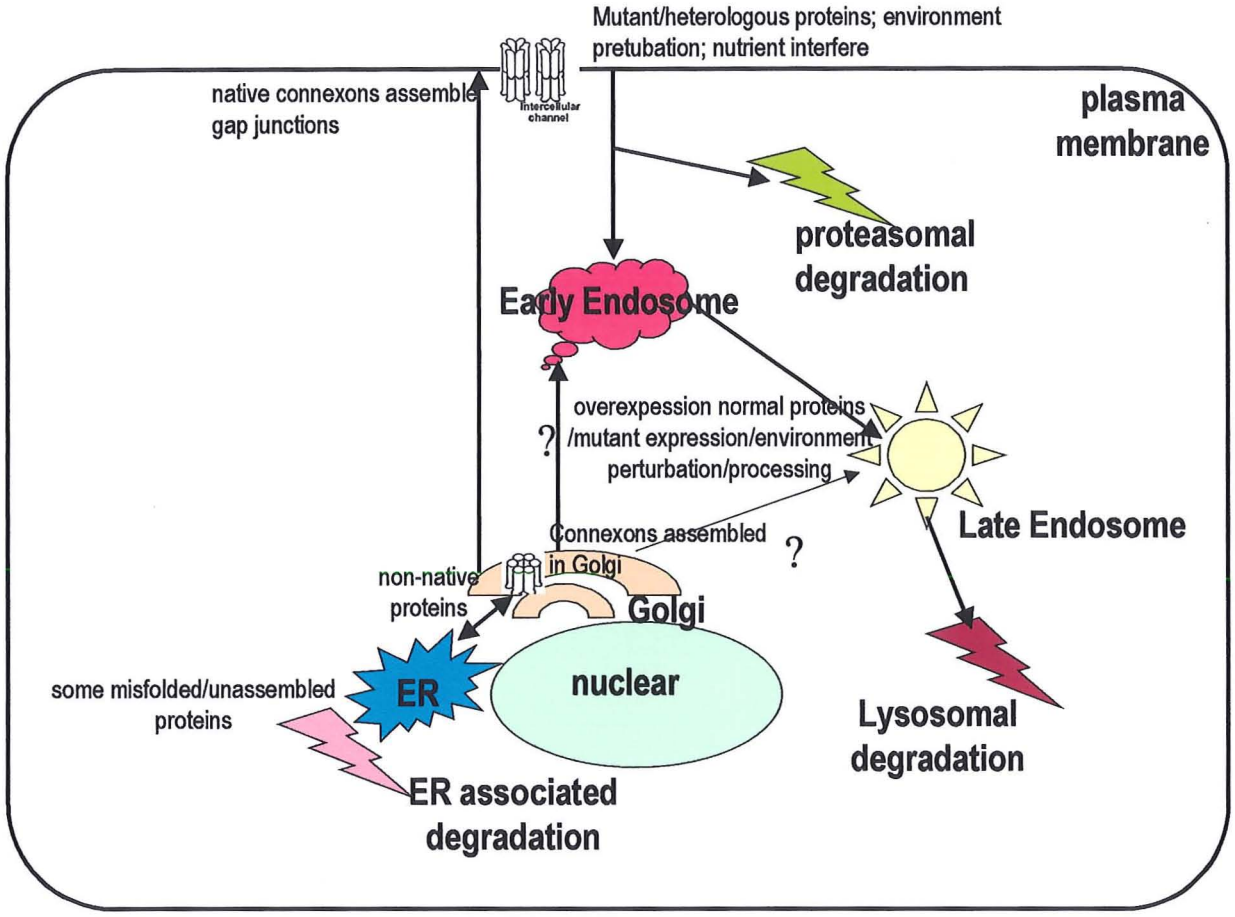

Figure 29: Model for the degradation pathways of connexins. Connexins are synthesised in ER and transmitted into the trans-Golgi network, subsequently targeting to cell surface or early endosome. Connexins are degraded through proteasomal and /or lysosomal pathways.

5.1 Both microtubules and microfilaments regulate relocation of the Connexin 43 and hDlg complex into the cytoplasm in W12GPXYcells.

Staining with Phalloidin-TRITC clearly revealed significant differences in actin filament distribution between W12G and W12GPXY cells (Figure 30 A). W12G cells appeared polygonal in shape and made extensive contacts with neighbouring cells while W12GPXY cells displayed an elongated phenotype with many cell projections and barbed points on the cell membranes; the overall level of cell-cell contact appearing much reduced in comparison with W12G. Cytoplasmic actin filament bundles were evenly spread in W12G cells, but were more abundant in W12GPXY cells (refer to Fig. 19). After treatment with Cytochalasin B to distrupt actin filaments, actin concentrated into plaques and speckles in the cytoplasm, more obviously in W12GPXY cells (refer to Fig. 23). Immunofluorescence with an anti-tubulin antibody revealed the microtubule network in the cytoplasm of untreated W12G and W12PXY cells. Nocodazole treatment resulted in aberrant accumulation of tubulin all through the cytoplasm (Figure 30 B).

When Cytochalasin B was used to disrupt actin filaments in W12G cells, Connexin 43 remained localised in well-defined membrane plaques although a little more cytoplasmic protein could be observed than in the untreated cells (Figure 31 A panel B). Little change in hDlg location was observed: most membrane staining remained with a little of the protein located as a diffuse stain in the cytoplasm (Figure 31 A panel A). There was no co-localisation of hDlg and Connexin 43 in Cytochalasin B treated W12G cells (Figure 31 A panel C). In Cytochalasin B treated W12GPXY cells, the cytoplasmic co-localisation of hDlg and Connexin 43 seen in untreated cells was retained, (Figure 31 A panels D-E). These data indicate that both Connexin 43 and hDlg membrane targeting in W12G cells does not, or at least not completely, rely on functional microfilaments. Furthermore, redistribution of Connexin 43 and hDlg in W12GPXY cells does not result from rearrangement of the actin cytoskeleton.

After treatment of W12G cells with Nocodazole, the most striking change was that most of cell surface Connexin 43 relocated to the cytoplasm in a perinuclear distribution (Figure 31 B panel H). In Nocodazole treated W12G cells, most hDlg could be detected in the cytoplasm rather than on plasma membrane (Figure 31 B panel G), although there was still no co-staining observed with Connexin 43. In

Nocodazole treated W12GPXY cells, hDlg showed some perinuclear localisation but was mostly located diffusely throughout the cytoplasm (Figure 31 B panel J). Furthermore, in W12GPXY cells treated with Nocodazole, Connexin 43 remained localised with hDlg (Figure 31 B panel K, L). Taken together, these findings indicated that microtubules are involved in the normal membrane localisation of Connexin 43 and hDlg in W12G cells but that the relocation of the two proteins into the cytoplasm of W12GPXY cells is not a direct result of reorganisation of the micro-tubular system.

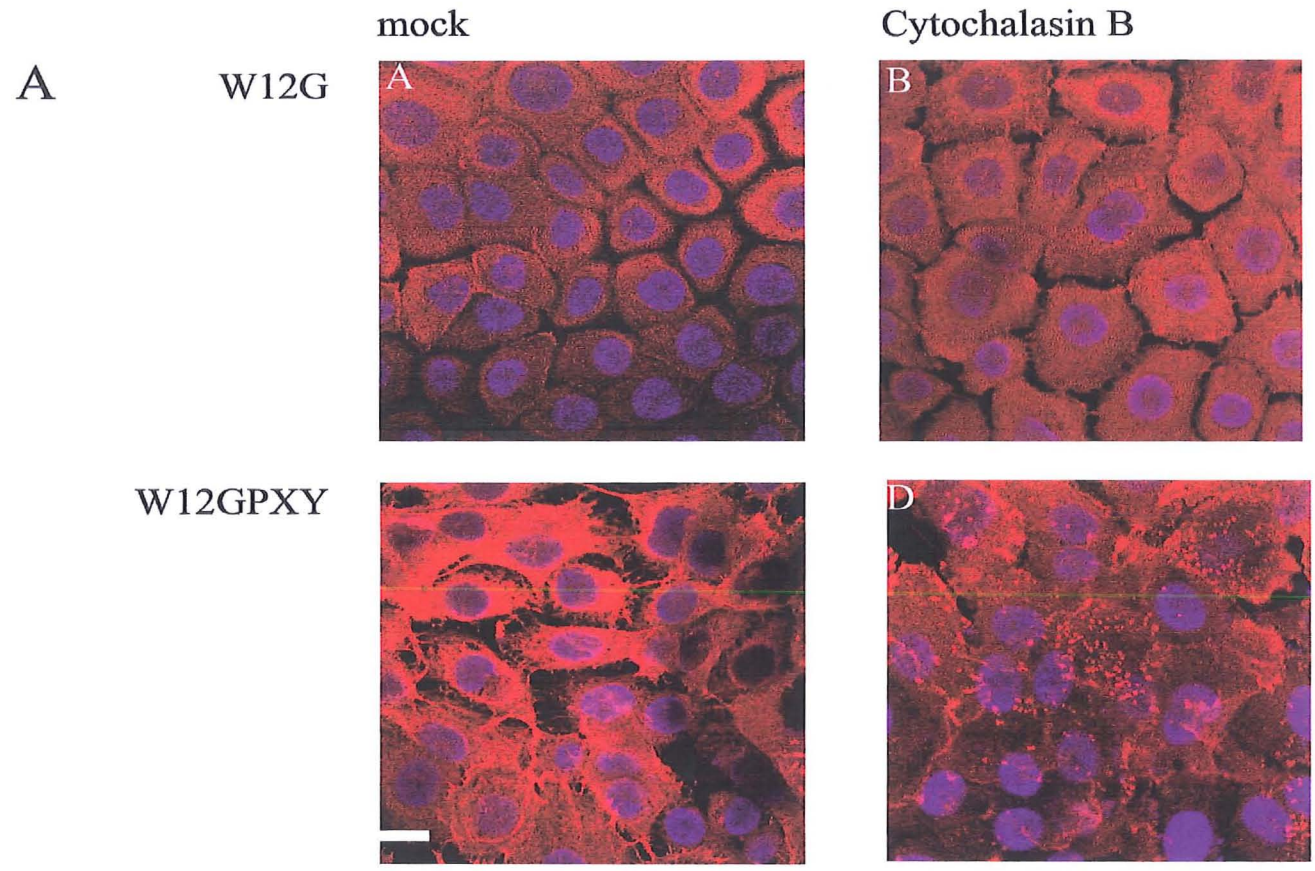

Figure 30: Effect of disruption of the cytoskeleton of W12G and W12GPXY cells.
A: Phalloidin stain of Cytochalasin B treated cells. A, C, mock-treated W12G V W12GPXY cells; B, D Cytochalasin B treated W12G and W12GPXY cells. Nuclei are stained with DAPI. Bar=10μm.

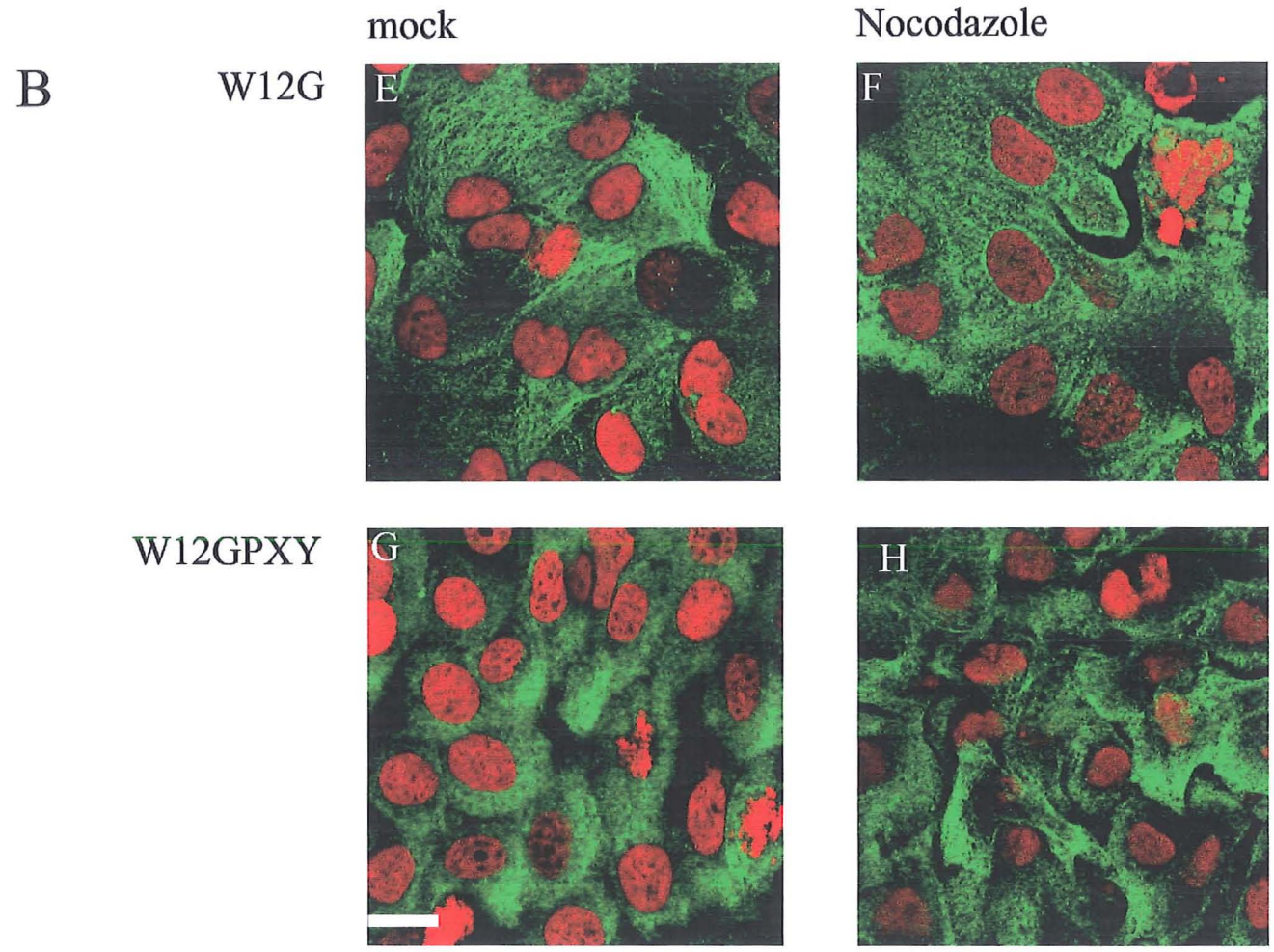

B: Immunofluorescence staining with an anti-tubulin antibody of Nocodazole treated cells. E, G., mock-treated W12G V W12GPXY cells; F, H Nocodazole treated W12G and W12GPX cells. Nuclei are stained with propidium iodide. Bar=10μm.

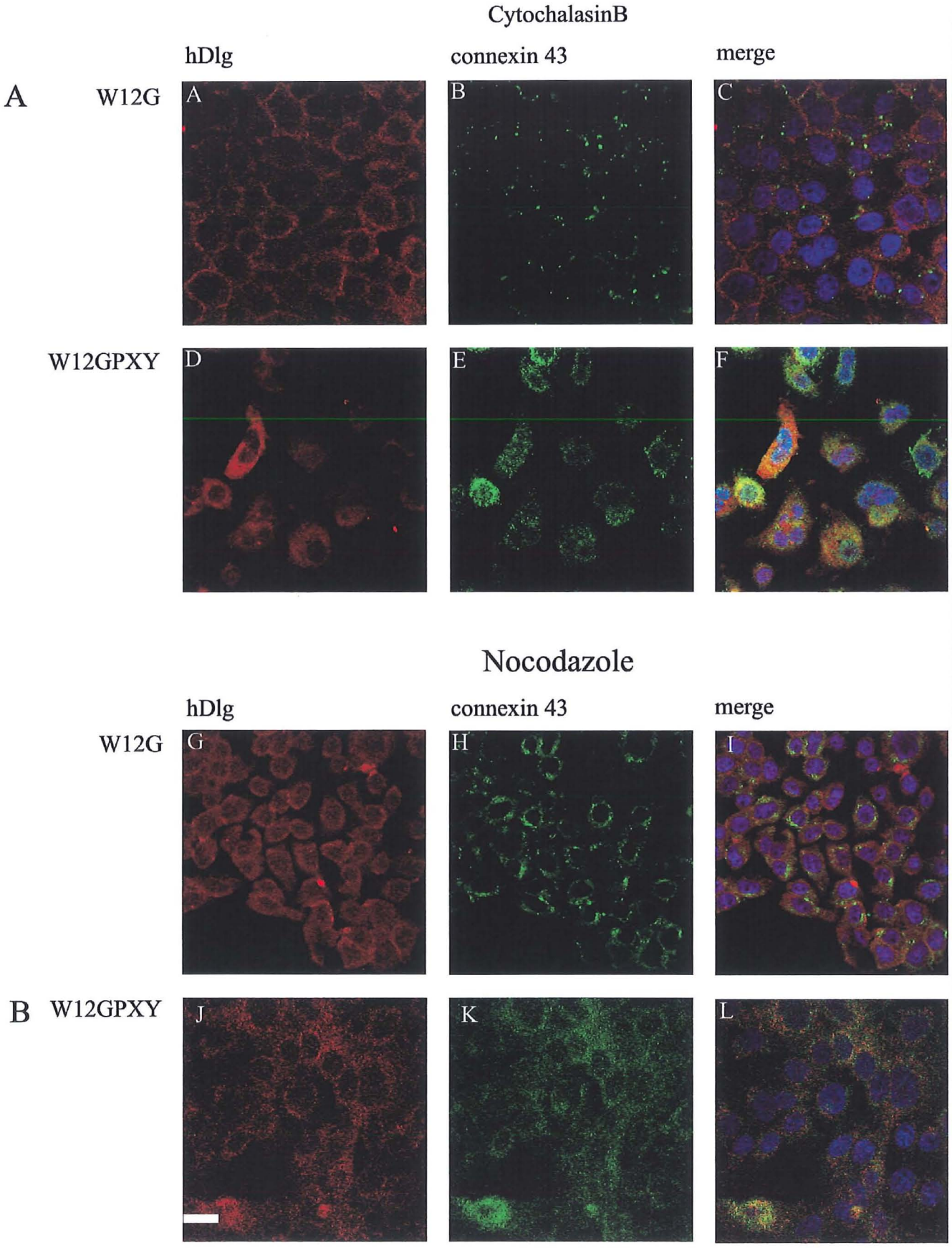
CytochalasinB
hDlg
connexin 43
merge
A
W12G
A
B
C
W12GPXY
D
E
F
Nocodazole
hDlg
connexin 43
merge
W12G
G
H
I
B
W12GPXY
J
K
L

Figure 31: Effect of disruption of the cytoskeleton on distribution of Connexin 43 and hDlg in W12G and W12GPXY cells. Nuclei are stained with DAPI. Bar=10μm.
A: Effect of Cytochalasin B. Panel A-C, W12G cells, panel D-F W12GPXY cells; A, D hDlg stain; B, E Connexin 43 stain; C, F merged image of A, B and D, E respectively. Note lack of effect of Cytochalasin B in distribution of hDlg and Connexin 43.

B: Effect of Nocodazole. Panel G-I, W12G cells, panel J-L W12GPXY cells; G, J hDlg stain; H, K Connexin 43 stain; I, L merged image of G, H and J, K respectively. Note lack of effect of Nocodazole in distribution of hDlg and Connexin 43.

5.2 hDlg and Connexin 43 were not blocked in the trans-Golgi network

It is important to investigate where in the cytoplasm hDlg associated with Connexin 43 to understand the mechanism of hDlg in the trafficking and degradation of Connexin 43. In different systems, Connexin 43 was reported to distribute into three main subcellular locations: plasma membrane-associated gap-junction plaques, a perinuclear population, and intracellular vesicles (Lampe and Lau, 2000; Defamie et al., 2001). Previous studies demonstrated that perinuclear Connexin 43 probably was assembled in the trans-Golgi network, while intracellular vesicle-like distribution of Connexin 43 was probably involved in the lysosomal pathway (Das et al., 2001; Qin et al., 2003). My results showed there was les than 3% of total Connexin 43 staining on cell membrane in W12GPXY cells, but most of Connexin 43 ($\geq$ 97%) was in the cytoplasmic compartments. Therefore, it was important to know whether Connexin 43 binding to hDlg occurred either prior to or post the trans- Golgi network.

Co-staining with an anti-Golgi marker of both Connexin 43 and hDlg was used to define whether these proteins accumulated in the Golgi apparatus in W12GPXY cells. As shown in (Fig. 32 (B, E)), the Golgi maker stained compartments were perinuclear while the majority of either Connexin 43 or hDlg (Fig. 32 (A, D)) localized in other cytoplasmic regions. Not surprisingly, there was some co-localization of Golgi with both proteins (Fig. 32 (C, F)). These data indicated both hDlg and Connexin 43 transited through the trans-Golgi network but suggested that the cytoplasmic association of the two proteins in W12GPXY cells happened not in the Golgi but in other cytoplasmic compartments.

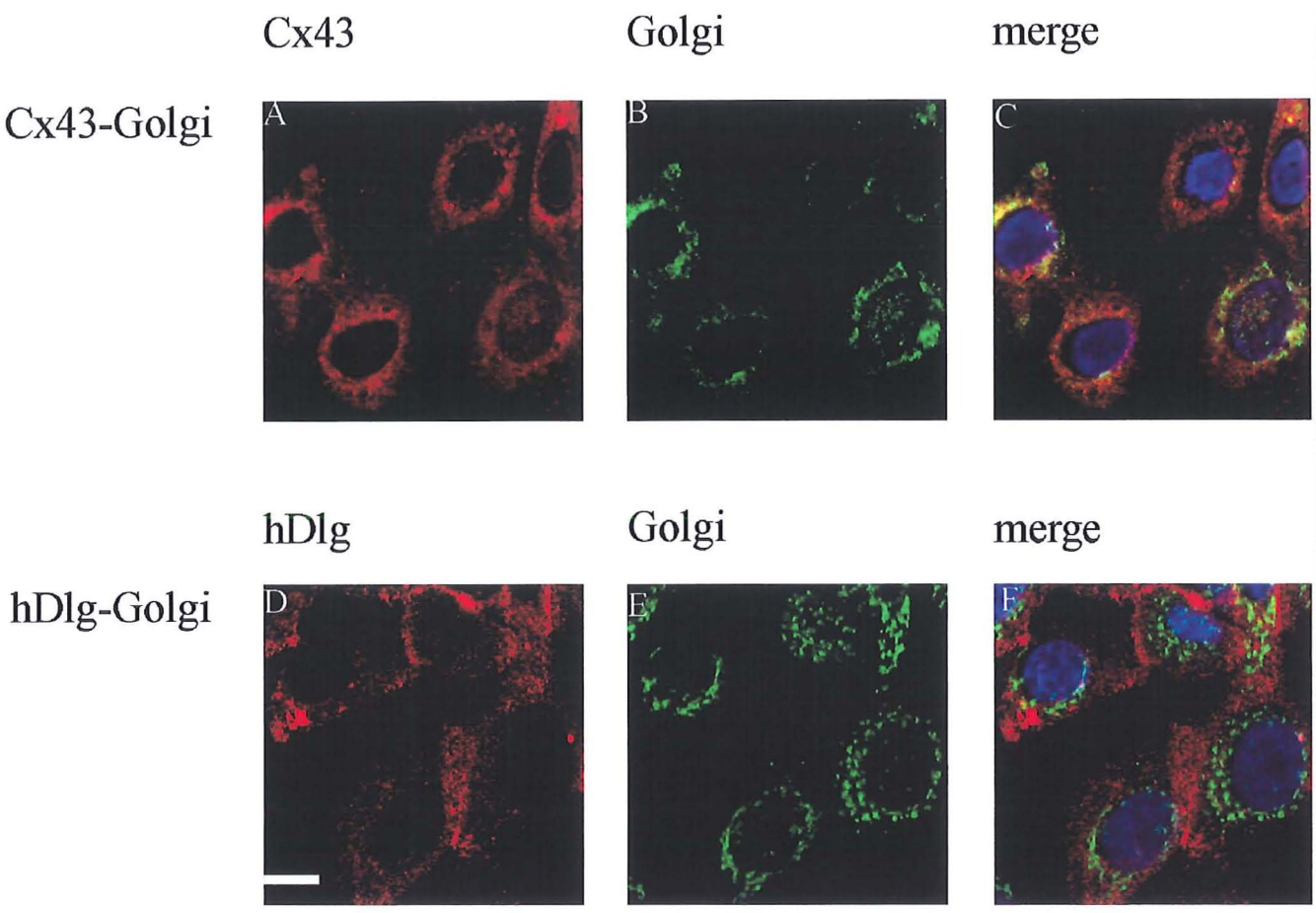

Figure 32: Co- immunofluorescene of either hDlg or Connexin 43 with Golgi maker (anti-GM 130) in W12GPXY cells. A, B and C, Cx43-Golgi co-stain of W12GPXY cells; D, E and F, hDlg-Golgi co-staining of W12GPXY cells. A, Cx43 stain; D, hDlg stain; B and E, Golgi stains; C and F merge image of A, B and D, E respectively. Nuclei are stained with DAPI. Bar=20μm.

5.3 Sequestration of Connexin 43 and hDlg in endosome-lysosome compartments

Next, to determine the subcellular localization of the hDlg-Connexin 43 complex, both Connexin 43 and hDlg were co-stained with an early endosome maker, EEA1, in W12GPXY cells and also in C33a-PCT3Xflag-HPV18WtE6 transfected cells. In W12GPXY and C33a-PCT3Xflag-HPV18WtE6 transfected cells, most of Connexin 43 was found in cytoplasmic regions (Fig. 33 (B, H)) confirming our previous results. This coincided with the subcellular location of the early endosome maker (Fig. 33 (A, G)) and merging of Connexin 43 and EEA1 revealed strong co-localized immunofluorescence signals (Fig. 33 (C, I)). In contrast, in C33a-PCT3Xflag (control) and C33a-PCT3Xflag-HPV18MuE6 (I.E. E6 lacking the PDZbinding domain) transfected cells, EEA1 remained in endocytosomal staining (Fig. 33 (D, J)), but Connexin 43 remained in gap junction plaques at the cell contact points on the cell surface as in untransfected C33a cells (Fig. 33 (E, K)). There was no co-stain of Connexin 43 and EEA1 in these cells (Fig. 33 (F, L)). Similarly, hDlg was intracellularly localized with EEA1 in both W12GPXY and C33a-PCT3Xflag-HPV18WtE6 transfected cells, but not in C33a-PCT3Xflag and C33a-PCT3Xflag-HPV18MuE6 transfected cells. Thus, it was shown that most of hDlg and Connexin 43 association accumulated in early endosomes and strongly suggested Connexin 43 was intracellularly sequestered by high risk HPV E6 binding hDlg via a protein-protein interaction Fig. (34).

Subsequently, in order to determine the degradative route of the hDlg and Connexin 43 complex, cells were co-stained with a late endosome- lysosome maker, mannose 6-phospate receptor (MPR), and both hDlg and Connexin 43. Both Connexin 43 and hDlg co-localized with the late endosome-lysosome maker in both W12GPXY and C33a-PCT3Xflag-HPV18WtE6 transfected cells. Consistent with the early endosome

results, in the control C33a-PCT3Xflag and C33a-PCT3Xflag-HPV18MuE6 transfected cells, hDlg and Connexin 43 were found on the plasma membrane and separated from the mannose 6-phosphate receptor staining (Fig.35 and 36). These results indicated most of intracellular hDlg and Connexin 43 complexes were degraded via the lysosomal pathway through endosome compartments as a result of the action of high risk HPV E6 onco-function.

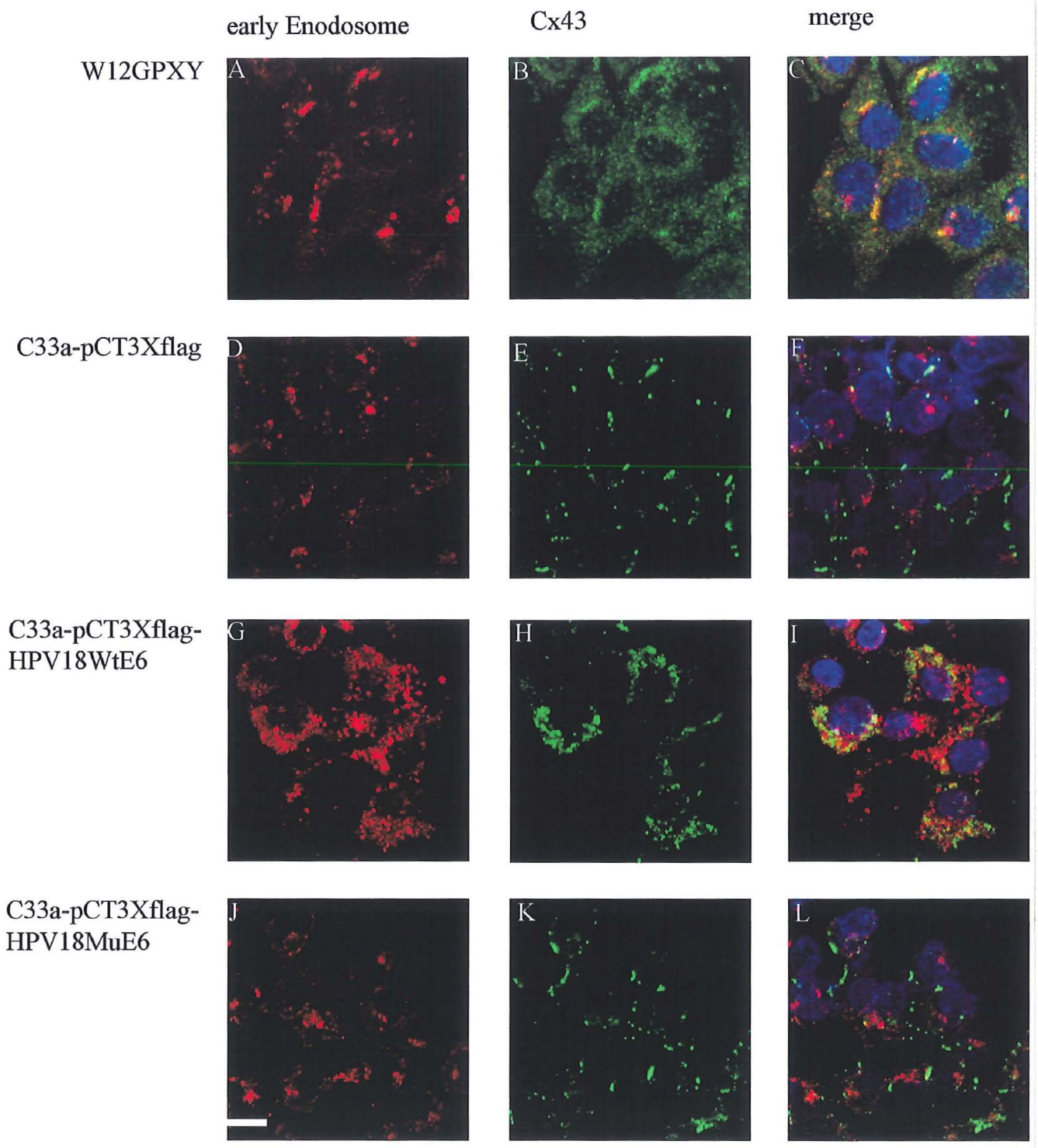

Figure 33: Co-immunofluorescene stains of early endosome maker, EEA1, and Connexin 43 in W12GPXY and transfected C33a cells. Nuclei are stained with DAPI. Panel A-C, W12GPXY cells; panel D-F C33a-PCT3Xflag cells; panel G-I,

C33a-PCT3Xflag-HPV18WtE6 cells; panel J-L, C33a-PCT3Xflag-HPV18MuE6. A, D, G and J, EEA1 stain; B, E, H and K Connexin 43 stain; C, F, and I L merged image of AB, DE, GH and JK respectively. Nuclei are stained with DAPI. Bar=10μm.

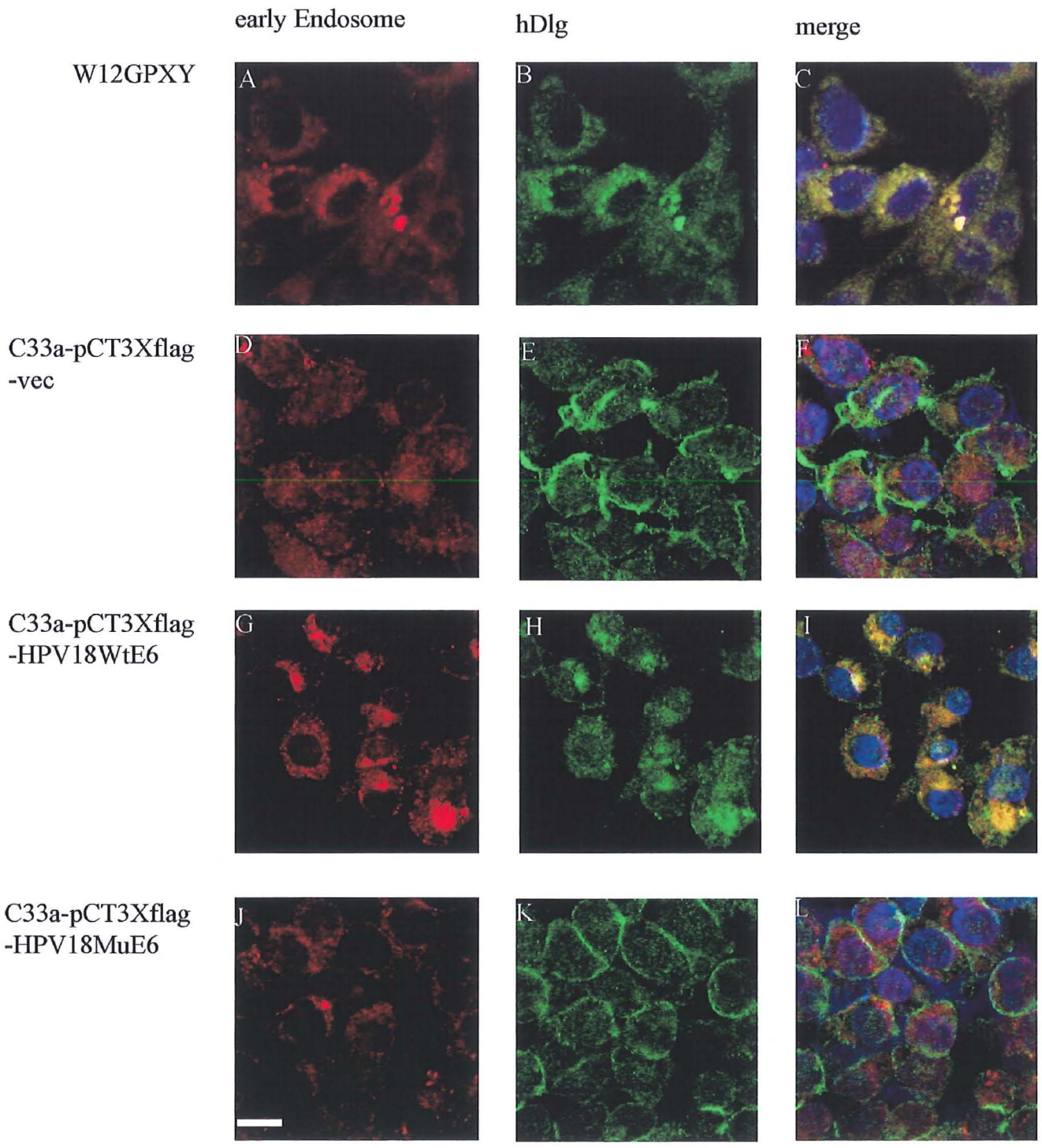

Figure 34: Co-immunofluorescene stains of early endosome maker, EEA1, and hDlg in W12GPXY and transfected C33a cells. Nuclei are stained with DAPI. Panel A-C, W12GPXY cells; panel D-F C33a-PCT3Xflag cells; panel G-I, C33a-PCT3Xflag-HPV18WtE6 cells; panel J-L, C33a-PCT3Xflag-HPV18MuE6. A, D, G and J, EEA1

stain; B, E, H and K hDlg stain; C, F, and I L merged image of AB, DE, GH and JK respectively. Nuclei are stained with DAPI. Bar=10μm.

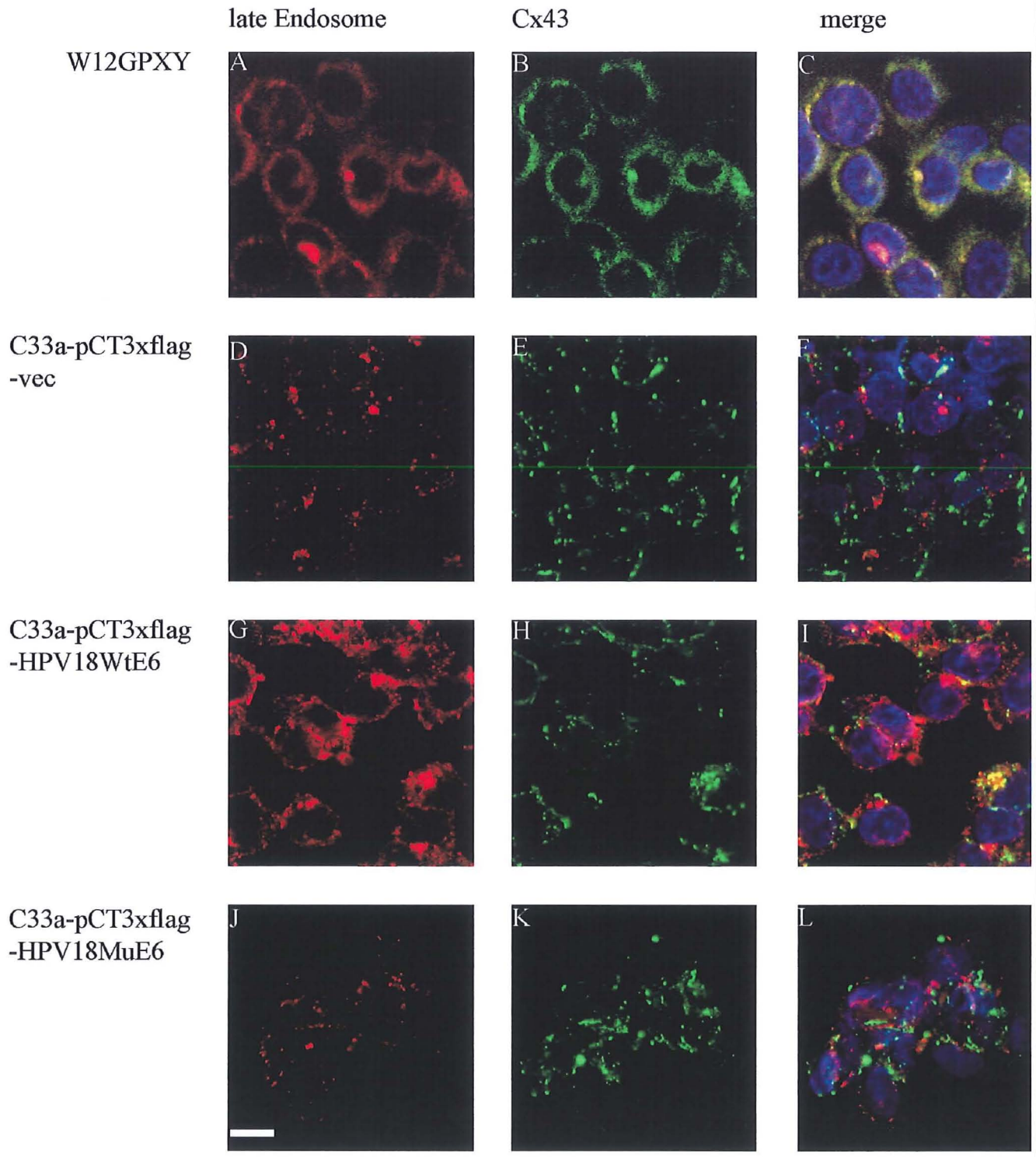

Figure 35: Co-immunofluorescene stains of late endosome and lysosome maker, MPR, and Connexin 43 in W12GPXY and transfected C33a cells. Panel A-C, W12GPXY cells; panel D-F C33a-PCT3Xflag cells; panel G-I, C33a-PCT3Xflag-

HPV18WtE6 cells; panel J-L, C33a-PCT3Xflag-HPV18MuE6. Nuclei are stained with DAPI. Bar=10μm.

A, D, G and J, MPR stain; B, E, H and K Connexin 43 stain; C, F, and I L merged image of AB, DE, GH and JK respectively.

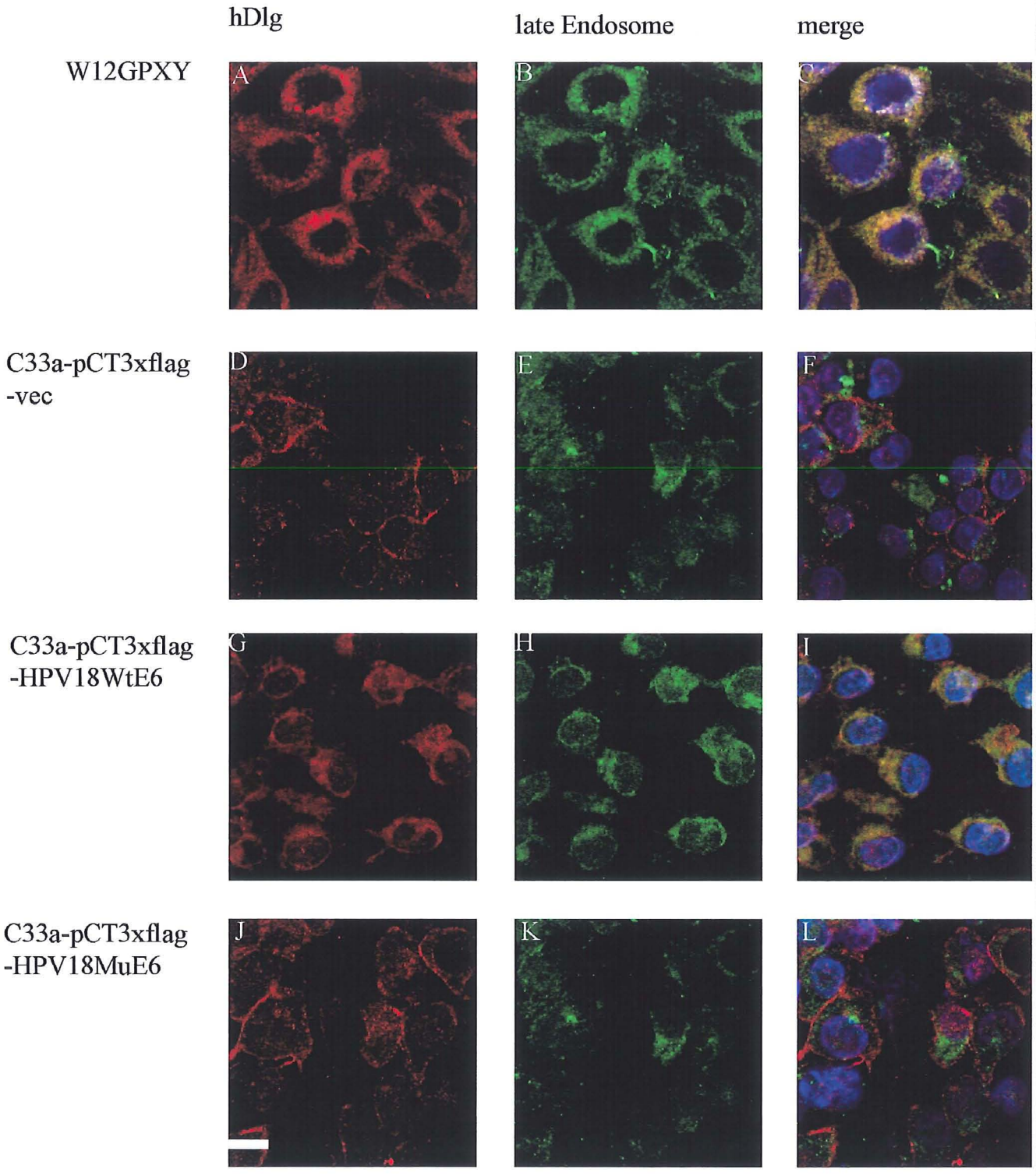

Figure 36: Co-immunofluorescene stains of late endosome and lysosome maker, MPR, and hDlg in W12GPXY and transfected C33a cells. Nuclei are stained with DAPI. Bar=10μm.

Panel A-C, W12GPXY cells; panel D-F C33a-PCT3Xflag cells; panel G-I, C33a-PCT3Xflag-HPV18WtE6 cells; panel J-L, C33a-PCT3Xflag-HPV18MuE6. A, D, G and J, MPR stain; B, E, H and K hDlg; C, F, and I L merged image of AB, DE, GH and JK respectively.

5.4 Most of hDlg-Connexin 43 complexes are degraded in the lysosomal pathway

As previous studies demonstrated that both Connexin 43 and hDlg could be degraded via a proteasomal pathway in several cell models (Liang and Beyer, 1995; Mantovani et al., 2001), it was interesting to investigate whether or not the proteasome also played a role in E6 mediated targeting of hDlg and Connexin 43. W12G, W12GPXY, C33a-PCT3Xflag-HPV18WtE6 and C33a-PCT3Xflag-HPV18MuE6 transfected cells were treated with proteasome inhibitors, MG132 and ALLN with mock controls; Western blot revealed a slightly increased Connexin 43 and hDlg levels in both W12GPXY cells and C33a-PCT3Xflag-HPV18WtE6 transfected cells after MG132 treatment, which was not obvious in W12G and C33a-PCT3Xflag-HPV18MuE6 transfected cells (Fig (37)). However, when double stained with hDlg and Connexin 43, the MG132 or ALLN treated W12GPXY cell showed besides the intrecellular staining, increased cell surface Connexin 43 gap junction plaques present on the plasma membrane Fig (38). This finding suggested a role for the proteasome in E6-mediated targeting of hDlg and Connexin 43 into the endosome/lysosome pathway.

Next, it was interesting to examine whether or not the endosome/lysosome pathway is the major degradative pathway for cytoplasmic hDlg and Connexin 43 complexes in W12GPXY and C33a-PCT3Xflag-HPV18WtE6 cells. After lysosome inhibited with NH_4Cl, western blot showed there was a remarkable increase in Connexin 43 and hDlg in W12GPXY and C33a-PCT3Xflag-HPV18WtE6 transfected cells, which was not noted in W12G and C33a-PCT3Xflag-HPV18MuE6 transfected cells Fig (39). From the co- immunofluorescence staining results, it was found there was increased Connexin 43 and hDlg observed in the cytoplasm compared to the untreated W12GPXY cells but no restoration of Connexin 43 into gap junction plaques. It also seemed that lysosomal inhibitor (NH_4Cl) could not affect Connexin 43 stability on

cell membrane and gap junction formation in W12G cells Fig (40). In summary, these data suggested the possibility that high risk HPV E6 could act as the trigger for hDlg and Connexion 43 association, relocation from the cell membrane and degradation in endosome/lysosome compartments. At least in part, proteasome is involved in the process.

W12G-W12GPXY and C33a-WtE6-C33a-MuE6 cells treated with MG132

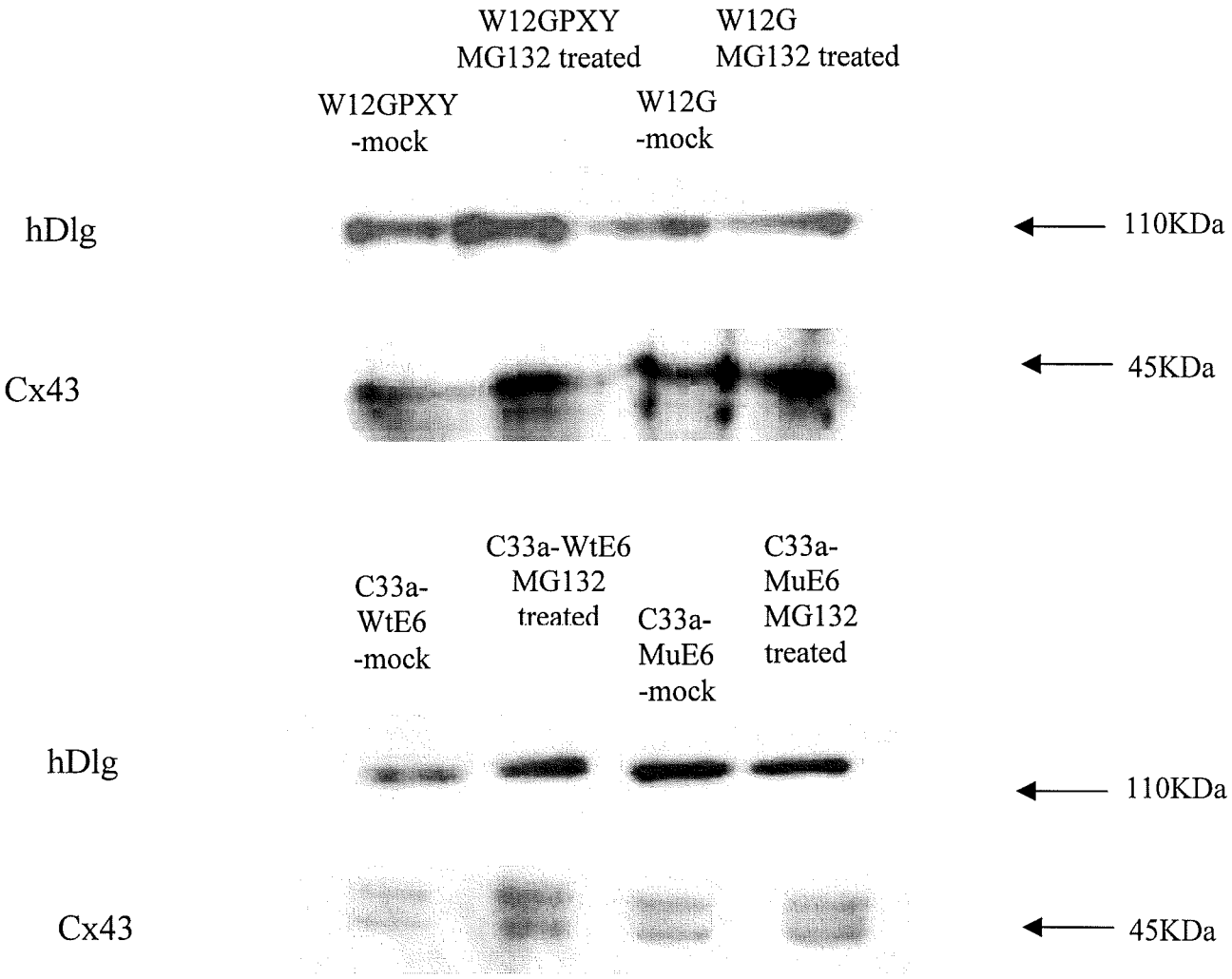

Figure 37. Western blot analysis of hDlg and Connexin 43 expression in W12G, W12GPXY, C33a-PCT3Xflag-HPV18WtE6 and C33a-PCT3Xflag-HPV18MuE6 transfected cells treated with proteasome inhibitor MG132. The sample loading between different cell types were not qualified.

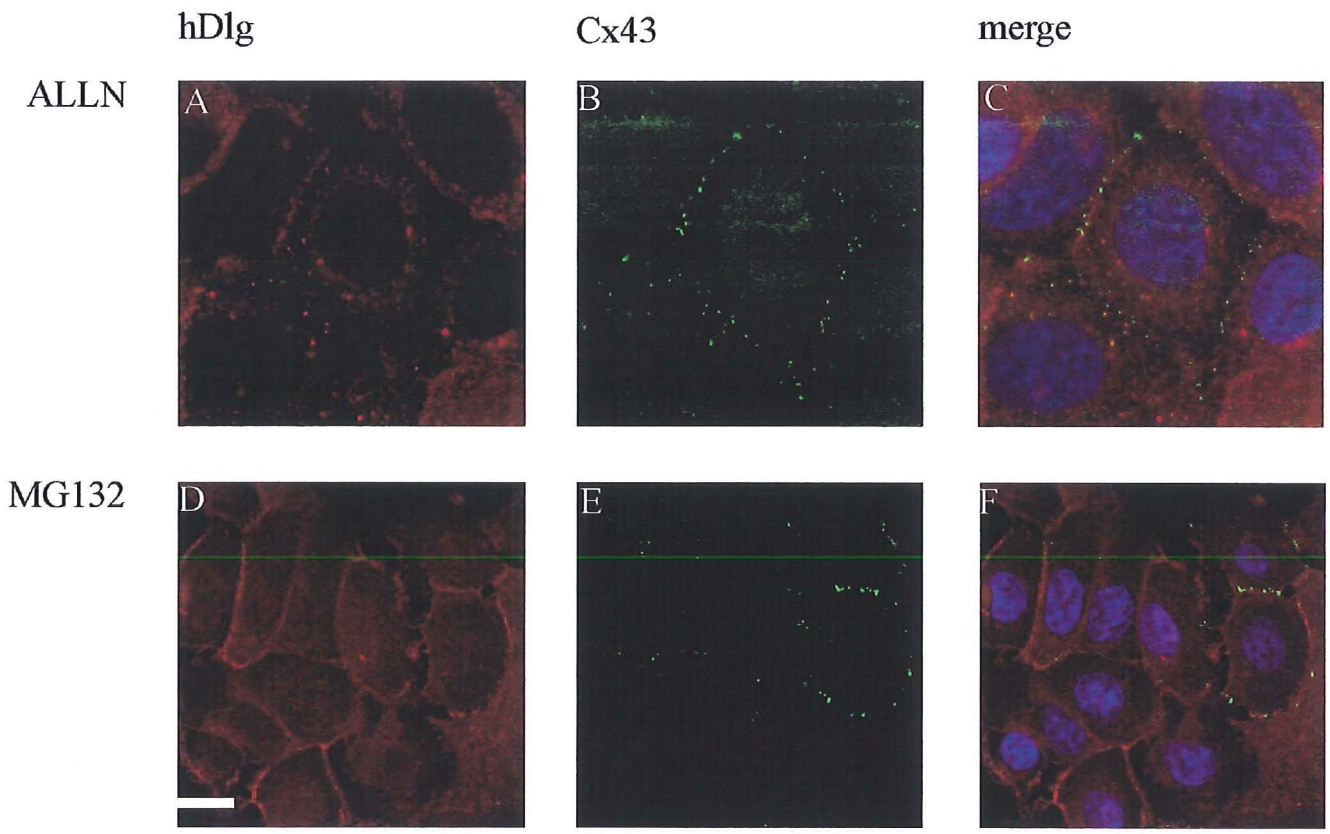

Figure 38: Co-immunofluorescene stains of Connexin 43 and hDlg in W12GPXY cells treated with proteasome inhibitor ALLN or MG132. Panel A-C, W12GPXY cells treated with ALLN; panel D-F, W12GPXY cells treated with MG132. A and D, hDlg stain; B and E, Connexin 43; C and F merged image of A and B, D and E, respectively. Nuclei are stained with DAPI. Bar=10μm.

W12G-W12GPXY and C33a-WtE6-C33a-MuE6 cells treated with NH_4Cl

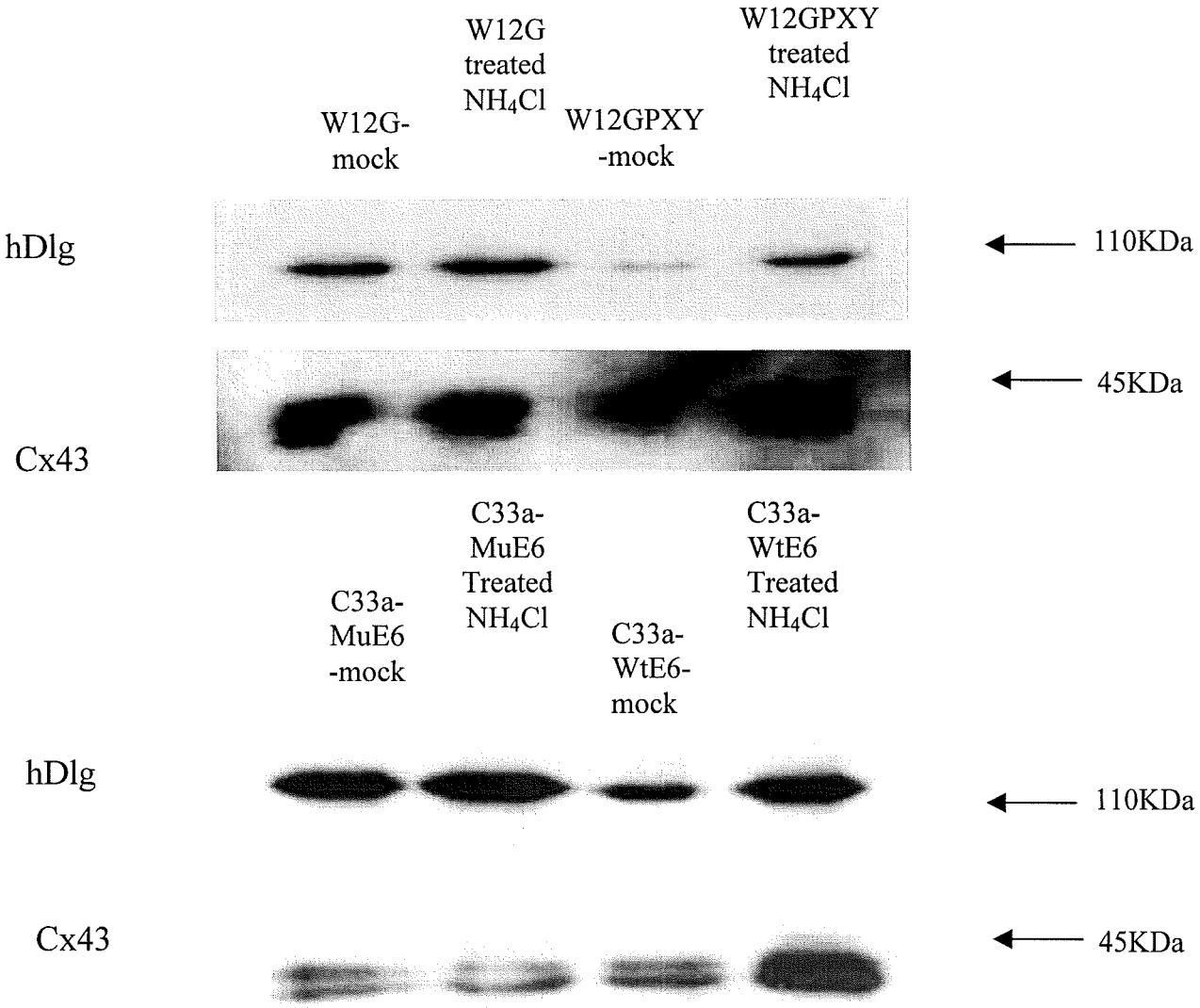

Figure 39: Western blot analysis of hDlg and Connexin 43 expression in W12G, W12GPXY, C33a-PCT3Xflag-HPV18WtE6 and C33a-PCT3Xflag-HPV18MuE6 transfected cells treated with lysosome inhibitor NH_4Cl. The sample loading between different cell types were not qualified.

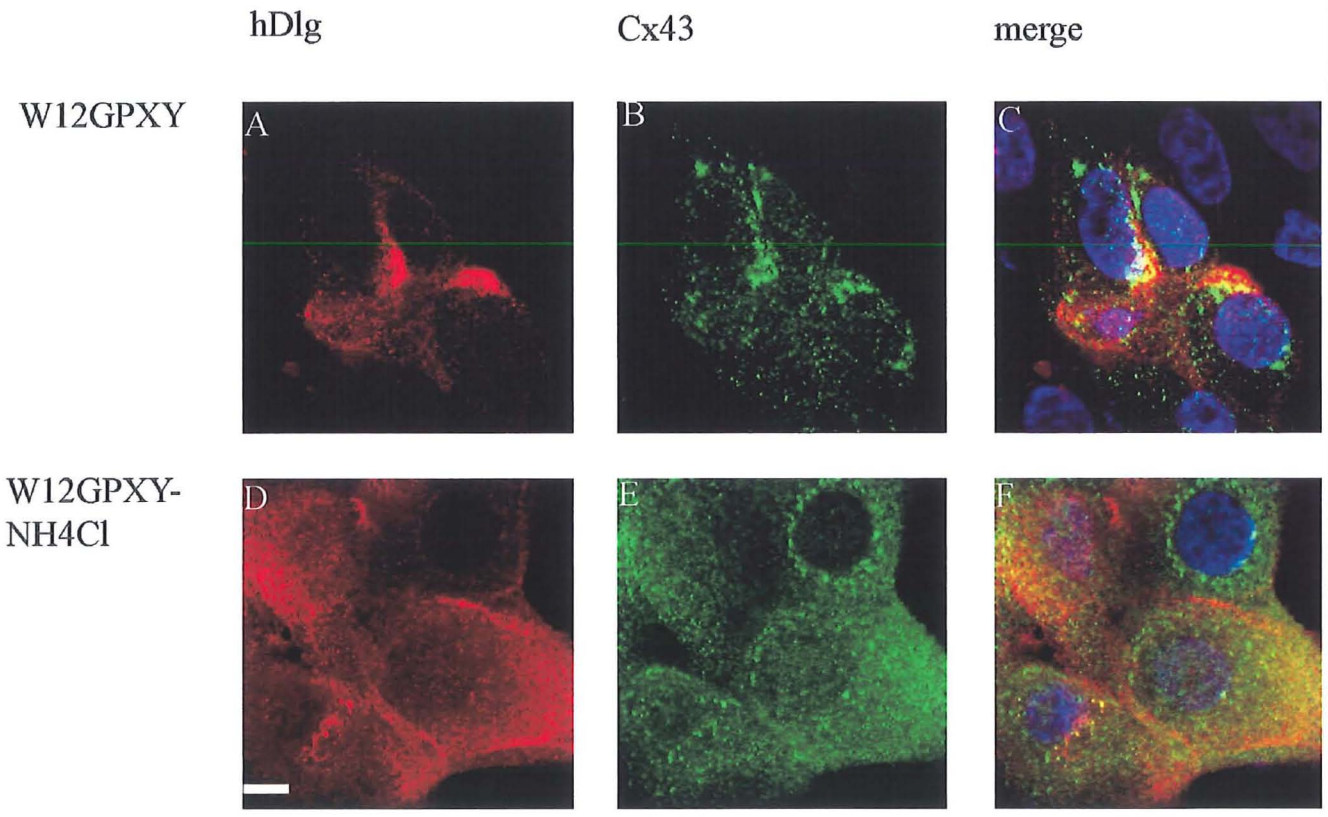

Figure 40: Co-immunofluorescene staining of Connexin 43 and hDlg in W12GPXY cells treated with lysosome inhibitor NH_4Cl. Panel A-C, W12GPXY control cells; panel D-F, W12GPXY cells treated with NH_4Cl. A and D, hDlg stain; B and E, Connexin 43; C and F merged image of A and B, D and E, respectively. Nuclei are stained with DAPI. Bar=10μm.

5.5 Discussion

Like other membrane associated proteins, both Connexin 43 and hDlg are synthesised in the ER and pass through the trans-Golgi network to the plasma membrane. Furthermore, connexins have assembled as connexons after exiting from the Golgi network but form gap junction plaques only in the plasma membrane. Previous studies suggested that Connexin 43 from the Golgi network was prevalent in vesicular carriers that traffic along microtubules and actin filaments to reach the plasma membrane (Paulson et al., 2000; Martin et al., 2001), while hDlg movement to the cell surface was more dependant on microtubules (Hanada et al., 2000). To investigate the mechanism underlying aberrant trafficking of cytoplasmic Connexin 43 and hDlg protein complexes in W12GPXY cells, I disturbed microtubules with nocodazole or actin filaments with Cytochalasin B. These results showed that neither Connexin 43 nor hDlg trafficking was strongly affected by actin filament disruption, but was very sensitive to microtubule distribution. I also showed that cytoplasmic hDlg and Connexin 43 aggregates in W12GPXY cells were not blocked in the Golgi apparatus. These results suggested that while microtubules played a role in both Connexin 43 and hDlg transport, the altered Connexin 43 and hDlg subcellular distribution caused by E6 did not result primarily from rearrangement of cytoskeleton.

A remarkable pathology change in many invasive cancers and in malignant cell lines is the loss of connexin expression and GJIC. W12GPXY cells were developed as an HPV16 positive primary cervical malignant cell line; in these cells, transferring of LY by gap junctions was found deficient although Connexin 43, the most common gap junctions protein, mRNA and protein expression were still on average maintained at a high level. The reason for this paradox has now been shown to be the loss of Connexin 43 from gap junctions and targeting through binding hDlg into the

endosome/lysosome degradation pathway. These findings are consistent with a previous report in which retrovirally delivered connexins continued to be expressed in malignant breast tumor cells but gap junction plaques were absent (Qin et al., 2002). It was proposed that in these connexin expressing tumour cells, GJIC deficiently could be due to the instability of connexins at the plasma membrane or defects in the secretory pathway involved in delivering connexins to the cell surface for gap junction assembly. Unlike other plasma membrane proteins, Connexin 43 undergoes rapid turnover with a half-life of only 1–2 h (Laird et al., 1991). Previous studies showed that both the proteasome and lysosomes were involved in Connexin 43 degradation in tumor cells (Qin et al., 2003); the lysosomal pathway was proposed to degrade endocytosed connexins and the proteasomal pathway was the route of cytosolic and misfolded protein degradation, however, the relative contribution of each pathway to Connexin 43 and hDlg turnover remains unclear.

It was shown in both W12GPXY and C33a-PCT3Xflag-HPV18WtE6 cells that the majority of Connexin 43 associated with hDlg and co-localised in the early endosome and late endosome/lysosome compartments. After treatment with NH_4Cl to inhibit lysosomal degradation, both Connexin 43 and hDlg accumulated in the lysosomes but were not restored to cell membrane junctions. This suggested that Connexin and hDlg degradation occurred in the lysosomes, but that E6 worked on the protein complexes at an earlier step in Connexin 43 and hDlg trafficking. One possibility is that in these GJIC-deficient tumor cells, newly synthesized vesicular Connexin 43 transports from trans-Golgi network and interacts with high risk HPV E6/hDlg, the whole protein complex is directly targeted to the lysosomes for degradation via the endosomal system without firstly transporting to the plasma membrane. This may partly explain how some tumor cells could continue expressing Connexin 43 but could not form

Connexin 43 gap junction plaques on cell membrane. Consistent with this, it was reported that in MDA-MB-231 breast tumor cells the newly synthesized Connexin 43 (as monomers or oligomers) may traffic from an early secretory compartment, e.g. Golgi network, directly to the endosome/lysosome for degradation without necessarily firstly reaching the plasma membrane, in a "by-pass" mechanism (Qin etal., 2003). Another group reported that prolonged treatment of bovine aortic endothelial cells with TGF-β1 causes increased expression, synthesis and accumulation of Connexin 43 in a lysosomal compartment; interestingly, there were no internalized gap junctions observed within the cytoplasm or within lysosomes (Larson et al., 2001). Thus, it is possible that in this case, Connexin 43 was also routed directly to lysosomes before reaching the plasma membrane through the proposed by-pass pathway.

Another possibility is that the E6/hDlg complexes target isolated connexons in cytoplasm or even cooperate with proteasome activity on the cell membrane for internalisation in the endosomes before the connexons can associate in gap junction plaques and form intercellular junctions. Interestingly, when W12GPXY cells were treated with proteasome inhibitors, there was modest recovery of gap junction plaques on the cell membrane and intercellular transferring of LY, and reduced Connexin 43 accumulation in cytoplasm. This suggested involvement of proteasomal activity in Connexin 43 redistribution and degradation in these cells. Moreover, hDlg was reported as being a specific target of high risk HPV E6 for proteasome mediated degradation (Mantovani et al., 1995). Together, these data would be consistent with the hypothesis that E6/hDlg associations could promote connexon internalisation via proteasome activity on the cell membrane that could destroy gap junction plaque stability and importantly result in Connexin 43 and hDlg association. Furthermore, this Connexin 43 proteasomal mediated degradation hypothesis was also supported by

data for other integral membrane proteins including the epithelial Na^+ channel and growth hormone receptors going through proteasomal related degradation (Staub et al., 1997; Gover et al., 1997).

It is important to note that although it was shown that Connexin 43 and hDlg complexes were found in the endosome/lysosomes, it is still not clear whether Connexin 43 and hDlg were cleaved and degraded there, because the antibodies available can not necessarily distinguish intact from cleaved peptides of Connexin 43 and hDlg. It was noted in Chapter 3. that in W12GPXY cells, Connexin 26 and Connexin 30 still formed many gap junction plaques, in spite of the loss of Connexin 43 from the cell membrane. In the contrast, from previous reports it seemed that whole gap junction plaque areas, no matter what connexin types, might be internalized to form gap junction annular vesicles that were transported and degradated in the endosomal/lysosomal compartments (Bjorkman, 1962; Larsen et al., 1979). It will be interesting to investigate whether E6/hDlg specifically disassembled Connexin 43 from the whole gap junctions and only internalized Connexin 43 from the cell membrane that vitally affected gap junction component and functions.

In summary, our study revealed that both lysosomes and proteasomes play distinctly important roles in Connexin 43 degradation and functional gap junction formation on the cell membrane, and it elucidated the complementary mechanism and co-operation of the two different degradation pathways in Connexin 43 degradation and gap junction assembly.

Chapter 6. DISCUSSION, CONCLUSION AND FUTURE WORK

It has been reported that gap junctional intercellular communication was frequently decreased or absent in cells treated with tumor promoting agents. The observations were made on various cell types of wide range tissues and species using both *in vitro* and *in vivo* models (Kanno and Matsui, 1968; Jamakosmanovic and Loewenstein, 1968; Kivtovskikh et al., 1991). It was hypothesised that gap junctional intercellular communication may play a key role in carcinogenesis progression and the gap junction proteins, connexins, may act as tumour suppressors, since transfecting cells with an expression vector for wild type connexins can revert the phenotype of the tumor cells (Loewenstein, 1979, Peeble et al., 2003). Moreover, it was demonstrated that expression of viral oncogenes such as v-src, BPV-4 E8 and SV-40 large T-antigen could result in loss of gap junction intercellular communication (Loewenstein, 1985; Fitzgerald et al., 1993; Faccini et al., 1996, NaHK et al., 2000). Gap junctional intercellular communication was also inhibited in HPV 16 related tumorigenesis (Campo, 2002). During HPV-associated carcinogenesis, loss of GJIC occurred in the late stage of the progression (Aasen et al., 2003).

One of the main aims of this project was to investigate the mechanism of loss of gap junctional intercellular communication in the W12GPXY cell line, a model of later stages of high-risk HPV-induced cervical carcinogenesis. While, the microarray results presented have demonstrated there was no obvious connexin expression change at a transcription level between immortal W12G and malignant W12GPXY cells, immunofluorecence staining showed that Connexin 43 protein, was absent from many W12GPXY cells and redistributed into the cytoplasm in the remainder. This correlated

with the absence of LY transfer between W12GPXY cells. Interestingly, in W12GPXY cells, immunofluorscence also showed that Connexin 26 and Connexin 30 could still form gap junctional plaques on the cell membrane, suggesting that as a result of the loss of Connexin 43, a change in gap junction properties rather than a complete loss of coupling has occurred. Connexin 26 and Connexin 30 can form gap junctions that are not permeable to LY transfer (Brissette et al., 1994; Marziano et al., 2003), which was also shown in W12GPXY cells.

Phosphorylation is one of the most common post-translational modifications for connexins, particularly of Connexin 43, primarily on serine and tyrosine amino acids. It was found that v-Src tyrosine kinase could phosphorylate Connexin 43 directly on two distinct tyrosine sites, Y247 and Y265, and the activated epidermal growth factor receptor acts indirectly through activated MAP kinase on three serine site (S255, S279 and S282) to alter Connexin 43 phosphorylation (Crow et al., 1992; Lau et al., 1992). Furthermore, it has been shown that activation of several other kinases including protein kinase A, protein kinase C, p34(cdc2)/cyclin B kinase and casein kinase 1, can lead to phosphorylation at 12 of the 21 serine, and two of the six tyrosine, residues in the C-terminal region of connexin 43 (Lampe and Lau, 2004). Previous studies demonstrated that Connexin 43 underwent several phosphorylation events that could affect a broad variety of Connexin 43-associated processes, such as the trafficking, assembly/disassembly, degradation, as well as the gating of gap junction channels (Kurata and Lau, 1990; Zhou et al., 1994; Laird et al., 1995; Lin et al., 2001). Furthermore, it was found that phosphorylated Connexin 43 correlated with reduced gap junctions on the cell surface in Rous sarcoma virus transformed fibroblast cells and in ras transformed cells total Connexin 43 expression was found decreased and phosphorylated

level was increased (Crow et al., 1990; Brissette et al., 1991). In HPV-16 transformed or in cells overexpressing HPV-16 E5, it was shown that inhibited expression of Connexin 43 was the main reason for a decrease in gap junction formation, although there was increased, virus-induced Connexin 43 phosphorylation (Ennaji et al., 1994; Tomakidi et al., 2000). In the latter case, it was proposed that E5 contributed to Connexin 43 down-regulation and phosphorylation. However, E5 was overexpressed in these transformed cells while, in contrast, E5 could not be detected in high risk HPV genome-integrated cervical cancer cell lines (Tanimoto et al., 1992; Corden et al., 1999). In contrast with E5 causing a decrease in Connexin 43 expression, data from this project showed there was no change in Connexin 43 quantitative expression or phosphorylated isoform distribution between W12G and W12GPXY cells, suggesting that phosphorylation probably was not the central effector for Connexin 43 redistribution into the cytoplasm and the consequent loss of gap junctions on the cell membrane in W12GPXY cells.

E6, one of the two major oncogenes expressed by high risk HPVs, displays multiple oncogenic properties besides interfering with the p53 pathway, and it alone was sufficient to induce malignant carcinoma in transgenic animals (Song et al., 1999; Liu et al., 1999). Previous studies suggested a possibility by which E6 could affect Connexin 43 accumulation in cytoplasm and loss from the cells. The finding that PDZ_2 containing proteins could be targets of high risk HPV E6 suggested a possible mechanism for E6 mediated loss of Connexin 43, as Connexin 43 had previously been shown to bind to the PDZ_2 protein ZO-1.

A special four amino acid motif in the C-termini of high risk HPV E6 was shown to interact with the second PDZ domain of proteins, such as hDlg, hScrib and SAP97, and the binding was required for E6 induced epithelial hyperplasia in vivo (Thomas et al.,

2001; Nguyen et al., 2003). Most of these proteins belong to the membrane-associated guanylate kinase homologue family (Thomas et al., 2001). MAGUK family members can also interact with cell adhesion molecules, cytoskeletal proteins and components of second message cascades (Garner et al., 2000; Hung and Sheng, 2001).

Unlike other MAGUKs, hDlg contains a proline-rich amino-terminal domain with two potential SH3 domain binding sites (Ren et al., 1993; Lue et al., 1994). The presence of these consensus binding sites suggests that hDlg might participate in signaling pathways by forming protein complexes via the SH3 domains of other proteins. T lymphocytes $p56^{lck}$, a known tyrosine kinase, was found to directly bind to the site within the amino-terminal segment of hDlg containing the proline-rich domain. These results provide evidence of a novel function of hDlg in coupling tyrosine kinases in cell signalling pathways (Hanada et al., 1997).

Dlg, is required for the proper assembly and function of adherens junctions (Wood and Bryant, 1991; Wood et al., 1996). It has been shown recently that Dlg is predominantly localized at the adherens junctions of the epidermis, intestine, and pharynx of embryos and adult nematodes (Firestein and Rongo, 2004). Dlg-deficient embryos exhibited abnormal adherens junction formation and disorganization of the actin cytoskeleton without any change in E-cadherin localization (Firestein and Rongo, 2004). It was demonstrated that human intestinal epithelial cells express several forms of hDlg whose changes in phosphorylation state correlate with the initiation of differentiation. Moreover, by using an RNA interference approach, hDlg is shown to be necessary for adherens junction integrity and for functional differentiation of human intestinal epithelial cells. Finally, hDlg was shown to bind to p85/ phosphatidylinositol 3-kinase (PI3K) and both

proteins are part of a common macromolecular complex with E-cadherin at the sites of cell-cell contact (Laprise et al., 2004).

Recently, it was shown that hDlg might also act as a determinant in E-cadherin-mediated adhesion and signaling in mammalian epithelial cells (Laprise et al., 2004). The reduction of hDlg expression levels by RNAi in intestinal cells not only severely alters adherens junction integrity but also prevents the recruitment of p85/PI3K to E-cadherin-mediated cell-cell contacts; and PI3K and hDlg are associated with E-cadherin in a common macromolecular complex in living differentiating intestinal cells. The complex interaction requires the association of hDlg with E-cadherin and with Src homology domain 2 domains of the p85/PI3K subunit. Phosphorylation of hDlg on serine and threonine residues prevents its interaction with the p85 Src homology domain 2 in subconfluent cells, whereas phosphorylation of hDlg on tyrosine residues is essential (Laprise et al., 2004). There are several phosphorylated sites in the amino terminal region of hDlg and it was found that p38MAPK is involved in the phosphorylation process. When high risk HPV E6s target to hDlg, it was purposed that the binding could perturb hDlg phosphorylation process and consequently promote degradation of hDlg.

The cadherin/catenin complex plays important roles in cell adhesion, signal transduction, as well as the initiation and maintenance of structural and functional organization of cells and tissues. ZO-1 works as a cross-linker between cadherin/catenin complexes and the actin-based cytoskeleton through direct interaction with α-catenin and actin filaments at its amino- and carboxyl-terminal halves, respectively, and ZO-1 is a functional component in the cadherin-based cell adhesion system (Itoh et al., 1997). There were reports that MAGUK proteins especially ZO-1 were involved in Connexin 43 assembly and targeting to the cell membrane to gap junction plaques and high risk HPV E6 seems

to target MAGUK proteins e.g. hDlg and hScrib. I propose that E6 can target Connexin 43 via these junction-associated MAGUK proteins. Several reports have shown MAGUK proteins, such as ZO-1, could bind directly to Connexin 43 on the plasma membrane and the binding could influence membrane Connexin 43 assembly and stability (Toyofuku et al., 1998; Baker et al., 2002). Furthermore, chemical disruption of gap junctional intercellular communication could result in aberrant cytoplasmic co-localised Connexin 43 and ZO-1 complexes (Defamie et al., 2001). In this project, I found another membrane protein from the MAGUK family, hDlg, co-stained with Connexin 43 in the cytoplasm. Point mutation and co-immunoprecipitation studies clearly confirmed the association between hDlg and Connexin 43 via its second PDZ domain in W12GPXY cells. Moreover, Connexin 43 and hDlg were initially expressed on cell surface, but both of them were endocytosed and colocalised together when the cells were transfected with HPV 18 E6. Recently, it was reported that hDlg could interact with Connexin 32 and the binding was potentially involved in hepatotumorigenesis in Connexin 32 null mice (Dr David C. Spray, unpublished data, presented at the 2005 International Gap Junction Conference). All these data suggest that hDlg plays an important role in assembly and stability of Connexin 43 on the cell membrane during progression of some tumors. It would be important to explore whether other PDZ_2 containing proteins from MAGUKs family also interact with connexins and regulate gap junction composition.

Interestingly, it was noted that Connexin 43 and hDlg were localised on plasma membrane and there seemed to be no co-localisation of the two proteins in the cytoplasm in W12G cells, although the HPV16 genome also had integrated into the host cell genome and E6 and E7 oncoproteins were expressed. However, it was found that there

was around a three-fold increase in levels of E6 in W12GPXYcells and while E6 only appeared in the nucleus in W12G cells, but also translocated into the cytoplasm in W12GPXYcells. It was proposed that the majority of the cytoplasmic E6 binds to hDlg in W12GPXY cells and acts as a trigger for formation of a hDlg/Connexin 43 complex leading to their redistribution from the plasma membrane to the cytoplasm. SiRNA and Leptomycin B experiments confirmed this hypothesis. Furthermore, experiments with C33a cells showed that E6 mediated association and relocation of hDlg and Connexin 43 is a general phenotype not specific to W12GPXY cells.

Whether Connexin 43 and E6 interacted with hDlg via the same PDZ domain is still under investigation. It is possible that that Connexin 43 and E6 have different binding sites in hDlg. The binding between E6 and hDlg via the second PDZ domain could improve the binding affinity of hDlg associated with Connexin 43 through regulation of intramolecular interaction between multiple domains of hDlg; in the cytoplasm, hDlg could actually exist as a scaffold for the triple protein complex composed of E6, hDlg and Connexin 43. This idea is indirectly supported by observation that some MAGUK proteins' PDZ_2 ligand binding could intramolecularly affect the binding affinity of other protein interaction domains (Wu et al., 2000; Imamura et al., 2002).

Another hypothesis is that E6 and Connexin 43 could competitively associate with hDlg via the same binding site in its second PDZ domain and hDlg binding with Connexin 43 is vital for the latter's cell membrane stability. So increasing cytoplasmic E6 could block hDlg composing a precise protein complex with Connexin 43 on the cell surface and subsequently result in Connexin 43 existing in an unstable environment and a failure to assemble on the cell membrane leading to retention in the cytoplasm.

A third idea is that hDlg probably associates with Connexin 43 when they traffic together from the post-Golgi network to the cell membrane, E6 binding to hDlg could disrupt the trafficking of the complex and activate cellular protein quality control systems causing hDlg associated with Connexin 43 to undergo an unusual alternative transport and degradation pathway, which is consistent the observation that most of Connexin 43 was degraded via the lysosomal pathway in tumor cells (Qin et al., 2003).

High risk HPV E6 can associate with paxillin, and overexpression of HPV16 E6 can lead to actin filament cytoskeleton disruption that is a characteristic of many malignant tumor cells (Tong and Howley, 1997). It was noticed that drebrin, an actin associated protein also reported to bind with Connexin 43 (Butkevich et al., 2004), was found increased in W12GPXY cells from the microarray analysis (details in Table 9).

Establishment and maintenance of epithelial cell polarity relies on finely tuned protein networks comprising cell surface molecules, cytoplasmic adaptors, and enzymes connected to the actin cytoskeleton. hDlg is involved in cell polarity and is regarded as an important tumor suppressor, which could affect cellular molecular scaffolds to repress cell signalling pathways, and profoundly disrupt the epithelial cytoarchitecture to perturb cell shape and function. E6 binding to hDlg was found correlated with actin cytoskeleton disorganization and morphological transformation in human keratinocytes (Watson et al., 2003). It was also demonstrated that Dlg could bind to dEB1 (microtubule-binding protein--cytoskeletal), and disruption of the cellular microtubule network could cause aberrant hDlg distribution in MDCK cells (Brumby et al., 2004; Iizuka-Kogo et al., 2005). This suggests that microtubules can influence hDlg cytoplasmic trafficking and membrane targeting. It was shown that disruption of the actin cytoskeleton could perturb connexin trafficking and cell membrane assembly (Thomas et al., 2001; Hernandez-

Blazquez et al., 2001). Moreover, microtubules were required for gap junction assembly and connexin trafficking from several independent observations (Martin et al., 2001; Lauf et al., 2002). Thus, high risk HPV could indirectly disrupt cell membrane gap junction maintenance with binding to hDlg by affecting actin filament or microtubule network distribution. Results from this project confirmed the cytoskeleton disruption by increased levels of E6 and there was more influence of microtubules than actin filaments in transport of hDlg and Connexin 43.

Similar to other plasma membrane proteins, gap junction proteins are delivered to the cell surface through secretory pathways. Connexins are translated in the rough endoplasmic reticulum and most of them subsequently transit from the endoplasmic reticulum through the trans-Golgi network, during this procedure connexins are oligomerized into connexons (Musil and Goodenough, 1993; Sarma et al., 2002). Interestingly, Connexin 43 is degraded at a rate (half life only 1.5-5 h) much faster than most other cell surface proteins (Musil et al., 1990; Beardslee et al., 1998). Although the degradation of Connexin 43 has been shown to be sensitive to inhibitors of either the lysosome or of the proteasome (Hatanaka et al., 2004), how connexins are targeted for degradation and whether this process can be regulated to affect intercellular communication is unknown.

In tumor cells, it was reported that Connexin 43 undergoes both proteasome and lysosome degradation; lysosomes play a key role in degrading not only internalized Connexin 43 from the plasma membrane but also Connexin 43 delivered from early secretory compartments in breast tumor cells. Protesomal degradation regulates the stability of phosphorylated Connexin 43 and appears to promote the internalization of Connexin 43 from the cell surface (Qin et al., 2003). My data suggest that reducing

Connexin 43 degradation with proteasome inhibitors (but not with lysosome inhibitor) was associated with a striking increase in gap junction assembly compared to control cells under basal conditions. Proteasome degradation seemed to be working on Connexin 43 stability and assembly, and gap junction plaques could be restored by treatment with effective proteasome inhibitors in Connexin 43 assembly-inefficient cells. Interestingly, there was no obvious Connexin 43 degradation via the proteasome on the plasma memebrane in W12G and C33a-PCT3Xflag-HPV18MuE6 transfected cells (refer to Fig. 35). In contrast, it was suggested that the major degradation of cytoplasmic Connexin 43 happened in the endosome/lysosome degradation pathway. It seems possible that the proteasome works as a disessembling factor leading to an unusual trafficking of Connexin 43 from cell membrane to the lysosomes. These results were consistent with the observation that most Connexin 43 resided in endocytic vesicles/compartments and Connexin 43 gap junction plaques were lost from the cell membrane in high risk HPV positive tumor cells highly expressing E6.

Formerly, it was reported that oncogenic human papillomavirus E6 proteins targeted hDlg for proteasome-mediated degradation and proteasome inhibitors could override the capacity of E6 to degrade hDlg (Gardiol et al., 1999). Previous studies also indicated that PDZ containing proteins could mediate sorting of cell membrane proteins between recycling endosomes and lysosome degradation (Cao et al., 1999). My results are consistent with high risk E6 associating with hDlg and regulating its proteasomal degradation, but I also showed that in W12GPXY cells and C33a cells overexpressing HPV 18 E6, hDlg was transported to late endosomes and lysosomes from the early endosomes. Furthermore, it was consistent that the endogenous hDlg accumulated in the cytoplasm when the W12GPXY cells were treated with lysosomal inhibitor. More

importantly, due to most of hDlg co-localising together with Connexin 43 in endocytic compartments of W12GPXY cells, it would seem that lysosomal degradation was the major destination for hDlg in these cells. However, both the lysosome and the proteasome could be involved in the degradation of hDlg. The proteasome probably is mainly acting around the cell membrane, with E6-mediated ubiquitination of hDlg possibly resulting in membrane Connexin 43 disassembly and internalization. Most cytoplasmic hDlg interacted with Connexin 43 in vesicles and the associated complex was delivered to the lysosomal degradation compartments.

There were several reports showing ZO-1, another PDZ containing MAGUK protein, frequently interacted with Connexin 43 on the plasma membrane and the binding was probably regulated by the c-Src signalling pathway (Sorgen et al., 2004). From data generated in this thesis, I draw a novel hypothesis about ZO-1 and hDlg in the loss of GJIC in high risk HPV-associated invasive carcinogenesis. hDlg may be more involved in Connexin 43 trafficking and internalization in endocytosis, but ZO-1 is probably more important for Connexin 43 cell membrane stability and gap junction assembly. Immunoprecipitation of Connexin 43 with hDlg and ZO-1 from different cellular compartments will explore whether there is competition between ZO-1 and hDlg binding to Connexin 43 on the cell membrane and in the cytoplasm.

To understand the details of the components of the cytoplasmic Connexin 43 complex, further, immunoprecipitation from cell extracts, which treated with RNA interference against hDlg, will highlight whether E6 is involved in the interaction via hDlg and forms a triple protein complex with hDlg-Connexin 43 in the cytoplasm, or if Connexin 43 interacts with hDlg at the same binding site with E6. Moreover, it will help define the

mechanisms of hDlg suppression in tumorgenesis. It will be interesting to investigate the invasive characteristics of W12GPXY cells to understand the importance of cell membrane gap junctions in tumorgenesis progression in these cells because Connexin 43 gap junction plaques were supposed to be back on the cell membrane once the cells treated with Leptomycin B or expressing si RNA against HPV-16 E6.

The E6 oncoprotein together with E7 provides the major transforming activity of high risk HPVs. The combination of E6 and E7 genes is normally retained and expressed in cervical carcinomas, which is sufficient for transformation and causing carcinoma. It was found that expression of both E6 and E7 proteins alone without other viral gene products could lead to the transformation of rodent fibroblasts and human keratinocytes, however, the induction of transformation by E7 was much less efficiently and the presence of E6 greatly enhanced the frequency (Bedell et al., 1989; Halbert et al., 1991; Band et al., 1991). However, HPV16 E7 was found associated with F-actin directly and disrupted actin cytoskeletal polymerisation (Rey et al., 2000); furthermore, it was reported there was microtubule-associated morphological alteration in E7 targeted pRb-deficient astrocytoma cells (Dirks et al., 1997).

Possibilities for further work

In the future, there are several questions worth investigating:

- It will be important to investigate whether the binding of E6, hDlg and Connexin 43 is a triplex protein complex or there are other proteins also involved for the association.

- It will be important to investigate whether E7 cooperates with E6 to reorganize the trafficking and membrane targeting of Connexin 43 and whether the collaboration of the two oncoproteins results in a new model of hDlg and Connexin 43 degradation.

- E5 has been shown to be important in Connexin 43 down-regulation and phosphorylation, and it also can affect cell membrane protein trafficking. It is important to know whether E5 is a co-effector with E6 for the loss of Connexin 43 gap junction in W12GPXY cells.

- The sequence of the PDZ2 domains between ZO-1 and hDlg are quite similar. It will be interesting to know whether ZO-1 is also associated with high risk HPV E6. It will be interesting to investigate whether other PDZ contain proteins from the MAGUK family are also involved in connexin trafficking and assembly like hDlg and ZO-1.

- In this project, evidence showed that W12GPXY cells still have Connexin 26 and Connexin 30 gap junctions although Connexin 43 was lost from gap junctions. It will be interesting to investigate what molecules can no longer be transported between cells when Connexin 43 is deleted from the gap junction plaques. Such molecules will probably play important roles in cell proliferation control, cell apoptosis signal system and the cancer cell invasion process.

- Using the abundant information from the microarray data analysis, it will be interesting to identify what are the key gene transcription changes during the late stages of HPV positive cervical cancer.

- From previous studies and this project, it was shown high risk HPV E6 can associate with hDlg in the PDZ2 domain. It will be interesting to investigate the binding capacity of E6 of other HPV types from the low risk group or the high risk HPV that infect either cutaneous or mucosal organs (e.g., HPV 5, HPV 6, HPV 1 and HPV 18), which maybe important in the different mechanisms of HPV positive lesions.

- Although results in this project have shown the PDZ binding site mutated Connexin 43 cannot associate with hDlg, it is still worth designing PDZ2 mutation to confirm the association and identify the binding amino acid motif in the PDZ2 domain of hDlg.

REFERENCES

Aasen, T., Hodgins, M. B., Edward, M. and Graham, S. V. (2003). The relationship between connexins, gap junctions, tissue architecture and tumour invasion, as studied in a novel in vitro model of HPV-16-associated cervical cancer progression. *Oncogene* 22, 6025-6036.

Aasen Trond (2003). The role of gap junctions and connexins in squamous epithelial differentiation and HPV-associated carcinogenesis. *PhD thesis*, Glasgow University. Glasgow, U.K.

Alford AI, Rannels DE (2001). Extracellular matrix fibronectin alters connexin43 expression by alveolar epithelial cells. *Am J Physiol Lung Cell Mol Physiol.* 280, 680-688.

Allen F, Tickle C, Warner A (1990). The role of gap junctions in patterning of the chick limb bud. *Development.* 108, 623-634.

Anderson JM. Cell signalling: MAGUK magic (1996). *Curr Biol.* 6, 382-384.

Androphy EJ, Hubbert NL, Schiller JT, Lowy DR. (1987). Identification of the HPV-16 E6 protein from transformed mouse cells and human cervical carcinoma cell lines. *EMBO J.* 6, 989-992.

Antinore MJ, Birrer MJ, Patel D, Nader L, McCance DJ (1996). The human papillomavirus type 16 E7 gene product interacts with and trans-activates the AP1 family of transcription factors. *EMBO J.* 15, 1950-1960.

Arvan P, Zhao X, Ramos-Castaneda J, Chang A (2002). Secretory pathway quality control operating in Golgi, plasmalemmal, and endosomal systems. *Traffic.* 3, 771-780.

Asaba N, Hanada T, Takeuchi A, Chishti AH (2003). Direct interaction with a kinesin-related motor mediates transport of mammalian discs large tumor suppressor homologue in epithelial cells. *J Biol Chem.* 278, 8395-8400.

Asamoto M, Takahashi S, Imaida K, Shirai T, Fukushima S (1994). Increased gap junctional intercellular communication capacity and connexin 43 and 26 expression in rat bladder carcinogenesis. *Carcinogenesis.* 15, 2163-2166.

Asamoto M, Toriyama-Baba T, Krutovskikh V, Cohen SM, Tsuda H (1998). Enhanced tumorigenicity of rat bladder squamous cell carcinoma cells after abrogation of gap junctional intercellular communication. *Jpn J Cancer Res.* 89, 481-486.

Anumonwo JM, Taffet SM, Gu H, Chanson M, Moreno AP, Delmar M. (2001). The carboxyl terminal domain regulates the unitary conductance and voltage dependence of connexin40 gap junction channels. Circ Res. 88, 666-667.

Aznavoorian S, Murphy AN (1993). Molecular aspects of tumor cell invasion and metastasis. *Cancer.* 71, 1368-1383.

Bager Y, Kenne K, Krutovskikh V, Mesnil M, Traub O, Warngard L(1994). Alteration in expression of gap junction proteins in rat liver after treatment with the tumour promoter 3,4,5,3',4'-pentachlorobiphenyl. *Carcinogenesis.* 15, 2439-2443.

Baker, T. S., Caspar, D. L. D. & Murakami, W. T. (1983). Polyoma virus 'hexamer' tubes consist of paired pentamers. *Nature,* 303, 446–448.

Baker, T. S., Drak, J. & Bina, M. (1989). The capsid of small papova viruses contains 72 pentameric capsomeres: direct evidence from cryoelectron-microscopy of simian virus 40. *Biophys. J.* 55, 243–253.

Band V, De Caprio JA, Delmolino L, Kulesa V, Sager R (1991). Loss of p53 protein in human papillomavirus type 16 E6-immortalized human mammary epithelial cells. *J Virol.* 65, 6671-6676.

Barbosa MS, Edmonds C, Fisher C, Schiller JT, Lowy DR, Vousden KH (2003). The region of the HPV E7 oncoprotein homologous to adenovirus E1a and Sv40 large T antigen contains separate domains for Rb binding and casein kinase II phosphorylation . *EMBO J.* 9, 153-160.

Bargiello TA, Saez L, Baylies MK, Gasic G, Young MW, Spray DC (1987). The Drosophila clock gene per affects intercellular junctional communication. *Nature*. 328, 686-691.

Barker RJ, Price RL, Gourdie RG (2003). Increased association of ZO-1 with connexin43 during remodeling of cardiac gap junctions. *Circ Res.* 90, 317-324.
Beardslee M, J. Laing, E. Beyer and J. Saffitz (1998). Rapid turnover of connexin43 in the adult rat heart. *Circ. Res.* 83, 629–635.

Bedell MA, Jones KH, Grossman SR, Laimins LA (1989). Identification of human papillomavirus type 18 transforming genes in immortalized and primary cells. *J Virol.* 63, 1247-1255.

Beer DG, Neveu MJ, Paul DL, Rapp UR, Pitot HC (1988). Expression of the c-raf protooncogene, gamma-glutamyltranspeptidase, and gap junction protein in rat liver neoplasms. *Cancer Res.* 15, 1610-1617.

Behrens J, Jerchow BA, Wurtele M, Grimm J, Asbrand C, Wirtz R, Kuhl M, Wedlich D, Birchmeier W (1998). Functional interaction of an axin homolog, conductin, with beta-catenin, APC, and GSK3beta. Science. 24, 596-599.

Benharouga M, Haardt M, Kartner N, Lukacs GL (2001). COOH-terminal truncations promote proteasome-dependent degradation of mature cystic fibrosis transmembrane conductance regulator from post-Golgi compartments. *J Cell Biol* 153, 957–970.

Bergoffen J, Scherer SS, Wang S, Scott MO, Bone LJ, Paul DL, Chen K, Lensch MW, Chance PF, Fischbeck KH (1993). Connexin mutations in X-linked Charcot-Marie-Tooth disease. *Science*. 262, 2039-2042.

Berthoud VM, Westphale EM, Grigoryeva A, Beyer EC (2000). PKC isoenzymes in the chicken lens and TPA-induced effects on intercellular communication. *Invest Ophthalmol Vis Sci.* 41, 850-858.

Bevans CG, Kordel M, Rhee SK, Harris AL (1998). Isoform composition of connexin channels determines selectivity among second messengers and uncharged molecules. *J Biol Chem.* 273, 2808-2816.

Bjorkman N.A (1962). Study of the ultrastructure of the granulosa cells of the rat ovary. *Acta Anat. (Basel)* 51,125–147.

Bilder, D., Li, M. and Perrimon, N. (2000). Cooperative regulation of cell polarity and growth by Drosophila tumor suppressors. *Science.* 289, 113-116.

Bosch FX, Munoz N. (2002). The viral etiology of cervical cancer. *Virus Res.* 89, 183-190.

Bossinger O, Schierenberg E (1992). Cell-cell communication in the embryo of Caenorhabditis elegans. *Dev Biol.* 151, 401-409.

Boyer SN, Wazer DE, Band V (1996). E7 protein of human papilloma virus-16 induces degradation of retinoblastoma protein through the ubiquitin-proteasome pathway. *Cancer Res.* 56, 4620-4624.

Bosch FX, Lorincz A, Munoz N, Meijer CJ, Shah KV (2002). The causal relation between human papillmavirus and cervical cancer. *J Clin Pathol.* 55, 244-265.

Brandner JM, Houdek P, Husing B, Kaiser C, Moll I (2004). Connexins 26, 30, and 43: differences among spontaneous, chronic, and accelerated human wound healing. *J Invest Dermatol.* 122, 1310-1320.

Brehm A, Miska EA, McCance DJ, Reid JL, Bannister AJ, Kouzarides T (1998). Retinoblastoma protein recruits histone deacetylase to repress transcription. *Nature.* 391, 597-601.

Breitling R, Armengaud P, Amtmann A, Herzyk P. (2004). Rank products: a simple, yet powerful, new method to detect differentially regulated genes in replicated microarray experiments. *FEBS Lett.* 573, 83-92.

Breitling R, Amtmann A, Herzyk P. (2004). Iterative Group Analysis (iGA): a simple tool to enhance sensitivity and facilitate interpretation of microarray experiments. *BMC Bioinformatics*. 5, 34.

Brenman JE, Topinka JR, Cooper EC, McGee AW, Rosen J, Milroy T, Ralston HJ, Bredt DS (1998). Localization of postsynaptic density-93 to dendritic microtubules and interaction with microtubule-associated protein 1A. *J Neurosci.* 18, 8805-8813.

Briggs MW, Adam JL, McCance DJ (2001). The human papillomavirus type 16 E5 protein alters vacuolar H(+)-ATPase function and stability in Saccharomyces cerevisiae. *Virology*. 280, 169-175.

Brissette JL, Kumar NM, Gilula NB, Hall JE, Dotto GP (1994). Switch in gap junction protein expression is associated with selective changes in junctional permeability during keratinocyte differentiation. *Proc Natl Acad Sci U S A*. 91, 6453-6457.

Brissette JL, Kumar NM, Gilula NB, Dotto GP (1991). The tumor promoter 12-O-tetradecanoylphorbol-13-acetate and the ras oncogene modulate expression and phosphorylation of gap junction proteins. *Mol Cell Biol.* 11, 5364-5371.

Brumby A, Secombe J, Horsfield J, Coombe M, Amin N, Coates D, Saint R, Richardson H (2004). A genetic screen for dominant modifiers of a cyclin E hypomorphic mutation identifies novel regulators of S-phase entry in Drosophila. *Genetics*. 168, 227-251.

Bruzzone R, White TW, Paul DL (1994). Expression of chimeric connexins reveals new properties of the formation and gating behavior of gap junction channels. *J Cell Sci.* 107, 955-967.

Budunova IV, Williams GM (1994). Cell culture assays for chemicals with tumor-promoting or tumor-inhibiting activity based on the modulation of intercellular communication. *Cell Biol Toxicol.* 10, 71-116.

Butkevich E, Hulsmann S, Wenzel D, Shirao T, Duden R, Majoul I (2004). Drebrin is a novel connexin-43 binding partner that links gap junctions to the submembrane cytoskeleton. *Curr Biol.* 14, 650-658.

Campo MS (2002). Animal models of papillomavirus pathogenesis. *Virus Res.* 89, 249-261.

Cao TT, Deacon HW, Reczek D, Bretscher A, von Zastrow M (1999). A kinase-regulated PDZ-domain interaction controls endocytic sorting of the beta2-adrenergic receptor. *Nature.* 401, 286-290.

Carico E, Atlante M, Bucci B, Nofroni I, Vecchione A (2001). E-cadherin and alpha-catenin expression during tumor progression of cervical carcinoma. *Gynecol Oncol.* 80, 156-161.

Carystinos GD, Alaoui-Jamali MA, Phipps J, Yen L, Batist G (2001). Upregulation of gap junctional intercellular communication and connexin 43 expression by cyclic-AMP and all-trans-retinoic acid is associated with glutathione depletion and chemosensitivity in neuroblastoma cells. *Cancer Chemother Pharmacol.* 47, 126-132.

Carystinos, G. D., Bier, A. and Batist, G. (2001). The role of connexin-mediated cell-cell communication in breast cancer metastasis. *J. Mammary Gland Biol. Neoplasia* 6, 431-440.

Cavatorta, A. L., Fumero, G., Chouhy, D., Aguirre, R., Nocito, A.L., Giri, A. A., Banks, L. and Gardiol D. (2004). Differential expression of the human homologue of drosophila discs large oncosupressor in histologic samples from human papillomavirus-associated lesions as a marker for progression to malignancy. *Int. J. Cancer* 111, 373-380.

Chen JJ, Reid CE, Band V, Androphy EJ (1995). Interaction of papillomavirus E6 oncoproteins with a putative calcium-binding protein. *Science*. 269, 529-531.

Chan SY, Delius H, Halpern AL, Bernard HU (1995). Analysis of genomic sequences of 95 papillomavirus types: uniting typing, phylogeny, and taxonomy. *J Virol*. 69, 3074-3083.

Cheng S, Schmidt-Grimminger DC, Murant T, Broker TR, Chow LT (1995). Differentiation-dependent up-regulation of the human papillomavirus E7 gene reactivates cellular DNA replication in suprabasal differentiated keratinocytes. *Genes Dev*. 9, 2335-2349.

Chittenden T, Livingston DM, Kaelin WG Jr (1991). The T/E1A-binding domain of the retinoblastoma product can interact selectively with a sequence-specific DNA-binding protein. *Cell*. 65, 1073-1082.

Choudhry R, Pitts JD, Hodgins MB (1997). Changing patterns of gap junctional intercellular communication and connexin distribution in mouse epidermis and hair follicles during embryonic development. *Dev Dyn*. 210, 417-430.

Churchill GC, Louis CF (1998). Roles of Ca2+, inositol trisphosphate and cyclic ADP-ribose in mediating intercellular Ca2+ signaling in sheep lens cells. *J Cell Sci.* 111, 1217-1225.

Cohen-Salmon M, Ott T, Michel V, Hardelin JP, Perfettini I, Eybalin M, Wu T, Marcus DC, Wangemann P, Willecke K, Petit C (2002). Targeted ablation of connexin26 in the inner ear epithelial gap junction network causes hearing impairment and cell death. *Curr Biol*. 12, 1106-1111.

Cole WC, Garfield RE (1986). Evidence for physiological regulation of myometrial gap junction permeability. Am J Physiol. 251, 411-420.

Conrad, M., V. J. Bubb, and R. Schlegel (1993). The human papillomavirus type 6 and 16 E5 proteins are membrane-associated proteins which associate with the 16-kilodalton pore-forming protein. J. Virol. 67, 6170-6178.

Cope LM, Irizarry RA, Jaffee HA, Wu Z, Speed TP. (2004). A benchmark for Affymetrix GeneChip expression measures. Bioinformatics. 20, 323-331.

Craven SE, Bredt DS (1998). PDZ proteins organize synaptic signaling pathways. *Cell.* 93, 495-498.

Crow DS, Beyer EC, Paul DL, Kobe SS, Lau AF (1990). Phosphorylation of connexin43 gap junction protein in uninfected and Rous sarcoma virus-transformed mammalian fibroblasts. *Mol Cell Biol.* 10, 1754-1763.

Crow DS, Kurata WE, Lau AF. (1992). Phosphorylation of connexin43 in cells containing mutant src oncogenes. *Oncogene.* 7, 999-1003.

Crum CP, Barber S, Symbula M, Snyder K, Saleh AM, Roche JK (1990). Coexpression of the human papillomavirus type 16 E4 and L1 open reading frames in early cervical neoplasia. *Virology.* 178, 238-246.

Crusius K, Rodriguez I, Alonso A (2000). The human papillomavirus type 16 E5 protein modulates ERK1/2 and p38 MAP kinase activation by an EGFR-independent process in stressed human keratinocytes. *Virus Genes.* 20, 65-69.

Cruciani V, Leithe E, Mikalsen SO (2003). Ilimaquinone inhibits gap-junctional communication prior to Golgi fragmentation and block in protein transport. *Exp Cell Res.* 287, 130-142.

Cripe TP, Haugen TH, Turk JP, Tabatabai F, Schmid PG, Durst M, Gissmann L, Roman A, Turek LP (1987). Transcriptional regulation of the human papillomavirus-16 E6-E7 promoter by a keratinocyte-dependent enhancer, and by viral E2 trans-activator and repressor gene products: implications for cervical carcinogenesis. *EMBO J.* 6, 3745-3753.

Daley, Ellen M (1998). Clinical update on the role of HPV and cervical cancer. *Cancer Nurs* 21, 31-35.

Das Sarma J, Lo CW, Koval M (2001). Cx43/beta-gal inhibits Cx43 transport in the Golgi apparatus. *Cell Commun Adhes.* 8, 249-252.

Davy CE, Jackson DJ, Wang Q, Raj K, Masterson PJ, Fenner NF, Southern S, Cuthill S, Millar JB, Doorbar J (2002). Identification of a G(2) arrest domain in the E1 wedge E4 protein of human papillomavirus type 16. *J Virol.* 76, 9806-9818.

de Boer CJ, van Dorst E, van Krieken H, Jansen-van Rhijn CM, Warnaar SO, Fleuren GJ, Litvinov SV (1999). Changing roles of cadherins and catenins during progression of squamous intraepithelial lesions in the uterine cervix. *Am J Pathol.* 155, 505-515.

de Villiers EM, Gissmann L, zur Hausen H (1981). Molecular cloning of viral DNA from human genital warts. *J Virol.* 1981 40, 932-935.

Defamie N, Mograbi B, Roger C, Cronier L, Malassine A, Brucker-Davis F, Fenichel P, Segretain D, Pointis G (2001). Disruption of gap junctional intercellular communication by lindane is associated with aberrant localization of connexin43 and zonula occludens-1 in 42GPA9 Sertoli cells. *Carcinogenesis.* 22, 1537-1542.

Delmar, M., Coombs, W., Sorgen, P., Duffy, H. S. and Taffet, S. M. (2004). Structural bases for the chemical regulation of Connexin 43 channels. *Cardiovasc. Res.* 62, 268-275.

Denk C, Hulsken J, Schwarz E (1997). Reduced gene expression of E-cadherin and associated catenins in human cervical carcinoma cell lines. *Cancer Lett.* 120, 185-193.
Desaintes C, Demeret C (1996). Control of papillomavirus DNA replication and transcription. *Semin Cancer Biol.* 7, 339-347.

Dhar AK, Roux MM, Klimpel KR (2001). Detection and quantification of infectious hypodermal and hematopoietic necrosis virus and white spot virus in shrimp using real-time quantitative PCR and SYBR Green chemistry. *J Clin Microbiol.* 39, 2835-2845.

Dhar AK, Roux MM, Klimpel KR (2002). Quantitative assay for measuring the Taura syndrome virus and yellow head virus load in shrimp by real-time RT-PCR using SYBR Green chemistry. *J Virol Methods*. 104, 69-82.

Diez J.A, S. Ahmad and W. H. Evans (1999). Assembly of heteromeric connexons in guinea-pig liver en route to the Golgi apparatus, plasma membrane and gap junctions. *Eur. J. Biochem.* 262, 142–148.

Dimitratos, S. D, Woods, D.F., Stathakis, D.G. and Bryant, P.J. (1999). Signaling pathways are focused at specialized regions of the plasma membrane by scaffolding proteins of the MAGUK family. *Bioessays* 21, 912-921.

Dimitratos SD, Woods DF, Bryant PJ (1997). Camguk, Lin-2, and CASK: novel membrane-associated guanylate kinase homologs that also contain CaM kinase domains. *Mech Dev*. 63, 127-130.

Dimitratos SD, Woods DF, Stathakis DG, Bryant PJ (1999). Signaling pathways are focused at specialized regions of the plasma membrane by scaffolding proteins of the MAGUK family. *Bioessays*. 21, 912-921.

Dirks PB, Patel K, Hubbard SL, Ackerley C, Hamel PA, Rutka JT (1997). Retinoic acid and the cyclin dependent kinase inhibitors synergistically alter proliferation and morphology of U343 astrocytoma cells. *Oncogene*. 15, 2037-2048.

Doorbar, J., S. Ely, J. Sterling, C. McLean, and L. Crawford. (1991). Specific interaction between HPV-16 E1-E4 and cytokeratins results in collapse of the epithelial cell intermediate filament network. *Nature* 352, 824-827.

Doyle DA, Lee A, Lewis J, Kim E, Sheng M, MacKinnon R (1996). Crystal structures of a complexed and peptide-free membrane protein-binding domain: molecular basis of peptide recognition by PDZ. *Cell*. 85, 1067-1076.

Drain PK, Holmes KK, Hughes JP, Koutsky LA. (2002). Determinants of cervical cancer rates in developing countries. *Int J Cancer*. 100, 199-205.

Duffy HS, Delmar M, Spray DC (2002). Formation of the gap junction nexus: binding partners for connexins. *J Physiol Paris*. 96, 243-249.

Duffy MJ (1998). Cancer metastasis: biological and clinical aspects. *Ir J Med Sci*. 16,: 4-8.

Ellgaard L, Molinari M, Helenius A (1999). Setting the standards: quality control in the secretory pathway. *Science*. 286, 1882–1888.

Ennaji MM, Schwartz JL, Mealing G, Belbaraka L, Parker C, Parentaux M, Jouishomme H, Arella M, Whitfield JF, Phipps J (1995). Alterations in cell-cell communication in human papillomavirus type 16 (HPV16) transformed rat myoblasts. *Cell Mol Biol*. 41, 481-498.

Enomoto T, Yamasaki H (1984). Lack of intercellular communication between chemically transformed and surrounding nontransformed BALB/c 3T3 cells. *Cancer Res*. 44, 5200-5203.

Ennaji MM, Schwartz JL, Mealing G, Belbaraka L, Parker C, Parentaux M, Jouishomme H, Arella M, Whitfield JF, Phipps J (1995). Alterations in cell-cell communication in human papillomavirus type 16 (HPV16) transformed rat myoblasts. *Cell Mol Biol*. 41, 481-498.

Evans WH, Martin PE (2002). Gap junctions: structure and function. *Mol Membr Biol*. 19, 121-136.

Faccini AM, Cairney M, Ashrafi GH, Finbow ME, Campo MS, Pitts JD (1996). The bovine papillomavirus type 4 E8 protein binds to ductin and causes loss of gap junctional intercellular communication in primary fibroblasts. *J Virol*. 70, 9041-9045.

Fallon, R. F., and Goodenough, D. A. (1981). Five-hour half-life of mouse liver gap-junction protein. *J. Cell Biol*. 90, 521–526

Fanning AS, Anderson JM (1996). Protein-protein interactions: PDZ domain networks. *Curr Biol.* 6, 1385-1388.

Fehrmann F, Laimins LA (2003). Human papillomaviruses: targeting differentiating epithelial cells for malignant transformation. *Oncogene.* 22, 5201-5207.

Firestein, B. L. and Rongo, C. (2001). DLG-1 is a MAGUK similar to SAP97 and is required for adherens junction formation. *Mol. Biol. Cell.* 12, 3465-3475.

Fitzgerald DJ, Swierenga SH, Mesnil M, Piccoli C, Marceau N, Yamasaki H (1993). Gap junctional intercellular communication and connexin expression in normal and SV 40-transformed human liver cells in vitro. *Cancer Lett.* 7, 157-165.

Fitzgerald DJ, Mesnil M, Oyamada M, Tsuda H, Ito N, Yamasaki H (1989). Changes in gap junction protein (connexin 32) gene expression during rat liver carcinogenesis. *J Cell Biochem.* 41, 97-102.

Fleming TP, Ghassemifar MR, Sheth B (2000). Junctional complexes in the early mammalian embryo. *Semin Reprod Med.* 18, 185-193.

Fletcher WH, Shiu WW, Ishida TA, Haviland DL, Ware CF (1987). Resistance to the cytolytic action of lymphotoxin and tumor necrosis factor coincides with the presence of gap junctions uniting target cells. *J Immunol.* 139, 956-962.

Forge A, Becker D, Casalotti S, Edwards J, Evans WH, Lench N, Souter M (1999). Gap junctions and connexin expression in the inner ear. Novartis Found Symp. 219, 134-50.

Frattini MG, Laimins LA. (1994). Binding of the human papillomavirus E1 origin-recognition protein is regulated through complex formation with the E2 enhancer-binding protein. Proc Natl Acad Sci U S A. 91, 12398-12402.

Frese KK, Lee SS, Thomas DL, Latorre IJ, Weiss RS, Glaunsinger BA, Javier RT (2003). Selective PDZ protein-dependent stimulation of phosphatidylinositol 3-kinase by the adenovirus E4-ORF1 oncoprotein. *Oncogene.* 22, 710-721.

Fromaget C, el Aoumari A, Gros D (1992). Distribution pattern of connexin 43, a gap junctional protein, during the differentiation of mouse heart myocytes. *Differentiation.* 51, 9-20.

Fu CT, Bechberger JF, Ozog MA, Perbal B, Naus CC. (2004). CCN3 (NOV) interacts with connexin43 in C6 glioma cells: possible mechanism of connexin-mediated growth suppression. J Biol Chem. 279, 36943-36950.

Fujimoto K, Nagafuchi A, Tsukita S, Kuraoka A, Ohokuma A, Shibata Y (1997). Dynamics of connexins, E-cadherin and alpha-catenin on cell membranes during gap junction formation. *J Cell Sci.* 110, 311-322.

Funk JO, Waga S, Harry JB, Espling E, Stillman B, Galloway DA (1997). Inhibition of CDK activity and PCNA-dependent DNA replication by p21 is blocked by interaction with the HPV-16 E7 oncoprotein. *Genes Dev.* 11, 2090-2100.

Furuse M, Itoh M, Hirase T, Nagafuchi A, Yonemura S, Tsukita S, Tsukita S (1994). Direct association of occludin with ZO-1 and its possible involvement in the localization of occludin at tight junctions. *J Cell Biol.* 127, 1617-1626.

Gage JR, Meyers C, Wettstein FO (1990). The E7 proteins of the nononcogenic human papillomavirus type 6b (HPV-6b) and of the oncogenic HPV-16 differ in retinoblastoma protein binding and other properties. *J Virol.* 64, 723-730.

Gaietta, G., Deerinck, T. J., Adams, S. R., Bouwer, J., Tour, O., Laird, D. W., Sosinsky, G. E., Tsien, R. Y., and Ellisman, M. H. (2002). Multicolor and electron microscopic imaging of connexin trafficking. *Science* 296, 503–507.

Gao Q, Singh L, Kumar A, Srinivasan S, Wazer DE, Band V (2001). Human papillomavirus type 16 E6-induced degradation of E6TP1 correlates with its ability to immortalize human mammary epithelial cells. *J Virol.* 75, 4459-4466.

Gardiol D, Kuhne C, Glaunsinger B, Lee SS, Javier R, Banks L (1999). Oncogenic human papillomavirus E6 proteins target the discs large tumour suppressor for proteasome-mediated degradation. *Oncogene*. 18, 5487-5496.

Garner CC, Nash J, Huganir RL (2000). PDZ domains in synapse assembly and signalling. *Trends Cell Biol*. 10, 274-280.

Giepmans BNG, Moolenaar WH. (1998). The gap junction protein connexin 43 interacts with the second PDZ domain of the zonula occludens-1 protein. *Curr Biol* 8, 931–934.

Giepmans BN, Verlaan I, Hengeveld T, Janssen H, Calafat J, Falk MM, Moolenaar WH (2001). Gap junction protein connexin-43 interacts directly with microtubules. *Curr Biol*. 11, 1364-1368.

Giepmans BN, Verlaan I, Moolenaar WH (2001). Connexin-43 interactions with ZO-1 and alpha- and beta-tubulin. *Cell Commun Adhes*. 8, 219-23.

Giessmann D, Theiss C, Breipohl W, Meller K (2005). Decreased gap junctional communication in neurobiotin microinjected lens epithelial cells after taxol treatment. *Anat Embryol.* 209, 391-400.

Gissmann L, Wolnik L, Ikenberg H, Koldovsky U, Schnurch HG, zur Hausen H (1983). Human papillomavirus types 6 and 11 DNA sequences in genital and laryngeal papillomas and in some cervical cancers. *Proc Natl Acad Sci U S A.* 80, 560-563.

Gissmann L, Boshart M, Durst M, Ikenberg H, Wagner D, zur Hausen H (1984). Presence of human papillomavirus in genital tumors. *J Invest Dermatol*. 83, 26-28.

Gissmann L (1992). Human papillomaviruses and genital cancer. Semin *Cancer Biol*. 3, 253-261.

Glaunsinger BA, Lee SS, Thomas M, Banks L, Javier R (2000). Interactions of the PDZ-protein MAGI-1 with adenovirus E4-ORF1 and high-risk papillomavirus E6 oncoproteins. *Oncogene*. 19, 5270-5280.

Gomperts, S. N. (1996). Clustering membrane proteins: It's all coming together with the PSD-95/SAP90 protein family. *Cell* 84, 659-662.

Gonzalez-Mariscal L, Betanzos A, Avila-Flores A (2000). MAGUK proteins: structure and role in the tight junction. *Semin Cell Dev Biol*. 11, 315-324.

Goode S, Perrimon N (1997). Inhibition of patterned cell shape change and cell invasion by Discs large during Drosophila oogenesis. *Genes Dev*. 11, 2532-2544.

Corden SA, Sant-Cassia LJ, Easton AJ, Morris AG (1999). The integration of HPV-18 DNA in cervical carcinoma. *Mol Pathol*. 52, 275-282.

Govers R, van Kerkhof P, Schwartz AL, Strous GJ (1997). Linkage of the ubiquitin-conjugating system and the endocytic pathway in ligand-induced internalization of the growth hormone receptor. *EMBO J*. 16, 4851-4858.

Graeber SH, Hulser DF (1998). Connexin transfection induces invasive properties in HeLa cells. *Exp Cell Res*. 243, 142-149.

Grassmann K, Rapp B, Maschek H, Petry KU, Iftner T. (1996). Identification of a differentiation-inducible promoter in the E7 open reading frame of human papillomavirus type 16 (HPV-16) in raft cultures of a new cell line containing high copy numbers of episomal HPV-16 DNA. *J Virol*. 70, 2339-2349.

Craven, S. E., and D. S. Bredt. (1998). PDZ proteins organize synaptic signaling pathways. *Cell* 93, 495-498.

Greenberg, R. A., R. C. O'Hagan, H. Deng, Q. Xiao, S. R. Hann, R. R. Adams, S. Lichtsteiner, L. Chin, G. B. Morin, and R. A. DePinho. (1999). Telomerase reverse

transcriptase gene is a direct target of c-Myc but is not functionally equivalent in cellular transformation. *Oncogene*. 18, 1219-1226.

Grm HS, Banks L (2004). Degradation of hDlg and MAGIs by human papillomavirus E6 is E6-AP-independent. *J Gen Virol*. 85, 2815-2819.

Gu Z, Matlashewski G (1995). Effect of human papillomavirus type 16 oncogenes on MAP kinase activity. *J Virol*. 69, 8051-8056.

Guo Y, Martinez-Williams C, Rannels DE (2003). Gap junction-microtubule associations in rat alveolar epithelial cells. *Am J Physiol Lung Cell Mol Physiol*. 285, 1213-1221.

Gutstein DE, Morley GE, Tamaddon H, Vaidya D, Schneider MD, Chen J, Chien KR, Stuhlmann H, Fishman GI (2001). Conduction slowing and sudden arrhythmic death in mice with cardiac-restricted inactivation of connexin43. *Circ Res*. 88, 333-339.

Halbert CL, Demers GW, Galloway DA (1991). The E7 gene of human papillomavirus type 16 is sufficient for immortalization of human epithelial cells. *J Virol*. 65, 473-478.

Hanada T, Lin L, Chandy KG, Oh SS, Chishti AH. (1997). Human homologue of the Drosophila discs large tumor suppressor binds to p56lck tyrosine kinase and Shaker type Kv1.3 potassium channel in T lymphocytes. *J Biol Chem*. 272, 26899-26904.

Hanada T, Lin L, Tibaldi EV, Reinherz EL, Chishti AH (2000). GAKIN, a novel kinesin-like protein associates with the human homologue of the Drosophila discs large tumor suppressor in T lymphocytes. *J Biol Chem*. 275, 28774-28784.

Harris AL (2001). Emerging issues of connexin channels: biophysics fills the gap. *Q Rev Biophys*. 34, 325-472.

Harris BZ, Lim WA (2001). Mechanism and role of PDZ domains in signaling complex assembly. *J Cell Sci*. 114, 3219-3231.

Hashida T, Yasumoto S (1991). Induction of chromosome abnormalities in mouse and human epidermal keratinocytes by the human papillomavirus type 16 E7 oncogene. *J Gen Virol.* 72, 1569-1577.

Haskins J, Gu L, Wittchen ES, Hibbard J, Stevenson BR (1998). ZO-3, a novel member of the MAGUK protein family found at the tight junction, interacts with ZO-1 and occludin. *J Cell Biol.* 141, 199-208.

Hatanaka K, Kawata H, Toyofuku T, Yoshida K. (2004). Down-regulation of connexin43 in early myocardial ischemia and protective effect by ischemic preconditioning in rat hearts in vivo. *Jpn Heart J.* 45, 1007-10019.

Hawley-Nelson, P., K. H. Vousden, N. L. Hubbert, D. R. Lowy, and J. T. Schiller. (1989). HPV16 E6 and E7 proteins cooperate to immortalize human foreskin keratinocytes. *EMBO J.* 8, 3905-3910.

Havre PA, Yuan J, Hedrick L, Cho KR, Glazer PM (1995). p53 inactivation by HPV16 E6 results in increased mutagenesis in human cells. *Cancer Res.* 55, 4420-4424.

Hernandez-Blazquez FJ, Joazeiro PP, Omori Y, Yamasaki H (2001). Control of intracellular movement of connexins by E-cadherin in murine skin papilloma cells. *Exp Cell Res.* 270, 235-247.

Hertig CM, Butz S, Koch S, Eppenberger-Eberhardt M, Kemler R, Eppenberger HM (1996). N-cadherin in adult rat cardiomyocytes in culture. II. Spatio-temporal appearance of proteins involved in cell-cell contact and communication. Formation of two distinct N-cadherin/catenin complexes. *J Cell Sci.* 109, 11-20.

Herve JC, Sarrouilhe D (2002). Modulation of junctional communication by phosphorylation: protein phosphatases, the missing link in the chain. *Biol Cell.* 94, 423-432.

Higgins GD, Uzelin DM, Phillips GE, McEvoy P, Marin R, Burrell CJ (1992). Transcription patterns of human papillomavirus type 16 in genital intraepithelial

neoplasia: evidence for promoter usage within the E7 open reading frame during epithelial differentiation. *J Gen Virol.* 73, 2047-2057.

Hinck L, Nathke IS, Papkoff J, Nelson WJ (1994). Beta-catenin: a common target for the regulation of cell adhesion by Wnt-1 and Src signaling pathways. *Trends Biochem Sci.* 19, 538-542.

Hiratsuka M, Kishikawa Y, Narahara K, Inoue T, Hamdy SI, Agatsuma Y, Tomioka Y, Mizugaki M (2001). Detection of angiotensin-converting enzyme insertion/deletion polymorphisms using real-time polymerase chain reaction and melting curve analysis with SYBR Green I on a GeneAmp 5700. *Anal Biochem.* 289, 300-303.

Hirt L, Hirsch-Behnam A, de Villiers EM (1991). Nucleotide sequence of human papillomavirus (HPV) type 41: an unusual HPV type without a typical E2 binding site consensus sequence. *Virus Res.* 18, 179-189.

Homma N, Alvarado JL, Coombs W, Stergiopoulos K, Taffet SM, Lau AF, Delmar M (1998). A particle-receptor model for the insulin-induced closure of connexin43 channels. *Circ Res.* 83, 27-32.

Howley PM (1995). Chapter 65: Papillomavirus and their Replication. In: Field BN, Knipe DM, eds. Field's Virology, vol 2, 3rd ed. New York: Raven Press. 947-980

Howley PM and Lowy DR (2001). Virology, Vol 2. Fields BN, Knipe JB, Howly PM (eds). Lippincott/The Williams & Wilkins Co: Philadelphia PA. 2197-2230

Hough CD, Woods DF, Park S, Bryant PJ (1997). Organizing a functional junctional complex requires specific domains of the Drosophila MAGUK Discs large. *Genes Dev.* 11, 3242-3253.

Howley, P. M. (1996). Papillomaviridae: the viruses and their replication,. *In* B. N. Fields, D. M. Knipe, and P. M. Howley (ed.), Fields virology, 3rd ed. Lippincott-Raven Publishers, Philadelphia, Pa. p. 947-978

Hubert WG, Laimins LA (2002). Human papillomavirus type 31 replication modes during the early phases of the viral life cycle depend on transcriptional and posttranscriptional regulation of E1 and E2 expression. *J Virol.* 76, 2263-2273.

Huibregtse JM, Scheffner M, Howley PM (1991). A cellular protein mediates association of p53 with the E6 oncoprotein of human papillomavirus types 16 or 18. *EMBO J.* 10, 4129-4135.

Hummel M, Hudson JB, Laimins LA (1992). Differentiation-induced and constitutive transcription of human papillomavirus type 31b in cell lines containing viral episomes. *J Virol.* 66, 6070-6080.

Huibregtse JM, Scheffner M, Howley PM (1991). A cellular protein mediates association of p53 with the E6 oncoprotein of human papillomavirus types 16 or 18. *EMBO J.* 10, 4129-4135.

Huibregtse JM, Scheffner M, Howley PM (1993). Localization of the E6-AP regions that direct human papillomavirus E6 binding, association with p53, and ubiquitination of associated proteins. *Mol Cell Biol.* 13, 4918-4927.

Hung AY, Sheng M (2002). PDZ domains: structural modules for protein complex assembly. *J Biol Chem.* 277, 5699-5702.

Hurlin PJ, Foley KP, Ayer DE, Eisenman RN, Hanahan D, Arbeit JM (1995). Regulation of Myc and Mad during epidermal differentiation and HPV-associated tumorigenesis. *Oncogene.* 11, 2487-2501.

Hurtley S.M and A. Helenius (1989). Protein oligomerization in the endoplasmic reticulum. *Annu. Rev. Cell Biol.* 5, 277–307

Hyrc K, Rose B (1990). The action of v-src on gap junctional permeability is modulated by pH. *J Cell Biol.* 110, 1217-1226.

Ide N, Hata Y, Nishioka H, Hirao K, Yao I, Deguchi M, Mizoguchi A, Nishimori H, Tokino T, Nakamura Y, Takai Y (1999). Localization of membrane-associated guanylate kinase (MAGI)-1/BAI-associated protein (BAP) 1 at tight junctions of epithelial cells. *Oncogene*. 18, 7810-7815.

Iizuka-Kogo A, Shimomura A, Senda T (2005). Colocalization of APC and DLG at the tips of cellular protrusions in cultured epithelial cells and its dependency on cytoskeletons. *Histochem Cell Biol*. 123, 67-73.

Imamura F, Maeda S, Doi T, Fujiyoshi Y (2002). Ligand binding of the second PDZ domain regulates clustering of PSD-95 with the Kv1.4 potassium channel. *J Biol Chem*. 277, 3640-3646.

Irizarry RA, Hobbs B, Collin F, Beazer-Barclay YD, Antonellis KJ, Scherf U, Speed TP. (2003). Exploration, normalization, and summaries of high density oligonucleotide array probe level data. *Biostatistics*. 4, 249-264.

Isacson C, Kessis TD, Hedrick L, Cho KR (1996). Both cell proliferation and apoptosis increase with lesion grade in cervical neoplasia but do not correlate with human papillomavirus type. *Cancer Res*. 56, 669-674.

Ishidate T, Matsumine A, Toyoshima K, Akiyama T (2000). The APC-hDLG complex negatively regulates cell cycle progression from the G0/G1 to S phase. *Oncogene*. 19, 365-372.

Itoh M, Nagafuchi A, Moroi S, Tsukita S (1997). Involvement of ZO-1 in cadherin-based cell adhesion through its direct binding to alpha catenin and actin filaments. *J Cell Biol*. 138, 181-192.

Jamakosmanovic and Loewenstein. A (1968). Cellular uncoupling in cancerous thyroid epithelium. *Nature* 218, 775.

Jenson AB, Kurman RJ, Lancaster WD (1991). Tissue effects of and host response to human papillomavirus infection. *Dermatol Clin*. 9, 203-209.

Jeon S, Lambert PF (1995). Integration of human papillomavirus type 16 DNA into the human genome leads to increased stability of E6 and E7 mRNAs: implications for cervical carcinogenesis. *Proc Natl Acad Sci U S A*. 92, 1654-1658.

Jeon S, Allen-Hoffmann BL, Lambert PF (1995). Integration of human papillomavirus type 16 into the human genome correlates with a selective growth advantage of cells. *J Virol*. 69, 2989-2997.

Jiang M, Milner J (2002). Selective silencing of viral gene expression in HPV-positive human cervical carcinoma cells treated with siRNA, a primer of RNA interference. *Oncogene*. 21, 6041-6048.

Johnson RG, Meyer RA, Li XR, Preus DM, Tan L, Grunenwald H, Paulson AF, Laird DW, Sheridan JD (2002). Gap junctions assemble in the presence of cytoskeletal inhibitors, but enhanced assembly requires microtubules. *Exp Cell Res*. 275, 67-80.

Jones DL, Thompson DA, Munger K (1997). Destabilization of the RB tumor suppressor protein and stabilization of p53 contribute to HPV type 16 E7-induced apoptosis. *Virology*. 239, 97-107.

Jones DL, Alani RM, Munger K (1997). The human papillomavirus E7 oncoprotein can uncouple cellular differentiation and proliferation in human keratinocytes by abrogating p21Cip1-mediated inhibition of cdk2. *Genes Dev*. 11, 2101-2111.

Jordan, K., Chodock, R., Hand, A. R., and Laird, D. W. (2001). The origin of annular junctions: a mechanism of gap junction internalization. *J. Cell Sci.* 114, 763–773.

Jordan K, Solan JL, Dominguez M, Sia M, Hand A, Lampe PD, Laird DW (1999). Trafficking, assembly, and function of a connexin43-green fluorescent protein chimera in live mammalian cells. *Mol Biol Cell*. 10, 2033-2050.

Jou YS, Matesic D, Dupont E, Lu SC, Rupp HL, Madhukar BV, Oh SY, Trosko JE, Chang CC (1993). Restoration of gap-junctional intercellular communication in a

communication-deficient rat liver cell mutant by transfection with connexin 43 cDNA. *Mol Carcinog.* 8, 234-244.

Kadle R, Zhang JT, Nicholson BJ (1991). Tissue-specific distribution of differentially phosphorylated forms of Cx43. *Mol Cell Biol.* 11, 363-369.

Kanemitsu MY, Loo LW, Simon S, Lau AF, Eckhart W (1997). Tyrosine phosphorylation of connexin 43 by v-Src is mediated by SH2 and SH3 domain interactions. *J Biol Chem.* 272, 22824-22831.

Kanno and Matsui (1968). Cellular uncoupling in cancerous stomach epithelium. *Nature* 218, 775–776.

Kausalya PJ, Reichert M, Hunziker W (2001). Connexin45 directly binds to ZO-1 and localizes to the tight junction region in epithelial MDCK cells. *FEBS Lett.* 505, 92-96.

Kehmeier E, Ruhl H, Voland B, Stoppler MC, Androphy E, Stoppler H (2002). Cellular steady-state levels of "high risk" but not "low risk" human papillomavirus (HPV) E6 proteins are increased by inhibition of proteasome-dependent degradation independent of their p53- and E6AP-binding capabilities. *Virology.* 299, 72-87.

Kelsell DP, Di WL, Houseman MJ (2001). Connexin mutations in skin disease and hearing loss. *Am J Hum Genet.* 68, 559-68.

Khan SH, Wahl GM (1998). p53 and pRb prevent rereplication in response to microtubule inhibitors by mediating a reversible G1 arrest. *Cancer Res.* 58, 396-401.

Kidd JG, Roous P (1940). A transplantable rabbit carcinoma originating in a virus induced papilloma and containing the virus in masked or alter form. *J Exp Med* 71, 813-837

Kidder G.M, J. Rains and J. McKeon (1987). Gap junction assembly in the preimplantation mouse conceptus is independent of microtubules, microfilaments, cell flattening, cytokinesis. *Proc. Natl. Acad. Sci. USA* 84, 3718–3722.

Kikuchi T, Kimura RS, Paul DL, Adams JC (1995). Gap junctions in the rat cochlea: immunohistochemical and ultrastructural analysis. *Anat Embryol.* 191, 101-118.

Kim, E., DeMarco, S. J., Marfatia, S. M., Chishti, A. H., Sheng, M. and Strehler, E. E. (1998). Plasma membrane Ca2+ ATPase isoform 4b binds to membrane-associated guanylate kinase (MAGUK) proteins via their PDZ (PSD-95/Dlg/ZO-1) domains. *J. Biol. Chem.* 273, 1591-1595.

Kim E, Niethammer M, Rothschild A, Jan YN, Sheng M (1995). Clustering of Shaker-type K+ channels by interaction with a family of membrane-associated guanylate kinases. *Nature.* 378, 85-88.

King TJ, Fukushima LH, Hieber AD, Shimabukuro KA, Sakr WA, Bertram JS (2000). Reduced levels of connexin43 in cervical dysplasia: inducible expression in a cervical carcinoma cell line decreases neoplastic potential with implications for tumor progression. *Carcinogenesis.* 21, 1097-1109.

Kiyono, T., S. A. Foster, J. I. Koop, J. K. McDougall, D. A. Galloway, and A. J. Klingelhutz. (1998). Both Rb/p16INK4a inactivation and telomerase activity are required to immortalize human epithelial cells. *Nature.* 396, 84-88.

Kiyono T, Hiraiwa A, Fujita M, Hayashi Y, Akiyama T, Ishibashi M (1997). Binding of high-risk human papillomavirus E6 oncoproteins to the human homologue of the Drosophila discs large tumor suppressor protein. *Proc Natl Acad Sci U S A.* 94, 11612-11616.

Klingelhutz, A. J., S. A. Foster, and J. K. McDougall. (1996). Telomerase activation by the E6 gene product of human papillomavirus type 16. *Nature* 380, 79-82.

Klingelhutz AJ, Foster SA, McDougall JK (1999). Telomerase activation by the E6 gene product of human papillomavirus type 16. *Nature.* 380, 79-82.

Kornau HC, Schenker LT, Kennedy MB, Seeburg PH (1995). Domain interaction between NMDA receptor subunits and the postsynaptic density protein PSD-95. *Science*. 269, 1737-1740.

Koval M, Harley JE, Hick E, Steinberg TH (1997). Connexin46 is retained as monomers in a trans-Golgi compartment of osteoblastic cells. *J Cell Biol* 137, 847–857.

Krutovskikh VA, Oyamada M, Yamasaki H (1991). Sequential changes of gap-junctional intercellular communications during multistage rat liver carcinogenesis: direct measurement of communication in vivo. *Carcinogenesis.* 12, 1701-1706.

Krutovskikh VA, Mesnil M, Mazzoleni G, Yamasaki H (1995). Inhibition of rat liver gap junction intercellular communication by tumor-promoting agents in vivo. Association with aberrant localization of connexin proteins. *Lab Invest*. 72, 571-577.

Krutovskikh, V. and Yamasaki, H. (1997). The role of gap junctional intercellular communication (GJIC) disorders in experimental and human carcinogenesis. *Histol. Histopathol.* 12, 761-768.

Kumar NM, Gilula NB (1996). The gap junction communication channel. *Cell*. 84, 381-388.

Krutovskikh V, Mazzoleni G, Mironov N, Omori Y, Aguelon AM, Mesnil M, Berger F, Partensky C, Yamasaki H (1994). Altered homologous and heterologous gap-junctional intercellular communication in primary human liver tumors associated with aberrant protein localization but not gene mutation of connexin 32. *Int J Cancer*. 56, 87-94.

Krzyzek RA, Watts SL, Anderson DL, Faras AJ, Pass F (1980). Anogenital warts contain several distinct species of human papillomavirus. *J Virol*. 36, 236-44.

Kwak BR, Hermans MM, De Jonge HR, Lohmann SM, Jongsma HJ, Chanson M. (1995). Differential regulation of distinct types of gap junction channels by similar phosphorylating conditions. Mol Biol Cell. 6, 1707-1719.

Kuhne C, Gardiol D, Guarnaccia C, Amenitsch H, Banks L (2000). Differential regulation of human papillomavirus E6 by protein kinase A: conditional degradation of human discs large protein by oncogenic E6. *Oncogene*. 19, 5884-5891.

Kurata WE, Lau AF (1994). p130gag-fps disrupts gap junctional communication and induces phosphorylation of connexin43 in a manner similar to that of pp60v-src. *Oncogene*. 9, 329-35.

Kyo, S., M. Takakura, T. Taira, T. Kanaya, H. Itoh, M. Yutsudo, H. Ariga, and M. Inoue. (2000). Sp1 cooperates with c-Myc to activate transcription of the human telomerase reverse transcriptase gene (hTERT). *Nucleic Acids Res*. 28, 669-677.

Laird DW, Castillo M, Kasprzak L (1995). Gap junction turnover, intracellular trafficking, and phosphorylation of connexin43 in brefeldin A-treated rat mammary tumor cells. *J Cell Biol*. 131, 1193-203.

Laird DW, Puranam KL, Revel JP (1991). Turnover and phosphorylation dynamics of connexin43 gap junction protein in cultured cardiac myocytes. *Biochem J*. 273, 67-72.

Lahey T, Gorczyca M, Jia XX, Budnik V (1994). The Drosophila tumor suppressor gene dlg is required for normal synaptic bouton structure. *Neuron*. 13, 823-835.

Laird, D. W. (1996). The life cycle of a connexin: gap junction formation, removal, and degradation. *J. Bioenerg. Biomembr.* 28, 311–318

Lampe PD, Lau AF. (2004). The effects of connexin phosphorylation on gap junctional communication. *Int J Biochem Cell Biol*. 36, 1171-1186.

Lampe PD, TenBroek EM, Burt JM, Kurata WE, Johnson RG, Lau AF (2000). Phosphorylation of connexin43 on serine368 by protein kinase C regulates gap junctional communication. *J Cell Biol*. 26, 1503-1512.

Lampe PD, Lau AF (2000). Regulation of gap junctions by phosphorylation of connexins. *Arch Biochem Biophys*. 384, 205-215.

Lampe PD, Nguyen BP, Gil S, Usui M, Olerud J, Takada Y, Carter WG (1998). Cellular interaction of integrin alpha3beta1 with laminin 5 promotes gap junctional communication. *J Cell Biol.* 143, 1735-1747.

LaPorta RF, Taichman LB (1982). Human papilloma viral DNA replicates as a stable episome in cultured epidermal keratinocytes. *Proc Natl Acad Sci U S A.* 79, 3393-3397.

Laprise, P., Chailler, P., Houde, M., Beaulieu, J. F., Boucher, M. J., and Rivard, N. (2002). Phosphatidylinositol 3-Kinase Controls Human Intestinal Epithelial Cell Differentiation by Promoting Adherens Junction Assembly and p38 MAPK Activation. *J. Biol. Chem.* 277, 8226–8234.

Laprise, P., Viel, A. and Rivard, N. (2004). Human homolog of disc-large is required for adherens junction assembly and differentiation of human intestinal epithelial cells. *J. Biol. Chem.* 12, 10157-10166.

Laing, J. G., and Beyer, E. C. (1995). The Gap Junction Protein Connexin43 Is Degraded via the Ubiquitin Proteasome Pathway. *J. Biol. Chem.* 270, 26399–26403.

Laing JG, Tadros PN, Westphale EM, Beyer EC (1997). Degradation of connexin43 gap junctions involves both the proteasome and the lysosome. *Exp Cell Res.* 1997 Nov 1;236(2):482-92.

Liu X, Han S, Baluda MA, Park NH. HPV-16 oncogenes E6 and E7 are mutagenic in normal human oral keratinocytes. *Oncogene.* 14, 2347-2353.

Laird DW, Castillo M, Kasprzak L (1995). Gap junction turnover, intracellular trafficking, and phosphorylation of connexin43 in brefeldin A-treated rat mammary tumor cells. *J Cell Biol.* 131, 1193-1203.

Larsen W.J.,Tung H.N.,Murray S.A. and Swenson C.A. (1979) Evidence for the participation of actin microfilaments and bristle coats in the internalization of gap junction membrane. *J. Cell Biol.* 83, 576–587.

Larson D.M., Christensen T.G., Sagar G.D.V, and Beyer E.C. (2001) TGF-β1 induces an accumulation of connexin43 in a lysosomal compartment in endothelial cells. *Endothelium*. 8, 255–260.

Lau AF, Kanemitsu MY, Kurata WE, Danesh S, Boynton AL. (1992). Epidermal growth factor disrupts gap-junctional communication and induces phosphorylation of connexin43 on serine. *Mol Biol Cell*. 3, 865-874.

Lauf U, Giepmans BN, Lopez P, Braconnot S, Chen SC, Falk MM (2002). Dynamic trafficking and delivery of connexons to the plasma membrane and accretion to gap junctions in living cells. *Proc Natl Acad Sci U S A*. 99, 10446-10451.

Lee SS, Weiss RS, Javier RT (1997). Binding of human virus oncoproteins to hDlg/SAP97, a mammalian homolog of the Drosophila discs large tumor suppressor protein. *Proc Natl Acad Sci U S A*. 94, 6670-6675.

Leithe E, Rivedal E (2004). Ubiquitination and down-regulation of gap junction protein connexin-43 in response to 12-O-tetradecanoylphorbol 13-acetate treatment. *J Biol Chem*. 279, 50089-50096.

Lin R, Warn-Cramer BJ, Kurata WE, Lau AF (2001). v-Src phosphorylation of connexin 43 on Tyr247 and Tyr265 disrupts gap junctional communication. *J Cell Biol*. 154, 815-827.

Liu, J. P. (1999). Studies of the molecular mechanisms in the regulation of telomerase activity. *FASEB J.* 13, 2091-2104.

Liu Y, Chen JJ, Gao Q, Dalal S, Hong Y, Mansur CP, Band V, Androphy EJ (1999). Multiple functions of human papillomavirus type 16 E6 contribute to the immortalization of mammary epithelial cells. *J Virol*. 73, 7297-7307.

Lo W.K, A. Mills and J. F. Kuck (1994). Actin filament bundles are associated with fiber gap junctions in the primate lens. *Exp. Eye Res.* 58, 189–196.

Loewenstein. W.R. Loewenstein (1979). Junctional intercellular communication and the control of growth. *Biochim. Biophys. Acta* 560, 1–65.

Lowenstein WR (1985). Regulation of cell-to-cell communication by phosphorylation. *Biochem Soc Symp.* 50, 43-58.

Loewenstein, W.R., Kanno, Y (1966). Intercellular communication and the control of tissue growth : lackof communication between cancer cells. *Nature.* 209, 1248-1249

Longworth MS, Laimins LA (2004). Pathogenesis of human papillomaviruses in differentiating epithelia. *Microbiol Mol Biol Rev.* 68, 362-372.

Lucke T, Choudhry R, Thom R, Selmer IS, Burden AD, Hodgins MB (1999). Upregulation of connexin 26 is a feature of keratinocyte differentiation in hyperproliferative epidermis, vaginal epithelium, and buccal epithelium. *J Invest Dermatol.* 112, 354-361.

Lue RA, Marfatia SM, Branton D, Chishti AH (1994). Cloning and characterization of hdlg: the human homologue of the Drosophila discs large tumor suppressor binds to protein 4.1. *Proc Natl Acad Sci U S A.* 91, 9818-9822.

Lue RA, Brandin E, Chan EP, Branton D (1996). Two independent domains of hDlg are sufficient for subcellular targeting: the PDZ1-2 conformational unit and an alternatively spliced domain. *J Cell Biol.* 135, 1125-1137.

Lustig AJ (2004). Telomerase RNA: a flexible RNA scaffold for telomerase biosynthesis. *Curr Biol.* 14, 565-567.

Mantovani F, Massimi P, Banks L (2001). Proteasome-mediated regulation of the hDlg tumour suppressor protein. *J Cell Sci.* 114, 4285-4292.

Mao AJ, Bechberger J, Lidington D, Galipeau J, Laird DW, Naus CC (2000). Neuronal differentiation and growth control of neuro-2a cells after retroviral gene delivery of connexin43. *J Biol Chem.* 275, 34407-34414.

Marfatia SM, Morais Cabral JH, Lin L, Hough C, Bryant PJ, Stolz L, Chishti AH (1996). Modular organization of the PDZ domains in the human discs-large protein suggests a mechanism for coupling PDZ domain-binding proteins to ATP and the membrane cytoskeleton. *J Cell Biol.* 135, 753-766.

Marshall T, Pater A, Pater MM (1989). Trans-regulation and differential cell specificity of human papillomavirus types 16, 18, and 11 cis-acting elements. *J Med Virol.* 29, 115-126.

Martin PE, Blundell G, Ahmad S, Errington RJ, Evans WH (2001). Multiple pathways in the trafficking and assembly of connexin 26, 32 and 43 into gap junction intercellular communication channels. *J Cell Sci.* 114, 3845-3855.

Martin LG, Demers GW, Galloway DA (1998). Disruption of the G1/S transition in human papillomavirus type 16 E7-expressing human cells is associated with altered regulation of cyclin E. *J Virol.* 72, 975-985.

Martin PE, Steggles J, Wilson C, Ahmad S, Evans WH (2000). Targeting motifs and functional parameters governing the assembly of connexins into gap junctions. *Biochem J.* 349, 281-287.

Martin PE, Blundell G, Ahmad S, Errington RJ, Evans WH (2001). Multiple pathways in the trafficking and assembly of connexin 26, 32 and 43 into gap junction intercellular communication channels. *J Cell Sci.* 114, 3845-3855.

Mary H. Bunney, Claire Benton, Heather A. Cubie (1992). Viral warts: biology and treatment Chapter 3, Field's Virology. Oxford: Oxford University Press, 1992 Oxford, New York, Oxford University Press,. 2nd ed.

Marziano NK, Casalotti SO, Portelli AE, Becker DL, Forge A. (2003). Mutations in the gene for connexin 26 (GJB2) that cause hearing loss have a dominant negative effect on connexin 30. Hum Mol Genet. 12, 805-812.

Massimi P, Gammoh N, Thomas M, Banks L (2004). HPV E6 specifically targets different cellular pools of its PDZ domain-containing tumour suppressor substrates for proteasome-mediated degradation. *Oncogene*. 23, 8033-8039.

Matsumine A, Ogai A, Senda T, Okumura N, Satoh K, Baeg GH, Kawahara T, Kobayashi S, Okada M, Toyoshima K, Akiyama T (1996). Binding of APC to the human homolog of the Drosophila discs large tumor suppressor protein. *Science*. 272, 1020-1023.

Mayer BJ (2001). SH3 domains: complexity in moderation. *J Cell Sci.* 114, 1253-1263.

Mazzoleni G, Camplani A, Telo P, Pozzi A, Tanganelli S, Elfgang C, Willecke K, Ragnotti G (1996). Effect of tumor-promoting and anti-promoting chemicals on the viability and junctional coupling of human HeLa cells transfected with DNAs coding for various murine connexin proteins. *Comp Biochem Physiol C Pharmacol Toxicol Endocrinol.* 113, 247-256.

McGee AW, Topinka JR, Hahimoto K, Petrailia RS, Kakizawa S, Kauer F, Aguilera-Moreno A, Wenthold RJ, Kano M, Bredt DS (2001). PSD-93 knock-out mice reveal that neuronal MAGUKs are not required for development or function of parallel fiber synapses in cerebellum. *J Neurosci.* 21, 3085–3091.

McIntyre MC, Frattini MG, Grossman SR, Laimins LA (1993). Human papillomavirus type 18 E7 protein requires intact Cys-X-X-Cys motifs for zinc binding, dimerization, and transformation but not for Rb binding. *J Virol.* 67, 3142-50.

Mcmurray H.R; D. Nguyen; T.F. Westbrook; D.J. Mcance (2001). Biology of human papillomaviruses. *Int. J. Exp. Path* 182, 15-33.

McNutt NS, Hershberg RA, Weinstein RS (1971). Further observations on the occurrence of nexuses in benign and malignant human cervical epithelium. *J Cell Biol.* 51, 805-825.

McNutt NS, Weinstein RS. (1969). Carcinoma of the cervix: deficiency of nexus intercellular junctions. Science. 165, 597-599.

Mehta PP, Bertram JS, Loewenstein WR (1986). Growth inhibition of transformed cells correlates with their junctional communication with normal cells. *Cell.* 44, 187-196.

Mesnil M, Yamasaki H (1993). Cell-cell communication and growth control of norml and cancer cells: evidence and hypothesis. *Mol Carcinog.* 7, 14-17.

Meyer RA, Laird DW, Revel JP, Johnson RG (1992). Inhibition of gap junction and adherens junction assembly by connexin and A-CAM antibodies. *J Cell Biol.* 119, 179-189.

Migaud M, Charlesworth P, Dempster M, Webster LC, Watabe AM, Makhinson M, He Y, Ramsay MF, Morris RG, Morrison JH, O'Dell TJ, Grant SG (1998). Enhanced long-term potentiation and impaired learning in mice with mutant postsynaptic density-95 protein. *Nature.* 396, 433–439.

Missero C, Di Cunto F, Kiyokawa H, Koff A, Dotto GP (1996). The absence of p21Cip1/WAF1 alters keratinocyte growth and differentiation and promotes ras-tumor progression. *Genes Dev.* 10, 3065-3075.

Morais Cabral JH, Petosa C, Sutcliffe MJ, Raza S, Byron O, Poy F, Marfatia SM, Chishti AH, Liddington RC (1996). Crystal structure of a PDZ domain. *Nature.* 382, 649-652.

Moreno AP, Chanson M, Elenes S, Anumonwo J, Scerri I, Gu H, Taffet SM, Delmar M (2002). Role of the carboxyl terminal of connexin43 in transjunctional fast voltage gating. *Circ Res.* 90, 450-457.

Morley GE, Taffet SM, Delmar M (1996). Intramolecular interactions mediate pH regulation of connexin43 channels. *Biophys J.* 70, 1294-1302.

Munger K, Baldwin A, Edwards KM, Hayakawa H, Nguyen CL, Owens M, Grace M, Huh K (2004). Mechanisms of human papillomavirus-induced oncogenesis. *J Virol.* 78, 11451-11460.

Munger K, Howley PM (2002). Human papillomavirus immortalization and transformation functions. *Virus Res.* 89, 213-228.

Munoz N (2000). Human papillomavirus and cancer: the epidemiological evidence. *J Clin Virol*19, 1-5.

Murray AW, Fitzgerald DJ (1979). Tumor promoters inhibit metabolic cooperation in cocultures of epidermal and 3T3 cells. *Biochem Biophys Res Commun.* 91, 395-401.

Musil L.S, E. C. Beyer and D. A. Goodenough (1990). Expression of the gap junction protein connexin43 in embryonic chick lens: Molecular cloning, ultrastructural localization, and post-translational phosphorylation *J. Membr. Biol.* 116, 163–175.

Musil LS, Goodenough DA (1993). Multisubunit assembly of an integral plasma membrane channel protein, gap junction connexin43, occurs after exit from the ER. *Cell.* 74, 1065-1077.

Musil, L. S., Le, A. C., VanSlyke, J. K., and Roberts, L. M. (2000). Regulation of Connexin Degradation as a Mechanism to Increase Gap Junction Assembly and Function *J. Biol. Chem.* 275, 25207–25215.

Na HK, Wilson MR, Kang KS, Chang CC, Grunberger D, Trosko JE. (2000). Restoration of gap junctional intercellular communication by caffeic acid phenethyl ester (CAPE) in a ras-transformed rat liver epithelial cell line. Cancer Lett. 157, 31-38.

Nakamura, T. M., G. B. Morin, K. B. Chapman, S. L. Weinrich, W. H. Andrews, J. Lingner, C. B. Harley, and T. R. Cech. (1997). Telomerase catalytic subunit homologs from fission yeast and human. *Science* 277, 955-959.

Nakagawa S, Huibregtse JM (2000). Human scribble (Vartul) is targeted for ubiquitin-mediated degradation by the high-risk papillomavirus E6 proteins and the E6AP ubiquitin-protein ligase. *Mol Cell Biol.* 20, 8244-8253.

Nakahara T, Nishimura A, Tanaka M, Ueno T, Ishimoto A, Sakai H (2002). Modulation of the cell division cycle by human papillomavirus type 18 E4. *J Virol.* 76, 10914-10920.

Näthke, I. S., Hinck, L., Swedlow, J. R., Papkoff, J. and Nelson, W. J. (1994). Defining interactions and distributions of cadherin and catenin complexes in polarized epithelial cells. *J. Cell Biol.* 125,1341 -1352.

Naus CC (2002). Gap junctions and tumour progression. *Can J Physiol Pharmacol.* 80, 136-141.

Naus CC, Hearn S, Zhu D, Nicholson BJ, Shivers RR (1993). Ultrastructural analysis of gap junctions in C6 glioma cells transfected with connexin43 cDNA. *Exp Cell Res.* 206, 72-84.

Nelis E, Haites N, Van Broeckhoven C (1999). Mutations in the peripheral myelin genes and associated genes in inherited peripheral neuropathies. *Hum Mutat.* 13, 11-28.

Nguyen ML, Nguyen MM, Lee D, Griep AE, Lambert PF (2003). The PDZ ligand domain of the human papillomavirus type 16 E6 protein is required for E6's induction of epithelial hyperplasia in vivo. *J Virol.* 77, 6957-6964.

Niethammer M, Valtschanoff JG, Kapoor TM, Allison DW, Weinberg TM, Craig AM, Sheng M (1998). CRIPT, a novel postsynaptic protein that binds to the third PDZ domain of PSD-95/SAP90. *Neuron.* 20, 693-707.

Nelles E, Butzler C, Jung D, Temme A, Gabriel HD, Dahl U, Traub O, Stumpel F, Jungermann K, Zielasek J, Toyka KV, Dermietzel R, Willecke K (1996). Defective propagation of signals generated by sympathetic nerve stimulation in the liver of connexin32-deficient mice. *Proc Natl Acad Sci U S A.* 93, 9565-9570.

Nielsen PA, Baruch A, Shestopalov VI, Giepmans BN, Dunia I, Benedetti EL, Kumar NM (2003). Lens connexins alpha3Cx46 and alpha8Cx50 interact with zonula occludens protein-1 (ZO-1). *Mol Biol Cell.* 14, 2470-2481.

Nix SL, Chishti AH, Anderson JM, Walther Z (2000). hCASK and hDlg associate in epithelia, and their src homology 3 and guanylate kinase domains participate in both intramolecular and intermolecular interactions. *J Biol Chem.* 275, 41192-41200.

Oelze I, Kartenbeck J, Crusius K, Alonso A (1995). Human papillomavirus type 16 E5 protein affects cell-cell communication in an epithelial cell line. *J Virol.* 69, 4489-4494.

Pal JD, Liu X, Mackay D, Shiels A, Berthoud VM, Beyer EC, Ebihara L (2000). Connexin46 mutations linked to congenital cataract show loss of gap junction channel function. *Am J Physiol Cell Physiol.* 279, 596-602.

Pal JD, Berthoud VM, Beyer EC, Mackay D, Shiels A, Ebihara L (1999). Molecular mechanism underlying a Cx50-linked congenital cataract. *Am J Physiol.* 276, 1443-1446.

Panchin Y, Kelmanson I, Matz M, Lukyanov K, Usman N, Lukyanov S (2000). A ubiquitous family of putative gap junction molecules. *Curr Biol.* 10, 473-474.

Park TW, Fujiwara H, Wright TC (1995). Molecular biology of cervical cancer and its precursors. *Cancer.* 15, 1902-1913.

Patel D, Huang SM, Baglia LA, McCance DJ (1999). The E6 protein of human papillomavirus type 16 binds to and inhibits co-activation by CBP and p300. *EMBO J.* 18, 5061-5072.

Paulson AF, Lampe PD, Meyer RA, TenBroek E, Atkinson MM, Walseth TF, Johnson RG (2000). Cyclic AMP and LDL trigger a rapid enhancement in gap junction assembly through a stimulation of connexin trafficking. *J Cell Sci.* 113, 3037-3049.

Paznekas WA, Boyadjiev SA, Shapiro RE, Daniels O, Wollnik B, Keegan CE, Innis JW, Dinulos MB, Christian C, Hannibal MC, Jabs EW(2003). Connexin 43 (GJA1) mutations cause the pleiotropic phenotype of oculodentodigital dysplasia. *Am J Hum Genet.* 72, 408-418.

Peebles KA, Duncan MW, Ruch RJ, Malkinson AM. (2003). Proteomic analysis of a neoplastic mouse lung epithelial cell line whose tumorigenicity has been abrogated by transfection with the gap junction structural gene for connexin 43, Gja1. Carcinogenesis. 24, 651-657.

Perea SE, Massimi P, Banks L (2000). Human papillomavirus type 16 E7 impairs the activation of the interferon regulatory factor-1. *Int J Mol Med.* 5, 661-666.

Peters NS, Severs NJ, Rothery SM, Lincoln C, Yacoub MH, Green CR. (1994). Spatiotemporal relation between gap junctions and fascia adherens junctions during postnatal development of human ventricular myocardium. Circulation. 90, 713-725.

Phelan P, Starich TA (2001). Innexins get into the gap. *Bioessays.* 23, 388-396.

Phelps WC, Munger K, Yee CL, Barnes JA, Howley PM (1992). Structure-function analysis of the human papillomavirus type 16 E7 oncoprotein. *J Virol.* 66, 2418-2427.

Piepenhagen PA, Nelson WJ (1993). Defining E-cadherin-associated protein complexes in epithelial cells: plakoglobin, beta- and gamma-catenin are distinct components. *J Cell Sci.* 104, 751-762.

Pietenpol JA, Stein RW, Moran E, Yaciuk P, Schlegel R, Lyons RM, Pittelkow MR, Munger K, Howley PM, Moses HL (1990). TGF-beta 1 inhibition of c-myc transcription and growth in keratinocytes is abrogated by viral transforming proteins with pRB binding domains. *Cell.* 61, 777-785.

Pim D, Thomas M, Javier R, Gardiol D, Banks L (2000). HPV E6 targeted degradation of the discs large protein: evidence for the involvement of a novel ubiquitin ligase. *Oncogene.* 19, 719-725.

Plotkin LI, Manolagas SC, Bellido T (2002). Transduction of cell survival signals by connexin-43 hemichannels. *J Biol Chem.* 277, 8648-8657.

Puranam KL, Laird DW, Revel JP (1993). Trapping an intermediate form of connexin43 in the Golgi. *Exp Cell Res.* 206, 85-92.

Qin H, Shao Q, Curtis H, Galipeau J, Belliveau DJ, Wang T, Alaoui-Jamali MA, Laird DW (2002). Retroviral delivery of connexin genes to human breast tumor cells inhibits in vivo tumor growth by a mechanism that is independent of significant gap junctional intercellular communication. *J Biol Chem.* 277, 29132-29138.

Qin H, Shao Q, Igdoura SA, Alaoui-Jamali MA, Laird DW (2003). Lysosomal and proteasomal degradation play distinct roles in the life cycle of Cx43 in gap junctional intercellular communication-deficient and -competent breast tumor cells. *J Biol Chem.* 278, 30005-30014.

Rassat J., H. Robenek and H. Themenn (1982). Alterations of tight gap junctions in mouse hepatocytes following administration of colchicine. *Cell Tiss. Res.* 223, 187-200.

Reinstein E, Scheffner M, Oren M, Ciechanover A, Schwartz A (2000). Degradation of the E7 human papillomavirus oncoprotein by the ubiquitin-proteasome system: targeting via ubiquitination of the N-terminal residue. *Oncogene.* 19, 5944-5950.

Remm, M., A. Remm, and M. Ustav (1999). Human papillomavirus type 18 E1 protein is translated from polycistronic mRNA by a discontinuous scanning mechanism. *J. Virol.* 73, 3062-3070.

Ren, R., Mayer, B. J., Cicchetti, P., and Baltimore, D. (1993). Identification of a ten-amino acid proline-rich SH3 binding site. *Science.* 259, 1157-1161.

Reuver SM, Garner CC (1998). E-cadherin mediated cell adhesion recruits SAP97 into the cortical cytoskeleton. *J Cell Sci.* 111, 1071-1080.

Rey O, Lee S, Baluda MA, Swee J, Ackerson B, Chiu R, Park NH (2000). The E7 oncoprotein of human papillomavirus type 16 interacts with F-actin in vitro and in vivo. *Virology*. 268, 372-381.

Richard G (2000). Connexins: a connection with the skin. *Exp Dermatol*. 9, 77-96.

Richard G, Smith LE, Bailey RA, Itin P, Hohl D, Epstein EH Jr, DiGiovanna JJ, Compton JG, Bale SJ (1998). Mutations in the human connexin gene GJB3 cause erythrokeratodermia variabilis. *Nat Genet*. 20, 366-369.

Richard G, Brown N, Rouan F, Van der Schroeff JG, Bijlsma E, Eichenfield LF, Sybert VP, Greer KE, Hogan P, Campanelli C, Compton JG, Bale SJ, DiGiovanna JJ, Uitto J (2003). Genetic heterogeneity in erythrokeratodermia variabilis: novel mutations in the connexin gene GJB4 (Cx30.3) and genotype-phenotype correlations. *Invest Dermatol*. 120, 601-609.

Richman D.D; Whitley R.J; Hayden F.G. Clinical virology. Churchhill Livingstone Inc. 1997. Chapter 27, page 569-590.

Ririe KM, Rasmussen RP, Wittwer CT (1997). Product differentiation by analysis of DNA melting curves during the polymerase chain reaction. *Anal Biochem*. 245, 154-160.

Rivedal E, Mollerup S, Haugen A, Vikhamar G (1996). Modulation of gap junctional intercellular communication by EGF in human kidney epithelial cells. *Carcinogenesis*. 17, 2321-2328.

Ronco LV, Karpova AY, Vidal M, Howley PM (1998). Human papillomavirus 16 E6 oncoprotein binds to interferon regulatory factor-3 and inhibits its transcriptional activity. *Genes Dev*. 12, 2061-2072.

Roman A, Fife KH (1989). Human papillomaviruses: are we ready to type? *Clin Microbiol Rev*. 2, 166-190.

Rous P, Kidd JG (1936). The carcinogenic effect of a virus on tarred shin. *Science* 83, 468-469

Rook MB, van Ginneken AC, de Jonge B, el Aoumari A, Gros D, Jongsma HJ (1992). Differences in gap junction channels between cardiac myocytes, fibroblasts, and heterologous pairs. *Am J Physiol.* 263, 959-977.

Rouan F, White TW, Brown N, Taylor AM, Lucke TW, Paul DL, Munro CS, Uitto J, Hodgins MB, Richard G (2001). trans-dominant inhibition of connexin-43 by mutant connexin-26: implications for dominant connexin disorders affecting epidermal differentiation. *J Cell Sci.* 114, 2105-2113.

Rousset R, Fabre S, Desbois C, Bantignies F, Jalinot P (1998). The C-terminus of the HTLV-1 Tax oncoprotein mediates interaction with the PDZ domain of cellular proteins. *Oncogene*. 16, 643-654.

Rubin JB, Verselis VK, Bennett MV, Bargiello TA. (1992). A domain substitution procedure and its use to analyze voltage dependence of homotypic gap junctions formed by connexins 26 and 32. Proc Natl Acad Sci U S A. 89, 3820-3824.

Saez JC, Nairn AC, Czernik AJ, Spray DC, Hertzberg EL, Greengard P, Bennett MV (1990). Phosphorylation of connexin 32, a hepatocyte gap-junction protein, by cAMP-dependent protein kinase, protein kinase C and Ca2+/calmodulin-dependent protein kinase II. *Eur J Biochem.* 192, 263-273.

Saez, J. C., Berthoud, V. M., Branes, M. C., Martinez, A. D. and Beyer, E. C. (2003). Plasma membrane channels formed by connexins: their regulation and functions. *Physiol. Rev.* 83, 1359-1400.

Saffitz JE, Laing JG, Yamada KA (2000). Connexin expression and turnover : implications for cardiac excitability. *Circ Res.* 86, 723-728.

Samuel T, Weber HO, Funk JO (2002). Linking DNA damage to cell cycle checkpoints. *Cell Cycle*. 1, 162-168.

Sarma JD, Wang F, Koval M (2002). Targeted gap junction protein constructs reveal connexin-specific differences in oligomerization. *J Biol Chem.* 277, 20911-20918.

Schwarz E, Freese UK, Gissmann L, Mayer W, Roggenbuck B, Stremlau A, zur Hausen H (1985). Structure and transcription of human papillomavirus sequences in cervical carcinoma cells. *Nature.* 314, 111-114.

Schneider-Gadicke A, Schwarz E (1986). Different human cervical carcinoma cell lines show similar transcription patterns of human papillomavirus type 18 early genes. *EMBO J.* 5, 2285-2292.

Scheffner M, Whitaker NJ (2003). Human papillomavirus-induced carcinogenesis and the ubiquitin-proteasome system. *Semin Cancer Biol.* 13, 59-67.

Segretain D, Decrouy X, Dompierre J, Escalier D, Rahman N, Fiorini C, Mograbi B, Siffroi JP, Huhtaniemi I, Fenichel P, Pointis G (2003). Sequestration of connexin43 in the early endosomes: an early event of Leydig cell tumor progression. *Mol Carcinog.* 38, 179-187.

Severs NJ (2001). Gap junction remodeling and cardiac arrhythmogenesis: cause or coincidence? *J Cell Mol Med.* 5, 355-366.

Shieh BH, Zhu MY (1996). Regulation of the TRP Ca2+ channel by INAD in Drosophila photoreceptors. *Neuron.* 16, 991-998.

Shore, L., McLean, P., Gilmour, S. K, Hodgins, M. B. and Finbow, M. E. (2001). Polyamines regulate gap junction communication in Connexin 43-expressing cells. *Biochem. J.* 357, 489-495.

Singh D, Lampe PD (2003). Identification of connexin-43 interacting proteins. *Cell Commun Adhes.* 10, 215-220.

Sikerwar SS, Tewari JP, Malhotra SK (1981). Subunit structure of the connexons in hepatocyte gap junctions. *Eur J Cell Biol.* 24, 211-215.

Sohl G, Willecke K (2004). Gap junctions and the connexin protein family. *Cardiovasc Res.* 62, 228-232.

Solan JL, Fry MD, TenBroek EM, Lampe PD (2003). Connexin43 phosphorylation at S368 is acute during S and G2/M and in response to protein kinase C activation. *J Cell Sci.* 116, 2203-2211.

Song, S., Pitot, H. C. and Lambert, P. F. (1999). The human papillomavirus type 16 E6 gene alone is sufficient to induce carcinomas in transgenic animals. *J. Virol.* 73, 5887-5893.

Song, S., Liem, A., Miller, J. A. and Lambert, P. F. (2000). Human papillomavirus types 16 E6 and E7 contribute differently to carcinogenesis. *Virology* 267, 141-150.

Songyang Z, Fanning AS, Fu C, Xu J, Marfatia SM, Chishti AH, Crompton A, Chan AC, Anderson JM, Cantley LC (1997). Recognition of unique carboxyl-terminal motifs by distinct PDZ domains. *Science.* 275, 73-77.

Stanley MA, Browne HM, Appleby M, Minson AC (1989). Properties of a non-tumorigenic human cervical keratinocyte cell line. *Int J Cancer.* 43, 672-676.

Staub O, Gautschi I, Ishikawa T, Breitschopf K, Ciechanover A, Schild L, Rotin D (1997). Regulation of stability and function of the epithelial Na+ channel (ENaC) by ubiquitination. *EMBO J.* 16, 6325-6336.

Stauss MJ, Shaw EW (1949). Crystalline virus-like particles from skin papillomas characterized by intranuclear inclusion bodies. *Proc Soc Exp Biol Med.* 72, 46-50.

Stehle T, Schulz GE (1990). Three-dimensional structure of the complex of guanylate kinase from yeast with its substrate GMP. *J Mol Biol.* 211, 249-254.

Steinberg TH, Civitelli R, Geist ST, Robertson AJ, Hick E, Veenstra RD, Wang HZ, Warlow PM, Westphale EM, Laing JG (1994). Connexin43 and connexin45 form gap

junctions with different molecular permeabilities in osteoblastic cells. *EMBO J.* 13, 744-750.

Stevenson BR, Siliciano JD, Mooseker MS, Goodenough DA (1986). Identification of ZO-1: a high molecular weight polypeptide associated with the tight junction (zonula occludens) in a variety of epithelia. *J Cell Biol.* 103, 755-766.

Stoler MH, Wolinsky SM, Whitbeck A, Broker TR, Chow LT (1989). Differentiation-linked human papillomavirus types 6 and 11 transcription in genital condylomata revealed by in situ hybridization with message-specific RNA probes. *Virology.* 172, 331-340.

Stohr H, Weber BH (2001). Cloning and characterization of the human retina-specific gene MPP4, a novel member of the p55 subfamily of MAGUK proteins. *Genomics.* 74, 377-384.

Stoler MH (2003). The virology of cervical neoplasia: an HPV-associated malignancy. *Cancer J.* 9, 360-367.

Storey A, Almond N, Osborn K, Crawford L (1990). Mutations of the human papillomavirus type 16 E7 gene that affect transformation, transactivation and phosphorylation by the E7 protein. *J Gen Virol.* 71, 965-970.

Straight SW, Herman B, McCance DJ (1995). The E5 oncoprotein of human papillomavirus type 16 inhibits the acidification of endosomes in human keratinocytes. *J Virol.* 69, 3185-3192.

Stubenrauch F, Laimins LA (1999). Human papillomavirus life cycle: active and latent phases. *Semin Cancer Biol.* 9, 379-386.

Su LK, Vogelstein B, Kinzler KW (1993). Association of the APC tumor suppressor protein with catenins. *Science.* 262, 1734-1737.

Suchyna TM, Xu LX, Gao F, Fourtner CR, Nicholson BJ (1993). Identification of a proline residue as a transduction element involved in voltage gating of gap junctions. *Nature*. 365, 847-849.

Suzuki T, Ohsugi Y, Uchida-Toita M, Akiyama T, Yoshida M (1999). Tax oncoprotein of HTLV-1 binds to the human homologue of Drosophila discs large tumor suppressor protein, hDLG, and perturbs its function in cell growth control. *Oncogene*. 18, 5967-5972.

Tadvalkar G and Pinto da Silva P (1983). In vitro, rapid assembly of gap junctions is induced by cytoskeleton disruptors. *J Cell Biol* 96, 1279-1287.

Takahashi SX, Miriyala J, Colecraft HM (2004). Membrane-associated guanylate kinase-like properties of beta-subunits required for modulation of voltage-dependent Ca2+ channels. *Proc Natl Acad Sci U S A.* 101, 7193-7198.

Taliana L, Benezra M, Greenberg RS, Masur SK, Bernstein AM (2005). ZO-1: lamellipodial localization in a corneal fibroblast wound model. *Invest Ophthalmol Vis Sci.* 46, 96-103.

Tanaka M, Grossman HB (2001). Connexin 26 gene therapy of human bladder cancer: induction of growth suppression, apoptosis, and synergy with Cisplatin. *Hum Gene Ther*. 12, 2225-2236.

Tanimoto H (1992). Occurrence and expression of human papillomavirus type 16 genes in uterine cervical carcinomas. *Hiroshima J Med Sci*. 41, 71-77.

Theiss C, Meller K (2002). Microinjected anti-actin antibodies decrease gap junctional intercellular commmunication in cultured astrocytes. *Exp Cell Res*. 281, 197-204.

Thomas M, Banks L (1998). Inhibition of Bak-induced apoptosis by HPV-18 E6. *Oncogene*. 17, 2943-2954.

Thomas M, Laura R, Hepner K, Guccione E, Sawyers C, Lasky L, Banks L (2002). Oncogenic human papillomavirus E6 proteins target the MAGI-2 and MAGI-3 proteins for degradation. *Oncogene*. 21, 5088-5096.

Thomas M, Pim D, Banks L (1999). The role of the E6-p53 interaction in the molecular pathogenesis of HPV. *Oncogene*. 18, 7690-7700.

Thomas MA, Zosso N, Scerri I, Demaurex N, Chanson M, Staub O (2003). A tyrosine-based sorting signal is involved in connexin43 stability and gap junction turnover. *J Cell Sci.* 116, 2213-2222.

Thomas MA, Huang S, Cokoja A, Riccio O, Staub O, Suter S, Chanson M (2002). Interaction of connexins with protein partners in the control of channel turnover and gating. *Biol Cell.* 94, 445-456.

Thomas T, Jordan K, Laird DW (2001). Role of cytoskeletal elements in the recruitment of Cx43-GFP and Cx26-YFP into gap junctions. *Cell Commun Adhes.* 8, 231-236.

Tomakidi P, Cheng H, Kohl A, Komposch G, Alonso A (2000). Connexin 43 expression is downregulated in raft cultures of human keratinocytes expressing the human papillomavirus type 16 E5 protein. *Cell Tissue Res.* 301, 323-327.

Tong X, Howley PM (1997). The bovine papillomavirus E6 oncoprotein interacts with paxillin and disrupts the actin cytoskeleton. *Proc Natl Acad Sci U S A.* 29, 4412-4417.

Toomre, D., Keller, P., White, J., Olivo, J. C. & Simons, K (1999). Dual-color visualization of trans-Golgi network to plasma membrane traffic along microtubules in living cells. *J Cell Sci.* 112, 21-33.

Toyofuku T, Yabuki M, Otsu K, Kuzuya T, Hori M, Tada M. (1998) Direct association of the gap junction pro tein connexin-43 with ZO-1 in cardiac myocytes. *J Biol Chem.* 273,12725–12731.

Toyofuku T, Akamatsu Y, Zhang H, Kuzuya T, Tada M, Hori M (2001). c-Src regulates the interaction between connexin-43 and ZO-1 in cardiac myocytes. *J Biol Chem.* 276, 1780-1788.

Trosko JE, Chang CC (2001). Mechanism of up-regulated gap junctional intercellular communication during chemoprevention and chemotherapy of cancer. *Mutat Res.* 481, 219-229.

Trosko JE, Inoue T (1997). Oxidative stress, signal transduction, and intercellular communication in radiation carcinogenesis. *Stem Cells.* 2, 59-67.

Trosko JE, Ruch RJ (1998). Cell-cell communication in carcinogenesis. *Front Biosci.* 3, 208-236.

Tsukita, S., Furuse, M. and Itoh, M. (2001). Multifunctional strands in tight junctions. *Nat. Rev. Mol. Cell. Biol.* 2, 285 -293.

Tsunoda S, Sierralta J, Sun Y, Bodner R, Suzuki E, Becker A, Socolich M, Zuker CS (1997). A multivalent PDZ-domain protein assembles signalling complexes in a G-protein-coupled cascade. *Nature.* 388, 243-249.

Unwin N (1989). The structure of ion channels in membranes of excitable cells. *Neuron.* 3, 665-676.

van Veen TA, van Rijen HV, Wiegerinck RF, Opthof T, Colbert MC, Clement S, de Bakker JM, Jongsma HJ (2002). Remodeling of gap junctions in mouse hearts hypertrophied by forced retinoic acid signaling. *J Mol Cell Cardiol.* 34, 1411-1423.

VanSlyke JK, Deschenes SM, Musil LS (2000). Intracellular transport, assembly, and degradation of wild-type and disease-linked mutant gap junction proteins. *Mol Biol Cell.* 11, 1933-1946.

VanSlyke JK, Musil LS (2002). Dislocation and degradation from the ER are regulated by cytosolic stress. *J Cell Biol.* 157, 381-394.

Veldman, T., X. Liu, H. Yuan, and R. Schlegel. (2003). Human papillomavirus E6 and Myc proteins associate in vivo and bind to and cooperatively activate the telomerase reverse transcriptase promoter. *Proc. Natl. Acad. Sci. USA*. 100, 8211-8216.

Vessey CJ, Wilding J, Folarin N, Hirano S, Takeichi M, Soutter P, Stamp GW, Pignatelli M (1995). Altered expression and function of E-cadherin in cervical intraepithelial neoplasia and invasive squamous cell carcinoma. *J Pathol.* 176, 151-159.

Wang S.Sand A. Hildesheim (2003). Chapter 5: viral and host factors in human papillomavirus persistence and progression. *J. Natl. Cancer Inst. Monogr.* 31, 35–40.

Wang Y and B. Rose (1995). Clustering of Cx43 cell-to-cell channels into gap junction plaques: Regulation by cAMP and microfilaments. *J. Cell Sci.* 108, 3501–3508.

Wagner LM, Saleh SM, Boyle DJ, Takemoto DJ. (2002). Effect of protein kinase Cgamma on gap junction disassembly in lens epithelial cells and retinal cells in culture. Mol Vis. 8, 59-66.

Warner A. Gap junctions in development--a perspective. Semin Cell Biol. 1992 Feb;3(1):81-91.

Watabe M, Nagafuchi A, Tsukita S, Takeichi M (1994). Induction of polarized cell-cell association and retardation of growth by activation of the E-cadherin-catenin adhesion system in a dispersed carcinoma line. *J Cell Biol.* 127, 247-256.

Watson, R. A., Rollason T. P., Reynolds, G. M., Murray, P. G., Banks, L. and Roberts S. (2002). Changes in the expression of the human homologue of the Drosophila discs large tumour supressor protein in high-grade premalignant cervical neoplasias. *Carcinogenesis*. 23, 1791 –1796.

Watson RA, Thomas M, Banks L, Roberts S (2003). Activity of the human papillomavirus E6 PDZ-binding motif correlates with an enhanced morphological transformation of immortalized human keratinocytes. *J Cell Sci.* 116, 4925-4934.

Welsh MJ, Aster JC, Ireland M, Alcala J, Maisel H (1982). Calmodulin binds to chick lens gap junction protein in a calcium-independent manner. *Science*. 216, 642-644.

Werness BA, Levine AJ, Howley PM (1990). Association of human papillomavirus types 16 and 18 E6 proteins with p53. *Science*. 248, 76-79.

White, T. W. and Paul, D. L. (1999). Genetic diseases and gene knockouts reveal diverse connexin functions. *Annu. Rev. Physiol.* 61, 283-610.

White TW, Bruzzone R, Wolfram S, Paul DL, Goodenough DA (1994). Selective interactions among the multiple connexin proteins expressed in the vertebrate lens: the second extracellular domain is a determinant of compatibility between connexins. *J Cell Biol.* 125, 879-892.

White TW, Paul DL, Goodenough DA, Bruzzone R (1995). Functional analysis of selective interactions among rodent connexins. *Mol Biol Cell.* 6, 459-470.

Willecke, K., Eiberger, J., Degen, J., Eckardt, D., Romualdi, A., Guldenagel, M., Deutsch, U. and Sohl, G. (2002). Structural and functional diversity of connexin genes in the mouse and human genome. *Biol. Chem.* 383, 725-737.

Woods, D. F. and Bryant, P. J. (1991). The discs-large tumor supressor gene of Drosophila encodes a guanylate kinase homolog localized at septate junctions. *Cell.* 66, 451 – 464.

Woods DF, Hough C, Peel D, Callaini G, Bryant PJ (1996). Dlg protein is required for junction structure, cell polarity, and proliferation control in Drosophila epithelia. *J Cell Biol.* 134, 1469-1482.

Woods DF, Wu JW, Bryant PJ (1997). Localization of proteins to the apico-lateral junctions of Drosophila epithelia. *Dev Genet.* 20, 111-118.

Wu H, Reissner C, Kuhlendahl S, Coblentz B, Reuver S, Kindler S, Gundelfinger ED, Garner CC (2000). Intramolecular interactions regulate SAP97 binding to GKAP. *EMBO J.* 19, 5740-5751.

Wu JC, Tsai RY, Chung TH (2003). Role of catenins in the development of gap junctions in rat cardiomyocytes. *J Cell Biochem.* 88, 823-835.

Yamane Y, Shiga H, Asou H, Haga H, Kawabata K, Abe K, Ito E (1999). Dynamics of astrocyte adhesion as analyzed by a combination of atomic force microscopy and immuno-cytochemistry: the involvement of actin filaments and connexin 43 in the early stage of adhesion. *Arch Histol Cytol.* 62, 355-361.

Yamasaki H, Krutovskikh V, Mesnil M, Tanaka T, Zaidan-Dagli ML, Omori Y (1999). Role of connexin (gap junction) genes in cell growth control and carcinogenesis. *C R Acad Sci III.* 322, 151-159.

Yoshioka, N., H. Inoue, K. Nakanishi, K. Oka, M. Yutsudo, A. Yamashita, A. Hakura, and H. Nojima (2000). Isolation of transformation suppressor genes by cDNA subtraction: lumican suppresses transformation induced by v-src and v-K- ras. *J. Virol.* 74, 1008-1013.

Yotti LP, Chang CC, Trosko JE (1979). Elimination of metabolic cooperation in Chinese hamster cells by a tumor promoter. *Science.* 206, 1089-1091.
Zampighi G, Corless JM, Robertson JD (1980). On gap junction structure. *J Cell Biol.* 86, 190-198.

Zerfass-Thome K, Zwerschke W, Mannhardt B, Tindle R, Botz JW, Jansen-Durr P (1996). Inactivation of the cdk inhibitor p27KIP1 by the human papillomavirus type 16 E7 oncoprotein. *Oncogene.* 13, 2323-2330.

Zhang, Y. W., Kaneda, M. and Morita, I. (2003). The gap junction-independent tumor-suppressing effect of Connexin 43. *J. Biol. Chem.* 278, 44852-44856.

Zhang YW, Nakayama K, Nakayama K, Morita I (2003). A novel route for connexin 43 to inhibit cell proliferation: negative regulation of S-phase kinase-associated protein (Skp 2). *Cancer Res.* 63, 1623-1630.

Zhao W, Chow LT, Broker TR (1997). Transcription activities of human papillomavirus type 11 E6 promoter-proximal elements in raft and submerged cultures of foreskin keratinocytes. *J Virol.* 71, 8832-8840.

Zhou L, Kasperek EM, Nicholson BJ (1999). Dissection of the molecular basis of pp60(v-src) induced gating of connexin 43 gap junction channels. *J Cell Biol.* 144, 1033-1045.

Zimmer DB, Green CR, Evans WH, Gilula NB (1987). Topological analysis of the major protein in isolated intact rat liver gap junctions and gap junction-derived single membrane structures. *J Biol Chem.* 262, 7751-7763.

Zimmermann H, Degenkolbe R, Bernard HU, O'Connor MJ (1999). The human papillomavirus type 16 E6 oncoprotein can down-regulate p53 activity by targeting the transcriptional coactivator CBP/p300. *J Virol.* 73, 6209-6219.

zur Hausen H (1991). Human papillomaviruses in the pathogenesis of anogenital cancer. *Virology.* 184, 9-13.

zur Hausen H, de Villiers EM (1994). Human papillomaviruses. *Annu Rev Microbiol.* 48, 427-447.

zur Hausen H (1996). Papillomavirus infectionsa major cause of human cancers. *Biochem. Biophys. Acta* 111, 55-78.

zur Hausen H (1999). Papillomaviruses in human cancers. *Proc Assoc Am Physicians.* 111, 581-587.

zur Hausen H (2002). Papillomaviruses and cancer: from basic studies to clinical application. *Nat Rev Cancer*. 2, 342-350.

APPENDICES

Appendix 1

Homo sapiens gap junction protein, alpha 1, 43kDa (connexin 43) (GJA1), mRNA.

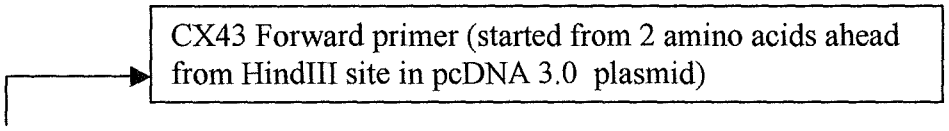

Wt CX43: atg ggt gac tgg agc gcc tta ggc aaa ctc ctt gac

Mu CX43: atg ggt gac tgg agc gcc tta ggc aaa ctc ctt gac

Amino acid sequence: start G D W S A L G K L L D

Wt CX43: aag gtt caa gcc tac tca act gct gga ggg aag gtg

Mu CX43: aag gtt caa gcc tac tca act gct gga ggg aag gtg

Amino acid sequence: K V Q A Y S T A G G K V

Wt CX43: tgg ctg tca gta ctt ttc att ttc cga atc ctg ctg ctg

Mu CX43: tgg ctg tca gta ctt ttc att ttc cga atc ctg ctg ctg

Amino acid sequence: W L S V L F I F R I L L L

Wt CX43: ggg aca gcg gtt gag tca gcc tgg gga gat gag cag

Mu CX43: ggg aca gcg gtt gag tca gcc tgg gga gat gag cag

Amino acid sequence: G T A V E S A W G D E Q

Wt CX43: tct gcc ttt cgt tgt aac act cag caa cct ggt tgt gaa

Mu CX43: tct gcc ttt cgt tgt aac act cag caa cct ggt tgt gaa

Amino acid sequence: S A F R C N T Q Q P G C E

Wt CX43: aat gtc tgc tat gac aag tct ttc cca atc tct cat gtg

Mu CX43: aat gtc tgc tat gac aag tct ttc cca atc tct cat gtg

Amino acid sequence: N V C Y D K S F P I S H V

Wt CX43: cgc ttc tgg gtc ctg cag atc ata ttt gtg tct gta ccc

Mu CX43: cgc ttc tgg gtc ctg cag atc ata ttt gtg tct gta ccc

Amino acid sequence: R F W V L Q I I F V S V P

Wt CX43: aca ctc ttg tac ctg gct cat gtg ttc tat gtg atg cga

Mu CX43: aca ctc ttg tac ctg gct cat gtg ttc tat gtg atg cga

Amino acid sequence: T L L Y L A H V F Y V M R

Wt CX43: aag gaa gag aaa ctg aac aag aaa gag gaa gaa ctc

Mu CX43: aag gaa gag aaa ctg aac aag aaa gag gaa gaa ctc

Amino acid sequence: K E E K L N K K E E E L

Wt CX43: aag gtt gcc caa act gat ggt gtc aat gtg gac atg cac

Mu CX43: aag gtt gcc caa act gat ggt gtc aat gtg gac atg cac

Amino acid sequence: K V A Q T D G V N V D M H

Wt CX43: ttg aag cag att gag ata aag aag ttc aag tac ggt att

Mu CX43: ttg aag cag att gag ata aag aag ttc aag tac ggt att

Amino acid sequence: L K Q I E I K K F K Y G I

Wt CX43: gaa gag cat ggt aag gtg aaa atg cga ggg ggg ttg

Mu CX43: gaa gag cat ggt aag gtg aaa atg cga ggg ggg ttg

Amino acid sequence: E E H G K V K M R G G L

Wt CX43: ctg cga acc tac atc atc agt atc ctc ttc aag tct atc

Mu CX43: ctg cga acc tac atc atc agt atc ctc ttc aag tct atc

Amino acid sequence: L R T Y I I S I L F K S I

Wt CX43: ttt gag gtg gcc ttc ttg ctg atc cag tgg tac atc tat

Mu CX43: ttt gag gtg gcc ttc ttg ctg atc cag tgg tac atc tat

Amino acid sequence: F E V A F L L I Q W Y I Y

Wt CX43: gga ttc agc ttg agt gct gtt tac act tgc aaa aga gat

Mu CX43: gga ttc agc ttg agt gct gtt tac act tgc aaa aga gat

Amino acid sequence: G F S L S A V Y T C K R D

Wt CX43: gat ccc tgc cca cat cag gtg gac tgt ttc ctc tct cgc

Mu CX43: gat ccc tgc cca cat cag gtg gac tgt ttc ctc tct cgc

Amino acid sequence: D P C P H Q V D C F L S R

Wt CX43: ccc acg gag aaa acc atc ttc atc atc ttc atg ctg gtg

Mu CX43: ccc acg gag aaa acc atc ttc atc atc ttc atg ctg gtg

Amino acid sequence: P T E K T I F I I F M L V

Wt CX43: gtg tcc ttg gtg tcc ctg gcc ttg aat atc att gaa ctc ttc

Mu CX43: gtg tcc ttg gtg tcc ctg gcc ttg aat atc att gaa ctc ttc

Amino acid sequence: V S L V S L A L N I I E L F

Wt CX43: tat gtt ttc ttc aag ggc gtt aag gat cgg gtt aag gga

Mu CX43: tat gtt ttc ttc aag ggc gtt aag gat cgg gtt aag gga

Amino acid sequence: Y V F F K G V K D R V K G

Wt CX43: aag agc gac cct tac cat gcg acc agt ggt gcg ctg

Mu CX43: aag agc gac cct tac cat gcg acc agt ggt gcg ctg

Amino acid sequence: K S D P Y H A T S G A L

Wt CX43: agc cct gcc aaa gac tgt ggg tct caa aaa tat gct tat

Mu CX43: agc cct gcc aaa gac tgt ggg tct caa aaa tat gct tat

Amino acid sequence: S P A K D C G S Q K Y A Y

Wt CX43: ttc aat ggc tgc tcc tca cca acc gct ccc ctc tcg cct

Mu CX43: ttc aat ggc tgc tcc tca cca acc gct ccc ctc tcg cct

Amino acid sequence: F N G C S S P T A P L S P

Wt CX43: atg tct cct cct ggg tac aag ctg gtt act ggc gac aga

Mu CX43: atg tct cct cct ggg tac aag ctg gtt act ggc gac aga

Amino acid sequence: M S P P G Y K L V T G D R

Wt CX43: aac aat tct tct tgc cgc aat tac aac aag caa gca agt

Mu CX43: aac aat tct tct tgc cgc aat tac aac aag caa gca agt

Amino acid sequence: N N S S C R N Y N K Q A S

Wt CX43: gag caa aac tgg gct aat tac agt gca gaa caa aat cga

Mu CX43: gag caa aac tgg gct aat tac agt gca gaa caa aat cga

Amino acid sequence: E Q N W A N Y S A E Q N R

Wt CX43: atg ggg cag gcg gga agc acc atc tct aac tcc cat gca

Mu CX43: atg ggg cag gcg gga agc acc atc tct aac tcc cat gca

Amino acid sequence: M G Q A G S T I S N S H A

Wt CX43: cag cct ttt gat ttc ccc gat gat aac cag aat tct aaa

Mu CX43: cag cct ttt gat ttc ccc gat gat aac cag aat tct aaa

Amino acid sequence: Q P F D F P D D N Q N S K

Wt CX43: aaa cta gct gct gga cat gaa tta cag cca cta gcc att

Mu CX43: aaa cta gct gct gga cat gaa tta cag cca cta gcc att

Amino acid sequence: K L A A G H E L Q P L A I

Wt CX43: gtg gac cag cga cct tca agc aga gcc agc agt cgt

Mu CX43: gtg gac cag cga cct tca agc aga gcc agc agt cgt

Amino acid sequence: V D Q R P S S R A S S R

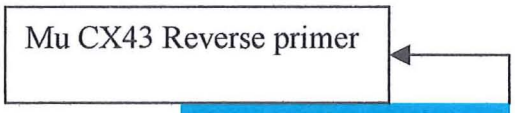

Wt CX43: gcc agc agc aga cct cgg cct gat gac ctg gag atc

Mu CX43: gcc agc agc aga cct cgg cct gat gac ctg gag atc

Amino acid sequence: A S S R P R P D D L E I

Wt CX43: tag

Mu CX43: tag

Amino acid sequence: Stop

Sequence result of Mu Cx 43 (from MBSU):

5' aac aat tct tct tgc cgc aat tac aac aag caa gca agt gag caa aac tgg gct aat tac agt gca gaa caa aat cga atg ggg cag gcg gga agc acc atc tct aac tcc cat gca cag cct ttt gat ttc ccc gat gat aac cag aat tct aaa aaa cta gct gct gga cat gaa tta cag cca cta gcc att gtg gac cag cga cct tca agc aga gcc agc agt cgt gcc agc agc aga cct TCG GTA CCA GTC GAC TCT AGA GGA TCC CGG GCT GAC TAC AAA GAC CAT GAC GGT GAT TAT AAA GAT CAT GAC ATC GAC TAC AAG GAT GAC GAT GAC AAG TAG 3'

Appendix 1: Homo sapiens gap junction protein, alpha 1, 43kDa (connexin 43) (GJA1), mRNA sequence. The forward primer for Mu Cx43 was started from the second amino acid ahead of HindIII site in pcDNA plasmid (the vector containing wild type human Cx43), the reverse primer for Mu Cx43 was labelled with blue background in Cx43 sequence. The deleted sequence for the last 7 amino acids in C-terminal were labelled with red. For more information see http:// www.ncbi.nlm.nih.gov/entrez/viewer.fcgi? db=nucleotide&val=4755136.
The recombined Mu Cx 43 plasmid was sequenced. The small letter sequence was from Cx43 cDNA and the capital letter sequence was from p3X FLAG-CMVTM-14 expression vector plasmid (E4901, Sigma).

Appendix 2

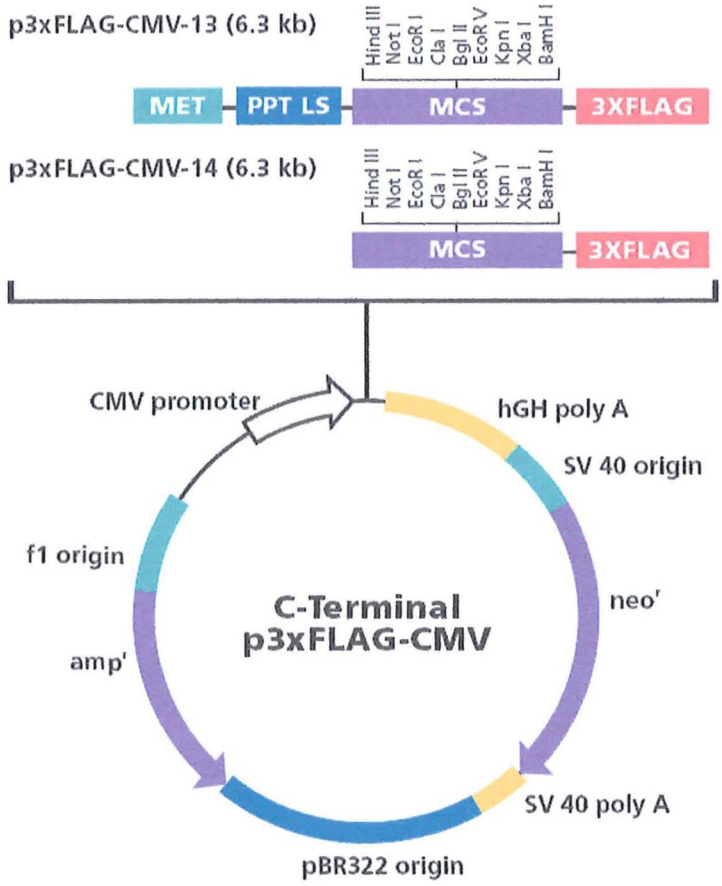

Multiple Cloning Site
(p3xFLAG-CMV-13* and p3XFLAG-CMV-14)

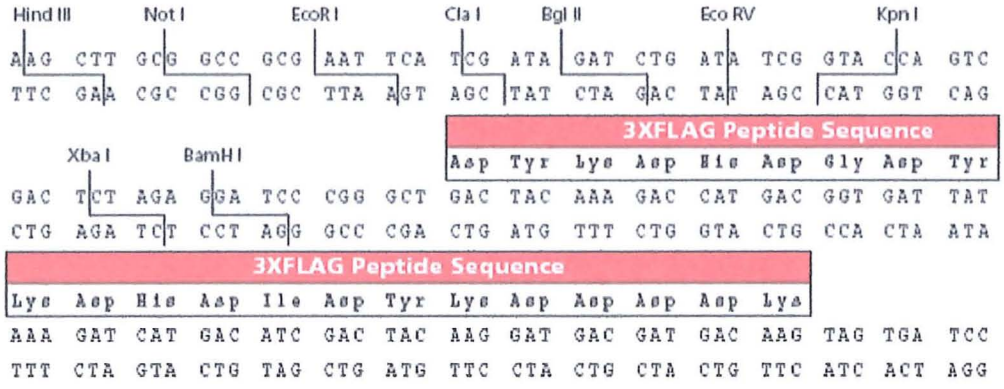

*For p3XFLAG-CMV-13, the Met-preprotrypsin leader sequence (PPT LS) precedes the FLAG coding sequence.

Appendix 2: p3X FLAG-CMVTM-14 expression vector plasmid (E4901, Sigma) plasmid. Used for cloning and transfecting wild and Tr378-382 mutant Connexin 43 constructs. For more information see http:// www.sigmaaldrich.com.

Appendix 3

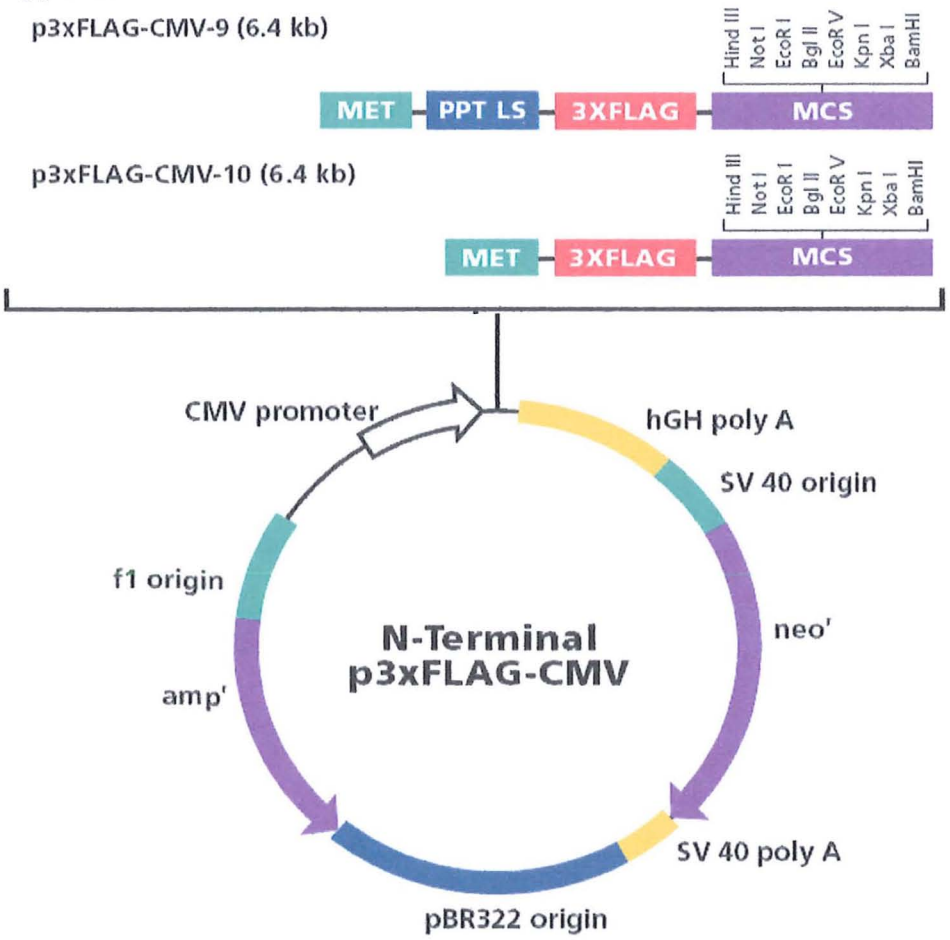

Multiple Cloning Site

(p3xFLAG-CMV-9* and p3xFLAG-CMV-10)

	3XFLAG Peptide Sequence														
Met*	Asp	Tyr	Lys	Asp	His	Asp	Gly	Asp	Tyr	Lys	Asp	His	Asp	Ile	
ATG	GAC	TAC	AAA	GAC	CAT	GAC	GGT	GAT	TAT	AAA	GAT	CAT	GAC	ATC	
TAC	CTG	ATG	TTT	CTG	GTA	CTG	CCA	CTA	ATA	TTT	CTA	GTA	CTG	TAG	

	3XFLAG Peptide Sequence								Not I		EcoR I				
Asp	Tyr	Lys	Asp	Asp	Asp	Asp	Lys								
GAT	TAC	AAG	GAT	GAC	GAT	GAC	AAG	CTT	GCG	GCC	GCG	AAT	TCA	TCG	ATA
CTA	ATG	TTC	CTA	CTG	CTA	CTG	TTC	GAA	CGC	CGG	CGC	TTA	AGT	AGC	TAT
								Hind III							

Bgl II		EcoR V			Kpn I			Xba I		Bam HI			
GAT	CTG	ATA	TCG	GTA	CCA	GTC	GAC	TCT	AGA	GGA	TCC	CGG	TG
CTA	GAC	TAT	AGC	CAT	GGT	CAG	CTG	AGA	TCT	CCT	AGG	CCC	AC

*For pFLAG-CMV-9, the Met-preprotrypsin leader sequence (PPT LS) precedes the FLAG coding sequence.

Appendix 3: p3X FLAG-CMVTM-10 expression vector plasmid (E4401, Sigma) plasmid. Used for cloning and transfecting wild and PDZ_2 binding site mutant HPV 18 E6 constructs. For more information see http:// www.sigmaaldrich.com.

Appendix 4

Gene	Probe set-ID	Fold change	Scanned raw data of W12G cells	Scanned raw data of W12GPXY cells
MMP1	204475_at	644.45	4.095627 4.122086 4.016399	12.04172 11.92974 11.39762
MMP10	205680_at	370.63	4.432889 4.459264 4.483434	10.22319 10.37197 8.391109
IGFBP3	212143_s_at	211.83	7.435301 7.904595 7.782328	12.48461 12.17823 12.59369
JAG1	209098_s_at	6.19	8.728028 8.659485 8.699817	10.56514 10.39518 9.939915
DBN1	202806_at	3.63	8.710068 8.625167 8.846464	8.023017 8.056138 8.106846

Appendix 4: Several raw scanned data samples of microarray results. MMP1, MMP10 and IGFBP 3 are the genes having huge fold change between W12G and W12GPXY cells, JAG1 and DBN1 are the genes have small huge fold change between W12G and W12GPXY cells. The scanned raw data was cauculated with ln. The raw data is consistent with microarray trend.

Appendix 5

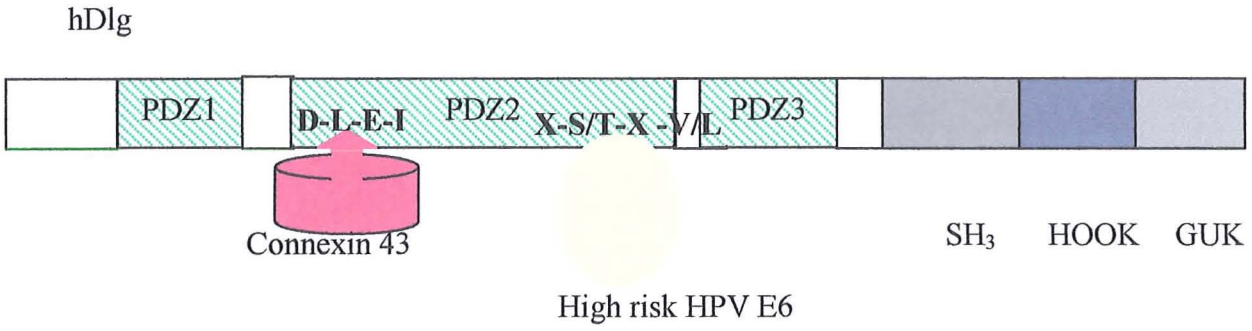

Appendix 5: Schematic diagram showing high risk HPV E6, and Connexin 43 binding in the PDZ2 domain in hDlg. The interaction sites were proposed different.

Appendix 6

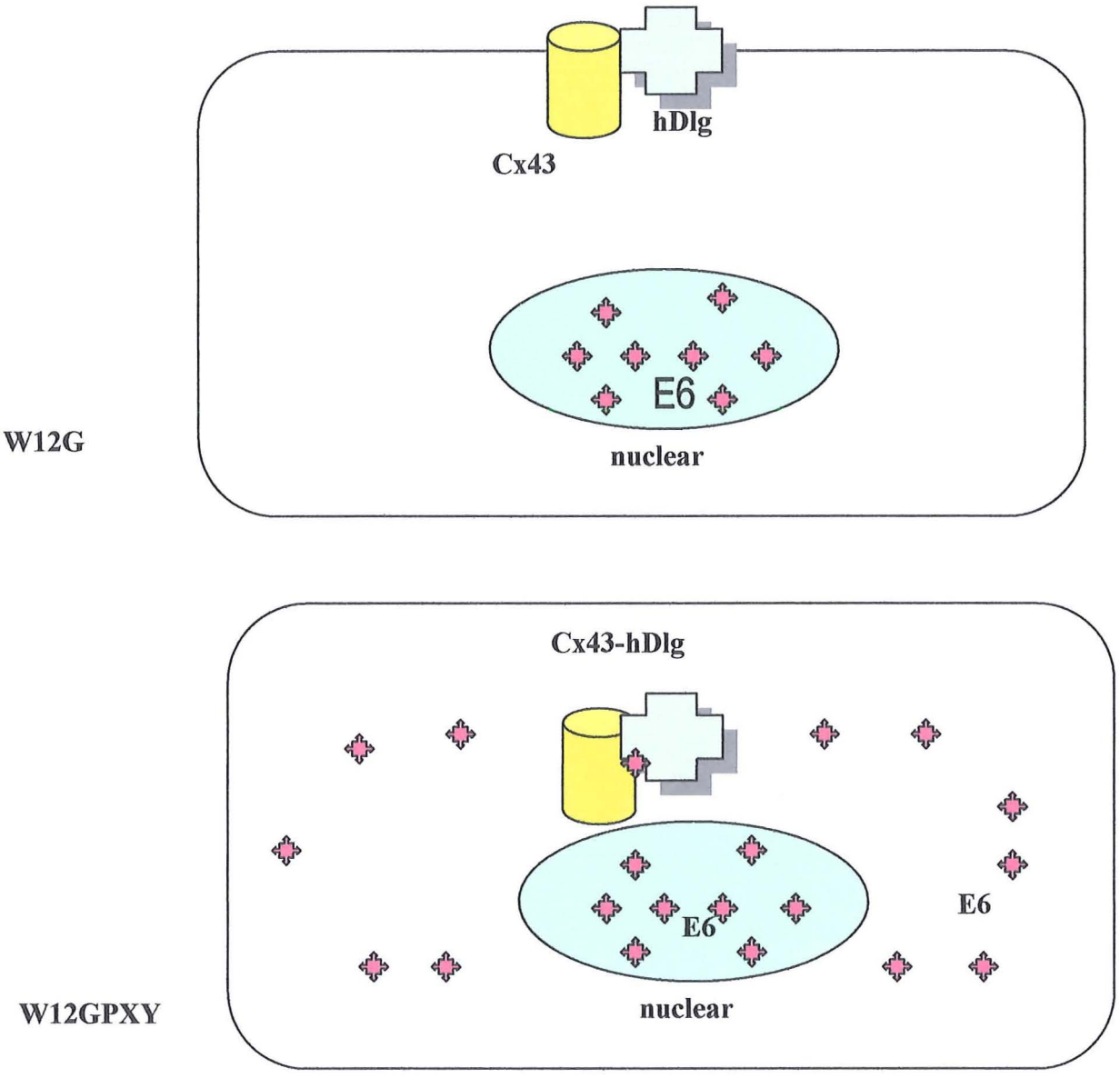

Appendix 6: Schematic diagram showing different location of HPV-16 E6, hDlg and Connexin 43 in W12G and W12GPXY cells. E6 is in nuclei, hdlg and Connexin are on the cell membrane in W12G cells; E6 is in nuclei and cytoplasm, hdlg and Connexin are associated with E6 in cytoplasm in W12GPXY cells.